A STUDY OF HEAT TRANSFER AND FLUID FLOW
IN THE ELECTROSLAG REFINING PROCESS

by

MANOJ KUMAR CHOUDHARY

B. Tech. Hons. (Chemical Engineering)
Indian Institute of Technology, Kharagpur
(1974)

M.S. (Chemical Engineering)
State University of New York at Buffalo
(1976)

SUBMITTED IN PARTIAL FULFILLMENT
OF THE REQUIREMENTS FOR THE
DEGREE OF

DOCTOR OF SCIENCE

at the

MASSACHUSETTS INSTITUTE OF TECHNOLOGY

June 1980

Signature of Author ______________________
Department of Materials Science
and Engineering, May 2, 1980

Certified by ______________________
Julian Szekely
Thesis Supervisor

Accepted by ______________________
Regis M. Pelloux
Chairman, Departmental Committee
on Graduate Students

A STUDY OF HEAT TRANSFER AND FLUID FLOW IN THE ELECTROSLAG REFINING PROCESS

by

MANOJ KUMAR CHOUDHARY

Submitted to the Department of Materials Science and Engineering on May 2, 1980 in partial fulfillment of the requirements for the degree of Doctor of Science

ABSTRACT

A mathematical model has been formulated to describe the electromagnetic field, fluid flow, heat transfer and solidification phenomena in electroslag refining systems.

The formulation is based on the simultaneous statement of Maxwell's equations written for the MHD approximation, the equations for turbulent fluid flow in the slag as caused by both electromagnetic and natural convection forces (due to temperature gradients) and the differential thermal energy balance equations with allowances made for the spatial distribution of heat generation rate in the slag, for the moving interfaces, for the transport of heat by metal droplets falling through the slag and for the release of latent heat in the mushy zone. The effective viscosity and the effective thermal conductivity in the slag are calculated by using a two equation model for turbulence. The equations are first stated in vector notations and then simplified for an axi-symmetric cylindrical coordinate system. An outline of the computational approach is also included.

The theoretically predicted pool profiles and temperature fields are found to be in reasonable agreement with experimental measurements reported in literature for a laboratory scale system. The predictive capability of the model makes it possible to relate the heat generation pattern, the temperature and the velocity fields, the casting rate and the pool profiles to the operating power and current, to the amount of slag used and to the geometry of the system.

Thesis Supervisor: Dr. Julian Szekely

Title: Professor of Materials Engineering

TABLE OF CONTENTS

Chapter		Page
	ABSTRACT	2
	TABLE OF CONTENTS	3
	LIST OF FIGURES	7
	LIST OF TABLES	12
	ACKNOWLEDGEMENTS	13
I	INTRODUCTION	14
II	LITERATURE SURVEY	17
	2.1 Mathematical Models for ESR	18
	2.2 Turbulent Recirculating Flows in Metallurgical Systems	23
III	FORMULATION OF MATHEMATICAL MODEL	27
	3.1 Process Description	27
	3.2 Summary of Basic Processes	28
	3.3 Assumptions Made in Model	30
	3.4 Statement of Mathematical Tasks	34
	3.5 Governing Equations for Flow and Heat Transfer Phenomena in the Electroslag Refining Process	35
	3.5.1 Maxwell's equations	35
	3.5.2 Fluid flow equations	39
	3.5.3 Heat transfer equations	45
	3.5.3A Heat transfer in slag	45
	3.5.3B Heat transfer in other portions of ESR	47
	3.5.4 Droplet Behavior	50
	3.5.4A Droplet radius	50
	3.5.4B Droplet motion in the slag	51
	3.5.4C Rate of heat removal by droplets from the slag	55

Chapter | Page

3.6 The Boundary Conditions 57

3.6.1 Boundary conditions for the magnetic field equation 57

3.6.2 Boundary conditions for the fluid flow equations 60

3.6.3 Boundary conditions for temperature 64

3.7 General Nature of Solutions 69

3.7.1 The nature of stirring 69

3.7.2 Relationship between velocity and current 72

3.7.3 Heat input vs. energy for stirring 73

3.7.4 Dimensionless form of governing equations 75

3.7.4A Dimensionless form of magnetic field equation 75

3.7.4B Dimensionless form of flow equations 76

3.7.4C Dimensionless form of the heat transfer equation 77

3.8 Concluding Remarks 79

Nomenclature 82

IV NUMERICAL SOLUTION OF GOVERNING EQUATIONS 91

4.1 Summary of Governing Equations and Boundary Conditions 91

4.1.1 Equations for magnetic field 91

4.1.2 Equations for fluid flow and heat transfer 92

4.1.3 Boundary conditions 93

4.2 Derivation of the Finite-Difference Equations 93

4.2.1 Expressions for interior nodes 98

4.2.2 Expressions for boundary nodes 103

4.3 Wall Function Approach 107

CHAPTER		Page
	4.4 Solution Procedure	114
	4.4.1 Flowsheet for computation	115
	4.4.2 Introduction to computer program	116
	4.4.3 Stability and convergence problems	116
	Nomenclature	125
V	COMPUTED RESULTS AND DISCUSSION	129
	5.1 Description of the System Chosen for Computation	129
	5.2 Physical Properties and Parameters Used in Computation	132
	5.3 Computational Details	140
	5.4 Results and Discussions	142
	5.4.1 Computed results on electromagnetic parameters	142
	5.4.2 Computed results on Fluid flow and heat transfer	153
VI	CONCLUSIONS AND SUGGESTIONS FOR FURTHER WORK	184
	6.1 Conclusions	184
	6.2 Suggestions for Further Work	189
	6.2.1 Suggestions for short term plans	190
	6.2.2 Suggestions for long term plans	190

Chapter		Page
APPENDICES		
A	A BRIEF NOTE ON PHASOR NOTATION	192
B	BOUNDARY CONDITIONS ON VORTICITY	196
C	CALCULATION OF RADIATION VIEW FACTORS	201
D	USE OF TEMPERATURE DEPENDENT ELECTRICAL CONDUCTIVITY IN THE SLAG	206
E	THE COMPUTER PROGRAM	208
	E.1 List of Fortran Symbols	208
	E.2 Program Listing	217
REFERENCES		273
BIOGRAPHICAL NOTE		280

List of Figures

Number		Page
3.1	Schematic sketch of the electroslag refining process	29
3.2	Physical concept of the process model	33
3.3	The effect of current on the maximum value of the linear velocity in the slag	74
4.1	Boundary conditions for the magnetic field intensity	95
4.2	Boundary conditions for fluid flow variables	96
4.3	Boundary conditions for temperature	97
4.4	A portion of the finite-difference grid	99
4.5	Illustration for calculating first order derivatives at boundaries	108
4.6	Domains for wall function method	110
4.7	Illustration for wall function approach	111

		Page
4.8	Simplified flow diagram for the computational scheme	117
5.1	Computed ratio of effective and atomic thermal conductivities in both slag and metal pools for operation with 1.7 kA (rms) and for an idealized metal pool shape and size.	139
5.2	Details on the grid configuration	141
5.3	Computed magnetic field intensity for operation with 1.7 kA (rms)	143
5.4	Computed current density vectors in slag for operation with 1.7 kA (rms)	145
5.5	Computed radial distribution of volumetric heat generation rate in slag for operation with 1.7 kA.	146
5.6	The effect of electrode penetration depth on heat generation rate in slag.	148
5.7	The effect of the amount of slag used on the heat generation rate in slag.	149
5.8	The effect of fill ratio on current distribution in the slag.	151

		Page
5.9	Computed and measured axial temperature profiles for ingot 15 (rms current = 1.7 kA) at r = 2.5 cm.	155
5.10	Computed temperature distribution at the slag-metal interface for ingot 15.	157
5.11	Results from Fig. 5.10 expressed in an alternative way.	159
5.12	Computed liquidus and solidus isotherms for ingot 15.	160
5.13	Computed and measured axial temperature profiles for ingot 17.	161
5.14	Computed liquidus and solidus isotherms for ingot 17.	163
5.15	Computed isotherms in slag for ingot 15.	164
5.16	The effect of electrode penetration depth on temperature distribution in the slag.	167
5.17	Computed streamline pattern in slag for ingot 15.	169

		Page
5.18	Computed velocity vectors in slag for operation with 1.7 kA and for a fill ratio of 0.325.	170
5.19	Computed velocity vectors in slag for operation with 1.7 kA and for a fill ratio of 0.09.	173
5.20	Radial distribution of buoyancy/electromagnetic contributions to vorticity, 2 cm below the electrode.	174
5.21	Computed distribution of turbulence kinetic energy in the slag for ingot 15.	175
5.22	Computed contours of the ratio effective thermal conductivity/atomic thermal conductivity in the slag for ingot 15.	177
5.23	Computed metal pool depths for different currents.	178
5.24	Variation of maximum pool depth with current.	179
5.25	Variation of casting rate with power.	181
A.1	Graphical representation of a phasor.	193

		Page
B.1	Evaluation of wall vorticity.	198
C.1	Schematic representation of the system for calculating view factors.	202

List of Tables

Number		Page
3.1	Summary of governing equations in vector notation	70
3.2	Summary of dimensionless variables	80
4.1	Summary of governing differential equations in cylindrical coordinate system	94
4.2	Description of the computer program	119
5.1	Composition of electrodes used in Mellberg's experiments	130
5.2	Remelting parameters in Mellberg's experiments	132
5.3	Physical property values used	134
5.4	Numerical values of parameters used in computation	136
5.5	Values for droplet parameters	182

ACKNOWLEDGEMENTS

I express my gratitude to Professor Julian Szekely for his invaluable guidance, assistance and encouragement during the course of this work. He has helped make my graduate study at MIT academically fruitful as well as an enjoyable experience.

I am grateful to Professors Thomas B. King, John F. Elliott, and Thomas W. Eagar for their interest in my research program.

I am indebted to my father and to other members of my family in India for their constant encouragement. Special gratitude to my wife, Saraswati, for too many contributions to mention.

I thank my friends for their advice and good wishes. One of them, Karin, deserves special thanks for her typing of the manuscript.

The financial support for this work from NSF is gratefully acknowledged.

CHAPTER I

INTRODUCTION

In recent years there has been a growing interest in the development of mathematical models for the representation of heat transfer and fluid flow phenomena in the electroslag refining process. While the earlier models concentrated on the calculations of pool profiles and temperature fields in the ingot, a more fundamental approach was taken in recently reported models where allowance has been made for the thermally and electromagnetically driven flow in the system. However, these latter models were primarily of theoretical interest because the shape and size of the molten metal pool had to be specified and because heat transfer in the mushy zone and in the ingot was neglected.

The work to be described in this thesis represents an attempt towards developing a predictive model for flow and thermal characteristics of the ESR process. The model developed in this work seeks mathematical representations for the electromagnetic field, for the turbulent recirculating flow in the slag (due to both electromagnetic and natural convection forces) and for heat transfer with phase change. It therefore involves the simultaneous statement of Maxwell's equations, equations for turbulent motion and the differential thermal energy balance equations. The model is then used to make predictions for a laboratory scale system reported in literature. The predictive capability of the model is utilized to investigate the interdependence of principal operating parameters.

Regarding the organization of this thesis, it is divided into six chapters in the following manner:

In Chapter 2, a literature survey is presented, which reviews mathematical models on ESR and on turbulent recirculating flow in metallurgical systems.

The formulation of the mathematical model is given in Chapter 3. After discussing the basic processes involved and the assumptions made, the governing differential equations are first written in vectorial forms so that some general conclusions can be drawn regarding the behavior of ESR systems. Then they are presented in the cylindrical coordinate system with axial symmetry. Boundary conditions are discussed and some dimensionless parameters are derived.

Numerical procedure used to solve the governing differential equations is outlined in Chapter 4.

Computed results on current distribution, heat generation pattern, velocity and temperature fields and pool profiles are discussed in Chapter 5. Wherever possible, these results are compared with experimental measurements available in literature.

Concluding remarks and some suggestions for further work in modelling of ESR process are made in Chapter 6.

Appendix A contains a brief note on phasor notation used for AC operation. Derivations of vorticity boundary conditions are discussed in Appendix B. Calculation of radiation view factors is outlined in Appendix C. The use of a temperature dependent electrical conductivity for slag is discussed in Appendix D and a listing of the computer program is presented in Appendix E.

CHAPTER II
LITERATURE SURVEY

The past decade has seen a rapid increase in the application of electroslag process in this country and in other industrialized nations. During the same period numerous papers dealing with both physical and mathematical modelling of ESR have been published. These models have resulted from a need to have a better understanding of the relationships among key process parameters so as to be able to devise effective strategies for controlling structure and composition of remelted ingots.

Mathematical models for the ESR process can be classified into two groups -- (1) those dealing with physical phenomena such as heat transfer, fluid flow and solidification (i.e. thermal and fluid flow models) [1-22] and (2) those dealing with chemical and electrochemical reactions (i.e. chemical models) [23-26]. The review presented here is restricted to thermal and fluid flow models for this is the category into which the present work falls.

From the point of view of mathematical modelling, the electroslag refining process represents a complex group of problems involving turbulent recirculating flow driven by electromagnetic and buoyancy forces, heat and mass transfer phenomena and phase change (both melting and solidification) with free boundaries. Because of the way ESR model described in this thesis has evolved, it appears best to divide this chapter into two sections. The first section reviews mathematical models for ESR and the second section presents an overview of literature on the mathematical modelling of turbulent recirculating flows in metallurgical systems.

2.1 Mathematical Models for ESR

Some of the earliest modelling work on ESR dealt with temperature distributions in the electrode. These involved the solution of one dimensional [2,3] or two dimensional [1,7] heat conduction problems with experimentally established boundary conditions. While these models were helpful in visualizing the relative magnitudes of various heat transfer mechanisms (i.e. conduction, convection and radiation) so far as the electrode was concerned, they could not provide insight into the local or the overall heat transfer rate between the electrode and the slag. The heat transfer coefficient between the electrode and the slag was, instead, used as an adjustable parameter to interpret measured temperature distributions in the electrode.

Most of the early models on ESR [4-12,18] have concentrated on the representation of thermal field in the ingot. While these models may differ in the form (e.g. transient vs. quasi steady state) or in the type of boundary conditions chosen (e.g. specified flux vs. specified temperature at the slag-metal interface) or in the way the release of latent heat is accounted for (e.g. adjustment of specific heat in the mushy zone vs. use of solidification models), the unifying themes behind these models are:

1) transport processes taking place in the slag are ignored with the boundary condition at the slag-metal interface being considered adjustable.

2) casting rate is used as an input to the model.

and 3) an effective thermal conductivity is used to account for convection in the metal pool.

These models then reduce to a set of heat conduction equations (with movement of slag-metal interface being accounted for) for the metal pool, for the mushy zone and for the solid ingot with appropriate boundary conditions. Some of these earlier models have been reviewed by Mitchell et al. [9] and by Ballantyne and Mitchell [12]. The models presented by Sun and Pridgeon [4], Carvajal and Geiger [8], Paton et al. [5,10], Ballantyne and Mitchell [12] and Jeanfils et al. [18] are transient in nature. While all these authors used the transient models to study the development of isotherms from the initial stages of remelting up to the attainment of quasi-steady state, Jeanfils et al. [18] also utilized their model to investigate the response of the system (as characterized by change in pool depth and mushy zone thickness) to specified changes (e.g. ramp, sinusoidal) in the melt rate.

Elliott and Maulvault [11] noted that the thermal conditions in an ESR system became reproducible in time after the ingot had grown to sufficient length (e.g. about 2.5 times the radius of the ingot when casting steels and other metals with similar conductivities) and developed a quasi steady state model for calculating thermal field in the ingot. This reduced the dimensionality of the problem without seriously affecting the scope of the model. Furthermore, the numerical scheme chosen by Elliott and Maulvault [11] allowed for arbitrary grid configurations. This in turn enabled them to concentrate the nodes in critical areas without excessive grid requirements.

Apart from being successful in the interpretation of experimental measurements on pool depth and on local solidification time in the mushy zone, these models [4-12,18] illustrated the influence of casting rate and the effective thermal conductivity on thermal fields in the ingot. Furthermore many of these papers provided measurements which were needed for model validation.

The inability of these models to generate predictive relationships among key process parameters such as power input, geometry, slag depth on one hand and melting rate, pool depth, width of the mushy zone etc. on the other hand stems from ignoring transport processes in the slag. The calculation of thermal fields in the slag necessitates the solution of electromagnetic field equations in order to obtain the local rate of heat generation in the slag. Furthermore there is vigorous convection in slag. The driving force for flow is provided by both electromagnetic and buoyancy forces and the flow, in general, is turbulent. The use of a spatially independent effective conductivity will not provide a realistic representation of convection in the slag. Thus a predictive model for the ESR process will have to seek additional mathematical representations for the electromagnetic force field, turbulent fluid flow field and for convective heat transfer in the slag.

This more fundamental approach has been taken in models published by Dilawari and Szekely [13,14,15], Kreyenberg and Schwerdtfeger [16] and Inoue and Iwasaki [21]. A review of these recent models as well as a survey on measurements of temperature and electric potential reported in the literature have been made by Kawakami and Goto [17].

The basic approach taken by the three groups of investigators is to first calculate the current paths for an assumed electrode melting tip shape (flat in references 13-16 and conical in reference 21) and then to solve fluid flow and convective heat transfer equations. Among these, Kreyenberg and Schwerdtfeger [16] considered fluid flow and heat transfer in the slag phase only while the other two groups examined the behavior of both metal and slag phases.

The approach of Kreyenberg and Schwerdtfeger [16] necessitated an assumed temperature distribution at the slag-metal interface. This assumed boundary condition was found to have a strong effect on calculated flow and temperature fields in the slag. The formulation presented by Dilawari and Szekely [15] was particularly comprehensive since it allowed for the turbulent nature of flow (in both liquid pools) and accounted for heat transfer between the slag and the falling metal droplets. Although the models put forward by Dilawari and Szekely [15] and Inoue and Iwasaki [21] were of fundamental interest, their practical use was limited because the shape and the size of the molten metal pool had to be specified and heat transfer in the mushy zone and in the solid ingot was neglected. These models, therefore, could not be addressed to the metallurgically important question of how to relate the shape and the size of the metal pool and the mushy zone to the operating parameters. Furthermore, the arbitrarily assumed pool shape precluded a meaningful comparison of experimentally measured temperature profiles below the slag-metal interface with predictions based on the model.

The work described in this thesis represents a significant step in our continuing efforts to develop a predictive model for ESR operations. The nature of the model, its scope and limitations are detailed in subsequent chapters.

Some applications of the model described in this thesis have already been published [19,20,22].

Before closing this section it should be pointed out that some studies have been made [27,28] to calculate segregation in ESR by solving interdendritic flow and temperature fields in simulated ESR ingots. The latter paper, in fact, investigated the suppression of macro-segregation by rotating the ingot. In both these papers, no account was taken of motion in the metal pool above the liquidus isotherm and electromagnetic effects were either avoided or ignored. Recently, however, Mehrabian and Ridder [29] have extended their model to account for motion in the metal pool (laminar motion caused by natural convection) and have elaborated on the important influence of fluid motion in the metal pool on solute redistribution in ingots. It will be a worthwhile exercise to combine some aspects of the model to be described in this thesis with models for calculating segregation so as to minimize uncertainties in specifying various boundary conditions in the latter models.

2.2 Turbulent Recirculating Flows in Metallurgical Systems

Some of the recent models of ESR (13-16, 19-22) have involved the solution of turbulent recirculating flow. These models have benefited greatly from experiences gained with modelling of such flows in connection with various metallurgical processes such as continuous casting (Szekely and Yadoya [30]), argon stirring (Szekely et al.[34]), deoxidation in the ASEA-SKF furnace (Szekely and Nakanishi [31]), induction stirring and melting (Szekely and Chang [32], Tarapore and Evans [33]) etc. It is to be noted that the computation of flow profiles in the latter two cases involved the simultaneous solution of Maxwell's and the Navier-Stokes equations. A growing interest in ladle metallurgy [37] operations to achieve bath homogenization (with respect to temperature and composition), deoxidation, degassing, inclusion removal, desulfurization etc. is likely to enhance the application of transport fundamentals in these systems. A detailed review of mathematical and experimental tools available for the study of transport phenomena in agitated ladle systems has been presented by Szekely [38].

The basic approach in the papers mentioned above has been to model the eddy transport terms through the use of an eddy viscosity (i.e. Boussinesq's proposal) which in turn is computed by solving additional equations. Unlike boundary layer flows or simple one dimensional flows where the spatial dependence of eddy viscosity can be given by an algebraic expression (e.g. mixing length hypothesis) or by a one equation model (which uses a differential equation for k, the turbulence kinetic energy and some suitable algebraic expression for l, the length scale of turbulence), turbulent recirculating flows, in general, require a two equation model (which uses two differential equations - one for k and another for some appropriate parameter of turbulence). Launder and Spalding [36] have reviewed various mathematical models of turbulence. Except Szekely and Yadoya [30] who used a one equation model, the rest of the papers listed above used a two equation model (Spalding's k-W model, where W is a statistical characteristic of turbulence). The computational algorithm employed in these papers used the Stream function-vorticity technique as detailed by Gosman et al. [39] Experimental proof for the predictions reported in these papers was in terms of tracer dispersion rates or in terms of surface velocities (for both laboratory and industrial systems) and thus was not very direct. Szekely et al. [34] measured velocity and turbulence kinetic energy in the water model of an argon stirred ladle. This study however was not conclusive because of the uncertainties regarding boundary conditions at the gas-liquid interface and because of inherent experimental inaccuracies involved in determining low velocities using a hot film anemometer.

In a recent study Szekely et al. [35] have reported accurate measurements (using a laser doppler anemometer) of time averaged and fluctuating velocities in a system in which recirculating motion was created by a moving belt.

They also refined the mathematical model by incorporating wall functions to represent momentum transfer in the vicinity of solid surfaces. This refinement is all the more necessary because the transport processes taking place in the vicinity of bounding surfaces are usually of more practical interest. A good agreement between measurements and predictions is found in this paper.[35]

In conclusion, it may be stated that while a great deal more work needs to be done to characterize gas agitated systems, the mathematical treatment of turbulent recirculating flows in single phases and for axial symmetry is relatively well developed and is supported by measurements made in both laboratory and plant scale systems.

CHAPTER III

FORMULATION OF MATHEMATICAL MODEL

In this chapter, a mathematical model is developed to describe flow and heat transfer phenomena in ESR systems. A brief description of the electroslag refining process is first presented so as to provide a clear perspective on the processes and components involved in the system.

3.1 Process Description

A detailed technical description of the ESR process is available in literature [40,41]. Figure 3.1 shows a sketch of a typical ESR system. As seen here a solid consumable electrode of the primary metal which may be cast or wrought or be composed of scrap is made one pole of a high current source (AC or DC) and a water cooled base plate is the other pole. A slag bath contained in the water cooled mold acts as ohmic resistance and the Joule heating produced in it melts the electrode tip. The metal droplets fall through the slag and collect in a pool on the base plate to solidify. The electrode is fed into the slag bath and the liquid metal solidifies progressively forming an ingot which now acts as the secondary electrode. An important feature of the process is that a slag skin is formed at the inner surface of the mold, which provides an electrical insulation separating the mold from the molten slag, the metal pool and the solidfying ingot. The most usual slag compositions fall within the system $CaF_2 + CaO + Al_2O_3$ and fulfill the basic requirements imposed by electrical and thermal conductivity, high temperature stability and phase behavior.

Refining takes place because of reactions between the metal and the slag in three stages:

i) during formation of a droplet on the electrode tip

ii) as the droplet falls through the slag, and

iii) at the slag-molten metal pool interface.

By suitable choice of slags, chemical and electrochemical reactions can either be encouraged or inhibited.

3.2 Summary of Basic Processes

The basic processes taking place during electroslag refining can be summarized as follows:

1) Passage of electric current through conducting media. This gives rise to spatially distributed joule heating in the slag. The interaction between current and the induced magnetic field results in Lorentz forces which cause circulation in slag and in metal pools.

2) Heat transfer, melting and solidification. Convective heat transfer takes place in the slag and in the metal pool. Metal droplets extract heat from the slag and get superheated. This superheat is released in the molten metal pool. Heat transport in other portions of

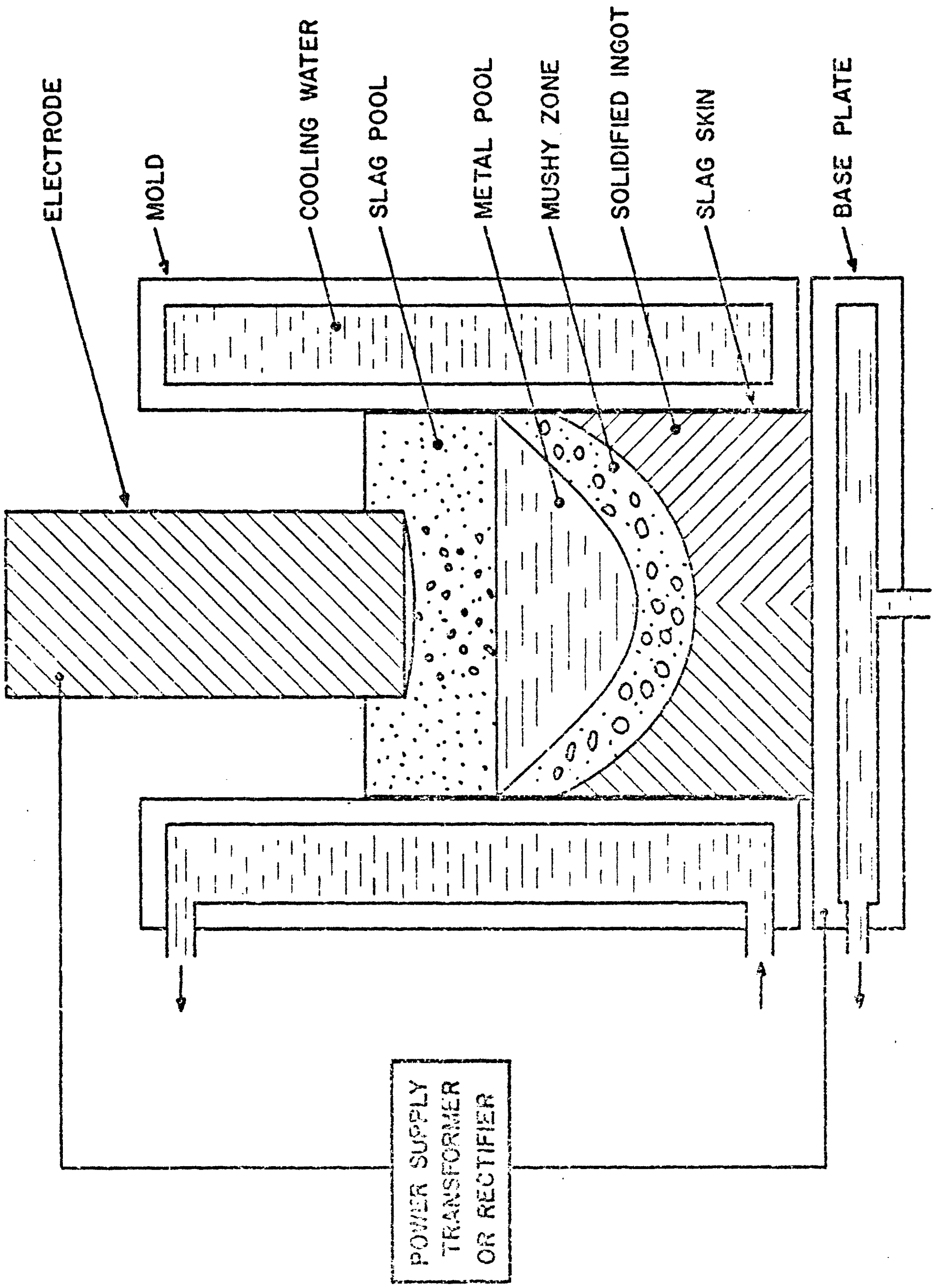

3.1 Schematic sketch of the electroslag refining process.

an ESR unit is characterized by conduction with account being taken of the movement of various interfaces. The electrode tip melts and solidification takes place in the mushy zone. Heat is removed through the mold by cooling water and there is radiative exchange of thermal energy between the free surface of the slag, the outer surface of the electrode and the inner surface of the mold.

3) Recirculation. There is recirculating motion in the slag and in the metal pool due to the combined effect of electromagnetic (Lorentz) and buoyancy (due to thermal gradients) driving forces. The fluid motion is, in general, turbulent.

4) Chemical and electrochemical reactions. This aspect of the ESR operation is not considered in the present work. The implications of ignoring chemical and electrochemical effects while modelling the thermal character of ESR are detailed in the next section.

3.3 Assumptions Made in Model

The physical concept of the process model is sketched in Fig. 3.2 which shows the coordinate system and the assumptions made regarding the geometry of the system.

The assumptions are as follows:

1) Cylindrical symmetry.

2) Slag-electrode and slag-metal boundaries are represented by horizontal surfaces. The assumption of a planar electrode melting tip is thought to be reasonable for large scale systems [42]. However, we have retained this assumption even for the small scale system considered in this work.

Other key assumptions made in the model are as follows:

3) Quasi-steady state.

4) The slag-metal interface is modelled as a rigid wall. This is thought to be reasonable in view of the modelling work reported by Campbell [42].

5) Fluid flow equations are solved for the slag phase only. Motion in the metal pool is accounted for by using an effective thermal conductivity. However, an attempt is made to deduce this parameter from the calculated flow field in the slag phase.

6) In most of the calculations electrical conductivity of the slag is assumed uniform. However, in some calculations the temperature dependence of electrical conductivity of slag is approximately accounted for.

7) The effect of metal droplets on the motion of the slag is neglected.

8) Effects associated with chemical and electrochemical reactions are not considered. There are two

aspects to these effects. The first is the influence of these processes on the nature of heat release in the slag and on motion of the slag. The second is the refining of metal as it is melted, passed through the slag, and collected in a pool at the top of the ingot. Since the present work is concerned with the flow and the thermal characteristics of ESR, the second aspect (i.e. refining) is not important here. It should be recognized, however, that even though the amount of matter involved in exchange reactions is quite small as compared to the total amount of metal being transferred from the electrode to the ingot, the thermal effects arising from concentration polarization and the enthalpy involved in various exchange reactions may influence the net heat supply rate in the regions of the slag near its interfaces with the electrode and the metal pool. These, in turn, will affect the melting rate of the electrode and the depth of molten metal pool.

9) The interaction between the electromagnetic force field and the turbulent fluctuations is neglected in absence of satisfactory methods for treating it.

10) An insulating slag skin is assumed to form on the interior surface of the mold.

Mathematical statements of these assumptions together with assumptions made in formulating the boundary conditions will be presented at appropriate places.

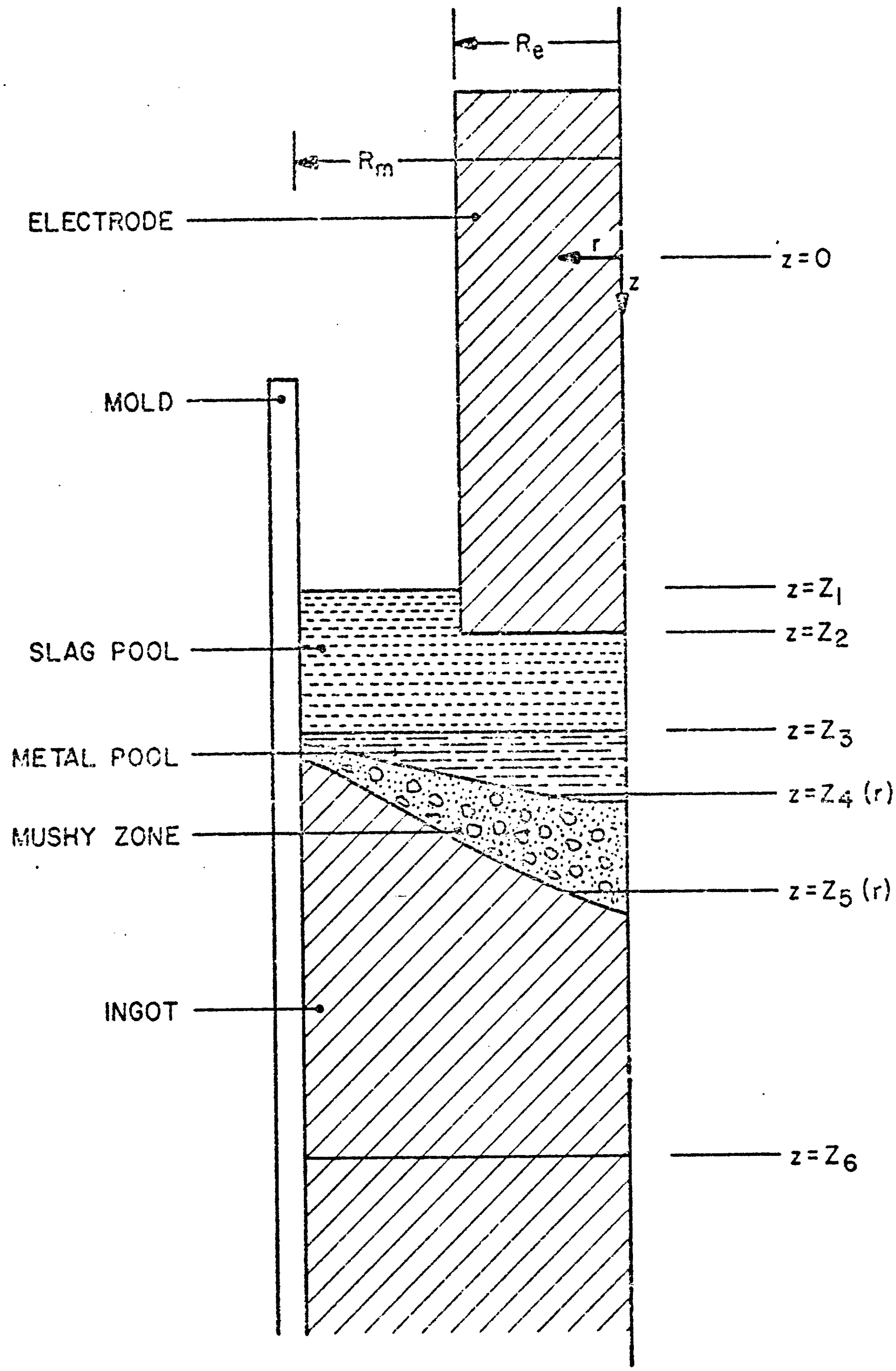

3.2 Physical concept of the process model.

3.4 Statement of the Mathematical Tasks

In context of the assumptions outlined above, the model to be developed in this work seeks mathematical representation for the following physical phenomena:

(1) Electromagnetic field

This is represented by the magnetohydrodynamic form of Maxwell's equations written for different portions of an ESR system and interconnected through boundary conditions. Solution of these equations gives spatial distributions of current densities, Joule heat and Lorentz forces.

(2) Recirculating flow in slag

This is represented by the turbulent Navier Stokes equations with due allowance for body forces (electromagnetic and natural convection). Turbulent viscosity is computed by solving two additional differential equations.

(3) Heat transfer and phase change

The mathematical statement of heat transfer phenomena in the system is given by convective heat transport equations. The convection terms in these equations account for heat transfer due to turbulent recirculating flow in the slag and heat transfer due to movement of various interfaces. In the slag, allowance has to be made for Joule heat generation and heat extraction by metal droplets and in the mushy zone account has to be taken of the release of latent heat.

3.5 Governing Equations for Flow and Heat Transfer Phenomena in the Electroslag Refining Process

Equations mentioned in the previous section are now presented. First the vectorial forms of these equations are given in order that some general conclusions can be obtained and then the equations are stated in the cylindrical coordinate system with axial symmetry.

3.5.1 Maxwell's Equations

Upon applying the MHD approximation, Maxwell's equations take the following form [43]:

(Faraday's Law) $$\underset{\sim}{\nabla} \times \underset{\sim}{E} = -\frac{\partial \underset{\sim}{B}}{\partial t} \qquad (3.1)$$

(Ampere's Law) $$\underset{\sim}{\nabla} \times \underset{\sim}{H} = \underset{\sim}{J} \qquad (3.2)$$

$$\underset{\sim}{\nabla} \cdot \underset{\sim}{B} = 0 \qquad (3.3)$$

$$\underset{\sim}{\nabla} \cdot \underset{\sim}{J} = 0 \qquad (3.4)$$

Here,

$\underset{\sim}{E}$ is the electric field, Volt/m

$\underset{\sim}{B}$ is the magnetic flux density, Weber/m^2 (or Teslas)

$\underset{\sim}{H}$ is the magnetic field intensity, Amp/m

$\underset{\sim}{J}$ is the current density, Amp/m^2

t is time, s

Furthermore, we have

$$\underset{\sim}{J} = \sigma(\underset{\sim}{E} + \underset{\sim}{V} \times \underset{\sim}{B}) \tag{3.5}$$

and

$$\underset{\sim}{B} = \mu_0 \underset{\sim}{H} \tag{3.6}$$

Where σ is the electrical conductivity in 1/Ohm-m, μ_0 is the magnetic permeability of free space in Henry/m and $\underset{\sim}{V}$ is the velocity of medium in m/s.

In brief, the meaning of these equations is as follows:

Eq. (3.1) relates the change in the magnetic flux density to the induced emf. Eq. (3.2) is Ampere's circuital law which relates the induced magnetic field intensity to current in the circuit. Eqs. (3.3) and (3.4) represent the continuity of the magnetic lines of force and conservation of current respectively.

Eqs. (3.1) through (3.6) can be combined [43] to give:

$$\frac{\partial \underset{\sim}{H}}{\partial t} = \eta \nabla^2 \underset{\sim}{H} + \underset{\sim}{\nabla} \times (\underset{\sim}{V} \times \underset{\sim}{H}) \tag{3.7}$$

where $\eta = \dfrac{1}{\sigma\mu_0}$ is called the magnetic diffusity.

Terms arising from the spatial dependence of σ have been neglected. Eq. (3.7), along with Eq. (3.4), contains all the information about $\underset{\sim}{H}$ included in Maxwell's equations.

By using dimensional relation, the ratio of the terms on the r·h·s of Eq. (3.7) is:

$$\frac{|\nabla \times (\underset{\sim}{V} \times \underset{\sim}{H})|}{|\eta \nabla^2 \underset{\sim}{H}|} = \frac{\text{magnetic convection}}{\text{magnetic diffusion}} \simeq 0\left(\frac{V_0 H_0/L}{\eta\ H_0/L^2}\right)$$

$$= 0\ (Re_m) \tag{3.8}$$

where $Re_m = V_0\, L \sigma \mu_0$ is called magnetic Reynolds number. L and V_0 are characteristic length and velocity respectively. In Eq. (3.8) the symbol 0(Q) stands for the order of magnitude of a physical quantity Q. For ESR systems, in general, $Re_m << 1$ and hence the convection term can be neglected [13]. The magnetic field equation then reduces to,

$$\frac{\partial \underset{\sim}{H}}{\partial t} = \eta \nabla^2 \underset{\sim}{H} \tag{3.9}$$

The electromagnetic body force (in N/m^3) is given by:

$$\underset{\sim}{F}_{be} = \underset{\sim}{J} \times \underset{\sim}{B} = \mu_0\ \underset{\sim}{J} \times \underset{\sim}{H} \tag{3.10}$$

In cylindrical coordinate system with axial symmetry

$(H_r = H_z = \frac{\partial}{\partial \theta} = 0)$, Eq. (3.9) can be written as

$$\sigma \mu_0 \frac{\partial H_\theta}{\partial t} = \frac{\partial}{\partial r} \left[\frac{1}{r} \frac{\partial}{\partial r} (r H_\theta)\right] + \frac{\partial^2 H_\theta}{\partial z^2} \tag{3.11}$$

In order to account for AC operation, phasor notation [43,44] (explained in Appendix A) is used. In this notation

$$H_\theta = \hat{H}_\theta e^{j\omega t}$$

$$J_r = \hat{J}_r e^{j\omega t}$$

$$\text{and} \quad J_z = \hat{J}_z e^{j\omega t} \qquad (3.12a,b,c)$$

Where $\hat{H}_\theta$, $\hat{J}_r$, $\hat{J}_z$ are the complex amplitudes of H_θ, J_r and J_z respectively, ω is the angular frequency and j is $\sqrt{-1}$. The momentary physical values of H_θ, J_r and J_z are the real parts of the complex functions given above.

In phasor notation, Eq. (3.11) takes the following form:

$$j\sigma\mu_0\omega\hat{H}_\theta = \frac{\partial}{\partial r}\left[\frac{1}{r}\frac{\partial}{\partial r}(r\hat{H}_\theta)\right] + \frac{\partial^2\hat{H}_\theta}{\partial z^2} \qquad (3.13)$$

which has to be solved for the real and imaginary parts. After solving Eq. (3.13) with appropriate boundary conditions, Eq. (3.2) can be used to calculate current densities as follows:

$$\hat{J}_r = -\frac{\partial\hat{H}_\theta}{\partial z}$$

$$\text{and} \qquad \hat{J}_z = \frac{1}{r}\frac{\partial}{\partial r}(r\hat{H}_\theta) \qquad (3.14a,b)$$

Using Eq. (3.10) and averaging [43,44] over the period $\frac{2\pi}{\omega}$ gives the following relationships for the time averaged components of electromagnetic body force:

$$F_r = -\frac{1}{2}\mu_0 \,\mathrm{Re}(\hat{H}_\theta \overline{\hat{J}_z})$$

$$\text{and} \quad F_z = \frac{1}{2}\mu_0 \,\mathrm{Re}(\hat{H}_\theta \overline{\hat{J}_r}) \qquad (3.15a,b)$$

where Re stands for the real part and the overhead bar denotes the complex conjugate. Similarly the time averaged heat generation rate per unit volume is given by:

$$Q_j = \frac{1}{2}\,\mathrm{Re}\left[\frac{\hat{J}_r\bar{\hat{J}}_r + \hat{J}_z\bar{\hat{J}}_z}{\sigma}\right] \qquad (3.16)$$

The electrical power input to the system is computed by using:

$$W = 2\pi \iint_{zr} Q_j(r,z)\; r\, dr\, dz \qquad (3.16a)$$

3.5.2 Fluid Flow Equations

Turbulent motion in the system is represented by the time-smoothed equations of continuity and motion (i.e. Navier-Stokes equations) written below in vectorial from [45]:

$$\underset{\sim}{\nabla} \cdot \underset{\sim}{\overline{V}} = 0 \qquad (3.17)$$

$$\rho(\bar{\underset{\sim}{V}} \cdot \underset{\sim}{\nabla})\bar{\underset{\sim}{V}} = -\underset{\sim}{\nabla}\bar{P} - \underset{\sim}{\nabla} \cdot \bar{\tau} + \bar{\underset{\sim}{F}}_b$$

inertial force — pressure force — viscous and Reynolds forces — body force

(3.18)

Here

ρ is the (average) density of the fluid

$\bar{V}$ is the velocity vector

$\bar{P}$ is the pressure

$\bar{\tau}$ is the stress tensor, which includes both viscous and Reynolds stresses $\overline{(\rho v_i' v_j')}$

$\bar{\underset{\sim}{F}}_b$ is the body force (per unit volume) vector which incorporates both electromagnetic and buoyancy driving forces and is given by

$$\bar{\underset{\sim}{F}}_b = \underset{\sim}{J} \mathrm{x} \underset{\sim}{B} + \rho[1-\beta(\bar{T}-T_o)]\underset{\sim}{g} \qquad (3.19)$$

Here

β is the coefficient of volume expansion

$\underset{\sim}{g}$ is the acceleration due to gravity

$\bar{T}$ is the temperature at a given location in the fluid

T_o is a reference temperature

The overhead bar in the above equations represents time-smoothed parameters. An assumption inherent in writing equations (3.17) and (3.18) is that the density variations due to temperature gradients are of importance only in producing buoyancy forces and density ρ is supposed to be evaluated at the reference temperature T_o.

Following Boussinesq [45], turbulent or Reynolds stresses can be computed using the same relationships which exist for viscous stresses in a Newtonian fluid but by replacing molecular viscosity of the fluid with a scalar turbulent viscosity. As mentioned in the previous chapter, turbulent viscosity is computed by using a suitable model of turbulence. In the present work a two equation model of turbulence, called the $k - \varepsilon$ model [46] is used. Here k is the turbulence kinetic energy per unit mass and ε is the dissipation rate of turbulence energy. As pointed out by Launder and Spalding [46], a wide variety of flows may be adequately represented by this model without adjustments to model parameters in the near wall regions. Also a comparison of the predictions of various models, with each other and with experiments has shown[46] the $k - \varepsilon$ model to be surpassed only by more complex "Reynolds - Stress" models. It should be noted, furthermore, that the equation for ε contains fewer terms, the exact form of the equation can be derived relatively easily and that ε appears directly as an unknown in the equation for k. The model postulates:

$$\mu_t = C_d \rho k^2/\varepsilon \qquad (3.20)$$

(turbulent viscosity)

Here C_d is a dissipation constant.

Distributions of k and ε in the flow field are represented by transport equations for scalar quantities. In vectorial form, these can be represented as [36,46] :

$$\rho(\underset{\sim}{\overline{V}} \cdot \underset{\sim}{\nabla}\phi) = \underset{\sim}{\nabla} \cdot \left(\frac{\mu_{eff}}{\sigma_\phi} \underset{\sim}{\nabla}\phi \right) + S_\phi \qquad (3.21a,b)$$

convective transport — viscous and turbulent diffusive transport — source

Here ϕ represents k or ε, σ_ϕ is the effective Prandtl number for transport of ϕ, μ_{eff} is the effective viscosity and is the sum of molecular viscosity (μ) and turbulent viscosity (μ_t) and S_ϕ represents the net rate (volumetric) of generation of ϕ.

Equation of motion and the transport equations for k and ε will now be given for an axisymmetric cylindrical coordinate system.

Upon introducing the vorticity, ξ

$$\xi = \frac{\partial \overline{V}_r}{\partial z} - \frac{\partial \overline{V}_z}{\partial r} \qquad (3.22)$$

and the stream function, ψ

$$\overline{V}_r = - \frac{1}{\rho r}\frac{\partial \psi}{\partial z} ,$$

$$\overline{V}_z = \frac{1}{\rho r}\frac{\partial \psi}{\partial r} \qquad (3.23\ a,b)$$

the equation of motion [Eq. (3.18)] can be written as the vorticity transport equation given below [39].

$$r^2\left[\frac{\partial}{\partial z}\left(\frac{\xi}{r}\frac{\partial\psi}{\partial r}\right) - \frac{\partial}{\partial r}\left(\frac{\xi}{r}\frac{\partial\psi}{\partial z}\right)\right] - \frac{\partial}{\partial z}\left[r^3\frac{\partial}{\partial z}\left(\mu_{eff}\frac{\xi}{r}\right)\right]$$
$$- \frac{\partial}{\partial r}\left[r^3\frac{\partial}{\partial r}\left(\mu_{eff}\frac{\xi}{r}\right)\right] + r^2\left(\frac{\partial\overline{F}_z}{\partial r} - \frac{\partial\overline{F}_r}{\partial z}\right) = 0 \qquad (3.24)$$

Using Eqns. (3.19), (3.15a,b) and (3.14a,b), the last term in the above equation can be shown to take the following form:

$$r^2\left(\frac{\partial\overline{F}_z}{\partial r} - \frac{\partial\overline{F}_r}{\partial z}\right) = -\left[\underbrace{r\mu_0 Re(\hat{H}_\theta \overline{J}_r)}_{\text{electromagnetic contribution}} + \underbrace{r^2\rho\beta g\left(\frac{\partial\overline{T}}{\partial r}\right)}_{\text{buoyancy contribution}}\right] \qquad (3.25)$$

In addition the following relationship exists between ξ and ψ:

$$\xi + \frac{\partial}{\partial z}\left(\frac{1}{\rho r}\frac{\partial\psi}{\partial z}\right) + \frac{\partial}{\partial r}\left(\frac{1}{\rho r}\frac{\partial\psi}{\partial r}\right) = 0 \qquad (3.26)$$

Transport equations for k and ε, in the axisymmetric cylindrical coordinate system, are given below:

<u>Transport Equation for k</u>

$$\frac{\partial}{\partial z}\left(k\frac{\partial\psi}{\partial r}\right) - \frac{\partial}{\partial r}\left(k\frac{\partial\psi}{\partial z}\right) - \frac{\partial}{\partial z}\left(r\frac{\mu_{eff}}{\sigma_k}\frac{\partial k}{\partial z}\right) - \frac{\partial}{\partial r}\left(r\frac{\mu_{eff}}{\sigma_k}\frac{\partial k}{\partial r}\right) = r\,S_k \qquad (3.27)$$

where $S_k = G - D$ (3.28)

$$G = 2\mu_t \left[\left(\frac{\partial \overline{V}_z}{\partial z}\right)^2 + \left(\frac{\partial \overline{V}_r}{\partial r}\right)^2 + \left(\frac{\overline{V}_r}{r}\right)^2 + \frac{1}{2}\left(\frac{\partial \overline{V}_r}{\partial z} + \frac{\partial \overline{V}_z}{\partial r}\right)^2 \right] \qquad (3.29a)$$

and $D = \rho\varepsilon$ (3.29b)

<u>Transport Equation for ε</u>

$$\frac{\partial}{\partial z}\left(\varepsilon \frac{\partial \psi}{\partial r}\right) - \frac{\partial}{\partial r}\left(\varepsilon \frac{\partial \psi}{\partial z}\right) - \frac{\partial}{\partial z}\left(r \frac{\mu_{eff}}{\sigma_\varepsilon} \frac{\partial \varepsilon}{\partial z}\right) - \frac{\partial}{\partial r}\left(r \frac{\mu_{eff}}{\sigma_\varepsilon} \frac{\partial \varepsilon}{\partial r}\right) = rS_\varepsilon \qquad (3.30)$$

where

$$S_\varepsilon = C_1 \frac{\varepsilon}{k} G - C_2 \rho \frac{\varepsilon^2}{k} \qquad (3.31)$$

As seen from Eqn. (3.28), the source S_k of the turbulence kinetic energy is made up of two terms G and D. The generation term, G, represents kinetic energy exchange between the mean flow and the turbulence. The dissipation term, D, represents the rate at which viscous stresses perform deformation work against the fluctuating strain rate. The origin and the form of these terms are discussed by Tennekes and Lumley [47] and by Hinze [48].

The source of ε, S_ε is also made up of a positive and a negative term. As in the previous case for S_k, the terms in Eqn. (3.31) represent interaction of turbulence with the mean flow and the self interaction of turbulence. The parameters σ_k, σ_ε, C_1, C_2 originate because of the assumptions made in representing diffusive action of turbulence by means of a gradient law (e.g. $\rho\,\overline{u'k'} = -\frac{\mu_t}{\sigma_k}\frac{\partial k}{\partial y}$) and in modelling source terms. The significance of these parameters and their estimation are discussed in reference 36.

3.5.3 Heat transfer equations

Equations for heat transfer phenomena taking place in different portions of an ESR system are given below.

3.5.3A Heat transfer in slag

The vectorial form of the convective heat transfer equation is written as [45]:

$$\underbrace{\rho\, C_p (\overline{\underset{\sim}{V}} \cdot \underset{\sim}{\nabla} \overline{T})}_{\text{convective transport}} = \underbrace{\underset{\sim}{\nabla} \cdot K_{eff}\, \underset{\sim}{\nabla} \overline{T}}_{\text{laminar and turbulent diffusive transport}} + \underbrace{S_T}_{\text{source}} \qquad (3.32)$$

Here

- C_p is the specific heat of slag
- $\overline{T}$ is the time-smoothed temperature
- S_T is the net volumetric heat generation rate in the slag
- K_{eff} is the effective thermal conductivity in the slag.

S_T, the source term in Eqn. (3.32) consists of two terms as shown below:

$$S_T = Q_j - Q_d \chi \tag{3.33}$$

where Q_j is the volumetric rate of Joule heat generation given by Eqn. (3.16) and Q_d is the rate at which heat is extracted (per unit volume) from the slag by the falling metal droplets. An expression for Q_d will be derived subsequently. χ in Eqn. (3.33) is defined as follows:

$$\begin{aligned} \chi &= 1 \quad \text{when } r \leq R_e \\ \chi &= 0 \quad \text{when } r > R_e \end{aligned} \tag{3.34a,b}$$

where R_e is the radius of the electrode. Conditions (3.34a,b) reflect the fact that droplets remove heat from the central column of the slag which has a radius equal to that of the electrode.

The effective thermal conductivity, K_{eff} is given by

$$K_{eff} = \underbrace{K}_{\substack{\text{molecular}\\ \text{conductivity}}} + \underbrace{K_t}_{\substack{\text{turbulent}\\ \text{conductivity}}} \tag{3.35}$$

After μ_t, the turbulent viscosity, has been calculated using the k-ε model, K_t can be evaluated by using,

$$\sigma_t = \frac{C_p \mu_t}{K_t} \simeq 1 \tag{3.36}$$

where σ_t is the turbulence Prandtl number. The convective transport term in Eqn. (3.32) accounts for the fluid velocity as well as the rise of the slag.

In the axisymmetric cylindrical coordinate system and using Eqns. (3.23a,b), Eqn. (3.32) can be written as:

$$r\rho C_p V_c \frac{\partial \bar{T}}{\partial z} + C_p\left[\frac{\partial}{\partial z}\left(\bar{T}\frac{\partial \psi}{\partial r}\right) - \frac{\partial}{\partial r}\left(\bar{T}\frac{\partial \psi}{\partial z}\right)\right] =$$

$$\frac{\partial}{\partial r}\left(K_{eff}\, r\frac{\partial \bar{T}}{\partial r}\right) + \frac{\partial}{\partial z}\left(K_{eff}\, r\frac{\partial \bar{T}}{\partial z}\right) + rS_T \qquad (3.37)$$

where V_c is the casting rate.

3.5.3B Heat transfer in other portions of ESR

The temperature distribution in the electrode, the molten metal pool, the mushy zone and the solid ingot can be expressed by the following general equation:

$$\rho_i C_{p_i}(\underset{\sim}{V}_i \cdot \underset{\sim}{\nabla} T) = \underset{\sim}{\nabla}\cdot K_i \underset{\sim}{\nabla} T + S_{T,i} \qquad (3.38\,a,b,c,d)$$

where, i = e (electrode), ℓ (metal pool),

m (mushy zone), s (solid ingot)

and $\underset{\sim}{V}_i$ accounts for the rise of the ingot surface (i.e. casting rate) and the downward movement of the electrode. $\underset{\sim}{V}_i$ has only the axial (i.e. z-direction) component.

For the coordinate being used, Eqn (3.38) can be written as:

$$r\rho_i \; C_{p_i} \; V_i \frac{\partial T}{\partial z} = \frac{\partial}{\partial r} (K_i \; r \frac{\partial T}{\partial r}) + \frac{\partial}{\partial z} (K_i \; r \frac{\partial T}{\partial z}) + r \; S_{T,i} \tag{3.39 a,b,c,d}$$

For the electrode, we have

$$V_e = V_t + V_c \tag{3.40}$$

where V_t is the speed of travel of electrode

$$S_{T,e} = 0 \tag{3.41}$$

For the metal pool

$$V_\ell = V_c \tag{3.42}$$

$$S_{T,\ell} = 0 \tag{3.43}$$

K_ℓ = effective thermal conductivity in the metal pool

$$= (1 + \Lambda) \; K_{m\ell} \tag{3.44}$$

where $K_{m\ell}$ is the atomic thermal conductivity of molten metal. The evaluation of Λ will be discussed in Chapter V.

For the mushy zone

$$V_m = V_c \tag{3.45}$$

$$S_{T,m} = V_c \rho_m \lambda \; \frac{\partial f_s}{\partial z} \tag{3.46}$$

where λ is the latent heat of fusion and f_s is the fraction of solids in the mushy zone. $S_{T,m}$ represents the rate of heat release (per unit volume) due to solidification.

For simplicity, a linear relationship will be assumed between f_s and T *, i.e.

$$f_s = \frac{T_{\ell,m} - T}{T_{\ell,m} - T_{s,m}} \tag{3.47}$$

where $T_{\ell,m}$ and $T_{s,m}$ are the liquidus and solidus temperatures of the metal. Then Eq. (3.36) can be written as

$$S_{T,m} = - \frac{V_c \rho_m \lambda}{T_{\ell,m} - T_{s,m}} \frac{\partial T}{\partial z} \tag{3.48}$$

For the ingot we have,

$$V_s = V_c \tag{3.49}$$

$$S_{T,s} = 0 \tag{3.50}$$

It is to be noted that Joule heating has been ingnored everywhere except in the slag. This is reasonable because electrical conductivity of the metal is very large.

The melting rate of the electrode is calculated by making a heat balance at the slag-electrode interface;

---

*The use of more complex relationships (e.g. solidification models) can be easily accommodated.

$$V_{me} = \left(q_{se} - K_e \left.\frac{\partial T}{\partial z}\right|_e \right) / (\rho_e \lambda_e) \tag{3.51}$$

where

q_{se} is heat flux from the slag to the electrode surface

$K_e \left.\frac{\partial T}{\partial z}\right|_e$ is heat flux conducted into the electrode

λ_e is the latent heat for melting of electrode.

q_{se} in Eq. (3.51) is evaluated either by using wall flux relation to be described later or by using

$$-q_{se} = - K \left.\frac{\partial T}{\partial z}\right|_{s\ell} \tag{3.52}$$

3.5.4 Droplet Behavior

In this section, expressions are developed to calculate heat transport by metal droplets falling through the slag. The treatment given here follows that of Dilawari and Szekely [15].

3.5.4A Droplet radius, r_d

For large electrodes, it has been suggested by Campbell [42] that metal droplets are formed at discrete locations on the tip of the electrode. The droplet radius r_d is, therefore, assumed independent of R_e. Then from dimensional arguments and by using experimental results, Campbell has given the following relationship,

$$r_d = \left(\frac{2.04\gamma}{g\,\Delta\rho}\right)^{1/2} \qquad (3.53a)$$

where γ is the interfacial tension between liquid slag and liquid metal, $\Delta\rho$ is the difference in density between the two liquids ang g is the acceleration due to gravity.

For small electrodes, the following relation is deduced by equating gravitational and surface tension forces:

$$r_d = \left(\frac{1.5\gamma R_e}{g\,\Delta\rho}\right)^{1/3} \qquad (3.53b)$$

3.5.4 B Droplet motion in the slag

Considering the slag to be stagnant (it is shown later that the slag velocity is substantially lower than the average falling velocity of the drop) and assuming the droplet to be a rigid sphere the equation describing the droplet motion takes the following form [49]:

$$4/3\ \pi r_d^{\,3}\ (\rho_d + \frac{\rho}{2})\ \frac{dU}{dt} = 4/3\ \pi\, r_d^{\,3}\Delta\rho g - C_D\ \pi r_d^{\,2}\rho\ \frac{U^2}{2} \qquad (3.54)$$

where

ρ_d is the density of metal droplet

ρ is the density of slag

C_D is the drag coefficient

U is the velocity

and $\Delta\rho$ is the difference in densities of the drop and the slag (i.e. $\rho_d - \rho$).

Eq. (3.54) can be written as follows:

$$\frac{dU}{U^2 - a^2} = - 3/8 \frac{C_D}{r_d} \frac{\rho}{\rho_d + 0.5\rho} dt \qquad (3.55)$$

where $a^2 = 8/3 \frac{\Delta\rho}{\rho} \frac{gr_d}{C_D}$ (3.56)

On integration, Eq. (3.55) yields:

$$U = \sqrt{\frac{A}{B}} \frac{e^{2\sqrt{AB}\,t} - 1}{e^{2\sqrt{AB}\,t} + 1} \qquad (3.57)$$

where $A = [\Delta\rho/(\rho_d + 0.5\rho)] g$

and $B = 3/8 \frac{C_D}{r_d} \frac{\rho}{\rho_d + 0.5\rho}$ (3.58a,b)

It follows from Eq. (3.57) that the terminal velocity of the droplet is given by:

$$U_t = \sqrt{\frac{A}{B}} \qquad (3.59)$$

Thus Eq. (3.57) can be written as

$$U = U_t \frac{e^{Ct} - 1}{e^{Ct} + 1} \qquad (3.60)$$

where $$C = 2A/U_t \tag{3.61}$$

If L_1 is the distance from the electrode tip to the slag-metal interface and τ is the residence time of the droplet, then

$$L_1 = \int_0^{\tau} U \, dt \tag{3.62}$$

Substituting Eq. (3.60) in the above equation gives:

$$\frac{(1 + e^{C\tau})^2}{4 e^{C\tau}} = e^{CL_1/U_t} \tag{3.63}$$

from which, the following expression can be deduced,

$$\tau = 1/C \ln \left[(m-1) + \sqrt{m^2 - 2m} \right] \tag{3.64}$$

where $$m = 2e^{2AL_1/U_t^2} \tag{3.65}$$

In the equations given above, C_D, the drag coefficient is not known and thus U_t is unknown. Following Dilawari and Szekely [15], U_t is estimated by using a correlation proposed by Hu and Kintner [50] who studied the steady motion of single drops of various organic liquids falling through stationary water. They concluded that the droplet motion can be represented in terms of two variables defined below:

$$Y = C_D \, We \, P_d^{0.15} \tag{3.66}$$

$$X = (Re_d/P_d^{0.15}) + 0.75 \tag{3.67}$$

where

$$We = \text{Weber number} = \frac{U_t^2 d_d \rho}{\gamma}$$

$$P_d = \text{a physical property group} = \frac{\rho\gamma^3}{g\mu^4}\frac{\rho}{\Delta\rho}$$

$$Re_d = \text{droplet Reynolds number} = \frac{U_t d_d \rho}{\mu}$$

$$d_d = \text{diameter of a droplet}$$

From Eq. (3.54) one can derive,

$$C_D = 4/3 \frac{\Delta\rho}{\rho}\frac{g d_d}{U_t^2} \tag{3.68}$$

Using definitions of C_D and We, Eq. (3.66) can be written as;

$$Y = 4/3 \frac{g d_d^2 \Delta\rho}{\gamma} P_d^{0.15} \tag{3.69}$$

Thus Y depends on physical properties of the system only. Hu and Kintner [50] proposed the following relationships between Y and X:

$$X = (0.75Y)^{0.784} \quad \text{for} \quad 2 < Y \leq 70$$

$$X = (22.22Y)^{0.422} \quad \text{for} \quad Y \geq 70 \tag{3.70a,b}$$

Once X is calculated using one of the above equations, U_t can be calculated as follows:

$$Re_d = (X - 0.75)\ P_d^{0.15}$$

which gives

$$U_t = \frac{Re_d \mu}{d_d\ \rho} \qquad (3.71)$$

3.5.4C Rate of heat removal by droplets from the slag

By assuming that heat transfer from the slag to a droplet can be characterized by a single heat transfer coefficient, h and an average temperature of the slag between the electrode tip and the slag-metal interface (T_B), one can write the following equation for heat balance on a single drop:

$$4/3\ \pi r_d^{\,3}\ \rho_d\ C_{P,d} \frac{dT_d}{dt} = h\ (T_B - T_d)\ 4\pi r_d^{\,2} \qquad (3.72)$$

With the initial condition, $t = 0$, $T_d = T_{me}$ where, T_d is the temperature of the drop and T_{me} is the melting temperature of the electrode.

The heat transfer coefficient, h can be estimated using the average velocity, U_{av} ($=L_1/\tau$) of the droplet in the slag, from suitable correlations [51]. In the present work a correlation proposed by Spelles [52] is used. This correlation is given below:

$$\frac{hd_d}{K} = 0.8 \; (d_d \; U_{av} \rho / \mu)^{1/2} \; (C_p \mu / K)^{1/3} \qquad (3.73)$$

where ρ, K, C_p, μ are respectively the density, the thermal conductivity, the specific heat and the viscosity of the slag.

Eq. (3.72) can be integrated to give the following expression for the final temperature, T_f of a droplet:

$$T_f = T_B - (T_B - T_{me}) \; e^{-S\tau} \qquad (3.74)$$

where

$$S = \frac{3h}{r_d \; C_{p,d} \; \rho_d} \qquad (3.75)$$

The rate at which heat is removed from the slag by the falling droplets is given by:

$$Q_s = \pi R_e^2 \; V_{me} \; \rho_e \; C_{p,d} \; (T_f - T_{me}) \qquad (3.76)$$

Where V_{me}, as defined by Eq. (3.51) is the melting rate of the electrode. Q_d, appearing in Eq (3.33) is obtained from:

$$Q_d = \frac{Q_s}{\pi R_e^2 L_1} \qquad (3.77)$$

i.e. droplets are assumed to remove heat uniformly from the volume of slag forming a central column of radius R_e and height L_1.

3.6 The Boundary Conditions

In this section expressions are developed for the dependent variables (or their gradients) on the bounding surfaces sketched in Fig. 3.2.

3.6.1 Boundary conditions for the magnetic field equation

Boundary conditions for Eq. (3.13) have to express the following physical constraints [43]:

(1) the continuity of the tangential component of the electric field across the phase boundaries, i.e.

$$\underset{\sim}{n} \times [\underset{\sim}{E}_1 - \underset{\sim}{E}_2] = 0 \qquad (3.78)$$

where $\underset{\sim}{n}$ is the unit vector normal to the boundary separating media 1 and 2. Eq. (3.78) is obtained by applying the integral form of Eq. (3.1) across the phase boundary.

(2) the statement of Ampere's Law [obtained by applying Stoke's theorem to Eq. (3.2)], i.e.

$$\oint \underset{\sim}{H} \cdot d\ell = \int \underset{\sim}{J} \cdot d\underset{\sim}{S} \qquad (3.79)$$

Eq. (3.79) states that the line integral of $\underset{\sim}{H}$ around the path enclosing an area through which a current is passing is equal to the current.

Constraints 1 and 2 are the statements of physical laws derivable from Maxwell's equations. In addition, the following assumptions have to be made:

(3) axial symmetry gives $\hat{H}_\theta = 0$ at $r = 0$ (3.80)

(4) at the free slag surface ($z = Z_1$, $R_e \le r \le R_m$) $\hat{J}_z = 0$

(5) at the upper boundary of electrode ($z = 0$, $0 \le r \le R_e$) $\hat{J}_r \simeq 0$

(6) at the lower boundary of ingot ($z=Z_6$, $0 \le r \le R_m$) $\hat{J}_r \simeq 0$.

Mathematical statements for these assumptions in terms of the magnetic field intensity, $\hat{H}_\theta$ are given below:

(1) at $z = 0$, $0 \le r \le R_e$, (upper boundary of electrode)

$$\frac{\partial \hat{H}_\theta}{\partial z} = 0 \tag{3.81}$$

$(\hat{J}_r = 0)$

(2) at $r = R_e$, $0 \le z \le Z_1$ (surface of electrode above slag)

$$\hat{H}_\theta = I_0/(2\pi R_e) \tag{3.82}$$

(Statement of Ampere's Law)

where I_0 is the maximum value of the total current.

(3) at $r = R_e$, $Z_1 \le z \le Z_2$ (vertical surface of electrode immersed in slag)

$$\frac{1}{\sigma} \hat{J}_z \Big|_e = \frac{1}{\sigma} \hat{J}_z \Big|_{s\ell} \tag{3.83}$$

(Continuity of $\hat{E}_z$)

(4) at $r = R_m$, $Z_1 \le z \le Z_6$ (slag-mold interface)

$$\hat{H}_\theta = \frac{I_0}{2\pi R_m} \tag{3.84}$$

(Ampere's Law)

(5) at $z = Z_2$, $0 \le r \le R_e$ (slag- electrode interface)

$$\frac{1}{\sigma} \hat{J}_r \Big|_e = \frac{1}{\sigma} \hat{J}_r \Big|_{s\ell}$$

(Continuity of $\hat{E}_r$)

which gives,

$$\frac{1}{\sigma} \frac{\partial \hat{H}_\theta}{\partial z}\Big|_e = \frac{1}{\sigma} \frac{\partial \hat{H}_\theta}{\partial z}\Big|_{s\ell} \tag{3.85}$$

(6) at $z = Z_1$, $R_e \le r \le R_m$ (free surface of slag)

$$\hat{H}_\theta = \frac{I_0}{2\pi r} \tag{3.86}$$

(from $\hat{J}_z = \frac{1}{r} \frac{\partial}{\partial r} (r\hat{H}_\theta) = 0$)

(7) at $z = Z_3$, $0 \le r \le R_m$ (slag-metal interface)

$$\frac{1}{\sigma} \frac{\partial \hat{H}_\Theta}{\partial z}\Big|_{s\ell} = \frac{1}{\sigma} \frac{\partial \hat{H}_\theta}{\partial z}\Big|_\ell \tag{3.87}$$

(continuity of $\hat{E}_r$)

(8) at $z = Z_6$, $0 \leq r \leq R_m$ (lower boundary of ingot)

$$\frac{\partial \hat{H}_\theta}{\partial z} = 0 \qquad (3.88)$$

$$(\hat{J}_r = 0)$$

It is to be noted that boundary conditions are stated in terms of $\hat{H}_\theta$ from which real and imaginary parts can be separated.

3.6.2 Boundary conditions for the fluid flow equations

In a physical sense the boundary conditions for the fluid flow equations have to express the following:

(1) Symmetry about the centerline

(2) The "no-slip" condition for the velocity at the solid boundaries (i.e. zero velocity at the stationary solid boundaries). As discussed in section 3.3, the slag-metal interface is assumed to be a rigid interface.

(3) At the free surface of the slag, the fluxes of momentum and turbulence quantities (k and ε) are assumed to be zero.

Since we use the vorticity transport equation, the above conditions have to be stated in terms of vorticity (ξ) and stream function (ψ). Furthermore, boundary conditions have to be stated for k and ε as well. The expressions for boundary conditions in terms of ξ and ψ.

are derived in texts on computational fluid dynamics [39,40] and a brief summary of these derivations are given in Appendix B. In this chapter, only the final form of the expressions are given. Also the wall function treatment for the turbulence quantities is discussed in the next chapter. With reference to Fig. 3.2 the boundary conditions for the flow equations are as follows:

(1) at $r = 0$, $Z_2 \leq z \leq Z_3$

$$\psi = \frac{\partial k}{\partial r} = \frac{\partial \varepsilon}{\partial r} = 0$$

and

$$\left(\frac{\xi}{r}\right)_0 = \frac{8}{\rho}\left[\frac{\psi_0 - \psi_2}{r_2^{\,2}} + \frac{\psi_1 - \psi_0}{r_1^{\,2}}\right]/(r_2^{\,2} - r_1^{\,2})\ ^*$$

(3.89a,b)

where suffixes 0, 1, 2 denote the points on the axis of symmetry and the adjacent grid nodes in the r-direction respectively.

(2) at $z = Z_1$, $R_e \leq r \leq R_m$ (free slag surface)

$$\psi = \frac{\xi}{r} = \frac{\partial k}{\partial z} = \frac{\partial \varepsilon}{\partial z} = 0 \qquad (3.90)$$

$\psi = 0$ follows from $\bar{V}_z = 0$ and $\xi = 0$ follows from $\mu_{eff}\left(\frac{\partial \bar{V}_r}{\partial z} + \frac{\partial \bar{V}_z}{\partial r}\right) = 0$ and from the definition of ξ (Eq.3.22).

---

*Derivation given in Appendix B

(3) at $z = Z_2$, $0 \leq r \leq R_e$ (slag-electrode interface)

$$\psi = 0 \tag{3.91a}$$

$$k = \varepsilon = 0 \,^{**} \tag{3.91b}$$

and

$$\left(\frac{\xi}{r}\right)_0 = \frac{3\,(\psi_0 - \psi_1)}{\rho r^2\,(z_1 - z_0)^2} - \frac{1}{2}\left(\frac{\xi}{r}\right)_1^{*} \tag{3.91c}$$

where suffixes 0 and 1 refer to a grid node on the boundary and to the adjacent node in z - direction, respectively.

(4) at $z = Z_3$, $0 \leq r \leq R_m$ (slag-metal interface)

$$\psi = 0 \tag{3.92a}$$

$$k = \varepsilon = 0 \,^{**} \tag{3.92b}$$

and

$$\left(\frac{\xi}{r}\right)_0 = \frac{3\,(\psi_0 - \psi_1)}{\rho r^2\,(z_1 - z_0)^2} - \frac{1}{2}\left(\frac{\xi}{r}\right)_1^{*} \tag{3.92c}$$

where suffixes have the same meaning as in the case of Eq. (3.91c).

---

* derivation given in Appendix B

** alternate and more realistic formulation through the use of wall functions is discussed in next chapter.

(5) at $r = R_e$, $Z_1 \leq z \leq Z_2$ (vertical surface of electrode immersed in slag)

$$\psi = 0 \tag{3.93a}$$

$$k = \varepsilon = 0^{**} \tag{3.93b}$$

and

$$\left(\frac{\xi}{r}\right)_0 = \frac{3}{\rho} \frac{(\psi_0 - \psi_1)}{(r_1 - r_0)^2 r_0 r_1} - \frac{1}{2}\left(\frac{\xi}{r}\right)_1 + \frac{\rho g \beta}{4 R_e \mu_{eff,1}} (r_1 - r_0)(T_o - T_1)^{*} \tag{3.93c}$$

where suffixes 0 and 1 refer to a grid point on the boundary and to the adjacent node in r - direction, respectively.

(6) at $r = R_m$, $Z_1 \leq z \leq Z_3$ (slag-mold interface)

$$\psi = 0 \tag{3.94a}$$

$$k = \varepsilon = 0^{**} \tag{3.94b}$$

and

$$\left(\frac{\xi}{r}\right)_0 = \frac{3}{\rho} \frac{(\psi_0 - \psi_1)}{(r_1 - r_0)^2 r_0 r_1} - \frac{1}{2}\left(\frac{\xi}{r}\right)_1 + \frac{\rho g \beta}{4 R_m \mu_{eff,1}} (r_1 - r_0)(T_o - T_1)^{*} \tag{3.94c}$$

---

* derivation discussed in Apendix B

** alternate and more realistic formulation through the use of wall functions is duscussed in next chapter.

where suffixes have the same meaning as in the case of Eq. (3.93c).

3.6.3 Boundary conditions for temperature

These boundary conditions have to express the following physical constraints:

(1) symmetry about the centerline

(2) continuity of heat fluxes at all the external surfaces and at the slag-metal interface.

(3) the electrode tip is at the liquidus temperature.

Again, with reference to Fig. 3.2, boundary conditions for the temperature equations can be written as follows:

(1) at $r = 0$, $0 \leq z \leq Z_6$

$$\frac{\partial T}{\partial r} = 0 \qquad (3.95)$$

(2) at $z = 0$, $0 \leq r \leq R_e$ (upper boundary of electrode) and at $z=Z_6$, $0 \leq r \leq R_m$ (lower boundary of ingot)

$$\frac{\partial T}{\partial z} = 0 \qquad (3.96)$$

(3) at $r = R_e$, $0 \leq z \leq Z_1$ (surface of electrode above slag)

$$-K \left.\frac{\partial T}{\partial r}\right|_e = \underset{\mathrm{I}}{h_c \,[\, T(R_e, z) - T_a]} + \epsilon_e \delta [\, T(R_e, z)^4$$

$$\underset{\mathrm{II}}{- \epsilon_s F_{es}(z)\, T_{s,av}{}^4 - \epsilon_m F_{em}\, T_m{}^4]} \qquad (3.97)$$

where

T_a	is the temperature of the gas
δ	is the Stefan-Boltzmann constant
$\epsilon_e, \epsilon_s, \epsilon_m$	are the emissivities of the dry electrode surface, the free surface of the slag and the inner surface of the mold respectively.
T_m	is the temperature of the inside surface of the mold above the slag
$T_{s,av}$	is the average temperature of the free surface of the slag
F_{es}	is the view factor between the electrode element and the slag surface
F_{em}	is the view factor between the electrode element and the mold wall.

It is understood here that the temperatures are in the absolute scale. The first term in Eq. (3.97) represents the convective exchange between the electrode surface and the ambient gas whereas the second term represents the radiative exchange between the electrode surface, the free slag surface and the inner surface of the mold. In order to fascilitate the calculation of view factors, the slag surface is represented by a single temperature, $T_{s,av}$ which is calculated from the following equation:

$$T_{s,av} = \frac{2\int_{R_e}^{R_m} T(r,Z_1)\,r\,dr}{(R_m^{\ 2} - R_e^{\ 2})} \tag{3.98}$$

(4) at $z = Z_1$, $R_e \le r \le R_m$ (free surface of slag)

$$K_{eff} \left.\frac{\partial T}{\partial z}\right|_{s\ell} = \delta\varepsilon_s [T_{s,av}^{\ 4} - \varepsilon_m F'_{sm} T_m^{\ 4} - \varepsilon_e F'_{se} T_{e,av}^{\ 4}] \tag{3.99}$$

where $T_{e,av}$ is the average temperature of the dry electrode

F'_{sm} is the view factor between the slag surface and the mold wall

and F'_{se} is the view factor between the free surface of the slag and the dry surface of the electrode.

As seen from Eq. (3.99), the convective heat loss from the slag surface to the ambient gas has been neglected. Also, in order to simplify calculations the slag surface and the electrode surface have been represented by their average temperatures.

View factors appearing in Eqns. (3.97) and (3.99) are calculated using the techniques discussed by Leunberger and Person [54]. The calculation procedure is outlined in Appendix C.

(5) at $r = R_e$, $Z_1 \leq z \leq Z_2$ (vertical surface of electrode immersed in slag)

$$K \left.\frac{\partial T}{\partial r}\right|_e = K \left.\frac{\partial T}{\partial r}\right|_{s\ell}^{*} \tag{3.100}$$

(6) at $z = Z_2$, $0 \leq r \leq R_e$ (slag-electrode interface)

$$T = T_{m,e} \tag{3.101}$$

(7) at $z = Z_3$, $0 \leq r \leq R_m$ (slag-metal interface)

$$- K_{eff} \left.\frac{\partial T}{\partial z}\right|_{s\ell}^{*} + \frac{Q_s}{\pi R_e^{\,2}} \chi = -K_\ell \left.\frac{\partial T}{\partial z}\right|_{\ell} \tag{3.102}$$

where Q_s is defined by Eq. (3.76) and χ is defined by Eq. (3.34a,b); i.e. the heat extracted by droplets from the slag is given uniformly to the liquid metal over an area $\pi R_e^{\,2}$.

---

*Alternate expressions for these fluxes can be given by wall function approach discussed in the next chapter.

(8) at $r = R_m$, $Z_1 \leq z \leq Z_3$ (slag-mold interface)

Since a solidified slag layer is assumed to exist at the inside wall of the mold, the temperature condition can be specified as $T = T_{\ell,s}$ (3.103a)

where $T_{\ell,s}$ is the melting temperature of the slag. Alternatively one may write

$$-K \left.\frac{\partial T}{\partial r}\right|_{s\ell}^{*} = h_{W,s} \quad (T - T_W) \tag{3.103b}$$

where $h_{W,s}$ is the overall heat transfer coefficient which describes the heat transfer from the molten slag/ slag skin interface to the cooling water in the mold. T_W is the average temperature of the cooling water.

(9) at $r = R_m$, $Z_3 \leq z \leq Z_6$

$$- K \left.\frac{\partial T}{\partial r}\right|_{i} = h_{W,i} \; (T - T_W) \tag{3.104}$$

where i stands for interfaces between various media (i.e. metal pool, mushy zone, solid ingot) and the mold. $h_{W,i}$ represents overall heat transfer coefficient at these interfaces.

---

* Alternate expressions for these fluxes can be given by wall function approach discussed in the next chapter.

3.7 General Nature of Solutions

The mathematical statement of the model is now complete. Before presenting the detailed results, it is worthwhile to discuss the general nature of solutions. The governing equations (in vectorial form) for the system are grouped together in Table 3.1.

3.7.1 The nature of stirring

Using Eqns. (3.10),(3.2) and (3.6), the electromagnetic body force $\underset{\sim}{F}_{be}$ can be written as follows:

$$\underset{\sim}{F}_{be} = \underset{\sim}{J} \times \underset{\sim}{B} = \frac{1}{\mu_0}(\underset{\sim}{\nabla} \times \underset{\sim}{B}) \times \underset{\sim}{B}$$

$$= \underbrace{-\underset{\sim}{\nabla}\left(\frac{1}{2\mu_0} B^2\right)}_{\mathrm{I}} + \underbrace{\frac{1}{\mu_0}(\underset{\sim}{B} \cdot \underset{\sim}{\nabla})\underset{\sim}{B}}_{\mathrm{II}} \tag{3.105}$$

Upon operating with $\underset{\sim}{\nabla}\times$ (i.e. curl) on the r.h.s. of Eq. (3.105), the first term vanishes. i.e.

$$\underset{\sim}{\nabla} \times \left(-\underset{\sim}{\nabla}\left(\frac{1}{2\mu_0} B^2\right)\right) = 0 \tag{3.106}$$

while in general,

$$\underset{\sim}{\nabla} \times \left(\frac{1}{\mu_0}(\underset{\sim}{B} \cdot \underset{\sim}{\nabla})\underset{\sim}{B}\right) \neq 0 \tag{3.107}$$

It follows therefore that the term I (called the magnetic pressure), cannot do any work <u>on a circulating fluid</u> and that the second term (II) is responsible for doing work.

Table 3.1 Governing equations for fluid flow and heat transfer in the ESR process

1. Maxwell's equations

$$\underset{\sim}{\nabla} \times \underset{\sim}{E} = -\frac{\partial \underset{\sim}{B}}{\partial t} \qquad \qquad \frac{\partial \underset{\sim}{H}}{\partial t} = \eta \nabla^2 \underset{\sim}{H}$$

$$\underset{\sim}{\nabla} \times \underset{\sim}{H} = \underset{\sim}{J} \qquad \text{OR}$$

$$\underset{\sim}{\nabla} \cdot \underset{\sim}{B} = 0 \qquad \qquad \underset{\sim}{\nabla} \cdot \underset{\sim}{J} = 0$$

$$\underset{\sim}{\nabla} \cdot \underset{\sim}{J} = 0$$

Constitutive equation

$$\underset{\sim}{B} = \mu_0 \underset{\sim}{H}$$

Ohm's law

$$\underset{\sim}{J} \cong \sigma \underset{\sim}{E}$$

2. Equations for fluid flow (in slag)

Equation of continuity

$$\underset{\sim}{\nabla} \cdot \underset{\sim}{\overline{V}} = 0$$

Equation of motion

$$\rho (\underset{\sim}{\overline{V}} \cdot \underset{\sim}{\nabla}) \underset{\sim}{\overline{V}} = -\underset{\sim}{\nabla} \overline{p} - \underset{\sim}{\nabla} \cdot \overline{\tau} + \left[\frac{1}{2} \mathrm{Re} (\underset{\sim}{\hat{J}} \times \underset{\sim}{\overline{\hat{B}}}) - \rho \left(1 - \beta (\overline{T} - T_0)\right) \underset{\sim}{g} \right]$$

Transport equation for k and ε

$$\rho (\underset{\sim}{\overline{V}} \cdot \underset{\sim}{\nabla} \phi) = \underset{\sim}{\nabla} \cdot \left(\frac{\mu_{eff}}{\sigma_\phi} \underset{\sim}{\nabla} \phi \right) + S_\phi$$

where $\phi = k$ or ε

3. Thermal energy equations

Heat transfer in slag

$$\rho C_p (\underset{\sim}{\overline{V}} \cdot \underset{\sim}{\nabla} \overline{T}) = \underset{\sim}{\nabla} \cdot K_{eff} \underset{\sim}{\nabla} \overline{T} + \frac{1}{2\sigma} \mathrm{Re}(\underset{\sim}{\hat{J}} \cdot \underset{\sim}{\overline{\hat{J}}}) - Q_d \chi$$

Heat transfer in other portions of ESR

$$\rho_i C_{p_i} (\underset{\sim}{V_i} \cdot \underset{\sim}{\nabla} T) = \underset{\sim}{\nabla} \cdot K_i \underset{\sim}{\nabla} T + S_{T,i}$$

where i = e (electrode), ℓ (metal pool),

m (mushy zone), s (solid ingot)

and V_i accounts for movement of various interfaces.

The inertial force in the equation of motion [Eq. (3.18)] can be written as

$$\rho(\underset{\sim}{\overline{V}}\cdot\underset{\sim}{\nabla})\underset{\sim}{\overline{V}} = \rho\left[(\underset{\sim}{\nabla}\times\underset{\sim}{\overline{V}})\times\underset{\sim}{\overline{V}}\right] + \rho\underset{\sim}{\nabla}\left(\frac{\overline{V}^2}{2}\right) \tag{3.108}$$

Introducing the definition of vorticity,

$$\underset{\sim}{\xi} = \underset{\sim}{\nabla}\times\underset{\sim}{\overline{V}} \tag{3.109}$$

we can rewrite Eq. (3.108) as follows:

$$\underbrace{\rho(\underset{\sim}{\xi}\times\underset{\sim}{\overline{V}})}_{\text{vortex force}} = -\rho\underset{\sim}{\nabla}\left(\frac{\overline{V}^2}{2}\right) + \rho(\underset{\sim}{\overline{V}}\cdot\underset{\sim}{\nabla})\underset{\sim}{\overline{V}} \tag{3.110}$$

From Eqs. (3.105) and (3.110), the analogy between $\underset{\sim}{F}_{be}$ and the vortex force is evident.

3.7.2 Relationship between velocity and current

Let us assume that the buoyancy driving force is small compared to the electromagnetic driving force (i.e. we operate with high current and with a small fill ratio) then Eqs. (3.18) and (3.19) can be combined to give:

$$\rho(\underset{\sim}{\overline{V}}\cdot\underset{\sim}{\nabla})\underset{\sim}{\overline{V}} = -\underset{\sim}{\nabla}\overline{P}_t - \underset{\sim}{\nabla}\cdot\overline{\tau} + \underset{\sim}{J}\times\underset{\sim}{B} \tag{3.111}$$

where $\overline{P}_t$ represents the sum of static pressure and gravitational force. If the inertial forces dominate (i.e. at high Reynolds number) then as a first approximation we may neglect the first two terms on the r.h.s. of Eq. (3.111). The order of magnitude of the remaining terms are:

$$O\left[\rho(\underset{\sim}{\bar{V}}\cdot\underset{\sim}{\nabla})\underset{\sim}{\bar{V}}\right] \simeq \frac{\rho V_0^2}{L}$$

$$O\left[\underset{\sim}{J} \times \underset{\sim}{B}\right] \simeq J_0 \times \mu_0 J_0 L \qquad (3.112a,b)$$

where J_0 is a characteristic current density of the system.

From Eqs. (3.112a) and (3.112b) we can write

$$\frac{\rho V_0^2}{L} \sim \mu_0 J_0^2 L \qquad (3.113)$$

i.e.

$$V_0 \sim J_0 \sqrt{\frac{\mu_0}{\rho}} \quad L$$

which indicates that the characteristic velocity is proportional to the current. Figure 3.3, taken from Dilawari and Szekely [15] shows the effect of current on the velocity in the slag phase. As seen here, under the isothermal conditions (i.e. in the absence of buoyancy driving forces) the relationship between the velocity and the current is linear.

3.7.3 Heat input vs. energy for stirring

From dimensional arguments it may be shown that:

$$\frac{\text{energy input for stirring}}{\text{energy input for heating}} \simeq O\left[\frac{(\underset{\sim}{J} \times \underset{\sim}{B})\cdot\underset{\sim}{V}}{J^2/\sigma}\right] \qquad (3.115a)$$

$$\simeq O\left[\frac{J_0^2 \mu_0 L V_0 \sigma}{J_0^2}\right] \qquad (3.115b)$$

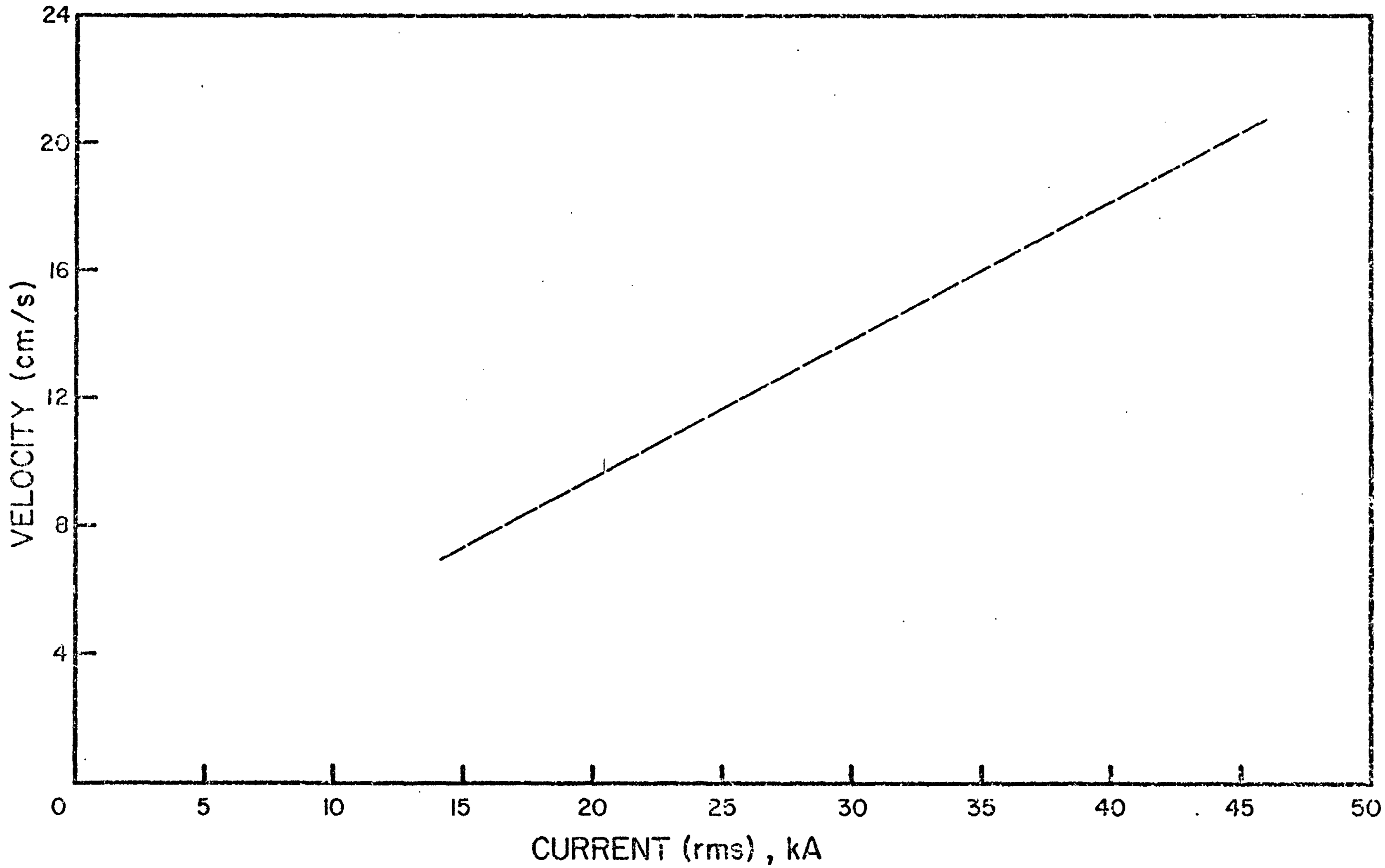

3.3 The effect of current on the maximum value of the linear velocity in the slag (from Dilawari and Szekely [15]).

$$\sim \left(\frac{\mu_0^3}{\rho} \right)^{1/2} L^2 \sigma J_0 \qquad (3.115c)^*$$

For illustrative purposes, let us assume $L = 0.5$ m, $\sigma = 250$ (ohm-m)$^{-1}$, $\rho = 3.0\times10^3$ kg/m^3, $J_0 = 40$ kA/m^2

$$\left(\frac{\mu_0^3}{\rho} \right)^{1/2} L^2 \sigma J_0 = \left[\frac{(1.25\times10^{-6})^3}{3\times10^3} \right]^{1/2} \times .25\times250\times4\times10^4$$

$$= 6.5 \times 10^{-5} << 1$$

3.7.4 Dimensionless form of governing equations

Let us now make the vector form of the governing equations dimensionless. This will generate parameters characterizing the behavior of the system.

3.7.4A Dimensionless form of magnetic field equation

Let us introduce the following dimensionless variables:

$$\underset{\sim}{\nabla}^* = L\,\underset{\sim}{\nabla} \qquad \hat{\underset{\sim}{H}}^* = \hat{\underset{\sim}{H}}/H_0$$

$$H_0 = I_0/L \qquad J_0 = I_0/L^2 \qquad (3.116)$$

then the magnetic field equation (Eq. (3.9)) can be written, in the phasor notation, as:

$$j\alpha\hat{\underset{\sim}{H}}^* = \nabla^{*2}\hat{\underset{\sim}{H}}^* \qquad (3.117)$$

where

---

*Using eq. (3.114)

$$\alpha = \omega\sigma\mu_0 L^2$$

$$= \frac{L^2\sigma\mu_0}{(1/\omega)}$$

$$= \frac{\text{characteristic time for magnetic diffusion}}{\text{characteristic period for electric current}} \qquad (3.118)$$

3.7.4B Dimensionless form of flow equations

In addition to dimensionless variables already defined in Eq. (3.116) let us introduce

$$V^* = \underset{\sim}{\bar{V}}/V_0 \qquad P^* = (\bar{P} - P_0)/\rho V_0^2$$

$$k^* = k/V_0^2 \qquad \varepsilon^* = \varepsilon L/V_0^3$$

$$T^* = (\bar{T} - T_{\ell,s})/(T_{\ell,m} - T_{\ell,s})$$

$$\underset{\sim}{J}^* = \underset{\sim}{J}L/H_0 \qquad (3.119)$$

then the equation of motion (Eq. (3.18)) can be written as

$$(\underset{\sim}{V}^*\cdot\underset{\sim}{\nabla}^*)\underset{\sim}{V}^* = -\underset{\sim}{\nabla}^*\underset{\sim}{P}^* - \underset{\sim}{\nabla}^* \underset{\sim}{\tau}^* + \left[N_1\frac{1}{2}\mathrm{Re}(\hat{\underset{\sim}{J}}^*\times\check{\underset{\sim}{B}}^*) + \{N_2 - N_3(T^*-\gamma)\}\frac{\underset{\sim}{g}}{g}\right] \qquad (3.120)$$

where

$$\tau^* = \tau/\rho V_0^2 = \text{(viscous + Reynolds force)/(inertial force)} \qquad (3.121)$$

$$N_1 = \mu_0 H_0^2/\rho V_0^2 = \text{(Lorentz force)/(inertial force)} \quad (3.122)$$

$$N_2 = gL/V_0^2 = \text{(Gravitational force)/(inertial force)} \quad (3.123)$$

$$N_3 = \beta g(T_{\ell,m} - T_{\ell,s})L/V_0^2 \quad (3.124)$$

$$= \text{(Buoyancy force)/(inertial force)}$$

$$\gamma = \frac{T_0 - T_{\ell,s}}{T_{\ell,m} - T_{\ell,s}} \quad (3.125)$$

similarly, the transport equations for k and ε [Eqs. (3.21a,b)] can be written as

$$\underset{\sim}{V}^* \cdot \underset{\sim}{\nabla}^* k^* = \frac{1}{Re_f} \underset{\sim}{\nabla}^* \cdot \left(\frac{\mu^*_{eff}}{\sigma_k} \underset{\sim}{\nabla}^* k^* \right) + S_k^* \quad (3.126)$$

where $$Re_f = \frac{\rho V_0 L}{\mu} \quad \text{(Reynolds no.)}$$

$$\mu^*_{eff} = \frac{\mu_t}{\mu} + 1 = \frac{\text{Effective viscosity}}{\text{Molecular viscosity}}$$

$$S_k^* = S_k L/\rho V_0^3 \quad (3.127a,b,c)$$

and

$$\underset{\sim}{V}^* \cdot \underset{\sim}{\nabla}^* \underset{\sim}{\varepsilon}^* = \frac{1}{Re_f} \underset{\sim}{\nabla}^* \cdot \left(\frac{\mu^*_{eff}}{\sigma_\varepsilon} \underset{\sim}{\nabla}^* \varepsilon^* \right) + S_\varepsilon^* \quad (3.128)$$

where $$S_\varepsilon^* = S_\varepsilon L^2/\rho V_0^4 \quad (3.129)$$

3.7.4C Dimensionless form of the heat transfer equation

Using dimensionless variables defined in Eqs. (3.116) and (3.119), the convective heat transfer equation for slag [Eq. (3.32)] can be written as,

$$(\underset{\sim}{V}^{*} \cdot \underset{\sim}{\nabla}^{*} T^{*}) = \frac{1}{Pe} \underset{\sim}{\nabla}^{*} \cdot K^{*}_{eff} \underset{\sim}{\nabla}^{*} T^{*} + N_T [\frac{1}{2} Re(\hat{\underset{\sim}{J}}^{*} \cdot \bar{\hat{\underset{\sim}{J}}}^{*}) - Q_d \chi\sigma / J_0^{2}] \qquad (3.130)$$

where

$$K^{*}_{eff} = \frac{K_t}{K} + 1 = \frac{\text{Effective thermal conductivity}}{\text{Molecular thermal conductivity}}$$

$$= Pr \frac{\mu_t}{\mu} + 1$$

$$= Pr (\mu^{*}_{eff} - 1) + 1 \qquad (3.131)$$

where $Pr = \frac{C_p \mu}{K}$ = Prandtl no.

$$N_T = \frac{J_o^{2}/\sigma}{\rho C_p V_o (T_{\ell,m} - T_{\ell,s})/L}$$

$$= \frac{\text{Heat generation by Joule effect}}{\text{Heat transport by convection}} \qquad (3.132)$$

$$Pe = \frac{\rho C_p V_o L}{K} = \text{Peclet no.} = Re_f \, Pr$$

$$= \frac{\text{Heat transport by convection}}{\text{Heat transport by conduction}}$$

By using the approach outlined here on Eq. (3.38), we can similarly define Peclet numbers for other portions of ESR. For example, below the slag-metal interface, we can define

$$Pe_{\ell} = \frac{\rho_{\ell} C_{p,\ell} V_{c,0}\, L}{K_{\ell}} \qquad (3.133)$$

where

$V_{c,0}$ is a reference casting rate

and

K_{ℓ} is effective thermal conductivity in metal pool.

Similarly, a group of other dimensionless parameters can be derived by considering the boundary conditions (e.g. Biot number at the ingot-mold interface).

The dimensionless parameters developed here and their physical interpretations are summarized in Table 3.2.

3.8 Concluding Remarks

A mathematical model has been formulated to describe the current distribution, fluid flow and heat transfer phenomena in the electroslag refining process. The model involves simultaneous statement of Maxwell's equations, equations for turbulent motion and convective heat transfer equations. The limitations of the model, in the form of assumptions made, are listed in section 3.3. On the positive side, the model accounts for some of the features of the ESR process which are considered

Table 3.2 Dimensionless parameters deduced from the governing equations

σ	$\omega\sigma\mu_0 L^2$	$\frac{\text{characteristic time for magnetic diffusion}}{\text{characteristic period for electric current}}$
N_1	$\mu_0 H_0^2/\rho V_0^2$	Lorentz force/Inertial force
N_2	gL/V_0^2	Gravitational force/Inertial force
N_3	$\beta g\Delta TL/V_0^2$	Buoyancy force/Inertial force
Re_f	$\rho V_0 L/\mu$	Inertial force/Viscous force ≡ Reynolds Number
N_T	$\dfrac{J_0^2/\sigma}{\rho C_p V_0 \Delta T/L}$	$\frac{\text{Heat generation rate due to Joule effect}}{\text{Heat transport rate by convection}}$
Pr	$C_p\mu/K$	Momentum diffusivity/Thermal diffusivity ≡ Prandtl number
Pe	$\rho C_p V_0 L/K$	Heat Transport by convection/Heat transport by conduction ≡ Peclet number
Pe_i	$\dfrac{\rho_i C_{p,i} V_{c,0} L}{K_i}$	Heat Transport due to movement of interface/ Heat Transport by conduction

crucial from the point of view of flow and heat transfer in the system. Thus, allowance has been made for both electromagnetic and buoyancy driving forces, for the spatial distribution of Joule heat release, for heat transport by metal droplets and for the release of latent heat in the mushy zone, etc.

Boundary conditions for the governing differential equations have been stated in section 3.6. Finally, brief discussions have been given on the general nature of the solution and the dimensionless parameters for the system.

Nomenclature

$\underset{\sim}{B}$	Magnetic flux density
C_1, C_2	Constants in $k - \varepsilon$ model
C_d	Dissipation rate constant
$C_p, C_{p,e}, C_{p,\ell}$ $C_{p,m}, C_{p,s}, C_{p,d}$	Specific heat of slag, electrode, molten metal, mushy zone, solid ingot and metal droplet
C_D	Drag coefficient
d_d	Diameter of a droplet
D	Dissipation term for turbulence kinetic energy
$\underset{\sim}{E}$	Electric field
f_s	Fraction of solids in the mushy zone
$\underset{\sim}{F}_b$	Body force (per unit volume) vector
$\underset{\sim}{F}_{be}$	Electromagnetic (Lorentz) body force vector
F_r, F_z	Radial and axial components of body force
F_{es}, F_{em}	Radiation view factors between the electrode element and slag,

Nomenclature (cont'd)

	electrode element and mold
F'_{sm}, F'_{se}	Radiation view factors between the slag surface and the mold, slag surface and the dry surface of electrode
g	Acceleration due to gravity
G	Generation term for turbulence kinetic energy
h	Heat transfer coefficient between the slag and a droplet
$h_{W,s}$	Overall heat transfer coefficient at the slag - mold interface
$h_{W,i}$	Overall heat transfer coefficients for the regions defined in equation (3.104)
$\underset{\sim}{H}, H_\theta, \hat{H}_\theta, H_0$	Magnetic field intensity, its component in the θ-direction, complex amplitude of H_θ, reference value
I_0	Amplitude of total current, also reference value for current

Nomenclature (cont'd)

j	$\sqrt{-1}$
$\tilde{J}, J_r, J_z, \hat{J}_r, \hat{J}_z$	Current density components in r- and z- direction and their complex amplitudes
$\bar{\hat{J}}$	Complex conjugate of $\hat{J}$
J_0	Reference current density
k	Kinetic energy (per unit mass) of turbulence
K, K_e, K_ℓ, K_m, K_s	Thermal conductivity of slag, electrode, molten metal (effective value), mushy zone and ingot
$K_{m\ell}$	Thermal conductivity (atomic) of molten metal
K_{eff}	Effective thermal conductivity (sum of molecular and turbulent contributions) in slag
K_t	Turbulent thermal conductivity in slag
L_1, L	Depth of slag below the electrode, characteristic length scale

Nomenclature (cont'd)

n	Normal vector
N_1	Ratio of (Lorentz force/ inertial force) Eq. (3.122)
N_2	Ratio of (Gravity force/ inertial force) Eq. (3.123)
N_T	Heat generation rate / Heat transport by convection, Eq. (3.132)
$\overline{P}, P_0$	Time - smoothed pressure, its reference value
Pe	Peclet no. for slag
Pe_ℓ	Peclet no. for metal pool
P_d	A physical property group for droplets
Pr	Prandtl no. for slag
Q_j	Rate of Joule heating (per unit volume)
Q_d	Rate of heat extraction (per unit volume) from slag by metal droplets

Nomenclature (cont'd)

Q_s	Rate of heat extraction from slag by metal droplets
r	Radial coordinate
r_d	Radius of a metal droplet
R_e	Radius of the electrode
R_m	Radius of the mold
Re_m	Magnetic Reynolds number
Re_f	Reynolds number for flow
Re_d	Droplet Reynolds number
S_T	Source term for temperature equation
S_k, S_ε	Source terms for k, ε
t	Time
$\overline{T}, T$	Temperature in the slag (time smoothed), elsewhere
T_a	Temperature of gas above the slag surface
T_B	Bulk temperature of the slag in the region $0 \leq r \leq R_e$

Nomenclature (cont'd)

T_f	Final temperature attained by a droplet
T_d	Temperature of a droplet
$T_{\ell,m}$	Liquidus temperature of the metal
$T_{\ell,s}$	Melting temperature of the slag
$T_{m,e}$	Melting temperature of electrode
$T_{s,m}$	Solidus temperature of the metal
T_W	Temperature of the cooling water
$T_{s,av}$	Average temperature of the slag surface
$T_{e,av}$	Average temperature of the dry electrode surface
U	Velocity of a metal droplet
U_{av}	Average velocity of a droplet
U_t	Terminal velocity of a droplet
$V_c, V_{c,0}$	Casting rate, its reference value
V_t	Rate of travel of electrode
$\bar{\underset{\sim}{V}}, V_0$	Time-smoothed velocity vector, its reference value

Nomenclature (cont'd)

$\overline{V}_r, \overline{V}_z$	Radial and axial components of velocity vector
W	Input power
We	Weber no.
X	Variable defined in Eq. (3.67)
Y	Variable defined in Eq. (3.66)
z	Axial coordinate
Z_1, Z_2, Z_3, Z_6	Position of free slag surface, melting tip of electrode, slag-metal interface, lower boundary of ingot

GREEK SYMBOLS

α	Characteristic time for magnetic diffusion / Characteristic period for electric current
β	Coefficient of thermal expansion of slag
γ	Interfacial tension between liquid metal and liquid slag
δ	Stefan - Boltzmann constant

Nomenclature (cont'd)

GREEK SYMBOLS

ε	Dissipation rate of turbulence energy
$\varepsilon_e, \varepsilon_s, \varepsilon_m$	Emissivity of electrode, slag, mold
ξ	θ - component of the vorticity vector
η	Magnetic diffusivity
λ	Latent heat of fusion of metal
Λ	Defined by Eq. (3.44)
μ	Viscosity of slag
μ_0	Magnetic permeability of free space
μ_{eff}	Effective viscosity of slag
ψ	Stream function
$\rho, \rho_e, \rho_\ell, \rho_m, \rho_s, \rho_d$	Density of slag, electrode, metal pool, mushy zone, solid ingot and droplet
$\sigma, \sigma_e, \sigma_m$	Electrical conductivity of slag, elctrode and metal

Nomenclature (cont'd)

GREEK SYMBOLS

$\sigma_k, \sigma_\varepsilon$	Prandtl number for k, ε
σ_t	Turbulence Prandtl number
$\bar{\tau}$	Sum of viscous and Reynolds stresses
τ	Residence time of a droplet
ω	Angular frequency of current
χ	Defined by Eqs. (3.34a,b)

Superscript

*	Dimensionless quantities

CHAPTER IV

NUMERICAL SOLUTION OF GOVERNING EQUATIONS

This chapter presents an outline of the numerical technique used for solving the differential equations developed in the previous chapter. After discussing the derivation of finite difference equations for the dependent variables, a brief treatment on the use of wall functions for representing heat and momentum transfer in the near wall regions is presented. The computational scheme and the computer program are discussed at the end of the chapter.

4.1 Summary of Governing Equations and Boundary Conditions

4.1.1 Equations for magnetic field

Let $\hat{H}_{\theta R}$ and $\hat{H}_{\theta I}$ denote the real and imaginary parts of $\hat{H}_{\theta}$ respectively, then Eq. (3.13) can be decomposed to give:

$$\frac{\partial}{\partial r}\left(\frac{1}{r}\frac{\partial}{\partial r}(r\hat{H}_{\theta R})\right) + \frac{\partial^2 \hat{H}_{\theta R}}{\partial z^2} = -\sigma\mu_0\omega\hat{H}_{\theta I} \qquad (4.1)$$

and

$$\frac{\partial}{\partial r}\left(\frac{1}{r}\frac{\partial}{\partial r}(r\hat{H}_{\theta I})\right) + \frac{\partial^2 \hat{H}_{\theta I}}{\partial z^2} = \sigma\mu_0\omega\hat{H}_{\theta R} \qquad (4.2)$$

It should be noted that,

$$|\hat{H}_{\theta}| = \left(\hat{H}^2_{\theta R} + \hat{H}^2_{\theta I}\right)^{1/2}$$

and that the phase angle

$$\beta_H = \tan^{-1}\left(\hat{H}_{\theta I}/\hat{H}_{\theta R} \right) \tag{4.3a,b}$$

Similarly from Eq. (3.14a,b) one can write;

$$\hat{J}_{rR} = \mathrm{Re}(\hat{J}_r) = -\frac{\partial \hat{H}_{\theta R}}{\partial z}$$

$$\hat{J}_{rI} = \mathrm{Im}(\hat{J}_r) = -\frac{\partial \hat{H}_{\theta I}}{\partial z}$$

$$|\hat{J}_r| = \left(\hat{J}_{zR}^{\,2} + \hat{J}_{zI}^{\,2} \right)^{1/2} \tag{4.4a,b,c}$$

and

$$\hat{J}_{zR} = \mathrm{Re}(\hat{J}_z) = \frac{1}{r}\frac{\partial}{\partial r}(r\hat{H}_{\theta R})$$

$$\hat{J}_{zI} = \mathrm{Im}(\hat{J}_z) = \frac{1}{r}\frac{\partial}{\partial r}(r\hat{H}_{\theta I})$$

$$|\hat{J}_z| = \left(\hat{J}_{zR}^{\,2} + \hat{J}_{zI}^{\,2} \right)^{1/2} \tag{4.5a,b,c}$$

4.1.2 Equations for fluid flow and heat transfer

Eqs. (3.24), (3.27), (3.30), (3.37), (3.39a,b,c,d) constitute the mathematical statement of the fluid flow and heat transfer phenomena in the system. These equations can be represented by the following general elliptic partial differential equation:

$$a_{1\phi} r\frac{\partial \phi}{\partial z} + a_\phi\left(\frac{\partial}{\partial z}\left(\phi\frac{\partial \psi}{\partial r}\right) - \frac{\partial}{\partial r}\left(\phi\frac{\partial \psi}{\partial z}\right) \right) - \frac{\partial}{\partial z}\left(b_\phi r \frac{\partial (c_\phi \phi)}{\partial z} \right) -$$

$$\frac{\partial}{\partial r}\left(b_\phi r \frac{\partial(c_\phi \phi)}{\partial r} \right) - rS_\phi = 0 \qquad (4.6)$$

where ϕ stands for the dependent variables $(\frac{\xi}{r}, \psi, k, \varepsilon, T)$. Values of the coefficients $a_{1\phi}, a_\phi$, b_ϕ, c_ϕ and the source term S_ϕ are listed in table 4.1.

4.1.3 Boundary conditions

Boundary conditions for the magnetic field intensity, $\hat{H}_\theta$ are stated in Fig. 4.1. Boundary conditions for fluid flow variables (i.e. $\frac{\xi}{r}, \psi, k$ and ε) are summarized in Fig. 4.2 and finally, boundary conditions for temperature are given in Fig. 4.3. In these figures the symbols e, sℓ, ℓ, m, s stand for electode, slag, metal pool, mushy zone, and solid ingot respectively.

4.2 Derivation of the Finite - Difference Equations

In this section, transformation of differential equations listed in section 4.1 to finite - difference forms is presented. This transformation involves the following steps:

1) The domain of integration is represented by a two dimensional (r,z) array of points called a grid.

2) A set of algebraic equations is derived, from the differential equations and the boundary conditions, which connect the values of the dependent variables at the grid nodes (points of intersection of grid lines)

Table 4.1 Summary of governing differential equations in cylindrical coordinate system

ϕ	$a_{1\phi}$	a_ϕ	b_ϕ	c_ϕ	S_ϕ
$\frac{\xi}{r}$	o	r^2	r^2	μ_{eff}	$\mu_o Re(\hat{H}_\Theta \bar{J}_r) + r\rho\beta g(\frac{\partial T}{\partial r})$
ψ	o	o	$\frac{1}{\rho r^2}$	1	$\frac{\xi}{r}$
k	o	1	μ_{eff}/σ_k	1	S_k [Eqs(3·28).(3·29a.b)]
ε	o	1	$\mu_{eff}/\sigma_\varepsilon$	1	S_ε [Eqs(3·29a).(3·31)]
T	$\rho C_p V_c$	c_p	K_{eff}	1	$Q_j - Q_d X$
	$\rho_e C_{p,e} V_e$	o	K_e	1	o
	$\rho_\ell C_{p,\ell} V_c$	o	K_ℓ	1	o
	$\rho_m C_{p,m} V_c$	o	K_m	1	$-V_c \rho_m \lambda / (T_{\ell,m} - T_{s,m}) \frac{\partial T}{\partial Z}$
	$\rho_s C_{p,s} V_c$	o	K_s	1	o

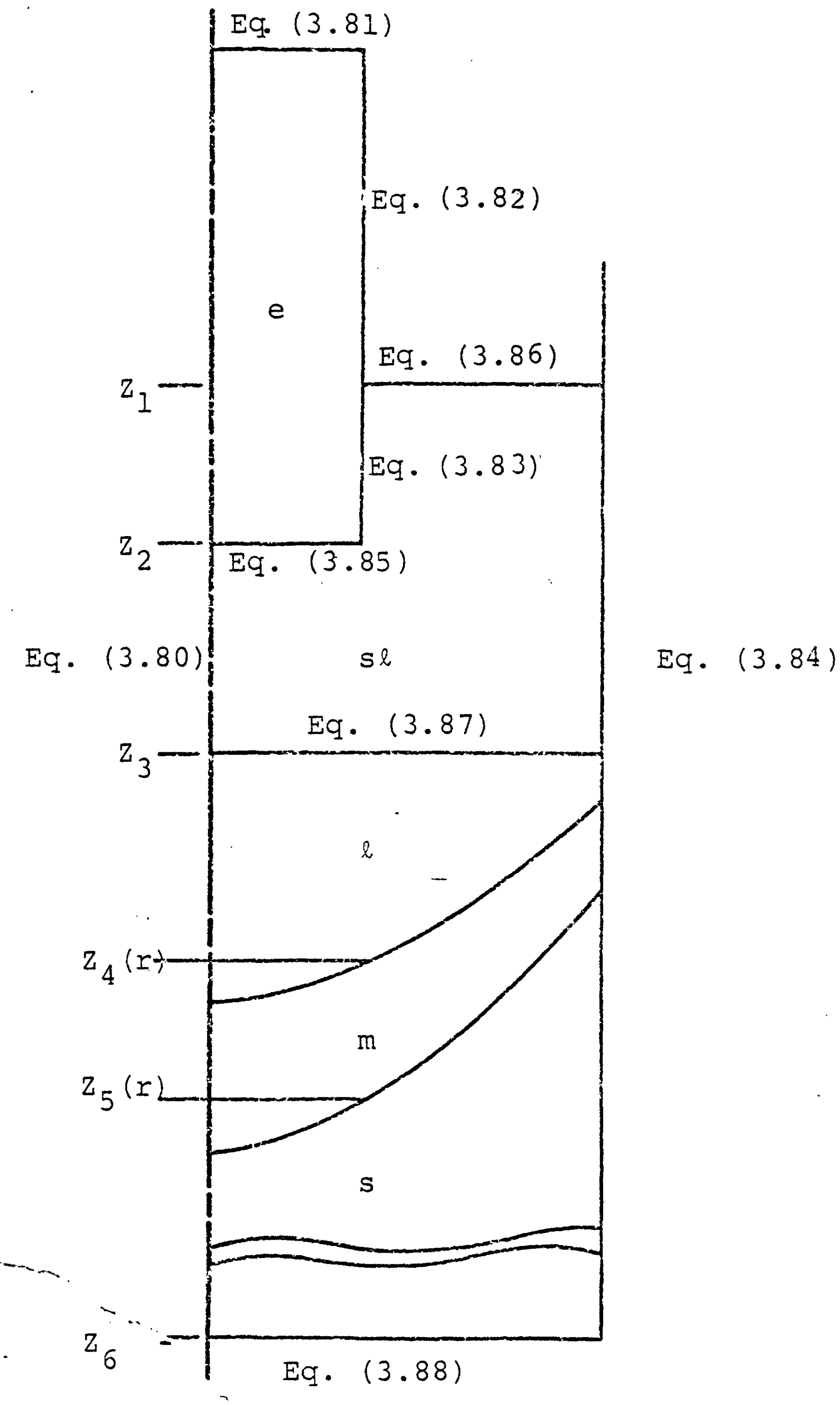

4.1 Boundary conditions for the magnetic field intensity.

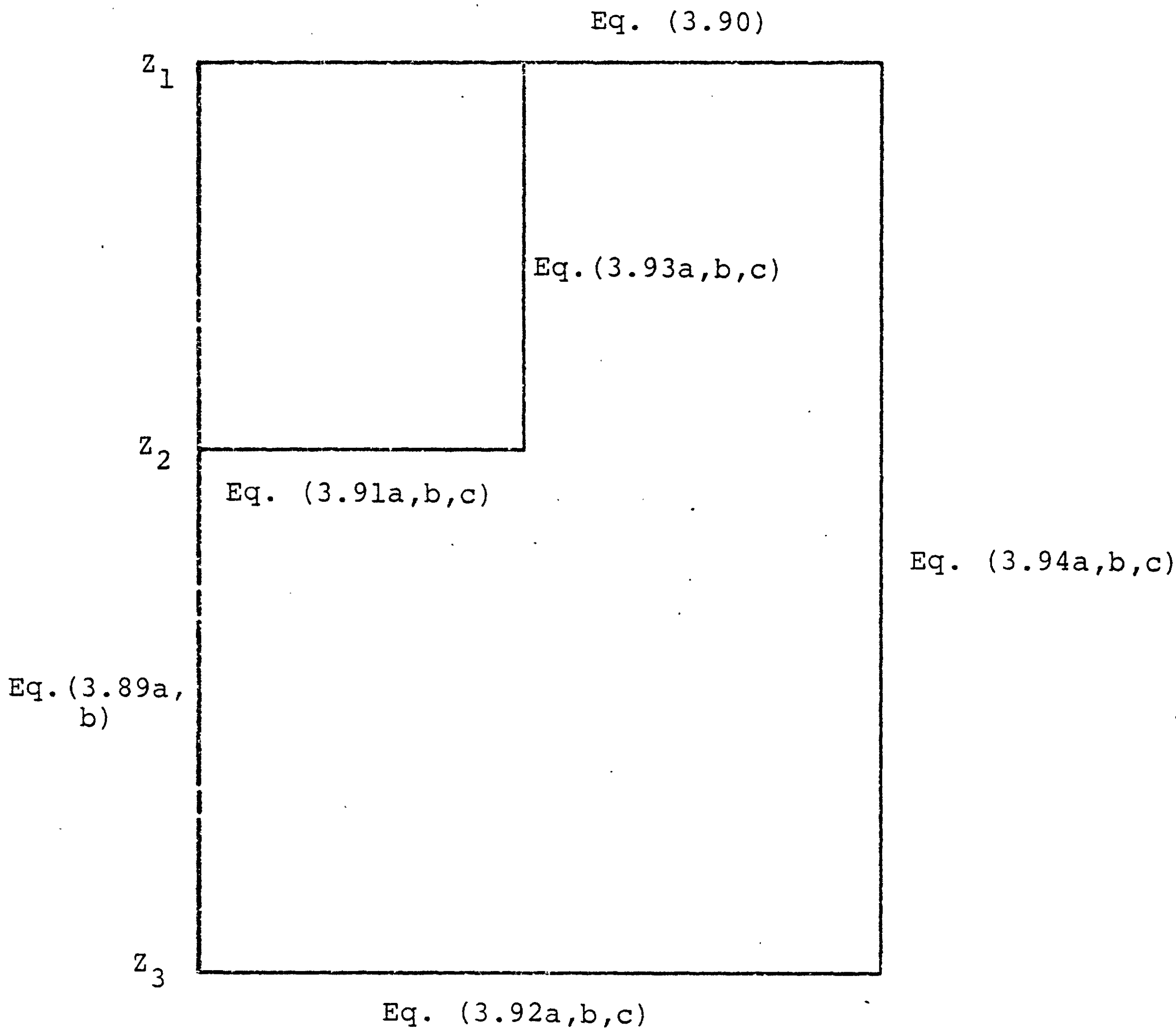

Fig. 4.2 Boundary conditions for fluid flow variables.

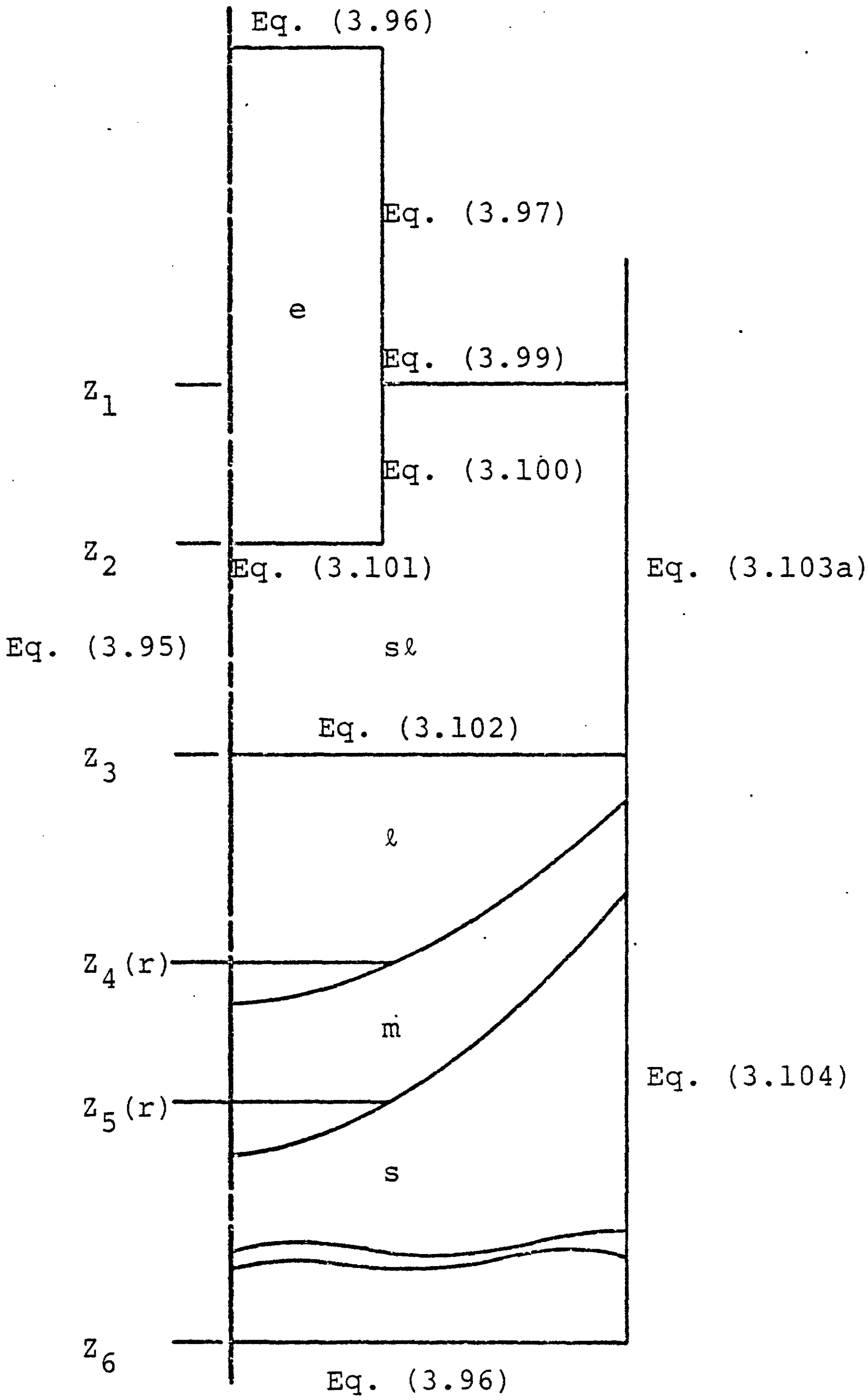

Fig. 4.3 Boundary conditions for temperature.

with each other and with other quantities.

4.2.1 Expressions for interior nodes

Fig. 4.4 shows a part of the orthogonal grid; with a typical node P and the surrounding nodes E,NE,N,NW,W,SW, SE. The neighboring nodes need not be equally spaced. The finite - difference equations are derived by using the technique described by Gosman et al [39]. A brief outline of this technique is presented with respect to the general elliptic equation [Eq. (4.6)]. The derivation of finite difference equations for the magnetic field intensity $(\hat{H}_{\theta R},\hat{H}_{\theta I})$ is analogous and only the final results will be given.

Let us proceed by integrating Eq. (4.6) over the area enclosed by the small rectangle, shown by the dotted lines in Fig. 4.4, which encloses the point P. The sides of this rectangle lie midway between the neighbouring grid lines. The double integral to be evaluated is

$$\underbrace{\int_{r_s}^{r_n}\int_{z_w}^{z_e}\left[a_{1\phi} r\,\frac{\partial\phi}{\partial z} + a_\phi\left(\frac{\partial}{\partial z}\left(\phi\frac{\partial\psi}{\partial r}\right) - \frac{\partial}{\partial r}\left(\phi\frac{\partial\psi}{\partial z}\right)\right)\right] dr\,dz}_{\text{convection terms}}$$

$$\underbrace{-\int_{r_s}^{r_n}\int_{z_w}^{z_e}\left[\frac{\partial}{\partial z}\left(b_\phi r\frac{\partial(c_\phi\phi)}{\partial z}\right) + \frac{\partial}{\partial r}\left(b_\phi r\frac{\partial(c_\phi\phi)}{\partial r}\right)\right] dr\,dz}_{\text{diffusion terms}}$$

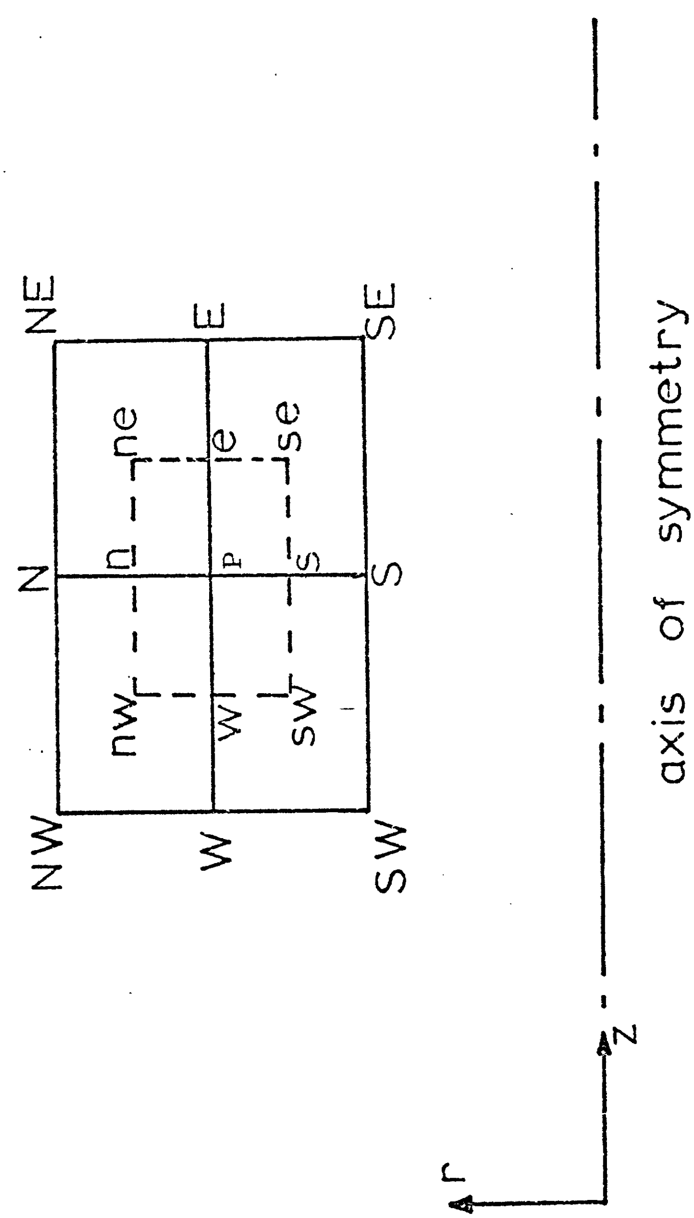

4.4 A portion of the finite-difference grid.

$$- \int_{r_s}^{r_n} \int_{z_w}^{z_e} rS_\phi \, dr \, dz = 0 \tag{4.7}$$

——source term—/

Following the details given by Gosman et al [39] and after some algebraic manipulation, we obtain the following successive substitution formula for ϕ which is valid for any interior point P in the integration field:

$$\phi_P = \frac{\sum\limits_{j=N,S,E,W} \left\{ \left[A_j' + c_{\phi,j}(b_{\phi,j} + b_{\phi,P}) B_j' \right] \phi_j \right\} + S_{\phi,P}}{\sum\limits_{j=N,S,E,W} \left\{ A_j' + c_{\phi,P}(b_{\phi,j} + b_{\phi,P}) B_j' \right\}} \tag{4.8}$$

where

$$A_j' = (A_j + A_{1j})/V_P \tag{4.9}$$

$$B_j' = B_j / \{ V_P (b_{\phi,j} + b_{\phi,P}) \} \tag{4.10}$$

with

$$A_E = \frac{a_{\phi,P}}{8}\left((\psi_{SE}+\psi_S-\psi_{NE}-\psi_N) + |\psi_{SE}+\psi_S-\psi_{NE}-\psi_N| \right)$$

$$A_W = \frac{a_{\phi,P}}{8}\left((\psi_{NW}+\psi_N-\psi_{SW}-\psi_S) + |\psi_{NW}+\psi_N-\psi_{SW}-\psi_S| \right)$$

$$A_N = \frac{a_{\phi,P}}{8}\left((\psi_{NE}+\psi_E-\psi_{NW}-\psi_W) + |\psi_{NE}+\psi_E-\psi_{NW}-\psi_W| \right)$$

$$A_S = \frac{a_{\phi,P}}{8}\left((\psi_{SW}+\psi_W-\psi_{SE}-\psi_E) + |\psi_{SW}+\psi_W-\psi_{SE}-\psi_E| \right)$$

(4.11a,b,c,d)

$$A_{1E} = -\frac{1}{4}a_{1\phi,P}(r_N - r_S) \tag{4.12a}$$

$$A_{1W} = \frac{1}{4}a_{1\phi,P}(r_N - r_S) \tag{4.12b}$$

$$A_{1N} = 0 \tag{4.12c}$$

$$A_{1S} = 0 \tag{4.12d}$$

$$B_E = \frac{b_{\phi,E} + b_{\phi,P}}{8} \frac{r_N - r_S}{z_E - z_P}(r_E + r_P) \tag{4.13a}$$

$$B_W = \frac{b_{\phi,W} + b_{\phi,P}}{8} \frac{r_N - r_S}{z_P - z_W}(r_W + r_P) \tag{4.13b}$$

$$B_N = \frac{b_{\phi,N} + b_{\phi,P}}{8} \frac{z_E - z_W}{r_N - r_P}(r_N + r_P) \tag{4.13c}$$

$$B_S = \frac{b_{\phi,S} + b_{\phi,P}}{8} \frac{z_E - z_W}{r_P - r_S}(r_S + r_P) \tag{4.13d}$$

and

$$V_P = \frac{1}{4}(z_E - z_W)(r_N - r_S)r_P \tag{4.14}$$

The form of the convection coefficients A_{js}, as given by Eqs. (4.11a,b,c,d) arises because of the "upwind differencing" used in representing the convection terms in Eq. (4.7).

Similarly Eqs. (4.1) and (4.2) can be integrated over the area enclosed by the rectangle sw,se,ne,nw in Fig. 4.4 and the two resulting algebraic equations can be solved to give the following expressions for $\hat{H}_{\theta R}$ and $\hat{H}_{\theta I}$ at any interior node P,

$$\hat{H}_{\theta R,P} = \sum_{j=N,S,E,W} \left\{ D_1\left(\frac{r_j}{r_p} D_j \hat{H}_{\theta R,j}\right) + D_2\left(\frac{r_j}{r_p} D_j \hat{H}_{\theta I,j}\right)\right\} \tag{4.15}$$

$$\hat{H}_{\theta I,P} = \sum_{j=N,S,E,W} \left\{ D_1\left(\frac{r_j}{r_p} D_j \hat{H}_{\theta I,j}\right) - D_2\left(\frac{r_j}{r_p} D_j \hat{H}_{\theta R,j}\right)\right\} \tag{4.16}$$

where

$$D_1 = \frac{S_1}{S_1^2 + S_2^2} \tag{4.17}$$

$$D_2 = \frac{S_2}{S_1^2 + S_2^2} \tag{4.18}$$

$$S_1 = \sum_{j=N,S,E,W} D_j \tag{4.19}$$

$$S_2 = 0.5\, \mu_0\, \omega \sigma_P \tag{4.20}$$

with

$$D_N = \frac{2r_P}{r_N + r_P} \cdot \frac{1}{(r_N - r_P)(r_N - r_S)}$$

$$D_S = \frac{2r_P}{r_S + r_P} \cdot \frac{1}{(r_P - r_S)(r_N - r_S)}$$

$$D_E = \frac{1}{(z_E - z_P)} \cdot \frac{1}{(z_E - z_W)}$$

$$D_W = \frac{1}{(z_P - z_W)} \cdot \frac{1}{(z_E - z_W)} \qquad (4.21a,b,c,d)$$

4.2.2 Expressions for boundary nodes

The successive substitution formulae given by Eqs. (4.15), (4.16) and (4.8) are valid for interior nodes. At the boundary nodes, the substitution relationships have to be derived using the boundary conditions shown in Fig. 4.1, 4.2 and 4.3. These boundary conditions are of the following general types:

(1) $\phi = \alpha_1$

i.e. the value of the variable at the boundary is a specified constant. For example, w.r.t. Fig. 4.1,

$$\hat{H}_\theta = 0 \qquad (\text{ at } r = 0,\ 0 \leq z \leq Z_6)$$

$$\hat{H}_\theta = \frac{I_0}{2\pi R_e} \qquad (\text{ at } r = R_e,\ 0 \leq z \leq Z_1) \qquad \text{etc.}$$

similarly w.r.t. Fig. 4.2

$$\psi = k = \varepsilon = 0 \qquad \text{at all rigid boundaries}$$

and w.r.t. Fig. 4.3

$$T = T_{m,e} \quad \text{at } z = Z_2,\ 0 \leq r \leq R_e$$

$$T = T_{\ell,s} \quad \text{at } r = R_m,\ Z_1 \leq z \leq Z_3$$

(2) $f(\underline{\phi}_i) = 0$

i.e. a functional relationship is specified among the dependent variables. The functional relationship f is such that it is possible to solve explicitly for a variable ϕ_j at the boundary node in terms of variables at the same and adjacent nodes. For example, w.r.t. Fig. 4.2

$$\left(\frac{\xi}{r}\right)_0 = \frac{3(\psi_0 - \psi_1)}{\rho r^2 (Z_1 - Z_0)^2} - \frac{1}{2}\left(\frac{\xi}{r}\right)_1 \quad \text{at } z = Z_3, 0 \leq r \leq R_m$$

where suffixes 0 and 1 refer to a grid node on the boundary and to the adjacent node in the z - direction, respectively.

(3) $p \dfrac{\partial\phi}{\partial n} + qF(\phi) = 0$

where $\frac{\partial\phi}{\partial n}$ is the gradient, normal to the boundary surface. These boundary conditions contain statements for the flux, normal to the bounding surfaces. For example, the symmetry boundary conditions, i.e.

$$\frac{\partial k}{\partial r} = \frac{\partial \varepsilon}{\partial r} = \frac{\partial T}{\partial r} = 0 \quad (p = 1 , q = 0)$$

fall in this class.

Other examples are (w.r.t. Fig. 4.3)

$$K \left.\frac{\partial T}{\partial r}\right|_i + h_{W,i}(T - T_W) = 0 \qquad \left(p = K_i, q = h_{W,i}, F(T) = T - T_W\right)$$

at $r = R_m$, $Z_3 \leq z \leq Z_6$

$$K_{eff} \left.\frac{\partial T}{\partial z}\right|_{sl} - \delta\varepsilon_s \left[T_{s,av}^4 - \varepsilon_m F'_{sm} T_m^4 - \varepsilon_e F'_{se} T_{e,av}^4 \right] = 0$$

at $z = Z_1$, $R_e \leq r \leq R_m$

$$(4) \quad p_1 \left.\frac{\partial \phi}{\partial n}\right|_1 + u = p_2 \left.\frac{\partial \phi}{\partial n}\right|_2$$

i.e. continuity of fluxes (or electric field) across an interface between media 1 and 2. For example, w.r.t. Fig. 4.1

$$\frac{1}{\sigma} \left.\frac{\partial \hat{H}_\theta}{\partial z}\right|_e = \frac{1}{\sigma} \left.\frac{\partial \hat{H}_\theta}{\partial z}\right|_{sl} \quad \text{at } z = Z_2,\ 0 \leq r \leq R_e$$

and

$$-K_{eff} \left.\frac{\partial T}{\partial z}\right|_{sl} + \frac{Q_S}{\pi R_e^2} \chi = - K_\ell \left.\frac{\partial T}{\partial z}\right|_\ell$$

at $z = Z_3$, $0 \leq r \leq R_m$

Boundary conditions of type 1 are specified, once and for all, at the beginning of the computation. The rest of the boundary conditions need updating after every iteration. Boundary conditions (3) and (4) involve calculating first order derivatives in a direction normal to the boundary. The calculation is illustrated below:

With reference to Fig. 4.5, let us suppose that AA' represents a boundary surface and that we wish to evaluate $\frac{\partial \phi}{\partial n}$ at node 0. Let 1 and 2 be adjacent nodes in the direction normal to AA' and that $01 = n_1$ and $02 = n_2$. Let us denote the values of ϕ at nodes 0,1, and 2 by ϕ_0, ϕ_1, and ϕ_2 respectively. Assuming a quadratic profile for ϕ we can write

$$\phi = \phi_0 + an + bn^2 \tag{4.22}$$

Then,

$$\phi_1 = \phi_0 + an_1 + bn_1^2 \tag{4.23}$$

and

$$\phi_2 = \phi_0 + an_2 + bn_2^2 \qquad (4.24$$

From Eqs. (4.23) and (4.24) we get,

$$\left.\frac{\partial\phi}{\partial n}\right|_0 = a = \frac{n_2^2(\phi_1 - \phi_0) - n_1^2(\phi_2 - \phi_0)}{(n_2 - n_1)n_1 n_2} \tag{4.25}$$

For the case when $\left.\frac{\partial\phi}{\partial n}\right|_0 = 0$ (e.g. symmetry, free surface boundary conditions for k,ε) we get,

$$\phi_0 = \left(\frac{n_2^2}{n_2^2 - n_1^2}\right)\phi_1 - \left(\frac{n_1^2}{n_2^2 - n_1^2}\right)\phi_2 \tag{4.26}$$

To illustrate let us consider the boundary condition for the energy equation at the free slag surface, i.e.

$$K_{eff}\left.\frac{\partial T}{\partial z}\right|_{sl} = \delta\varepsilon_S\left[T_{s,av}^4 - \varepsilon_m F'_{sm} T_m^4 - \varepsilon_e F'_{se} T_{e,av}^4\right] \tag{3.99}$$

By using Eq. (4.25) we get,

$$\left.\frac{\partial T}{\partial z}\right|_0 = \frac{n_2^2(T_1 - T_0) - n_1^2(T_2 - T_0)}{(n_2 - n_1)n_1 n_2}$$

$$= \frac{n_2^2 T_1 - n_1^2 T_2 - (n_2^2 - n_1^2)T_0}{(n_2 - n_1)n_1 n_2} \qquad (4.27)$$

Putting this in Eq. (3.99) gives,

$$T_0 = \frac{n_2^2}{n_2^2 - n_1^2} T_1 - \frac{n_1^2}{n_2^2 - n_1^2} T_2 - \frac{n_1 n_2}{n_1 + n_2} \delta \varepsilon_S \left[T_{s,av}^4 - \varepsilon_m F'_{sm} T_m^4 - \varepsilon_e F'_{se} T_{e,av}^4 \right] \qquad (4.28)$$

Thus at the end of an iteration, temperature at a node lying on the free surface of the slag can be updated using the above equation.

4.3 Wall Function Approach

One of the assumptions inherent in deriving the successive substitution formulae [Eq. (4.8)] is that the transport properties of the fluid vary so little between grid points that its value at a point such as e in Fig. 4.4 can be given by the arithmetic mean of the values at P and E. Thus,

$$b_{\phi,e} \simeq \frac{b_{\phi,P} + b_{\phi,E}}{2} \qquad (4.29)$$

It is known however that steep gradients of transport properties occur near the walls which bound a turbulent stream. In the immediate vicinity of the wall, the fluid

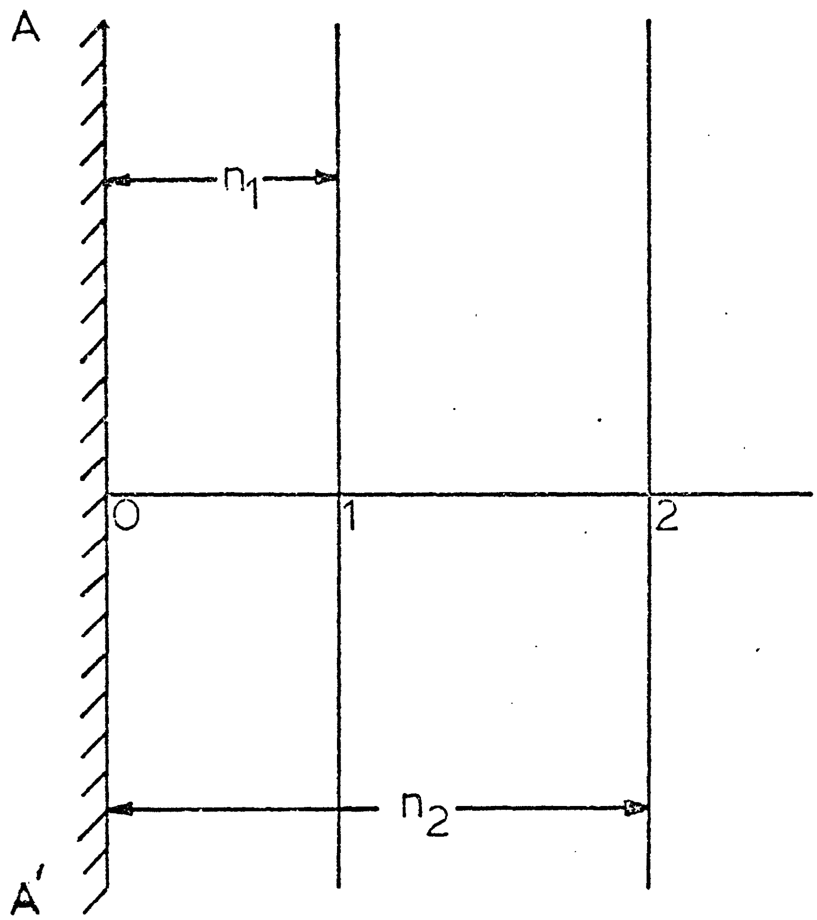

4.5 Illustration for calculating first order derivatives at boundaries.

is in laminar motion and the effective viscosity and thermal conductivity are very much lower than they are at even a short distance from the wall. The behaviour of the near wall region can be modelled either by using the low Reynolds number modelling method or by using the wall function method [46]. The latter method has been used more widely. It economizes computer time and storage and allows the introduction of additional empirical information in special cases, as when the wall is rough.

A brief treatment of wall function method for turbulence quantities (k and ε) and for heat transfer in the slag is given here. Fig. 4.6 shows the regions in the slag where wall function method has to be used. These regions which lie in the vicinity of various rigid walls are indicated by inclined lines and numbers 1, 2, 3, 4. Let us now illustrate the use of wall function approach w.r.t region 1 in Fig. 4.6. A portion of the grid in this region is shown in Fig. 4.7.

Let us assume that region 1 represents a constant shear layer with the value of shear stress being equal to τ_W. Let n represent distance from the wall, in the direction normal to the wall. Velocity distribution for this region can be written in terms of a "logarithmic law" [55]

$$V_+ = \frac{1}{\kappa} \ell n \, (E \, n^+) \qquad (4.30)$$

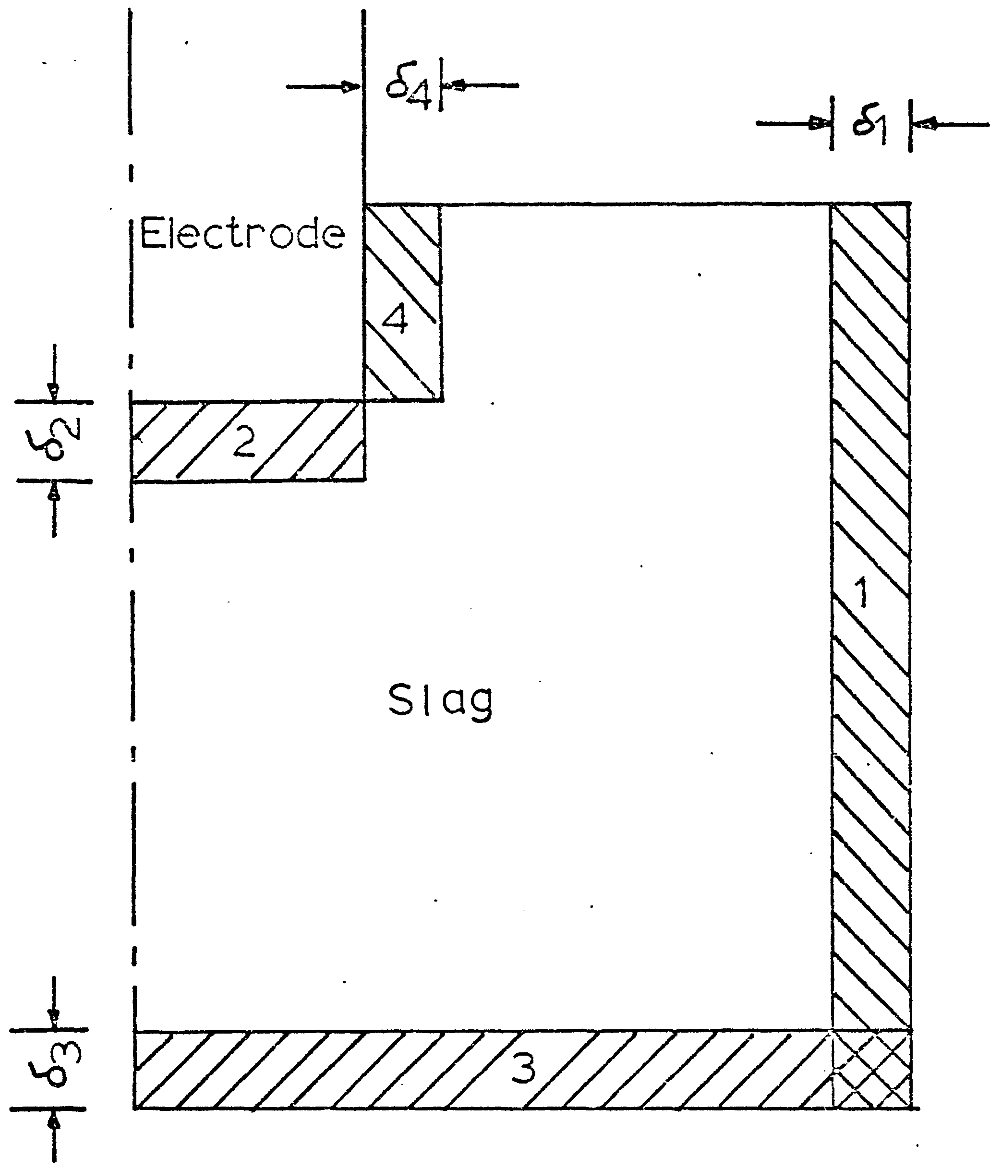

4.6 Domains for wall function method.

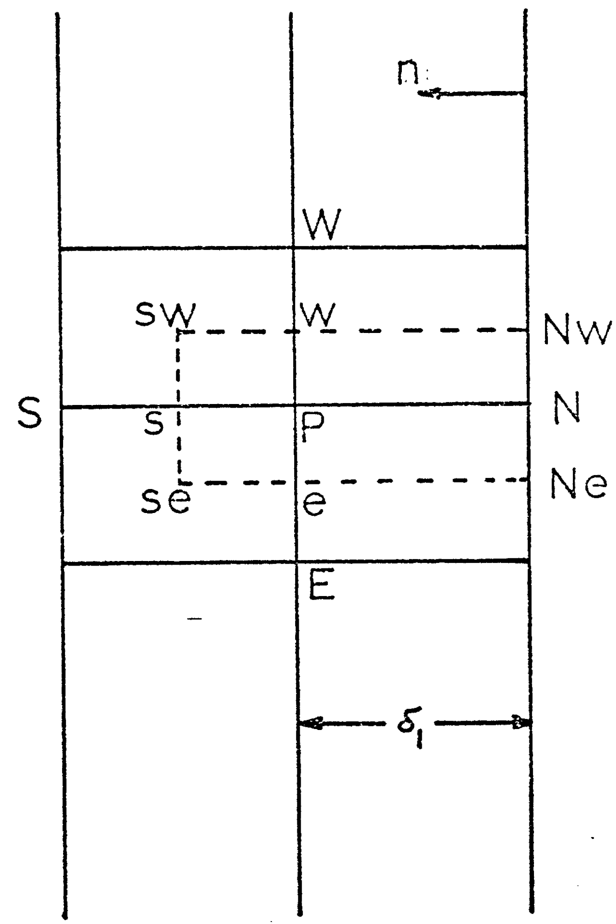

4.7 Illustration for wall function approach.

where κ = von Karman's constant = 0.4

E = a function of wall roughness, approximately equal to 9 for a smooth wall

$V_+ = V/V_\tau$ = dimensionless velocity parallel to wall (z-direction for Fig. 4.7)

V_τ = friction velocity = $\tau_W/(\rho C_d^{1/4} k^{1/2})$

$$n^+ = \rho \frac{nV_\tau}{\mu} = C_d^{1/4} \rho \, k^{1/2} n/\mu$$

= dimensionless distance from the wall.

For Eq. (4.30) to be valid, n^+ should be much larger than unity. For turbulent flow in a pipe, Pun and Spalding [55] suggest that $n^+ \geq 11.5$. Under these conditions, τ_W can be evaluated by using the following relationship [55],

$$\tau_W = \kappa C_d^{1/4} \rho \, V_p \, k_p^{1/2} / \ln \left[E \rho \delta_1 \, k_p^{1/2} \, C_d^{1/4}/\mu\right] \qquad (4.31)$$

The source term for the turbulence kinetic energy, S_k can be written as

$$S_k = G - D \qquad (3.28)$$

$$= \tau_W \frac{\partial V}{\partial n} - \frac{C_d \rho^2 k^2}{\mu_t} \qquad (4.32a)$$

$$= \tau_W \frac{\partial V}{\partial n} - \frac{C_d \rho^2 k^2}{\tau_W} \frac{\partial V}{\partial n} \tag{4.32b}$$

Near a wall, length scale of turbulence is porportional to distance from the wall and one can write [55]

$$\varepsilon_p = C_d^{3/4} k_p^{3/2} / (\kappa \delta_1) \tag{4.33}$$

Let us now discuss wall function for the transfer of heat. By using the analogy between heat and momentum transfer, it can be shown [56] that the local Nusselt number Nu_x can be given by a relationship of the following type*:

$$Nu_x = \frac{1/2 C_f' \, Re_x \, \sigma_\ell}{\sigma_t \{1 + \sqrt{1/2 \, C_f'} \, (\sigma_\ell / \sigma_t - 1) \, a\}} \tag{4.34}$$

where Re_x is the local Reynolds number

σ_ℓ is the Prandtl number of the fluid

σ_t is the turbulence Prandtl number

C_f' is the coefficient of skin friction defined as $1/2 C_f' = \tau_W / \rho V^2$

and 'a' is a parameter which makes an allowance for the transfer of heat through the viscous sublayer and depends on the ratio σ_ℓ / σ_t.

---

*Eq. (4.34) is valid in the absence of viscous dissipation or any other source of heat and for a constant wall temperature.

The final expression for the local flux of heat through the wall shown in Fig. 4.7 can be written as [55]:

$$-\frac{q_s}{\rho C_p V_p (T_p - T_N)} = \frac{\tau_w/\rho V_p^2}{\sigma_t \{1 + P\sqrt{\tau_W/\rho V_p^2}\}} \qquad (4.36)$$

with $$P = 9\,(\sigma_\ell/\sigma_t - 1)\,(\sigma_\ell/\sigma_t)^{-1/4} \qquad (4.37)$$

The differential equation (4.6) is integrated over the area enclosed by the rectangle sw, se, Ne, Nw in Fig. 4.7. In the case of turbulence kinetic energy, diffusion through the wall is set equal to zero and source term is given by Eq. (4.32b). Dissipation rate of turbulence energy, ε_p is calculated by using Eq. (4.33). In the case of energy equation, heat flux through the wall is replaced by Eq. (4.36).

4.4 Solution Procedure

The governing differential equations and their boundary conditions have now been converted into a set of algebraic equations. These equations will now have to be solved by an iterative technique. The solution procedure used in this work is the Gauss-Seidel method and uses successive substitution as compared to the "block-methods" which use matrix inversion techniques. Among the point methods, the Gauss-Seidel method is known to yield rapid convergence and is efficient from the view point of computer storage [39]. In the following subsections, the computational flowsheet will be provided together with a description of the computer program.

4.4.1 Flowsheet for computation

The equations for magnetic field intensity [Eqs. (4.1), (4.2)] are first solved to calculate the electromagnetic driving forces and the spatial distribution of the Joule heating rate. This involves using Eqs. (4.15) and (4.16) to update the values of $\hat{H}_{\theta R}$ and $\hat{H}_{\theta I}$ at the interior nodes and to use algebraic equivalent of boundary conditions to update the values at the boundary nodes. After convergence is obtained, the spatial distribution of current densities and the volumetric Joule heating rate are calculated using Eqs. (3.14 a,b) and (3.16). Next, the dependent variables for flow and heat transfer $\frac{\varepsilon}{r}$, ψ, k, ε, and T are taken up in the order indicated here. The procedure adopted can be summarized as follows:

(1) Each cycle of the iterative procedure is made up of IV subcycles where IV is the number of dependent variables.

(2) In each sub-cycle the domain of integration is scanned row by row and a single variable is updated. If the node being considered is an interior node, Eq. (4.8) is used; otherwise, the appropriate substitutional formula for the boundary node is used.

(3) When all of the sub-cycles have been completed, a new iteration cycle is commenced.

(4) The procedure is repeated until the changes in the values of the variables between successive iterations are less than a small specified quantity.

A simplified conceptual flow chart of the computational scheme is shown in Fig. 4.8.

4.4.2 Introduction to computer program

In this subsection a brief description of the computer program is given. The program was developed by following the outlines of the basic computer program published by Gosman et al [39]. However, extensive modifications and additions had to be made to tailor it for the present purposes. The program is subdivided into a number of subroutines, each one designed to perform a specific task. The listing of the computer program is given in Appendix E. The main features of this program are outlined in Table 4.2 which gives the names and the functions of various subroutines.

4.4.3 Stability and convergence problems

The search for a solution to the mathematical problem posed in Chapter III is based on the premise that the model describes the physics of the system adequately and that the set of differential equations together with

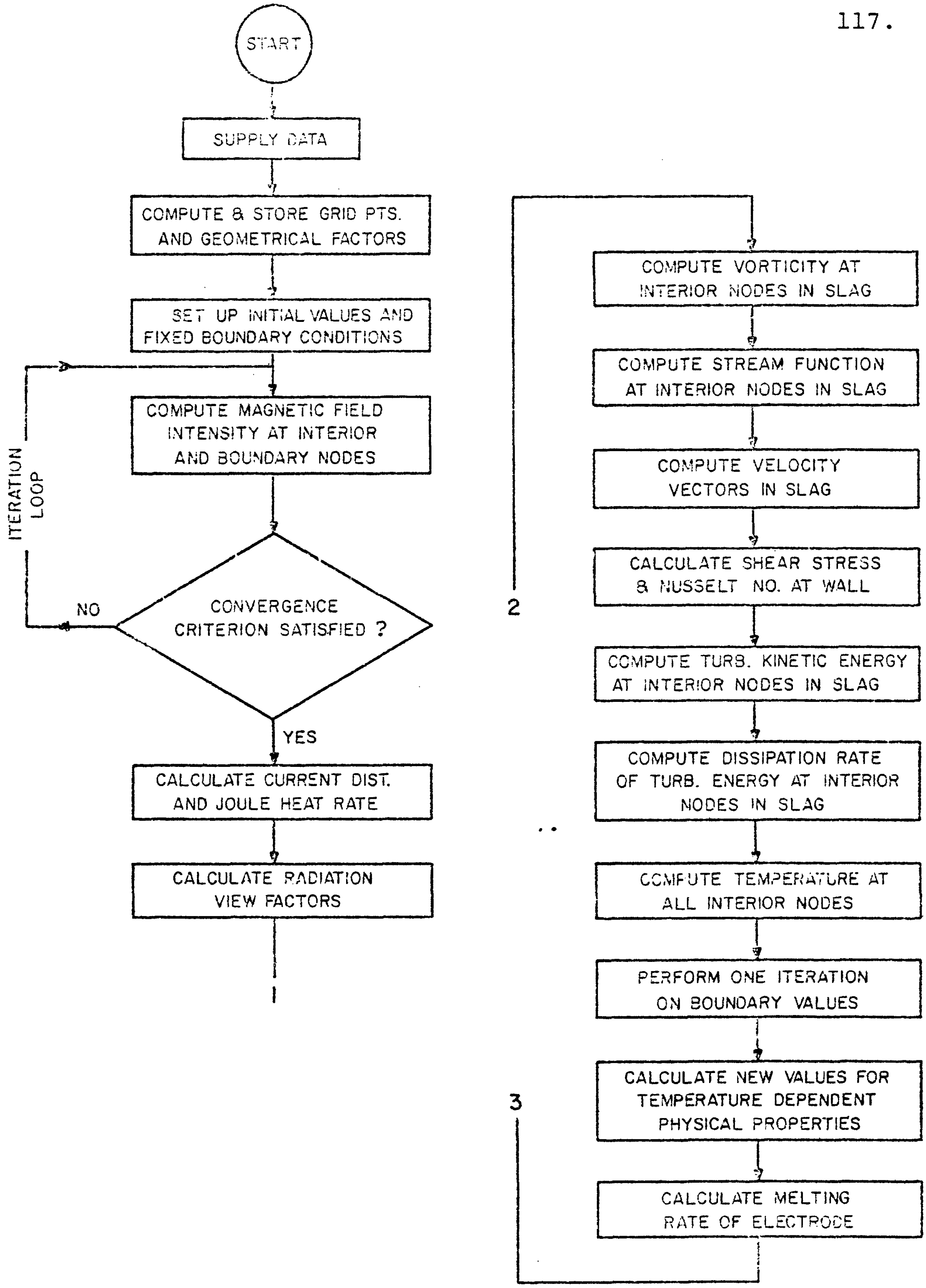

4.8 Simplified flow diagram for the computational scheme

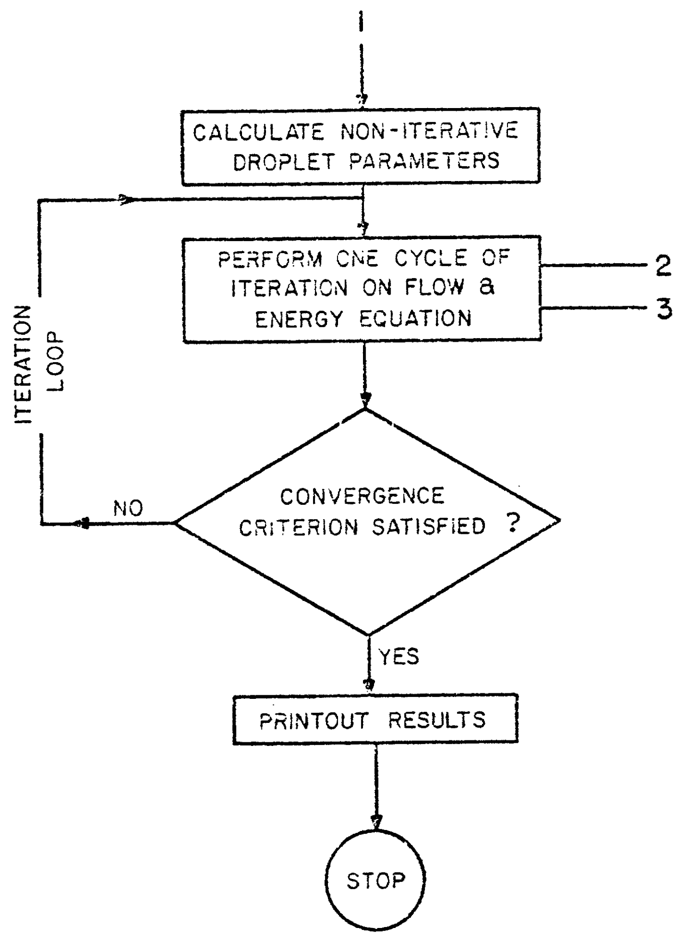

4.8 Continued

Table 4.2 Description of the Computer Program

Name	Function
MAIN	Starts the computations and controls the iteration procedure for flow and heat transfer variables.
BLOCK DATA	Supplies reference values for physical properties, values for operating parameters and dimensions of the system as well as control indices for the program.
CORD	Calculates coordinates of the grid nodes as well as D_j of Eqs. (4.13), (4.14) and B_j' of Eq. (4.6).
INIT	Provides initial values for the dependent variables and computes those prescribed boundary conditions for which no iteration is required.
FIELD	Solves for magnetic field intensity. Computes the distribution of current density and Joule heat and total power usage.
VF DROP	Calculates radiation view factors and droplet parameters.

EQN	Performs one cycle of iteration on the complete (both interior and boundary nodes) set of successive substitution equations by calling various subroutines. Also updates physical property values at the end of each iteration.
VORITY	Computes vorticity at the interior nodes in slag.
STRFUN	Computes stream function at the interior nodes in slag.
TURVAR	Computes turbulence kinetic energy and the dissipation rate of turbulence energy at the interior nodes in slag.
TEMPR	Computes temperature at all the interior nodes.
WALL	Computes shear stress and Nusselt no. at rigid boundaries.
BOUND	Computes dependent variables at those boundary nodes where iteration is required.
CONVEC	Calculates A_j' of Eq. (4.6) and makes modifications for incorporating wall functions.
SORCE	Calculates source term, $S_{\phi,p}$ of Eq. (4.6)

VELDIS	Calculates velocity distribution in the slag.
VISCOS	Calculates effective viscosity in the slag.
PROP	Allows the use of temperature dependent thermo-physical properties. Calculates the liquidus and the solidus isotherms and the melting rate of the electrode.
ADF	Calculates first order derivative by the three point quadratic approximation.
PRINT	Prints out calculated results.

their boundary conditions constitute a complete and a well-posed problem. Even when these conditions are fulfilled it requires a great deal of numerical experimentation to ensure that the solution procedure converges to the "correct" solution. Another important aspect of the solution procedure is the speed of convergence, since the computation time has to be realistically limited. A discussion on the factors which may influence the convergence, accuracy and the economy of the procedure is given by Gosman et al [39].

The computer program described earlier has evolved in stages and has involved considerable numerical experimentation. Following the practice in literature, the method of under-relaxation is used to reduce the chances of instability. If $\phi^{(N-1)}$ is the value of the variable calculated in the (N-1)th iteration and $\phi^{(N)}$ is the value which would be computed in the Nth iteration, then the value which is actually used in iteration N is computed from:

$$\phi = \alpha_{UR}\,\phi^{(N)} + (1 - \alpha_{UR})\,\phi^{(N-1)} \qquad (4.38)$$

where α_{UR} is called the under-relaxation parameter and is a number between 0 and 1. However, the rate of convergence of an iterative solution procedure can sometimes be improved by over-relaxation [39]. Mathematically, over-relaxation can be represented by an equation analogous to the above equation, i.e.,

$$\phi = \alpha_{OR}\, \phi^{(N)} + (1 - \alpha_{OR})\, \phi^{(N-1)} \qquad (4.39)$$

where α_{OR}, the over-relaxation parameter, lies between 1 and 2.

During numerical experimentation, the magnetic field equations were found to be very well behaved and over-relaxation was found to greatly enhance the rate of convergence. For the laboratory scale system discussed in the next chapter, $\alpha_{OR} = 1.5$ for $\hat{H}_{\theta R}$ and $\alpha_{OR} = 1.2$ for $\hat{H}_{\theta I}$ were found to give the optimum convergence rate.

In the case of other dependent variables ($\frac{\varepsilon}{r}$, ψ, k, ε, T), over-relaxation for the stream function and under-relaxation for the rest of the variables was found to be the best practice. The attempt to over-relax the vorticity equation lead to divergence.

To observe the convergence rate, two different criteria for convergence were employed. In one following Gosman et al [39], the maximum fractional change of ϕ in the field was dictated to be less than a prescribed value, i.e.;

$$[(\phi^{(N)} - \phi^{(N-1)})/\phi^{(N)}]_{max} \leq \varepsilon_1 \qquad (4.40)$$

Usually ε_1 has been set in the range of 0.001 to 0.005.

It sometimes happens that when the value of a variable at a particular node is much smaller than the values at surrounding nodes, fluctuations, in the small value will occur which are unacceptable by the above criterion, even though the rest of the field has converged. In this case an alternative criterion used by some other authors [32,35] was employed. This is given as

$$\frac{\sum|\phi^{(N)} - \phi^{(N-1)}|}{\sum|\phi^{N}|} \leq \varepsilon_2 \qquad (4.41)$$

where $\sum$ means summation over all the interior nodes. ε_2 has been set in the range 0.001 to 0.005.

The numerical solution was carried out on IBM 370 at MIT. Calculated results and discussions are given in the next chapter.

Nomenclature

$a_\phi, a_{1\phi}, b_\phi, c_\phi$	Coefficients in the general elliptic equation (4.6)
A'_j, B'_j	Coefficients in the general substitution formula, Eq. (4.8)
A_E, A_W, A_N, A_S	Coefficients in the convection terms of the general substitution formula, given by Eqs.(4.11a,b,c,d)
$A_{1E}, A_{1W}, A_{1N}, A_{1S}$	Coefficients accounting for the movement of interfaces, given by Eqs. (4.12a,b,c,d)
B_E, B_W, B_N, B_S	Coefficients in the diffusion terms of the general substitution formula, given by Eqs.(4.13a,b,c,d)
C_d	Dissipation rate constant
C'_f	Coefficient of skin friction
D_1, D_2	Terms in substitution formula for magnetic field intensity
D_N, D_S, D_E, D_W	Coefficients defined by Eqs.(4.21 a,b,c,d)
E	A function of wall roughness appearing in logarithmic law Eq. (4.30)

Nomenclature (cont'd)

$\hat{H}_\theta, \lvert\hat{H}_\theta\rvert$	Complex amplitude of magnetic field intensity in θ-direction, its magnitude
$\hat{H}_{\theta R}, \hat{H}_{\theta I}$	Real and imaginary parts of $\hat{H}_\theta$
$\hat{J}_r, \lvert\hat{J}_r\rvert$	Complex amplitude of current density in r-direction, its magnitude
$\hat{J}_{rR}, \hat{J}_{rI}$	Real and imaginary parts of $\hat{J}_r$
$\hat{J}_z, \lvert\hat{J}_z\rvert$	Complex amplitude of current density in z-direction, its magnitude
$\hat{J}_{zR}, \hat{J}_{zI}$	Real and imaginary parts of $\hat{J}_z$
k	Kinetic energy (per unit mass) of turbulence
Nu_x	Local Nusselt number
n, n^+	Dimensional, dimensionless distance normal to wall
P	Defined by Eq. (4.37).
Re_x	Local Reynolds number

Nomenclature (cont'd)

r	Radial coordinate
S_1, S_2	Defined by Eqs.(4.19),(4.20)
S_ϕ	Source term in the general elliptic equation (4.6)
T	Temperature
V_+, V	Dimensionless, dimensional velocity parallel to wall
V_τ	Friction velocity
z	Axial coordinate

GREEK SYMBOLS

α_{UR}, α_{OR}	Parameters for under and over relaxation
β_H	Phase angle of $\hat{H}_\theta$
$\delta_1, \delta_2, \delta_3, \delta_4$	Domains for the wall function approach
ε	Dissipation rate of turbulence energy
$\varepsilon_1, \varepsilon_2$	Convergence parameters defined by Eqs.(4.40),(4.41)

Nomenclature (cont'd)

ϕ	General notation for dependent variables
ξ	Vorticity
ψ	Stream function
σ_ℓ, σ_t	Prandtl number, turbulence Prandtl number
τ_w	Shear stress at wall
κ	von Karman's constant

CHAPTER V

COMPUTED RESULTS AND DISCUSSION

The model developed in Chapter III is now used to make predictions on the flow and thermal characteristics in an ESR system. Computed results presented in this chapter show typical temperature and velocity distributions and pool profiles as well as the interdependence of key process parameters, with the power input, fill ratio, amount of slag used and the position of the electrode as the independent variables and the casting rate, pool depth, velocity and temperature fields as the dependent variables. Wherever possible these predictions will be compared with experimental measurements available in the literature [57].

5.1 Description of the System Chosen for Computation

The experimental results, to which the predictions will be compared, are those reported by Mellberg[57] who studied the electroslag remelting of ball bearing steels in a laboratory scale system, using electrodes of 0.057 m diameter and a stationary water cooled copper mold of 0.1 m internal diameter. Remelting was done with alternating current and the mold was electrically insulated from the base plate. The electrode composition is given in Table 5.1 and the remelting parameters are given in Table 5.2.

Table 5.1 Composition of Electrodes Used by Mellberg

Components	C	Si	Mn	P	S	Cr	Al	O
Wt %	1.03	0.35	0.37	0.017	0.019	1.53	0.037	0.0025

Table 5.2 Remelting Parameters in Mellberg's Experiments

Ingot No.	Current, kA	Voltage V	Starting Slag Wt kg	Starting Slag Comp., Wt %				Casting rate cm/min
				CaF_2	CaO	Al_2O_3	SiO_2	
15	1.7	34	1.5	68	1	29	1	1.23
17	1.55	30	1.5	68	1	29	1	1.03

5.2 Physical Properties and Parameters Used in Computation

The computer program described in Chapter IV and included in the thesis as Appendix E allows for the temperature dependence of physical properties (μ, C_p, ρ, K) appearing in the model. As described in Chapter III, in order to keep the equation for magnetic field intensity decoupled from the flow and heat transfer equations, the model uses average values for the electrical conductivities of slag and metal. However, in some of the calculations an approximate allowance has been made for the temperature dependence of electrical conductivity of slag. In the absence of specific information on the temperature dependence of properties for the system being modeled, it was decided to perform calculations with constant values for the properties.

Physical property values used in the computation are listed in Table 5.3. The liquidus temperature, the density and the viscosity of the slag were estimated from data reported in reference 40 and its electrical conductivity was estimated from compilations made by Hajduk and El Gammal[58]. In the absence of better information, values for the specific heat, the thermal conductivity and the coefficient of volume expansion of the slag were taken the same as those used by Dilawari and Szekely[15]. The liquidus and the solidus temperature of the metal were given by Mellberg[57]. Values for the other properties were taken from Dilawari and Szekely[15] and from Elliott and Maulvault [11]. These values apply for pure iron or for intermediate carbon steels. The value for atomic thermal conductivity of molten metal was taken to be half of that for solid metal.

The dimensions of the system and the values for other parameters appearing in the model are shown in Table 5.4. The values for the constants C_1, C_2, C_d, σ_k, σ_ε of the k - ε model are those recommended by Launder and Spalding [46]. These recommendations were made on the basis of extensive examination of free turbulent flows. However, one must be aware that these are not universal constants and may change in different situations. The value for the convective heat transfer coefficient between the electrode surface and the ambient was suggested to be 17.2 $W/(m^2K)$ by Mendrykowski et al [3]. From experimental measurements, Maulvault [7] calculated this to be in the range 19 - 32 W/m^2 K. A value of 25 W/m^2 K was chosen for the present case. Values for heat transfer coefficients below the slag-metal interface were deduced from suggestions made by Elliott and Maulvault [11] and Ballantyne and Mitchell [12]. As seen in Table 5.4, below the slag-metal interface, heat removal by cooling water is represented by three heat transfer coefficients. Instead of using discontinuous values for heat transfer coefficient, as has been done here, it will certainly be

Table 5.3 Physical Property Values Used

K_e	thermal conductivity of electrode, 31.39	
$K_{s\ell}$	thermal conductivity of slag, 10.46	
K_m	thermal conductivity of mushy zone, 31.39	$\frac{W}{mK}$
K_s	thermal conductivity of solid ingot, 31.39	
$K_{m,\ell}$	thermal conductivity of molten metal, 15.48	
ρ_e	density of electrode, 7.2×10^3	
$\rho_{s\ell}$	density of slag, 2.85×10^3	$\frac{kg}{m^3}$
$\rho_\ell, \rho_m, \rho_s$	density of liquid metal, mushy zone, solid ingot, 7.2×10^3	
$C_{p,e}$	specific heat of electrode, 502	
$C_{p,s\ell}$	specific heat of slag, 837	$\frac{J}{kgK}$
$C_{p,\ell}, C_{p,m}, C_{p,s}$	specific heat of liquid metal, mushy zone, solid ingot, 753	
$T_{\ell,m}$	liquidus temperature of metal, 1723 K	
$T_{s,m}$	solidus temperature of metal, 1523 K	
$T_{\ell,s}$	liquidus temperature of slag, 1650 K	

β	coefficient of cubical expansion of slag, 1×10^{-4} K^{-1}
λ	latent heat of fusion of metal, 247 kJ/kg
σ_e, σ_m	electrical conductivity of electrode, metal, 7.14×10^5 mho/m
$\sigma_{s\ell}$	electrical conductivity of slag, 2.50×10^2 mho/m
ε_e	emissivity of electrode surface, 0.4
ε_s	emissivity of free slag surface, 0.6
γ	interfacial tension between molten slag and molten metal, 0.9 N/m
μ	viscosity of slag, 0.01 kg/m·s

Table 5.4 Numerical Values of Parameters Used In Computation

R_e	electrode radius, 0.0285 m	
R_m	mold inside radius, 0.05 m	
Z_1	free slag surface, 0.30 m	
Z_2	melting tip of electrode, 0.32 m	
Z_3	slag-metal interface, 0.37 m	
Z_6	lower boundary of the ingot, 0.73 m	
C_1	constant in $k - \varepsilon$ model, 1.44	
C_2	constant in $k - \varepsilon$ model, 1.92	
C_d	dissipation rate constant, 0.09	
σ_k	Prandtl number for k, 1.0	
σ_ε	Prandtl number for ε, 1.3	
μ_0	magnetic permeability, 1.26×10^{-6} Henry/m	
h_c	heat transfer coeffieicnt between the electrode and the gas, 25.1	$\frac{W}{m^2K}$
$h_{w,1}$	heat transfer coeffieicnt at the molten metal-mold interface, 272	

$h_{w,2}$	heat transfer coefficient at the mushy zone-mold interface, 272	$\frac{W}{m^2K}$
$h_{w,3}$	heat transfer coefficient at the ingot-mold interface, 188	$\frac{W}{m^2K}$
ω	angular frequency of current, 377 radians/s	
$\overline{I}_0$	total current (rms value), 1.4 - 2.5 kA	

more realistic to use heat transfer coefficient as a function of position if such information is available.

The evaluation of the parameter Λ which appears in Eq. (3.44) remains to be discussed. As seen from Eq. (3.44), ($1 + \Lambda$) represents the ratio of effective and atomic thermal conductivities in the metal pool. In the present work an attempt has been made to link this parameter to operating conditions by evaluating it from the computed flow field in the slag. Calculations were carried out for turbulent fluid flow and heat transfer in both the slag and the metal pool for the conditions when the shape of the metal pool was assumed cylindrical and its size predetermined. This approach is analogous to the one taken by Dilawari and Szekely [15]. A typical result on the computed ratios of effective and atomic thermal conductivities in both the slag and the metal pools is shown in Fig. 5.1. This figure represents computation for an operating current of 1.7 KA and for an assumed metal pool depth of 0.03 m. Calculations like these indicated that the average ratio of the effective and atomic thermal conductivities in the metal pool was about one third of the corresponding ratio for the slag pool, i.e.

$$\left(\frac{K_\ell}{K_{m\ell}}\right) = 1 + \Lambda \simeq \frac{1}{3}\left(\frac{K_{eff}}{K}\right)_{avg} \qquad (5.1)$$

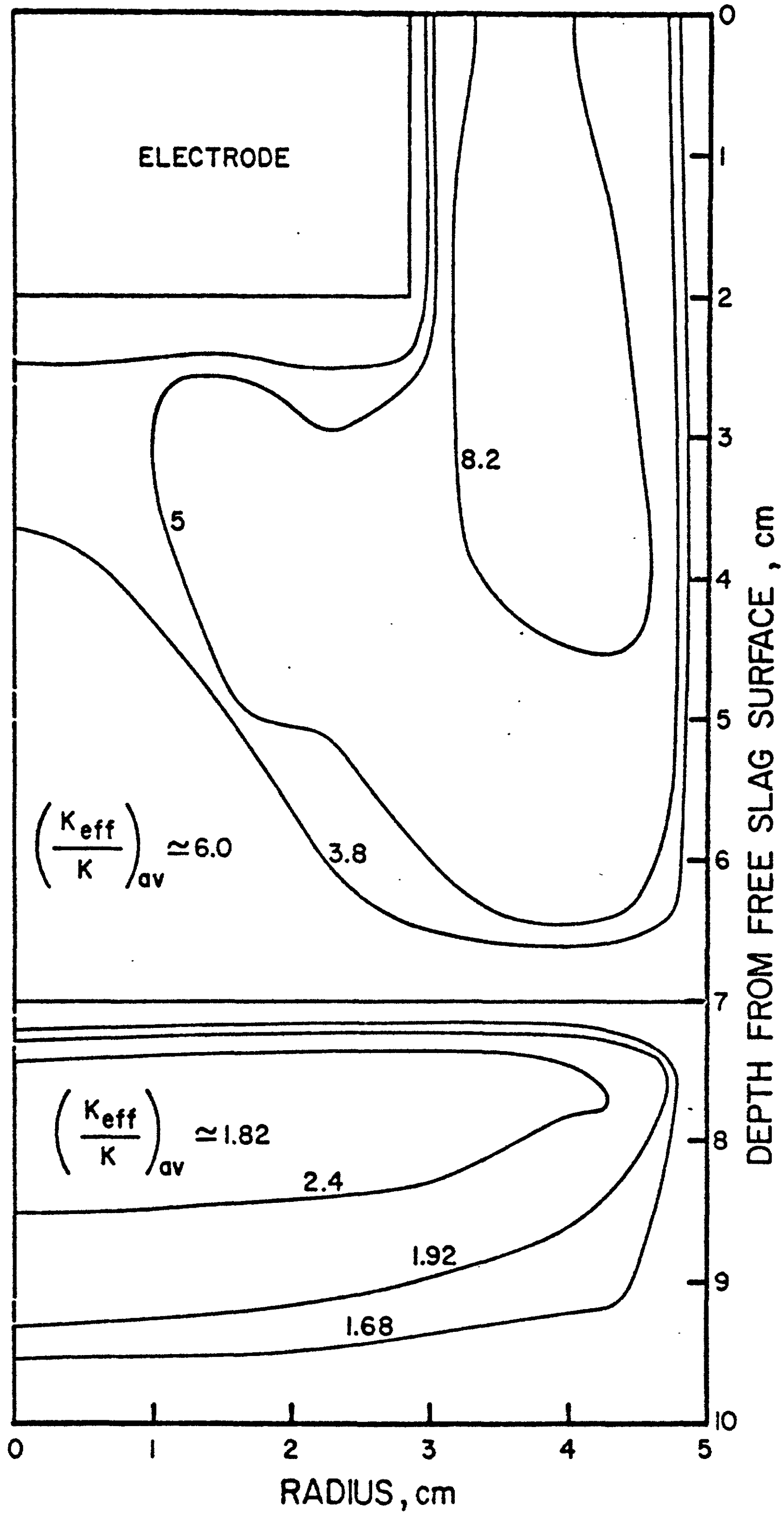

5.1 Computed ratio of effective and atomic thermal conductivities in both slag and metal pools for operation with 1.7 kA (rms) and for an idealized metal pool shape and size.

where, as mentioned before, K_ℓ and $K_{m\ell}$ denote the effective and the atomic thermal conductivities of the metal pool whereas K_{eff} and K denote the corresponding quantities for the slag. An attempt such as Eq. (5.1) appears crude at best and it is entirely possible that the value of the coefficient in this equation would differ from the value of 1/3 used in the present instance for different geometries and for much different current levels. Furthermore, according to the scheme chosen here, we only account for the mixing or dispersive action of turbulence in the metal pool, and the convective term in the equation for heat transport is still unaccounted for. These criticisms can not be taken care of unless the model is extended to calculate fluid flow in the metal pool. In the mean time, however, it does appear more reasonable to calculate the effective thermal conductivity in the metal pool from the model itself (albeit in an approximate manner) than selecting it to give a better agreement with the experimental measurements. For the results presented here, calculated values for Λ fell in the range 0.7 - 3.4.

5.3 Computational Details

The numerical scheme outlined in Chapter IV was used to solve the governing equations. Fig. 5.2 shows the grid which is typical of those used in the calculations presented in this chapter. As shown in this figure,

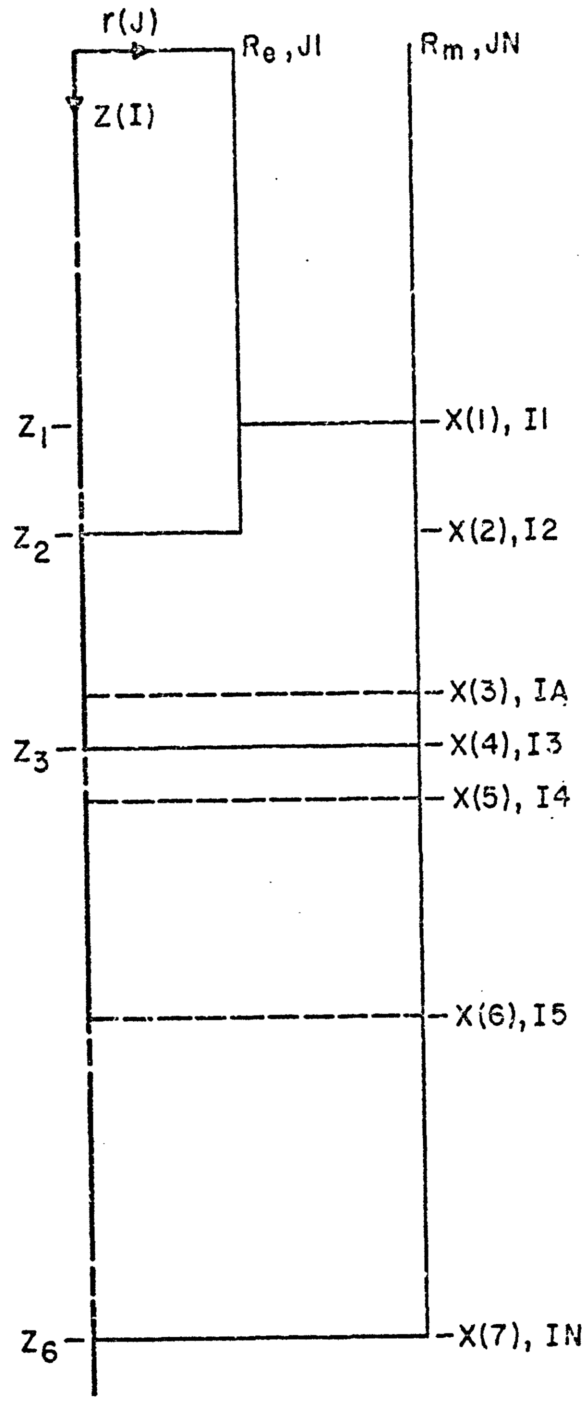

IN = 51, JN = 12

J1 = 7

I1 = 16, I2 = 19, IA = 24

I3 = 27, I4 = 31, I5 = 41

X(1) = 0.0285 m

X(2) = 0.3 m

X(3) = 0.361 m

X(4) = 0.37 m

X(5) = 0.38 m

X(6) = 0.43 m

X(7) = 0.73 m

R_e = 0.0285 m

R_m = 0.05 m

Fig. 5.2 Details on the grid configuration.

there are 51 I-lines (z-direction) and 12 J-lines (r-direction). While the spacing between the J-lines was kept the same in all the computations reported here, spacing between the I-lines was adjusted for various cases to concentrate nodes in the critical areas. The computations were carried out using the IBM 370 digital computer at MIT; the time interval involved in the computation was in the range of 100-200 seconds.

5.4 Results and Discussions

A selection of computed results on the electromagnetic aspect of the process is first presented and then results for the flow and thermal aspects are given. In the following discussions ingots 15 and 17 refer to operations with 1.7 kA and 1.55 kA (both rms values) respectively.

5.4.1 Computed results on electromagnetic parameters

Fig. 5.3 shows the radial distribution of the magnetic field intensity in the slag and in the metal calculated at different axial positions and for an operating current of 1.7 kA (rms). Curves 1 and 2 refer to calculations for the slag at vertical positions, 0.016 m and 0.044 m below the electrode respectively. Curves 3 and 4 refer to calculations for the metal at positions, 0.045 m and 0.22 m below the slag-metal interface

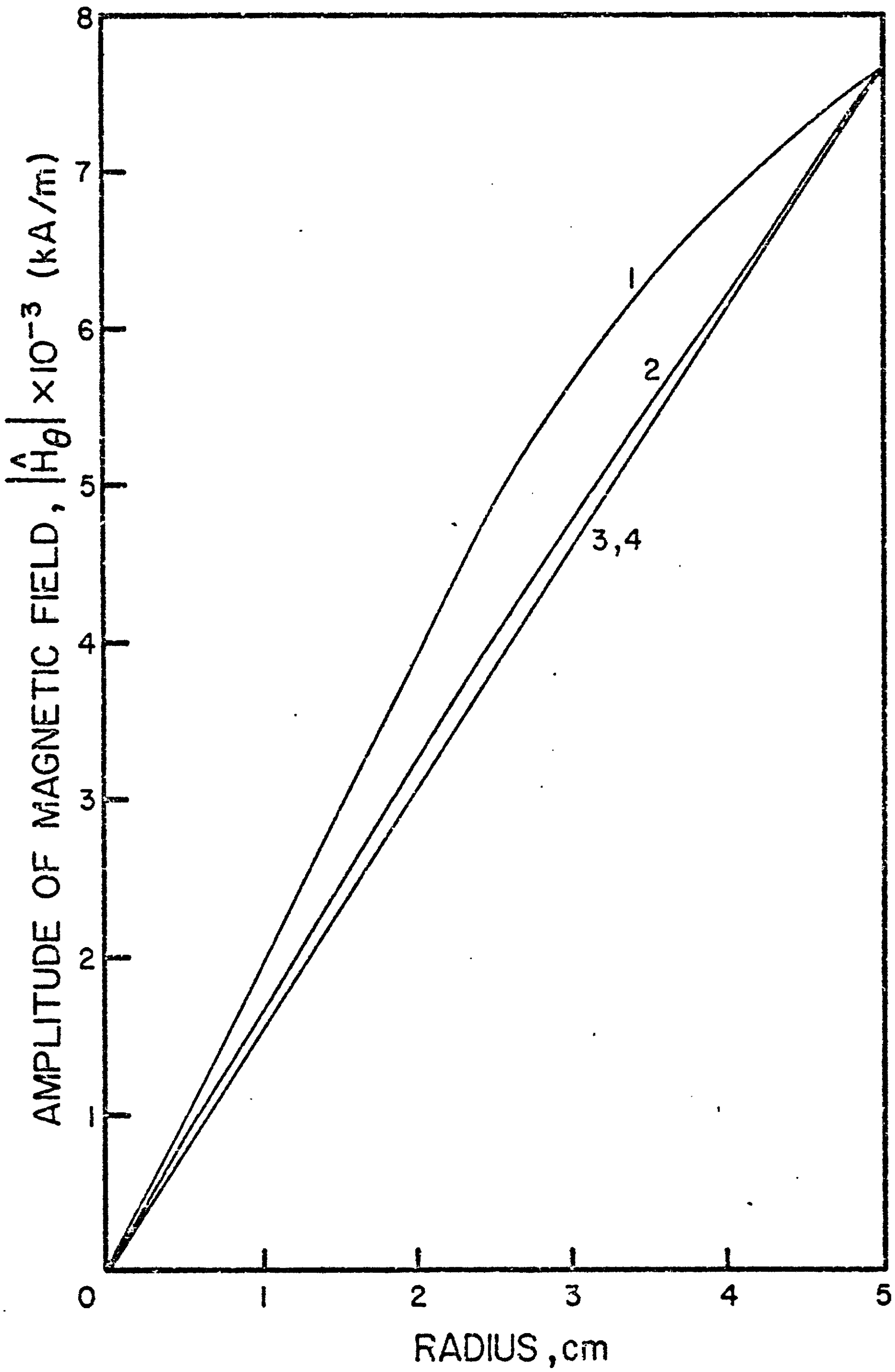

5.3 Computed magnetic field intensity for operation with 1.7 kA (rms).

1 1.6 cm below electrode
2 4.4 cm below electrode
3 4.5 cm below the slag-metal interface
4 22 cm below the slag-metal interface

respectively. As seen in this figure, the radial distribution of the magnetic field intensity in the metal is linear and the distributions at the two locations are identical. This implies that the current in the radial direction is negligible and that the axial component of the current is distributed uniformly across the cross section (with a density of 216 kA/m^2). In the slag, as can be inferred from curves 1 and 2, the radial component of current is finite and becomes small as the slag-metal interface is approached. This is readily seen in Fig. 5.4 which shows the current density vectors (length of a vector represents the rms value of current density) in the slag. The current path diverges in the vicinity of the electrode-slag interface but it becomes almost parallel as the slag-metal interface approaches.

Fig. 5.5 shows the radial distribution of volumetric Joule heat generation rate in the slag for the same two axial positions as in Fig. 5.3 (i.e. 0.016 m and 0.044 m below the electrode). In the vicinity of the slag-electrode interface, heat generation rate is quite high and the distribution is non-uniform. As is to be expected from the discussions given in connection with previous figures, the radial distribution of heat generation rate becomes uniform when the distance from the slag-electrode interface increases. The heat generation rates

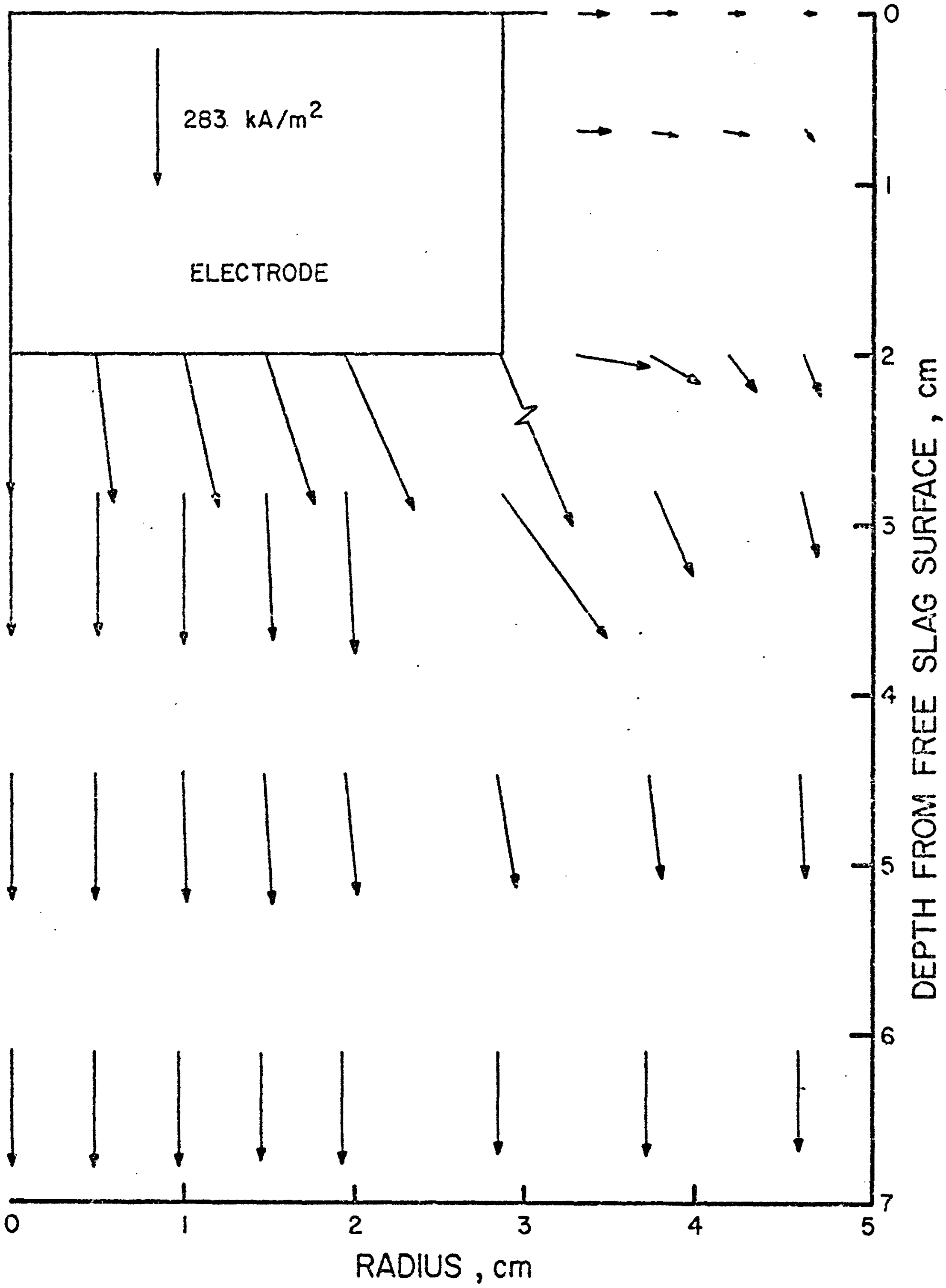

5.4 Computed current density vectors in slag for operation with 1.7 kA (rms).

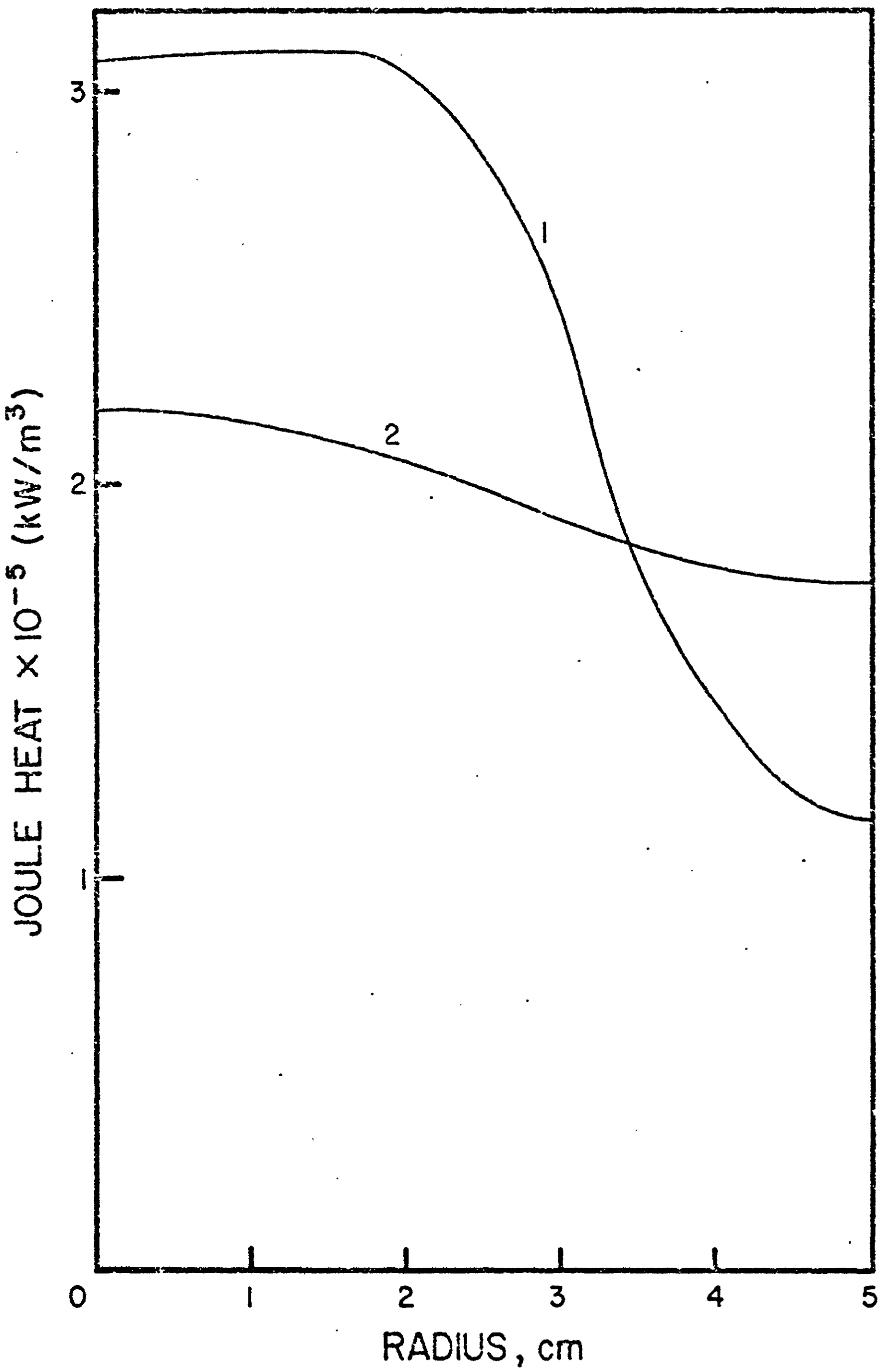

5.5 Computed radial distribution of volumetric heat generation rate in slag for operation with 1.7 kA.

1 1.6 cm below electrode

2 4.4 cm below electrode

are completely uniform in the ingot (65.45 kW/m^3) and in the upper portions of the electrode (621.6 kW/m^3).

Fig. 5.6 shows the effect of electrode penetration depth in the slag. Here the solid lines represent calculations already shown in Fig. 5.5 whereas the broken lines denote calculations where the electrode protrudes 0.01 m into the slag (as compared to 0.02 m for the previous case). The total amount of slag used (1.5 kg) and the power input (73 kW) were the same in both the cases. Curves 1 and 2 in this figure have the same meanings as in Fig. 5.5 As seen here, the case with a lower electrode penetration depth has a lower volumetric heat generation rate in the bulk portion of the slag. This is to be expected since the volume of slag below the electrode is larger in this case. The different heat generation patterns in the two cases will lead to different temperature distributions in the slag. This will be examined subsequently.

Fig. 5.7 shows the effect of the amount of slag used on the heat generation rate in the slag. Once again the solid lines represent the results already described in Fig. 5.5 whereas the broken lines represent calculations for a higher amount of slag (1.9 kg vs 1.5 kg for the former case). The electrode penetration depth (0.02 m) and the input power (73 kW) were the same in both the

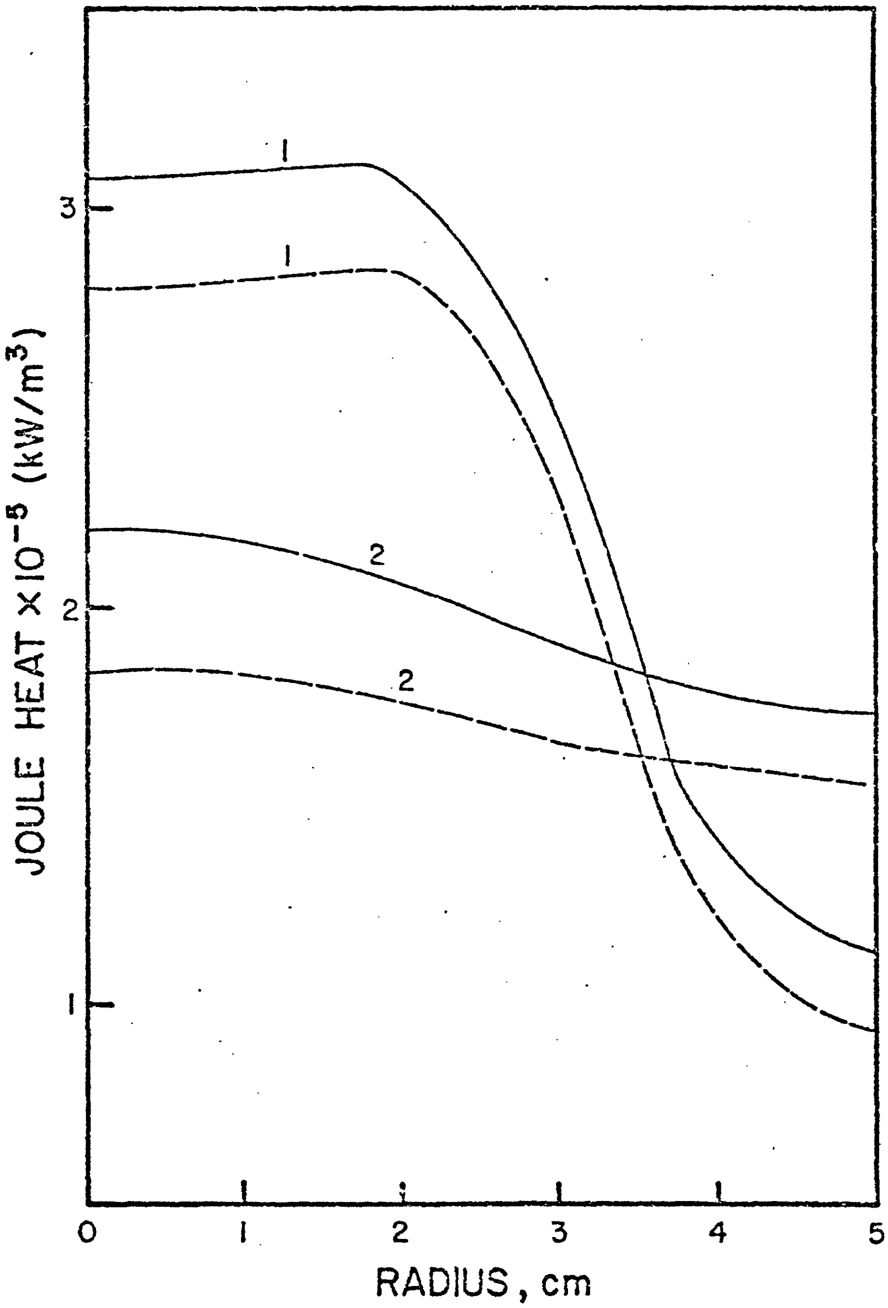

5.6 The effect of electrode penetration depth on heat generation rate in slag.

—— depth of penetration of electrode 2 cm, power 73 kW

--- depth of penetration of electrode 1 cm, power 73 kW

1 1.6 cm below electrode

2 4.4 cm below electrode

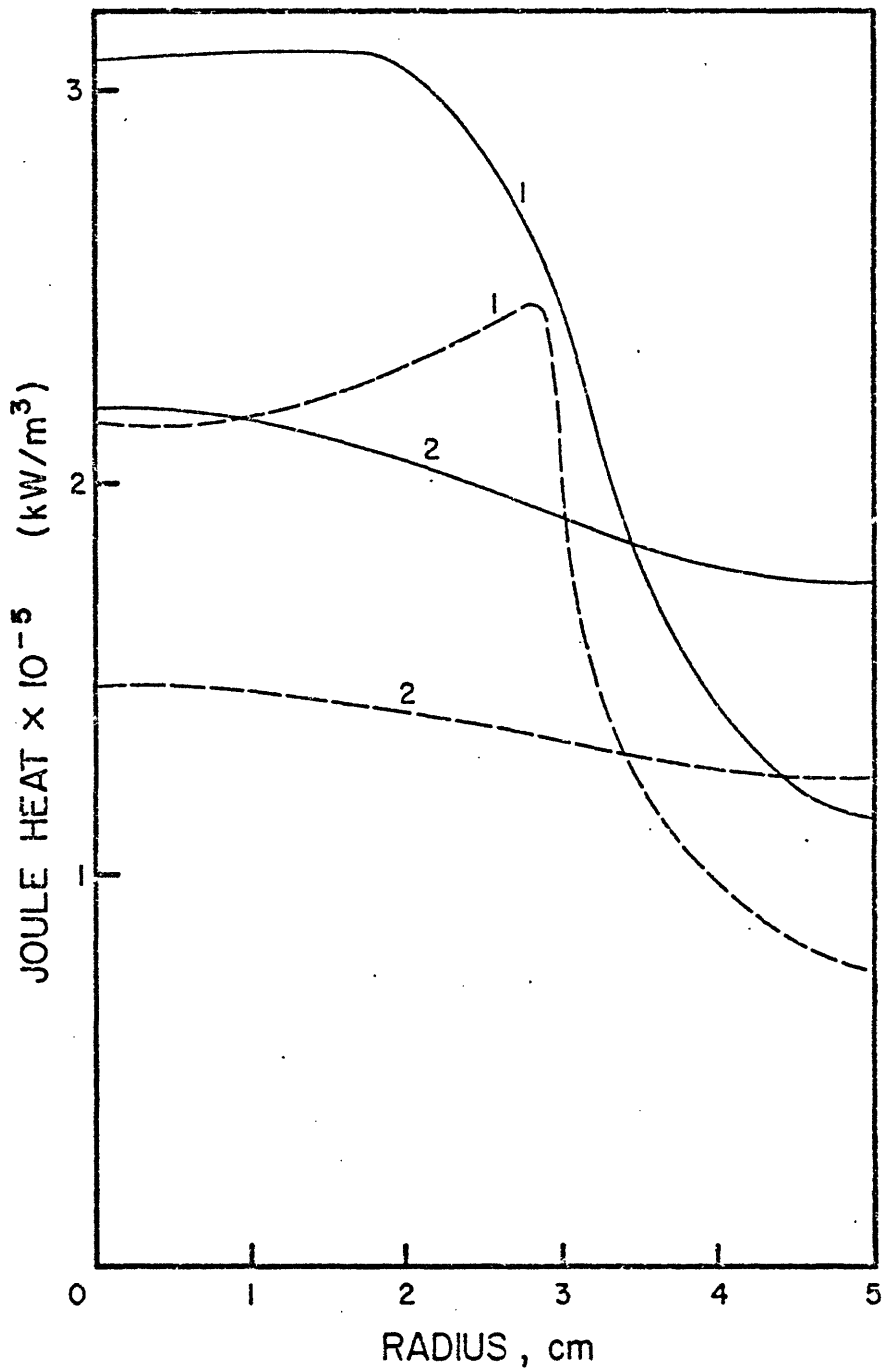

5.7 The effect of the amount of slag used on the heat generation rate in slag.

——	amount of slag 1.5 kg
----	amount of slag 1.9 kg
1	1.6 cm below electrode
2	4.4 cm below electrode

cases. As seen here, the larger volume of slag in the second case gives rise to a lower volumetric heat generation rate in the slag. Based on a uniform current distribution over the entire cross section of slag, the volumetric heat generation rate is 1.32×10^5 kW/m^3 for operation with 1.9 kg of slag as compared to 1.87×10^5 kW/m^3 for the other case. For both the lower electrode penetration depth and the larger amount of slag used, the resistance of the system was found to increase in accordance with the operating experience [62].

Fig. 5.8 shows the effect of fill ratio (cross sectional area of electrode/c·s·area of mold) on current distribution in the slag. The solid lines denote calculations for an electrode radius of 0.0285 m (Re_1) whereas the broken lines represent calculations for an electrode radius of 0.015 m (Re_2). The mold radius in both the cases is 0.05 m and the total current in each case is 1.7 kA. As in the case of previous figures, 1 and 2 denote vertical positions 0.016 m and 0.044 m below the electrode-slag interface. In the vicinity of the electrode and directly below it, there is an appreciable difference in the current density in the two cases with the lower fill ratio case having a much larger current density. The difference narrows as the radius increases. From the discussions given in section 3.7.2, we expect that a larger

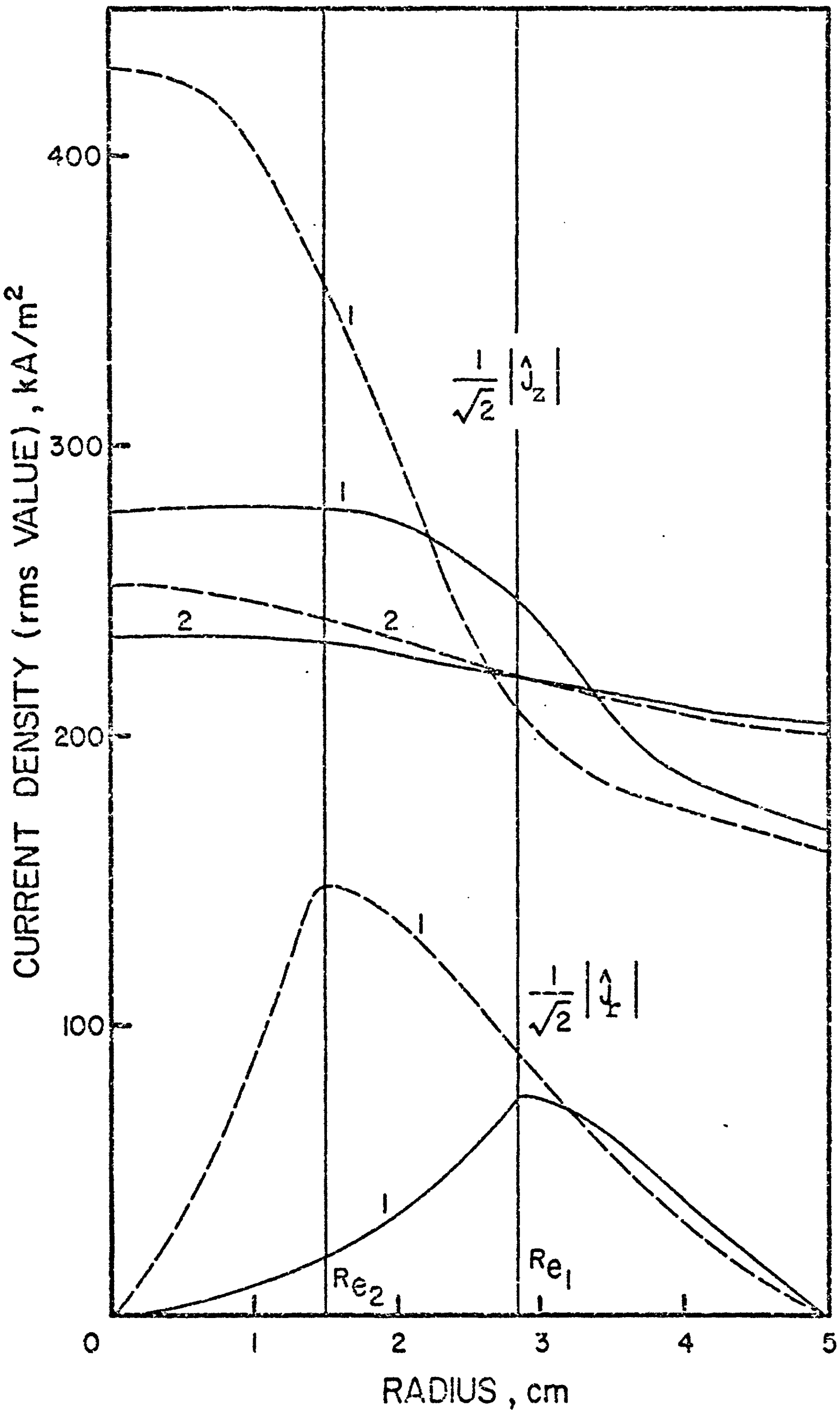

5.8 The effect of fill ratio on current distribution in the slag.

---	fill ratio	=	0.09	1	1.6 cm below electrode
——	fill ratio	=	0.325	2	4.4 cm below electrode

current density will give rise to increased velocity in the slag. This effect of the fill ratio will be examined subsequently. As the slag-metal interface is approached, the current density tends to be uniform and the difference in the two cases becomes small. Another effect of the reduced fill ratio is that the "effective cross section" for the passage of the current decreases, thereby increasing the electrical resistance of the system and the heat generation rate. Thus the total power input for the case with 0.015 m electrode radius (fill ratio = 0.09) is calculated to be 94 kW as compared to 73 kW for the case with 0.0285 m electrode radius (fill ratio = 0.32). The experimental observation of this effect is reported in the literature [61, 62].

Before closing this subsection, it should be noted that the computed current distribution and the heat generation pattern, and consequently fluid flow and temperature distrubution, will depend on the assumed shape of the electrode tip and on the assumptions made regarding the boundary conditions (e.g. insulating slag skin on the inside wall of the mold , the presence of a solidified slag crust on the submerged vertical wall of the electrode). As mentioned in Chapter III, the model developed in this work assumes a flat melting tip for the electrode and an insulating slag skin on the interior surface of the mold. The latter assumption is in accord with observations made in literature [40,41]. The assumption of a flat melting tip is made for computational convenience and ideally the shape of the electrode tip should be calculated using the mathematical model itself. However, this refinement to the model can only be accomplished if a more realistic understanding is developed of the melting process. This will require both experimental and analytical work.

The effect of a solidified slag crust on the submerged, curved surface of the electrode will be analogous to the effect of a reduced fill ratio since the effective c·s·area for current will decrease. Then, from discussions given in connection with Fig. 5.8, for the same total current, power requirement will be higher for this case and the current distribution will be less uniform. From the preceding discussions, the presence of a solidified slag crust on the electrode will be expected to increase the velocity in the slag. These observations are confirmed by calculations reported by Dilawari and Szekely [14,59].

5.4.2 Computed results on fluid flow and heat transfer

Results will now be presented for the temperature and velocity distributions in the system. Computed results on the temperature distribution will be compared with the limited measurements available.

It is noted that most of the calculations were carried out using a constant electrical conductivity of the slag. In some calculations, however, an allowance has been made for the temperature dependence of the electrical conductivity of the slag. The modifications required to the governing equations in order to accomplish this are discussed in Appendix D.

Fig. 5.9 shows a comparison between the experimentally measured axial temperature profile at a radial position r = 0.025 m and those predicted from the model. The discrete data points denote measurements, the broken line denotes predictions for the condition where the experimentally measured casting rate was used as an input to the model. The two solid lines denote predictions for the condition when the casting rate was computed from the model; curve I refers to calculations using a uniform electrical conductivity in the slag while curve II refers to calculations using a temperature dependent electrical conductivity in the slag. As discussed in Appendix D, temperature dependence of the electrical conductivity used in the calculations was deduced from experimental measurements reported by Mitchell and Cameron [60]. Power input in both the cases is kept the same (73 kW). It is seen that measurements correspond to a steeper axial temperature gradient in the vicinity of slag-metal interface than that

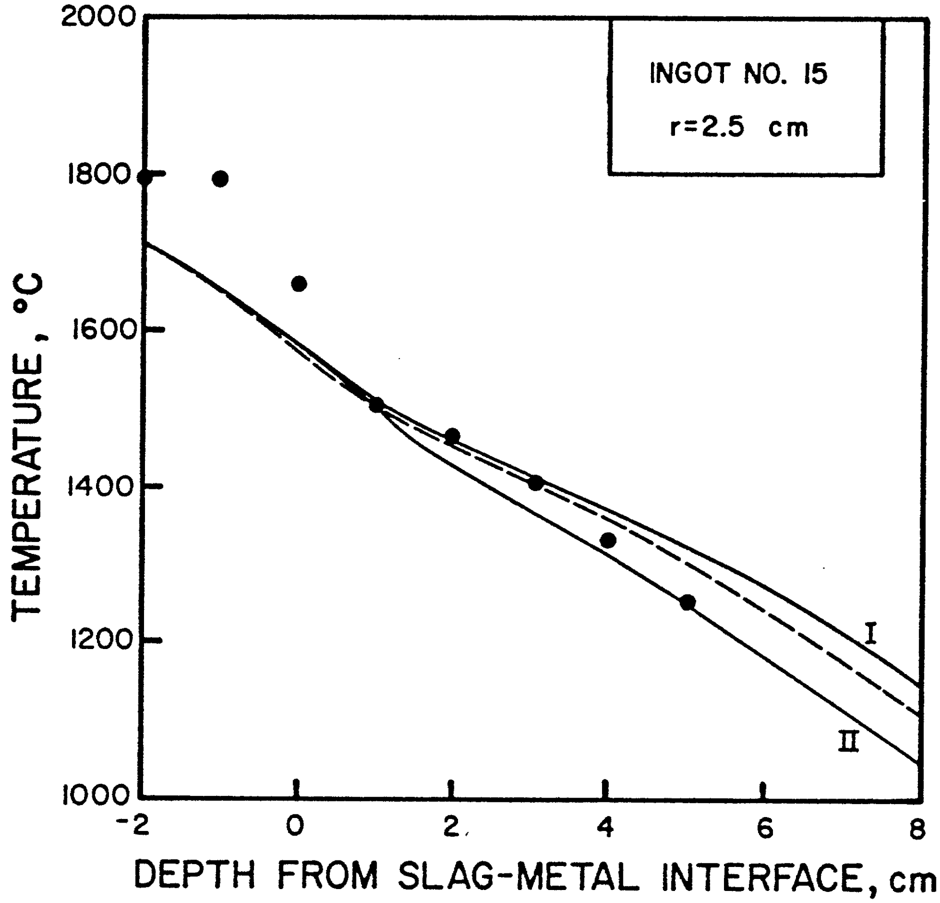

5.9 Computed and measured axial temperature profiles for ingot 15 (rms current = 1.7 kA) at r = 2.5 cm;

—— casting rate (V_c) calculated from the model

I uniform electrical conductivity in slag

II temperature dependent electrical conductivity in slag

--- experimentally measured value of V_c (0.74 m/hr) used as an input to the model

● measured values from Mellberg [57]

exhibited by the calculated results. This, as pointed out by Melberg, may partly be due to inaccuracies involved in experimentally defining the zero position. In general, all three curves shown in Fig. 5.9 provide a reasonable representation of the data points below the slag-metal interface. Curve II provides a somewhat better agreement with measurements primarily because in this case, calculated casting rate (0.7 m/hr) and effective thermal conductivity in the metal pool (27 W/mK) are lower than the corresponding values for case I (casting rate = 0.76 m/hr, effective thermal conductivity in metal pool = 30 W/mK).

One important derived quantity in these calculations is the radial temperature distribution at the slag-metal interface. Since there is not much difference in the three cases cited in Fig. 5.9, only the distribution for case I is discussed. This is shown in Fig. 5.10. As seen here there is quite an appreciable radial variation in the temperature (about 225°C in the present case). It is noted that several authors, when modelling pool profiles and the temperature fields in the ingot, used the temperature at the slag-metal interface as an arbitrarily adjustable boundary condition. The choice of this boundary condition may be critical, because this represents the coupling between the heat source in the slag and the heat transfer processes that take place within the ingot.

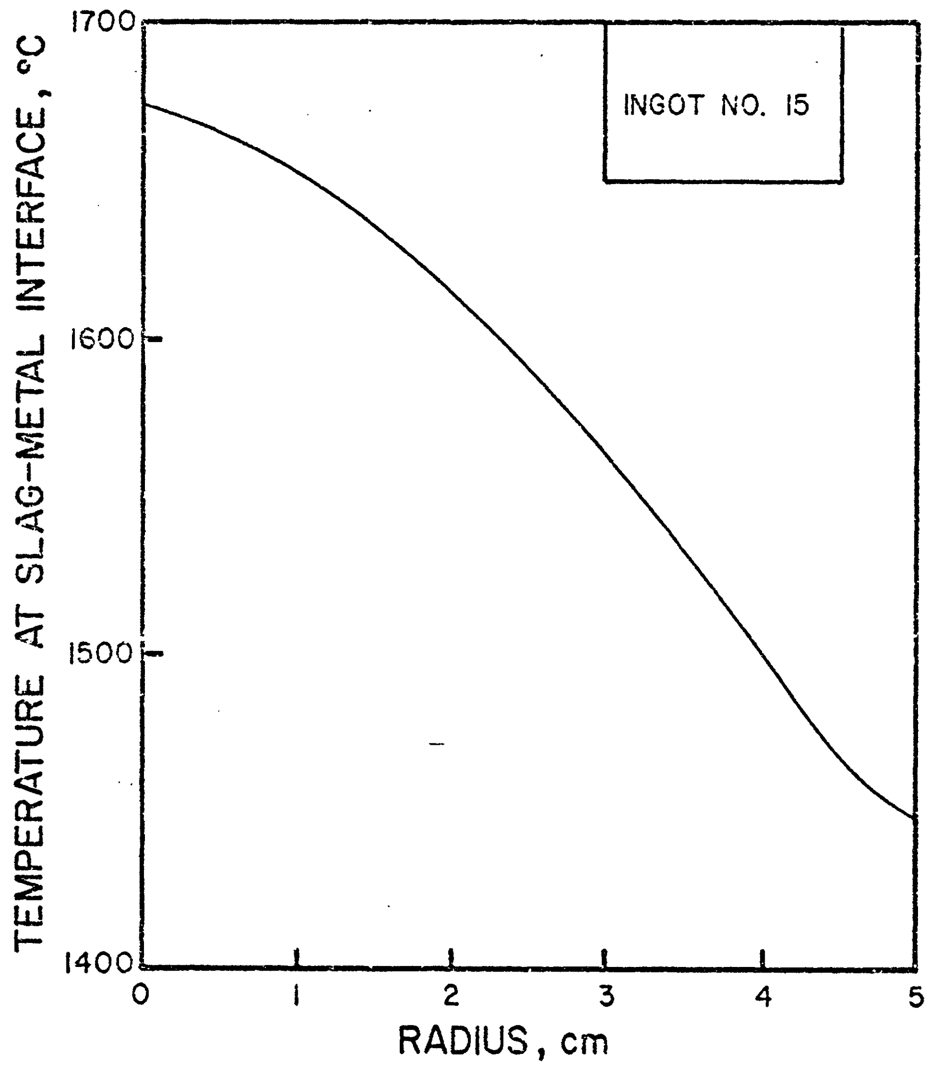

5.10 Computed temperature distribution at the slag-metal interface for ingot 15.

Fig. 5.11 shows an alternative way of expressing the radial distribution of temperature at the slag-metal interface. Here, $\ell n(\frac{T_{max}-T}{T_{max}-T_{min}})$ is shown plotted against $\ell n(\frac{r}{R_m})$ where T_{max} and T_{min} are the maximum (1675°C) and the minimum (1450°C) temperatures respectively and R_m is the radius of the mold. From this figure, it can be shown that

$$\frac{T_{max} - T}{T_{max} - T_{min}} \simeq \left(\frac{r}{R_m}\right)^{1.375} \qquad (5.2)$$

This type of relationship has been used by other authors to specify temperature distribution at the top of the ingot.

Fig. 5.12 shows the computed solidus and liquidus isotherms for the three cases that were represented in the previously given Fig. 5.9. Also shown, for the sake of comparison is a sulfur print reported by Mellberg, for corresponding operating conditions. It is seen that the sulfur print falls between the solidus and the liquidus curves, as one would expect. As before, curve II which represents computation with a temperature dependent electrical conductivity in the slag gives a closer agreement with the experimental measurements.

Fig. 5.13 shows a comparison between the experimentally measured and the theoretically predicted temperature profiles, for an ingot produced with a 1.55 kA current, at

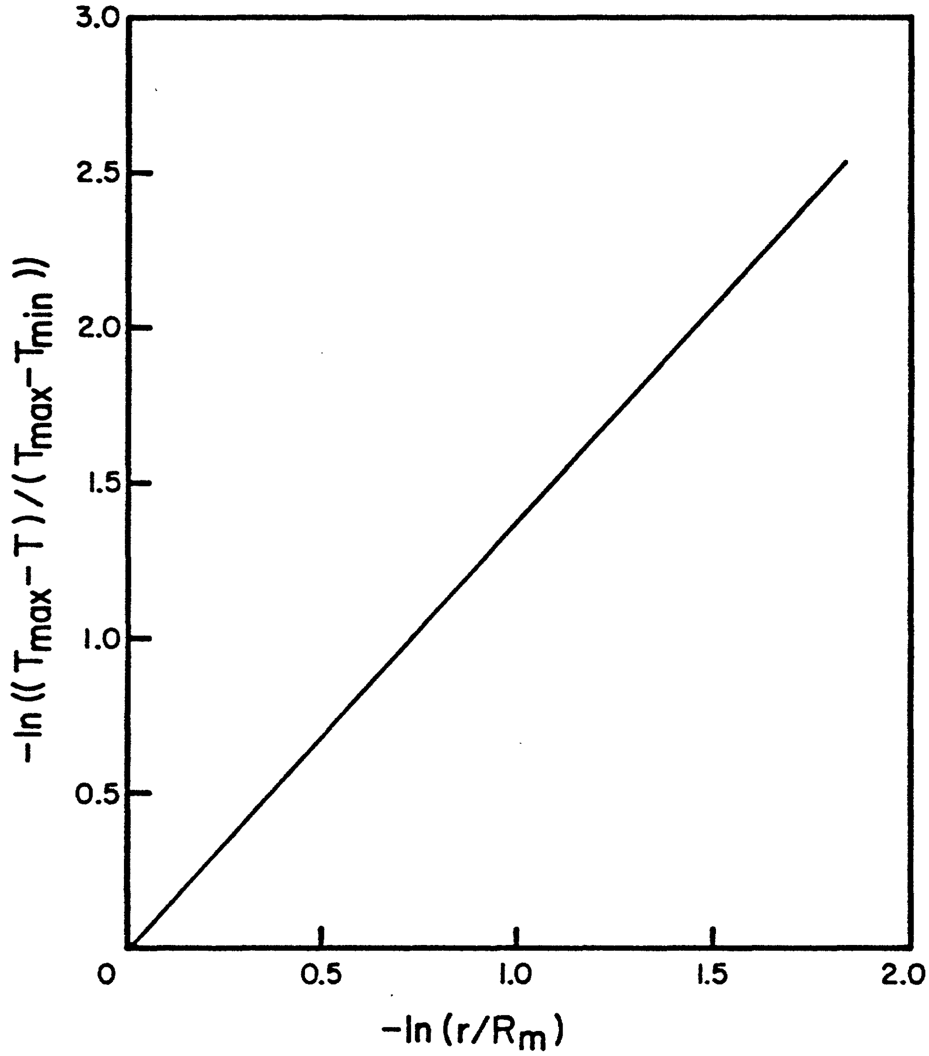

5.11 Results from Fig. 5.10 expressed in an alternative way.

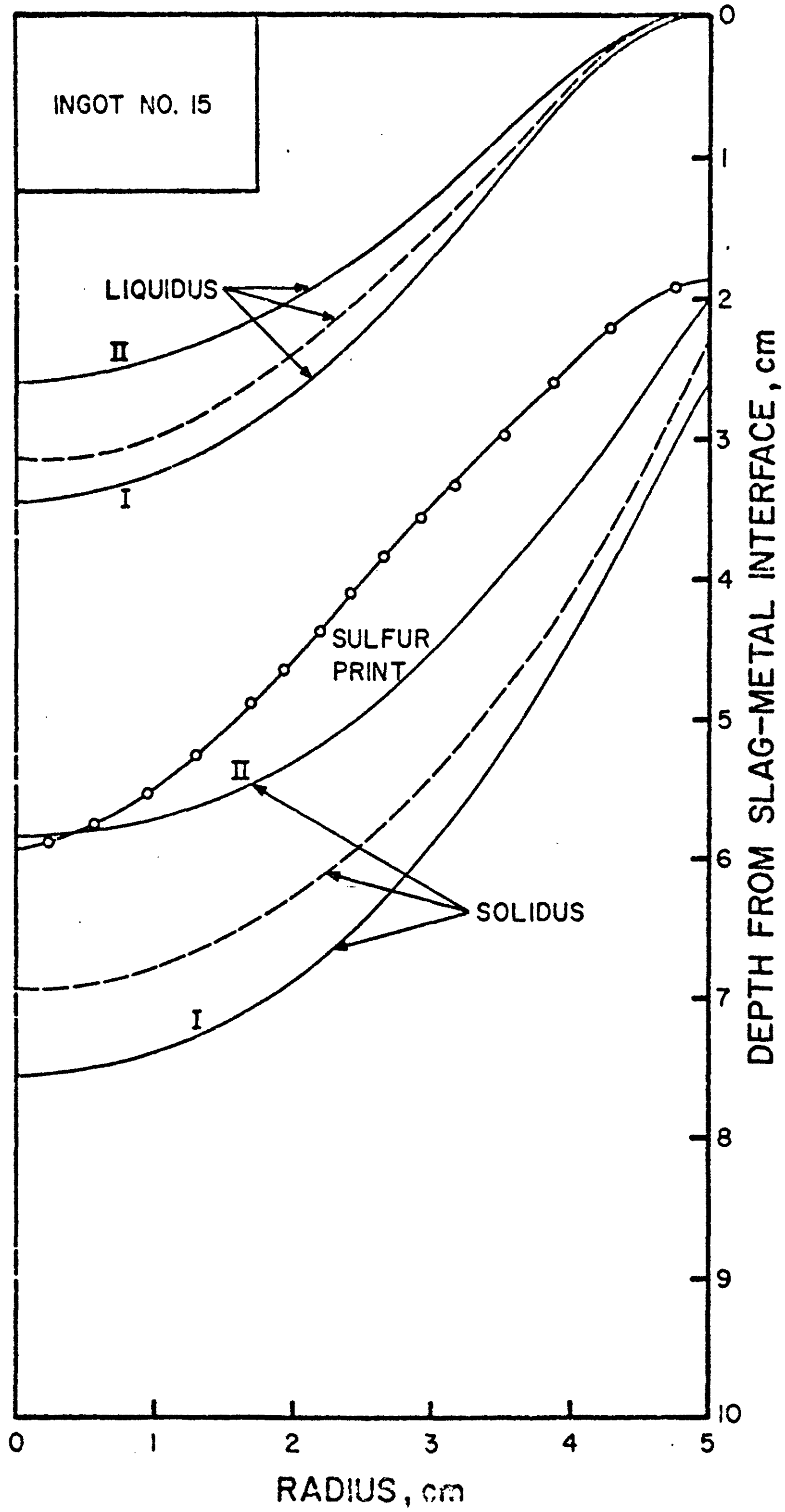

5.12 Computed liquidus and solidus isotherms for ingot 15. -0- sulfur print from Mellberg [57], rest of legends same as in Fig. 5.9.

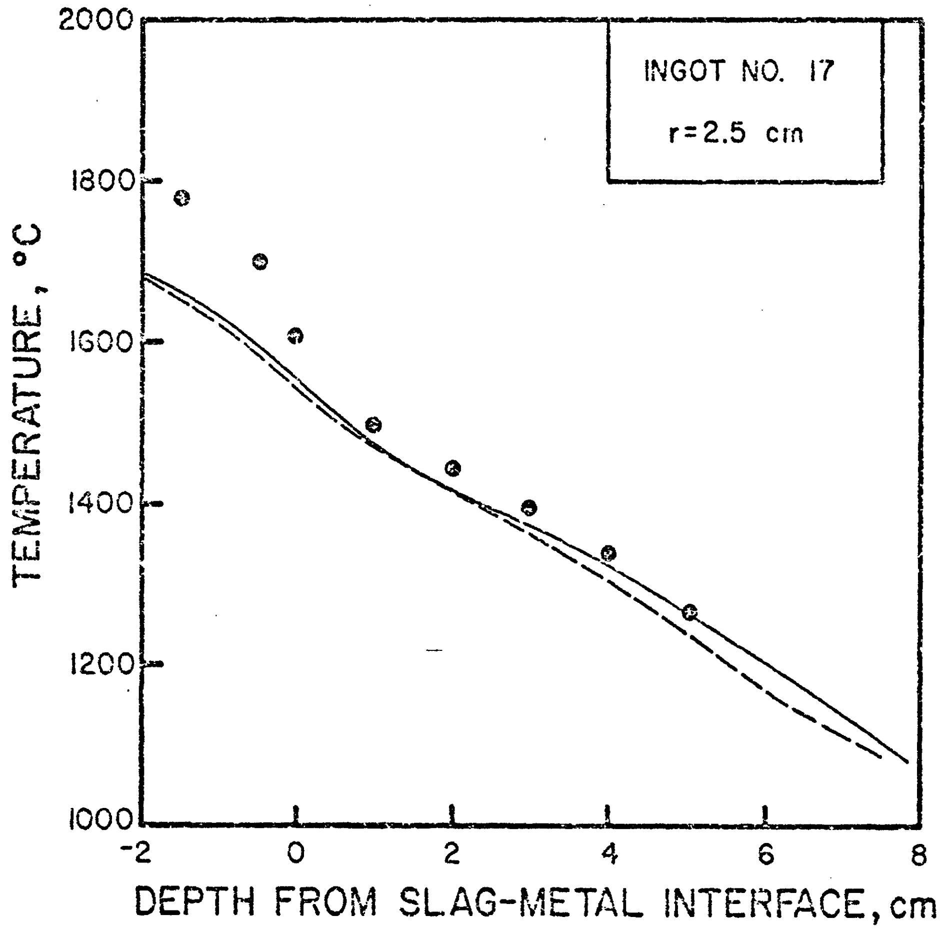

5.13 Computed and measured axial temperature profiles for ingot 17.

—— casting rate (V_c) calculated from the model

--- experimentally measured value of V_c (0.62 m/hr) used as an input to the model

• measured values from Mellberg [57]

the mid-radius position. Here again the solid line represents the predictions for a condition, when the casting rate was computed, while the broken line corresponds to predictions, where the experimentally determined casting rate was used as an input for the model. It is seen once again that there is reasonably good agreement between the measurements and the predictions below the slag-metal interface. The computed liquidus and solidus isotherms for these two cases are shown in Fig. 5.14. Also given for the purpose of comparison are some of the measured locations of the isotherms. It is seen that the solidus and the liquidus lines predicted by the two techniques are comparable, and that there is a somewhat better agreement between measurements and predictions for the case in which the casting rate is calculated from the model (0.64 m/hr vs. measured value of 0.62 m/hr).

Fig. 5.15 shows the computed isotherms in the slag for ingot 15. The solid lines represent calculations with a uniform electrical conductivity of the slag while the broken lines represent calculations with a temperature dependent electrical conductivity. As seen here, the latter case gives a lower maximum temperature (1787 °C vs. 1832 °C for the former case) with a little more uniform distribution. This is as expected since the electrical conductivity of the slag increases with temperature. It is seen that the

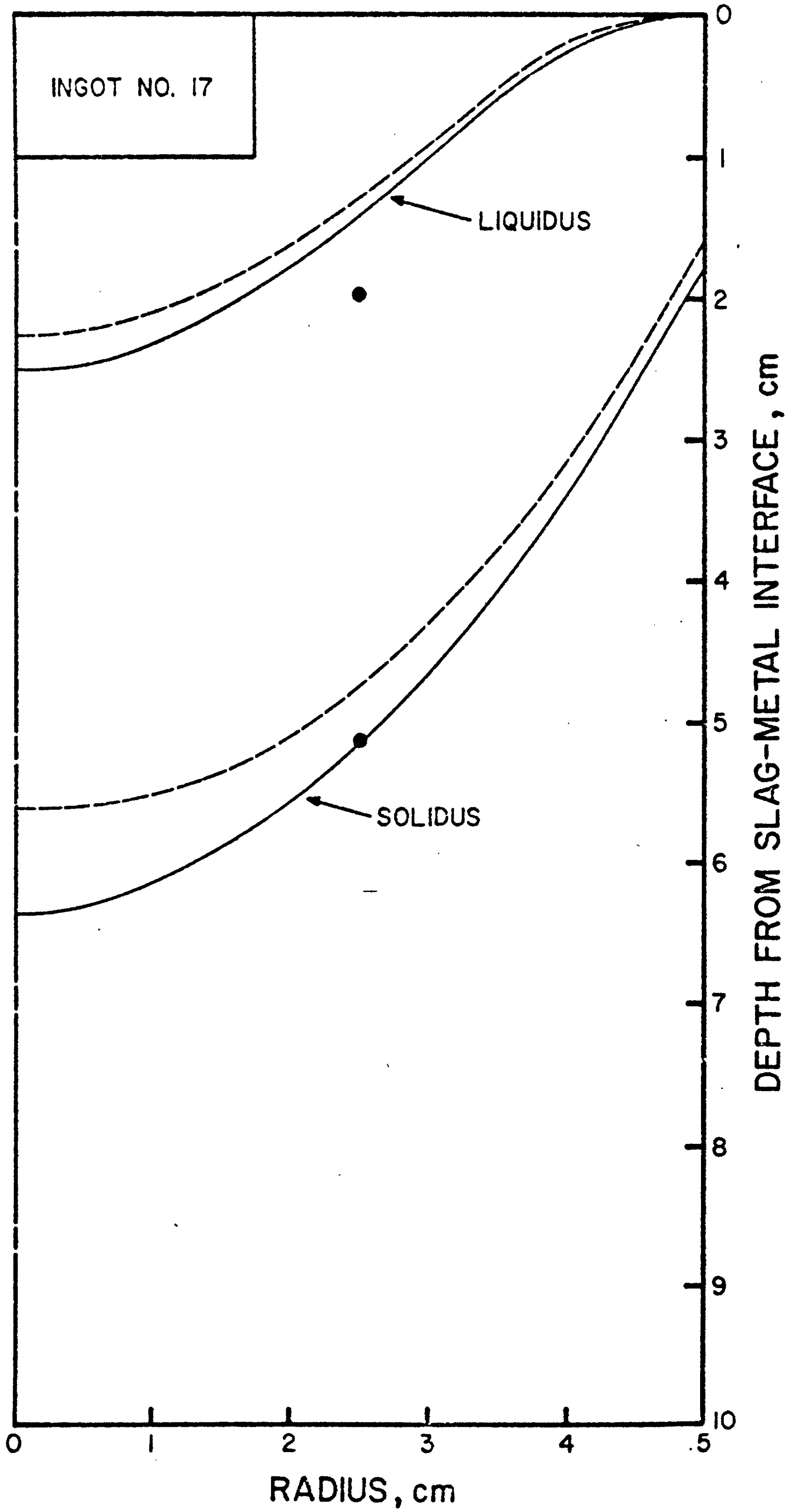

5.14 Computed liquidus and solidus isotherms for ingot 17.
Legends same as in Fig. 5.13.

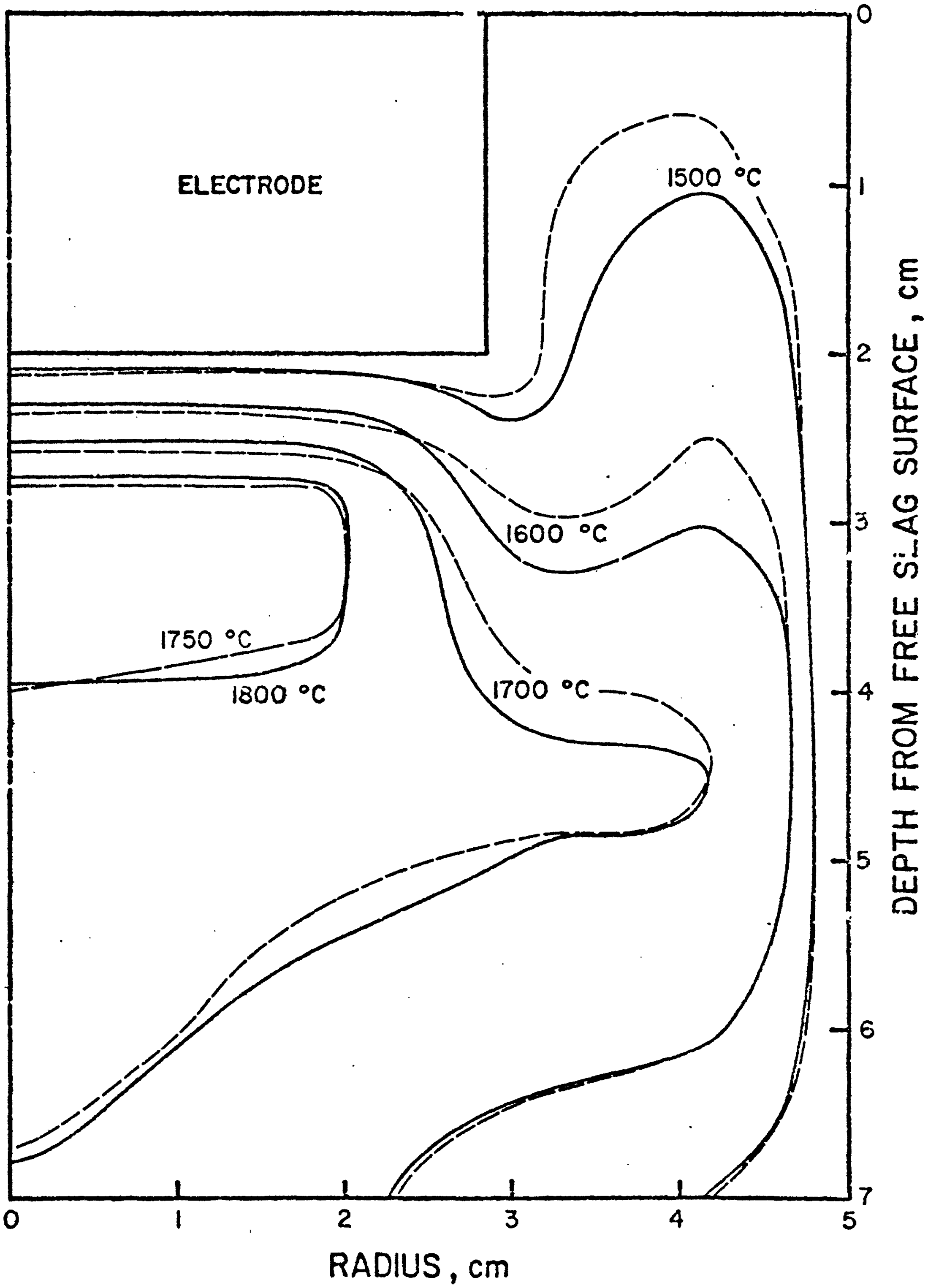

5.15. Computed isotherms in slag for ingot 15.

—— uniform electrical conductivity in slag

---- temperature dependent electrical conductivity in slag hottest region of the system is in the central portion, close to the electrode, but not in the immediate vicinity of the electrode.

It has to be stressed that at the surface of the electrode the temperature in the slag must equal the melting point of the electrode material, hence the positive axial temperature gradient in the immediate vicinity of the electrode. This positive axial temperature gradient is also consistent with the physical requirement that thermal energy has to be transferred from the slag to the electrode.

It should be noted that the temperature profiles depicted in Fig. 5.15 result from the combined effect of Joule heating and the convective fluid flow field in the slag phase. If convection had been neglected, one would have obtained unrealistically high temperatures in the vicinity of the electrode surface. An important effect of this convection, readily seen in Fig. 5.15, is the quite uniform temperature field in the central core of the slag; indeed, most of the temperature gradients appear to be confined to the vicinity of the wall.

This knowledge of the temperature field is of course quite important, if we wish to represent chemical reactions between the droplets and the slag, that may be temperature dependent.

Fig. 5.16 shows the effect of electrode penetration depth in the slag on the isotherms in the slag. The isotherms shown here are computed for an electrode penetration depth of 0.01 m. The amount of slag used (1.5 kg), the input power (73 kW) and the value used for the effective thermal conductivity in the metal pool (30 W/mK) are the same as in the case of Fig. 5.15. Comparing Figures 5.15 and 5.16 reveals that the temperatures in the bulk portion of the slag below the electrode are somewhat reduced when a lower electrode penetration depth is used (maximum temperature 1807 °C vs. 1832 °C for the other case). This is to be expected from the discussions given in connection with Fig. 5.6 where it was shown that a lower penetration depth resulted in a lower volumetric heat generation rate in the bulk portion of the slag. Also the casting rate is now reduced (0.61 m/hr vs. 0.76 m/hr for the other case). As is to be expected from the discussion given in connection with Fig. 5.9, the agreement with measured temperatures below the slag-metal interface was somewhat better. However, the temperature profiles in the ingot are not shown here, for the sake of brevity. Although the immersion depth of the electrode appears to have an important effect on the casting rate and hence on the position of liquidus and solidus isotherms, its effect on the temperature and velocity in

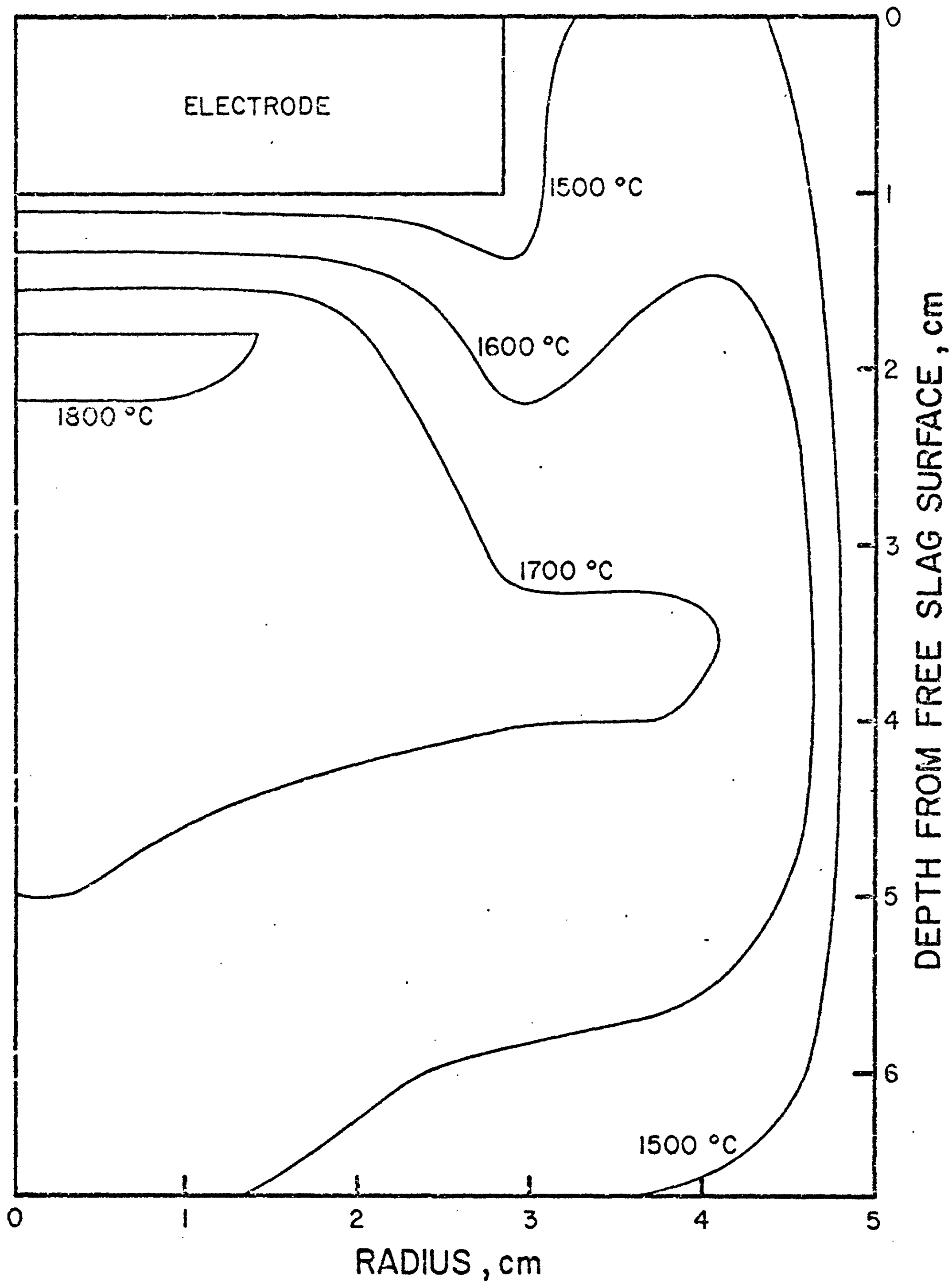

5.16 The effect of electrode penetration depth on temperature distribution in the slag.

the slag is less significant from the global viewpoint. Also, it should be noted that in practice, the immersion depth of the electrode is determined by the process itself. However , this aspect of the ESR process is yet to be modelled.

In the next few figures, calculated results on the flow and turbulent mixing in the slag are discussed. Fig. 5.17 shows the calculated stream lines in the slag for ingot 15. Computed velocity vectors in the slag are presented in Fig. 5.18. It follows from the discussions given in Chapter III that there are two principal forces that drive fluid motion in the slag -- the electromagnetic force field which in the present case would tend to generate an anti-clockwise circulation pattern and the buoyancy force field, which would tend to generate a clockwise circulation pattern in the bulk of the slag. It is seen in Figs. 5.17 and 5.18 that <u>for the case considered</u>, buoyancy forces tend to dominate in the bulk of the slag, producing a clockwise circulation pattern. The anti-clockwise circulation pattern in the annular space between the electrode and the mold results from the combined effects of buoyancy and electromagnetic forces (if buoyancy forces alone acted in the region one would obtain two circulating loops, as caused by a hotter fluid being located between the two cold surfaces, viz the electrode and

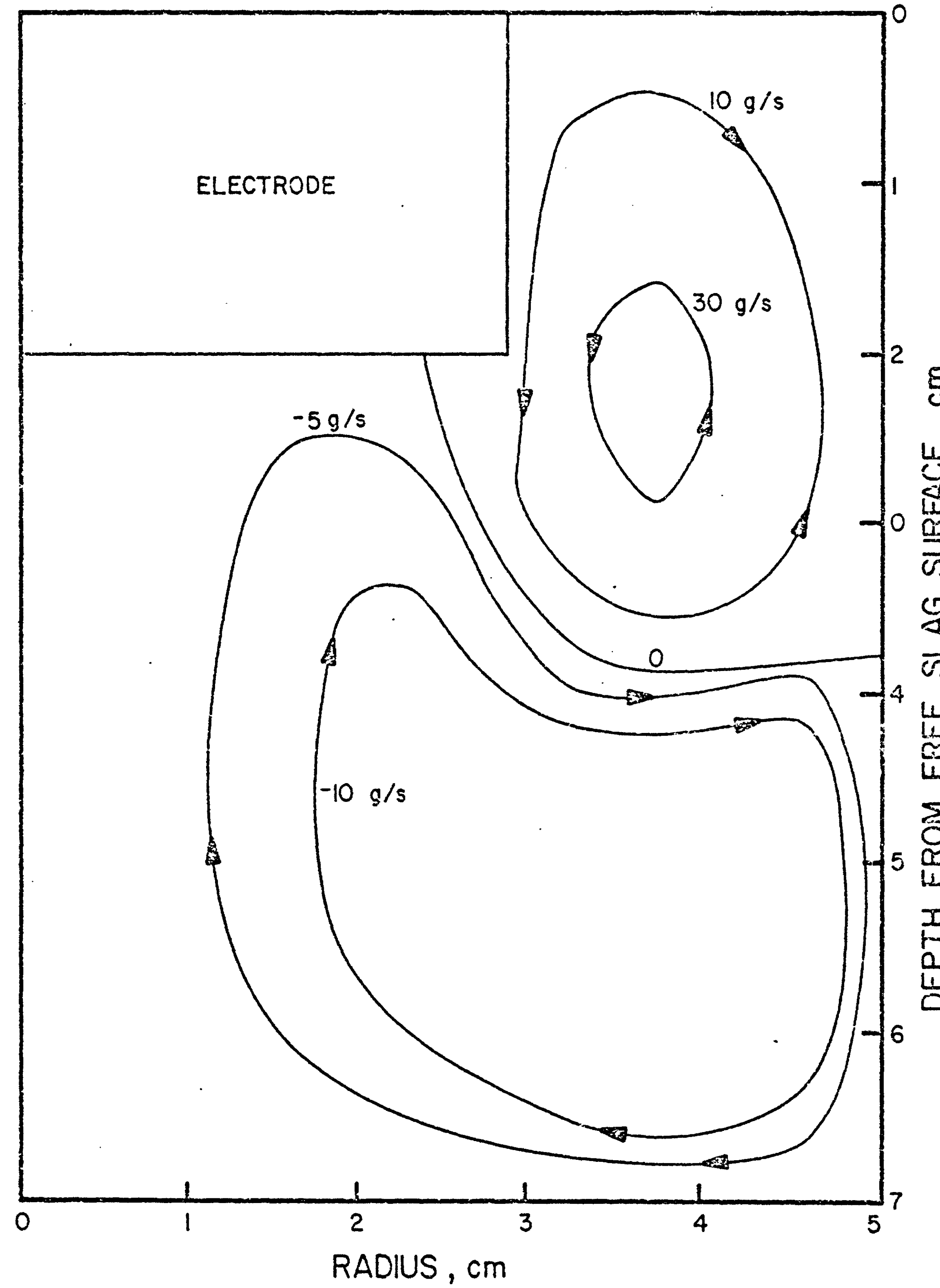

5.17 Computed streamline pattern in slag for ingot 15.

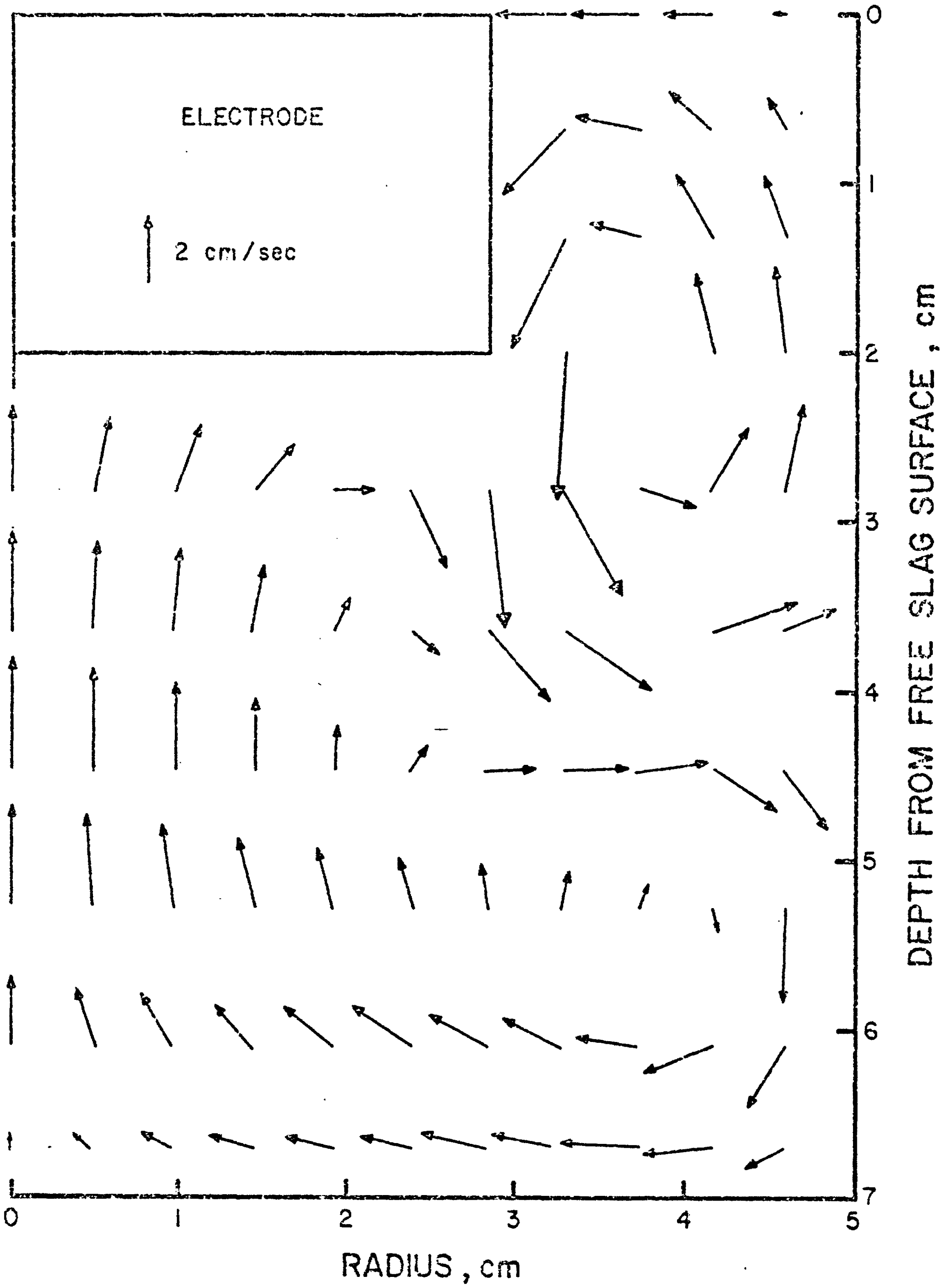

5.18 Computed velocity vectors in slag for operation with 1.7 kA and for a fill ratio of 0.325.

the mold wall). The absolute magnitude of the velocities calculated for the system, viz 0 - 5 cm/s are comparable to computed values reported in earlier papers describing fluid flow in ESR process [13-15].

The circulation is an important characteristic of ESR systems and it would be desirable to define the conditions under which either the electromagnetic or the buoyancy forces dominate the flow field. By dimensional arguments it may be shown that the following group may be used to define the nature of the circulation:

$$\phi = \frac{\mu_0 \bar{I}_0^{\,2}\left(1 - \frac{A_e}{A_m}\right)}{4\pi A_e L \rho \beta g \Delta T} \qquad (5.3)$$

where A_e and A_m are the cross sectional areas of the electrode and the mold respectively, L is the depth of the slag below the electrode, and $\bar{I}_0$ is the rms value of the total current.

The higher the value of ϕ the stronger is the domination of the electromagnetic forces. Thus the relative importance of electromagnetic stirring is increased by increasing the current, decreasing the fill ratio and decreasing the slag depth below the electrode.

These findings seem reasonable on physical grounds, because a diverging current field will produce a stronger J x B force. Extreme examples of this have been found in electroslag welding, using wire electrodes.

Figure 5.19 shows the velocity field computed for an identical current to Fig. 5.18 but for a greatly reduced fill ratio (0.09 as opposed to 0.32 in the previous case). It is clearly seen that under these conditions the flow is now dominated by electromagnetic forces. Also as expected from discussions given in connection with Fig. 5.8, the magnitude of the velocity increases when the fill ratio is decreased.

Fig. 5.20 shows the radial distribution of the ratio of buoyancy/electromagnetic contributions to vorticity, some 0.02 m below the electrode, computed for the cases that have been given in Figs. 5.18 and 5.19.

It is seen that buoyancy forces dominate in the vicinity of the walls because of the very steep radial temperature gradients. However, the curve drawn with the broken line, depicting the behavior of the system shown in Fig. 5.19 clearly indicates that the electromagnetic forces dominate in the central core for that case.

Fig. 5.21 shows the computed values for the turbulence kinetic energy in the slag for ingot 15. The maximum value for this parameter occurs in the annular space between the electrode and the mold and this value

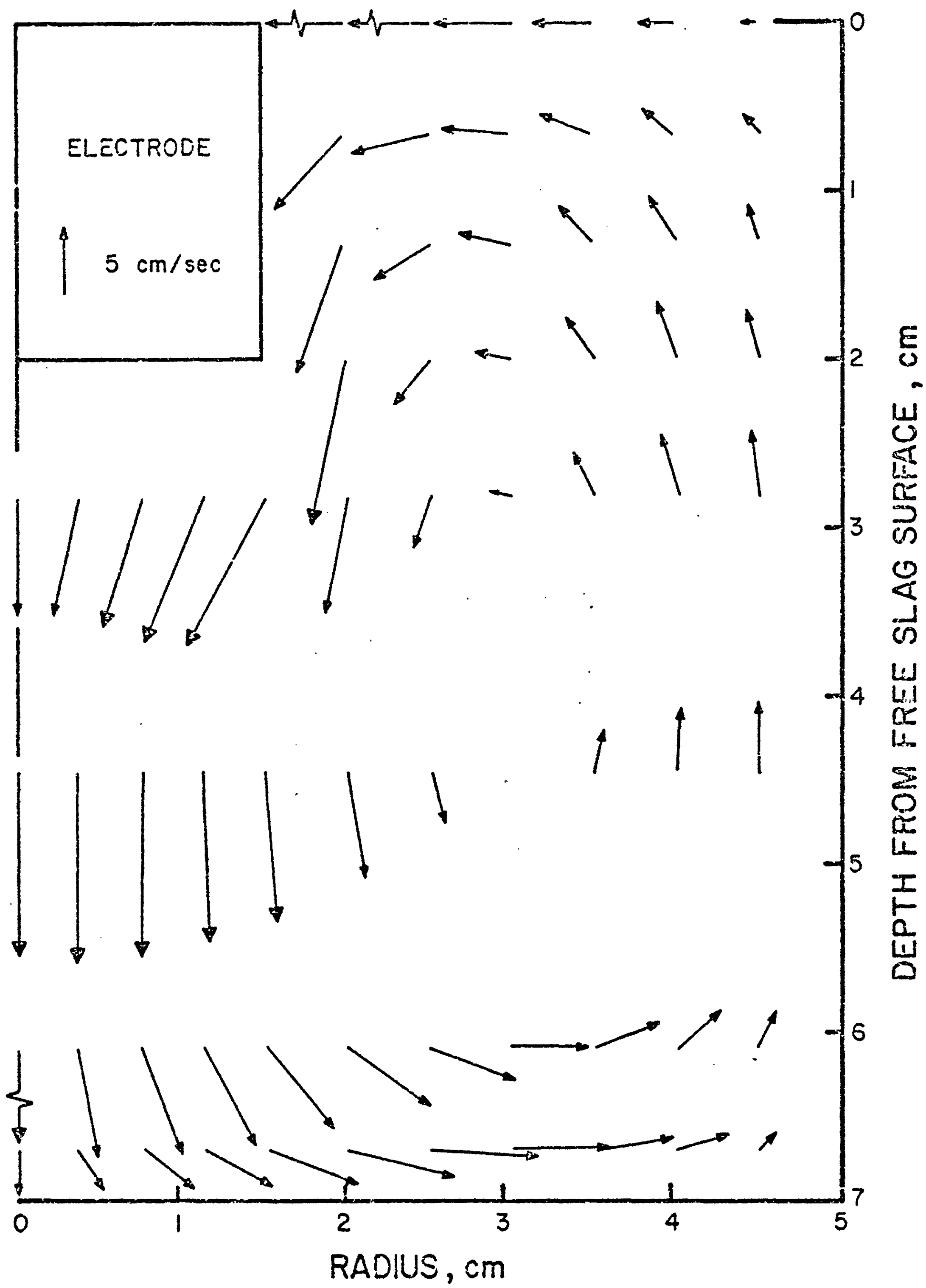

5.19 Computed velocity vectors in slag for operation with 1.7 kA and for a fill ratio of 0.09.

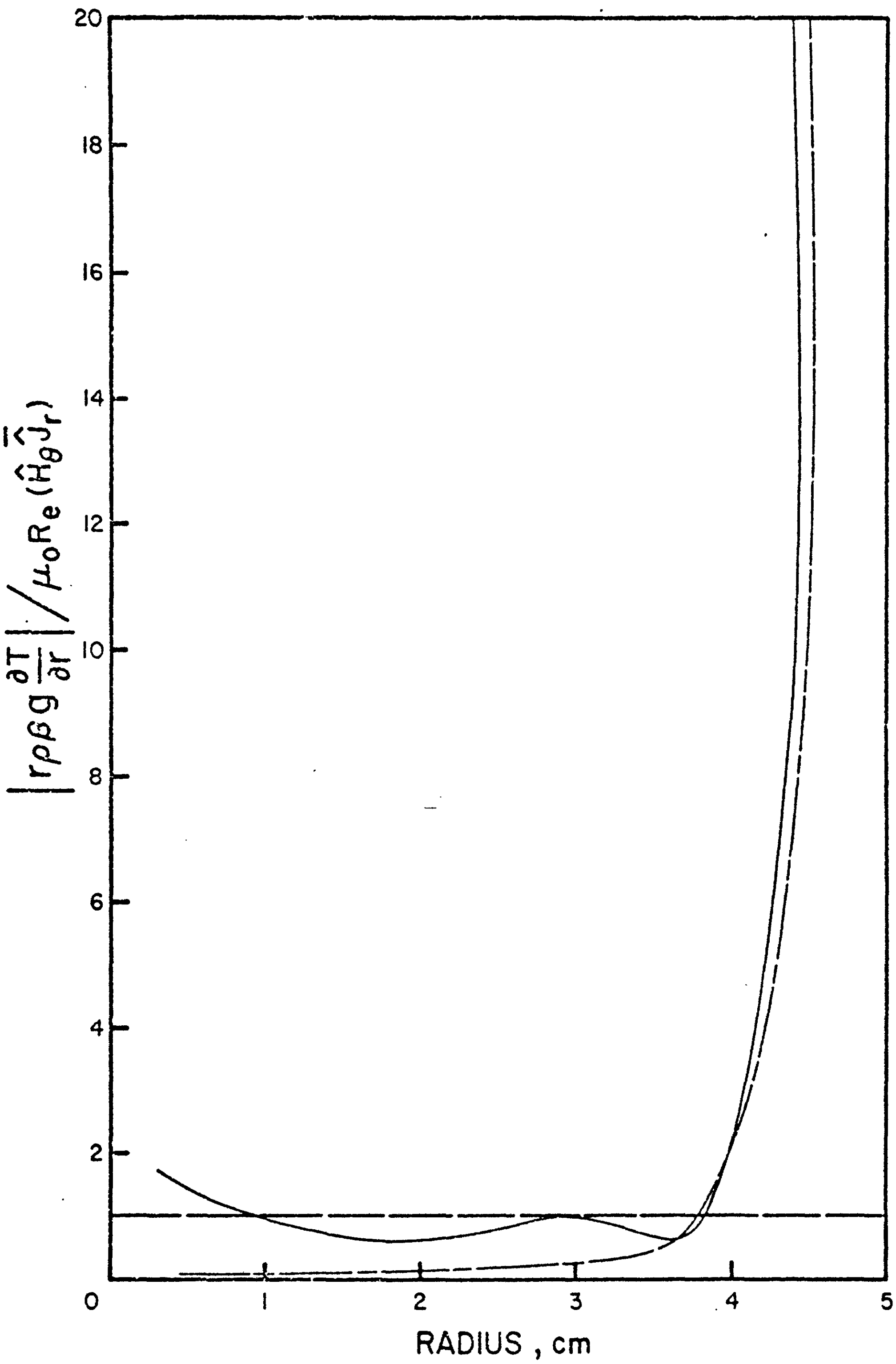

5.20 Radial distribution of buoyancy/electromagnetic contributions to vorticity, 2 cm below the electrode.

——— 1.7 kA, A_e/A_m = 0.325, ϕ [Eq.(5.3)]= 1.75

– – – 1.7 kA, A_e/A_m = 0.09 , ϕ [Eq.(5.3)]= 15

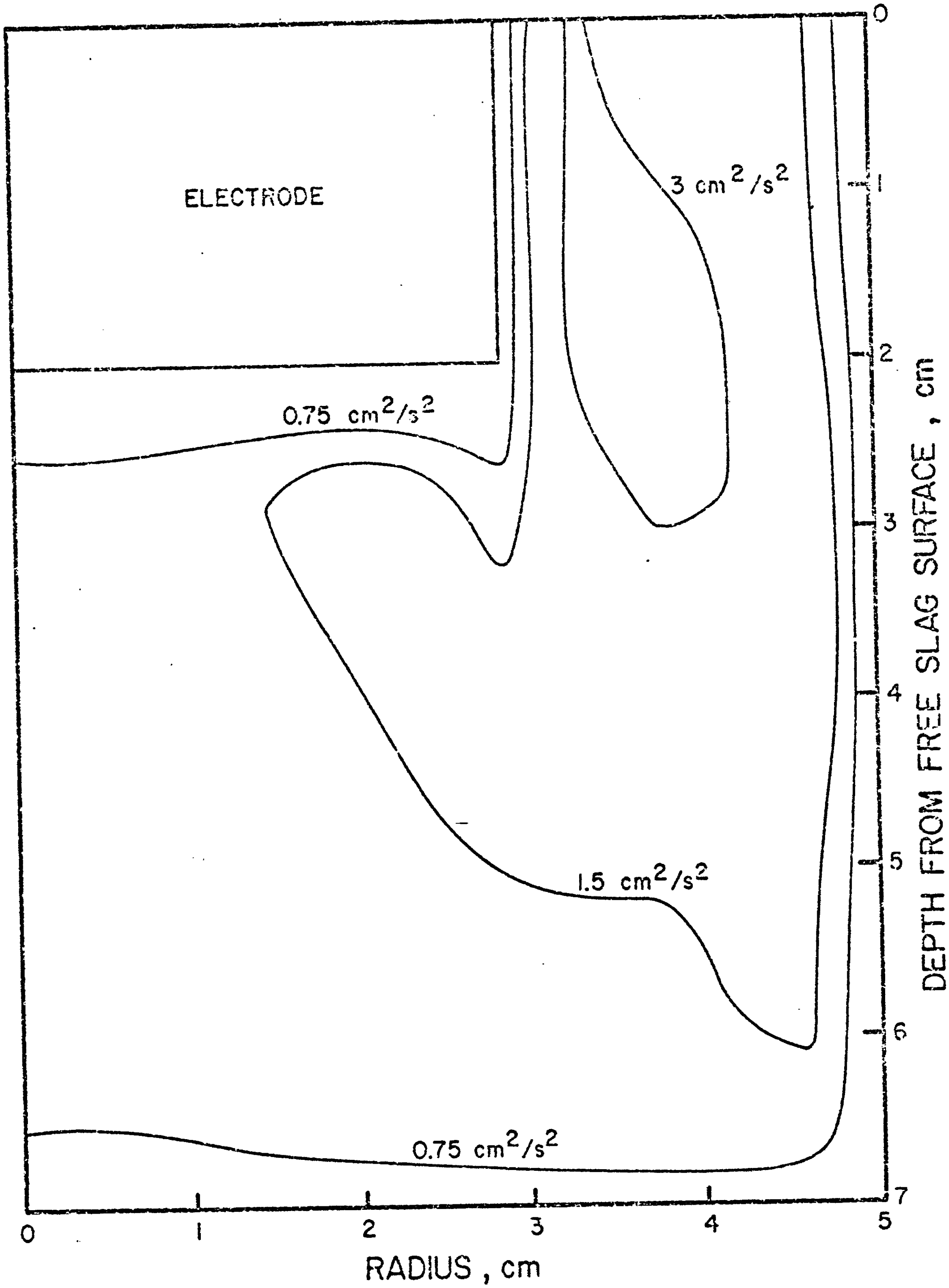

5.21 Computed distribution of turbulence kinetic energy in the slag for ingot 15.

is about 25% of the maximum kinetic energy of the mean motion.

Fig. 5.22 shows a plot of the ratio: effective thermal conductivity/atomic thermal conductivity in the slag for ingot 15. It is seen that the strong convective field does indeed produce turbulent conditions, corresponding to an appreciable enhancement of the effective thermal conductivity. As in the case of Fig. 5.21, the regions of the maximum effective conductivity correspond to the zones where the circulation has its maximum intensity -- a behavior that is consistent with physical reasoning.

The role of the current in determining the shape and the depth of the metal pool is examined in Figs. 5.23 and 5.24. Fig. 5.23 shows computed pool profiles for different current levels. The curves, drawn with the solid line, show that the higher the current, the deeper the pool profile. This finding has been established experimentally a long time ago; however, this is the first time that these experimental findings have been predicated from first principles. The curve drawn with the broken line (2A) depicts the computed pool profile

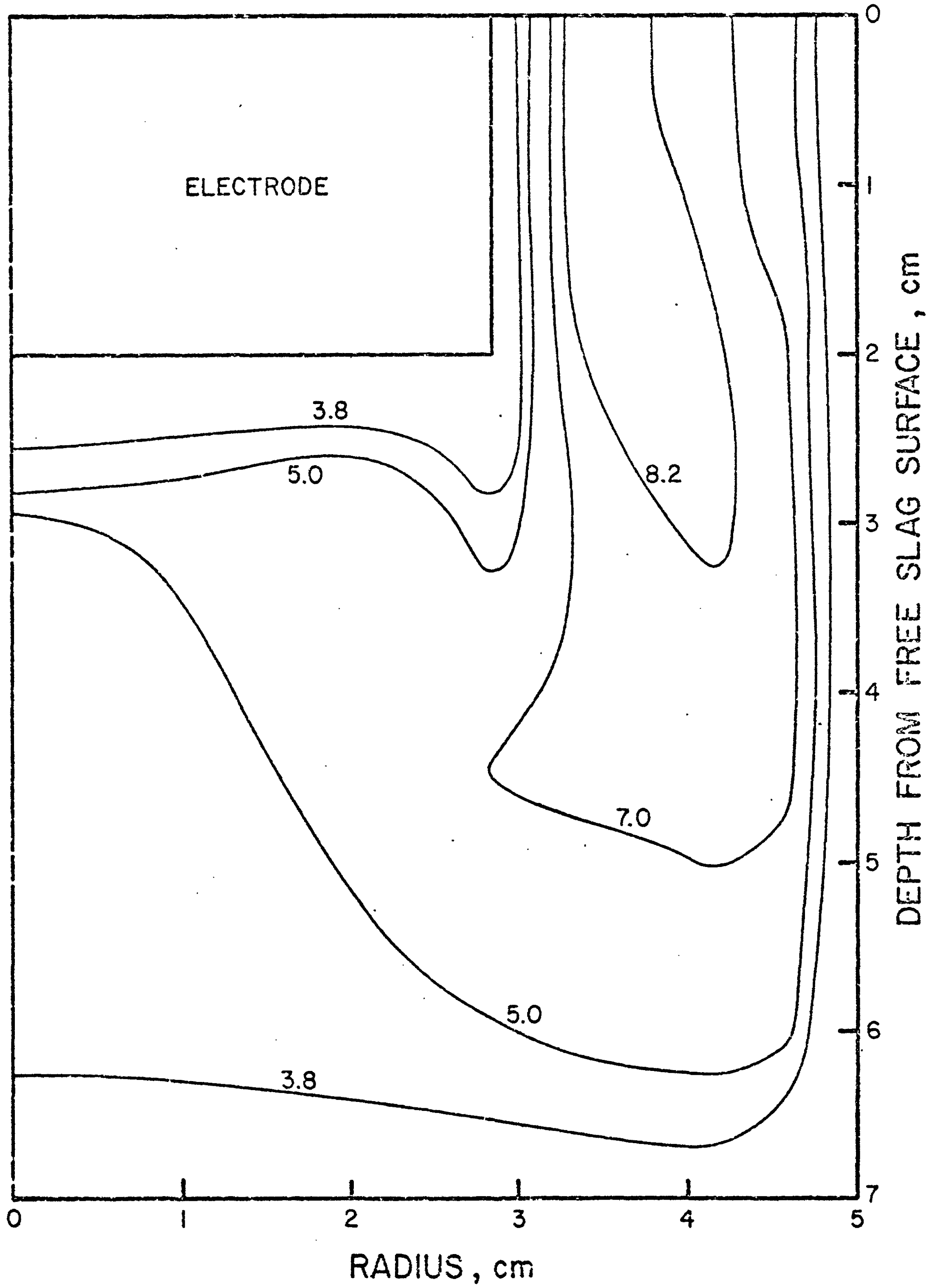

5.22 Computed contours of the ratio effective thermal conductivity/atomic thermal conductivity in the slag for ingot 15.

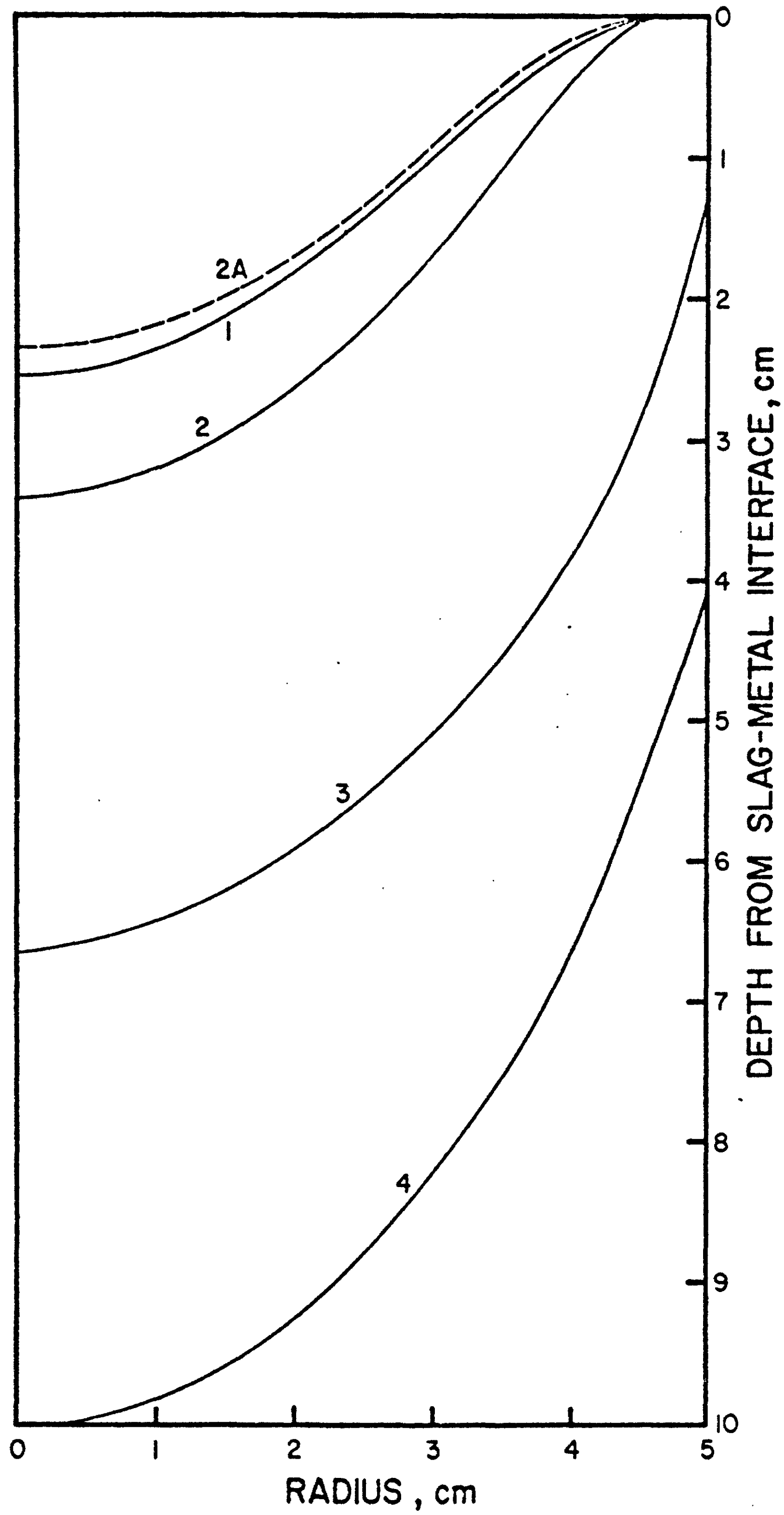

5.23 Computed metal pool depths for different currents.
1. 1.55 kA, 2. 1.7 kA, 3. 2.0 kA, 4. 2.5 kA
In all these cases amount of slag = 1.5 kg.
2A. Same power as 2 (73 kW), amount of slag = 1.9 kg.

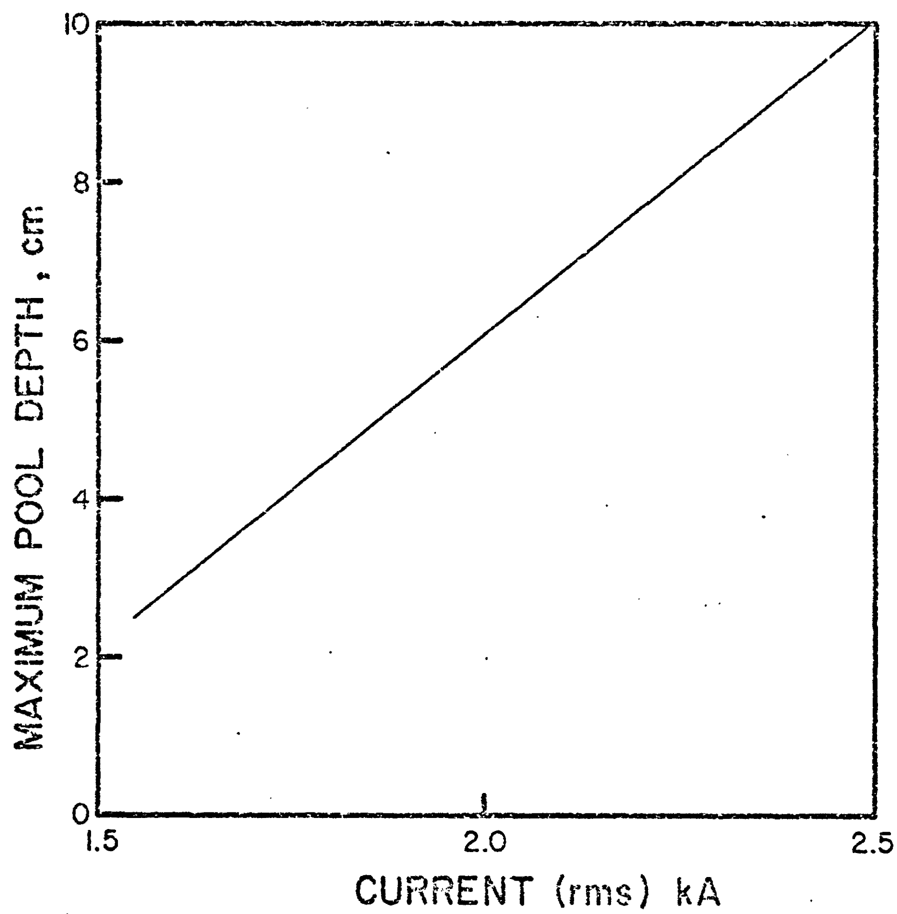

5.24 Variation of maximum pool depth with current.

for identical conditions of power to that given by (2) but for a greater amount of slag present (1.9 kg for the case 2A vs. 1.5 for the case 2). Heat loss from the slag to the mold wall for the case 2A was 30% higher than that for the case 2. This resulted in a smaller pool depth. Fig. 5.24 shows a plot of the computed maximum pool depth against the current used. Over the range examined the relationship is found to be linear. Fig. 5.25 shows a comparison between the theoretically predicted casting rates, as a function of power and the values reported experimentally by Mellberg [57]. It is seen that the agreement is not unreasonable. The predicted relationship between the casting rate and the power is linear. This again is consistent with operating experience [62].

Values for the parameters associated with a metal droplet are shown in Table 5.5. The superheat given this table is for operation with 1.7 kA (i.e. ingot 15). As seen here, the residence time of the droplet in the slag is very small. The average velocity of a droplet (0.28 m/s) is substantially larger than the velocity of slag and therefore the assumption of a quiescent slag made in calculating droplet para-

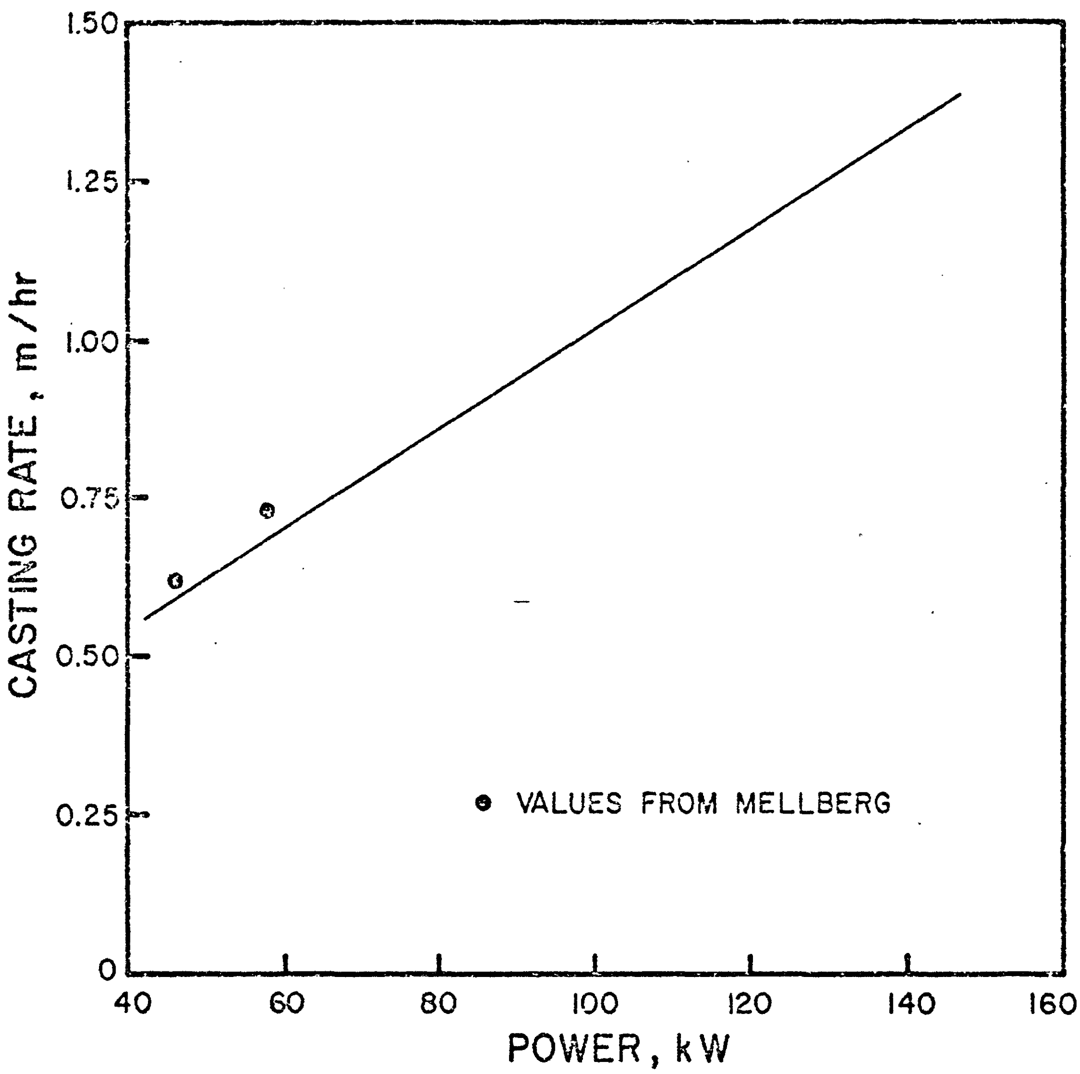

5.25 Variation of casting rate with power
• measured values from Mellberg [57].

Table 5.5 Values for Droplet Parameters

Parameter	Values
diameter, d_d	1.3 cm
residence time, τ	0.18 s
average velocity, $\bar{U}_{av}$	28 cm/s
superheat, $(T_f - T_{m,e})$	72 °C

meters (Section 3.5.4B) is reasonable.

This concludes the discussions of the computed results. The results presented in this chapter were selected to illustrate the predictive capability of the model developed in this work, and to investigate the interdependence of key process parameters. Concluding remarks are made in the next chapter.

CHAPTER VI

CONCLUSIONS AND SUGGESTIONS FOR FURTHER WORK

In this chapter concluding remarks are made and some suggestions are made for further work in mathematical modelling of ESR process.

6.1 Conclusions

In the work reported in this thesis a mathematical model has been developed to describe electromagnetic field, fluid flow, heat transfer and solidification phenomena in ESR systems. The model involved the simultaneous statement of Maxwell's equations, equations for turbulent flow and the differential thermal energy balance equations. These equations were first written in vectorial forms so that some general conclusions could be drawn regarding the behavior of ESR systems. Then the equations were presented in the cylindrical coordinate system with axial symmetry. The limitations of the model are inherent in the assumptions made in developing the model. While these assumptions are detailed in Section 3.3, some of the principal shortcomings of the model in its present form are as follows:

(1) Fluid flow equations are solved in the slag only. Motion in the metal pool is accounted for by using an effective thermal conductivity. However, as discussed in section 5.2, an attempt is made to deduce this parameter in the model itself.

(2) The model assumes a predetermined shape (flat) for the melting tip of the electrode and a known electrode penetration depth in the slag. Ideally these parameters should be calculated using the mathematical model. However, this refinement can be made only if a more realistic understanding is developed of the melting process.

(3) A constant value is used for the electrical conductivity of the slag. In some of the calculations presented in Chapter 5, an approximate allowance has been made for the temperature dependence of this parameter.

(4) Effects associated with chemical and electrochemical reactions are not considered.

On the positive side, the model accomplishes the following:

(1) It allows for turbulent flow in slag as caused by both electromagnetic and natural convection forces.

(2) It accounts for the spatial distribution of heat generation rate, the transport of heat by the metal droplets falling through the slag and for the movements of the ingot and the electrode.

(3) By integrating transport processes taking place in different portions of an ESR system, the model allows predictive relationships to be developed among key process parameters.

The governing differential equations developed in Chapter III were solved using a numerical technique outlined in Chapter IV to provide current distribution, velocity and temperature profiles for a laboratory scale system used by Mellberg[57]. In general the theoretical predictions for the temperature profiles and for the pool profiles were found to be in reasonable agreement with the experimental measurements, thereby indicating experimental support for the model.

The predictive capacity which is inherent in this model enables one to develop theoretical relationships predicting the interdependence of the key process parameters. For example, it has been possible to relate the heat generation pattern, the temperature and the velocity fields, the melting rate and the pool profiles to the operating power and current and to the geometry of the system.

The principal findings may be summarized as follows:

(1) The temperature at the slag-metal interface was found to be strongly spatially dependent. As seen from the work reported by Kreyenberg and Schwerdtfeger [16], the computed temperature and velocity distributions in the slag are strongly affected by the assumed temperature distribution at this interface and therefore it should be computed by the model rather than being specified arbitrarily.

(2) It was found that for a fixed geometry, the higher the current, the deeper was the pool profile; this

mode of operation also resulted in a faster casting rate. Over the range of parameters used in the computation, the relationship between maximum pool depth and the current and the relationship between casting rate and power were found to be linear.

(3) A deeper slag bath results in a larger heat loss through the mold wall. Thus for the same input power, a larger amount of slag gives rise to a lower pool depth.

(4) The depth of penetration of the electrode was found to have some effect on the slag temperature; more specifically the lower the penetration, the lower the slag temperature in the bulk and hence the lower the casting rate. However as mentioned before, in practice the electrode penetration is a factor that is determined by the process itself and this aspect of the problem is yet to be modelled.

(5) The model enables us to distinguish between the role buoyancy forces and electromagnetic forces play in driving the flow in the slag phase. It was found that the higher the current and the smaller the fill ratio, the more important was the role of electromagnetic forces. It has to be stressed, however, that in general, both these forces could play an important role in determining the flow field.

(6) The temperature distribution in the slag was found to be quite uniform with strong gradients in the vicinity of solid walls.

(7) The use of a temperature dependent electrical conductivity for slag gave a reduced maximum temperature in the slag and a somewhat more uniform temperature distribution. This resulted in a lower amount of heat being transported to the electrode and thus in a reduced casting rate.

(8) The ratio of effective/atomic thermal conductivity in the metal pool, computed according to suggestion outlined in section 5.2 was found to lie in the range of 1.7 to 4.5. This is consistent with values deduced from experimental works [6].

In closing, it is worthwhile to comment briefly on the principal differences and similarities between the present work and the earlier work reported by Dilawari and Szekely [13-15]. As mentioned in Chapter II, in the earlier work, the electromagnetic field, the fluid flow field and the temperature field were represented for an ESR system for a predetermined and idealized pool shape and size. Heat transfer phenomena in the mushy zone and in the ingot were ignored. While many of the transport equations and the boundary conditions used in the present work are identical to those used in the earlier work, the advances made in the present work are as follows:

(1) The shape and the size of the molten metal pool is no longer specified but calculated by solving heat transfer equations in the mushy zone and in the ingot. The present work allows for the incorporation of solidification models to represent the release of latent heat in the mushy zone.

(2) The model allows for the first time for a comparison to be made between the measured and the predicted pool profiles and temperature fields in the ingot.

(3) A more up-to-date model is used to represent the turbulent viscosity and the turbulent thermal conductivity in the slag. The model allows for special treatment of flow and heat transfer phenomena in the near wall regions.

6.2 Suggestions for Further Work

From the point of view of mathematical modelling, ESR process represents a fascinating, if complex, group of problems. The model described in this work was an attempt at grouping together the salient features of current distribution, fluid flow and heat transfer phenomena so that the model could be used to investigate the interdependence of key process parameters. A few suggestions are given here for some further work in the area of modelling of ESR process. The suggestions given here are limited to mathematical modelling but it should be recognized that physical modelling is a vast and extremely important area and that there is a need for a strong interaction between the two.

6.2.1 Suggestions for short term plans

These include the following:

(1) In the work reported in this thesis, limited measurements on a laboratory scale system were used. It would be desirable to have some measurements, specially on temperature distribution in the slag, available for a large scale system so as to be able to test the predictions of the model for this system.

(2) The model, in its present form, uses an effective thermal conductivity to account for convective heat transfer in the metal pool. The model can be extended to calculate flow in the metal pool. To achieve this it will be advantageous to employ a numerical scheme of the type used by Elliott and Maulvault [11] below the slag-metal interface.

(3) An attempt can be made to use the information on velocity and temperature distribution generated by the model in developing a kinetic model.

6.2.2 Suggestions for long term plans

These include the following:

(1) There is a strong need for both experimental and analytical work in order to develop a realistic under-

standing of melting phenomena at the slag-electrode interface.

(2) The model developed in this work can be extended to calculate fluid flow in the mushy zone so that it can be used to calculate macrosegregation in the ingot.

(3) Some preliminary calculations can be made for multiple electrode configurations. The modelling of multiple electrode system represents a major additional difficulty, because under these conditions axial symmetry is no longer observed.

(4) An approach similar to the one described in this thesis can be used to model the electroslag casting process.

APPENDIX A

A BRIEF NOTE ON PHASOR NOTATION

In dealing with sinusoidally time-varying quantities it is convenient to use phasor approach. A phasor is a complex number which can be represneted graphically as shown in Fig. A 1. The length of the line is equal to the magnitude of the complex number and the angle that the line makes with the positive real axis is the angle of the complex number. For example when the functional form is cosinusoidal, i.e. $A \cos(\omega t + \phi)$, the magnitude of the phasor is equal to the magnitude A of the cosinusoidal function and the angle of the phasor is equal to the phase angle ϕ of the function for $t = 0$. The real part of the phasor is $A \cos\phi$ which is the value of the function at $t = 0$. As seen from Fig. A.1, if the phasor is rotated about the origin in the counter-clockwise direction at the rate of ω rad/s, the time variation of its projection on the real axis describes the time variation of the cosinusoidal function. Using the terminology adopted in Chapters III and IV, a cosinusoidal function f can be represented, in phasor notation, as

$$f = \text{Re}\,[\hat{A}\, e^{j\omega t}] \tag{A.1}$$

where

$$\hat{A} = |\hat{A}|\, e^{j\phi} \tag{A.2}$$

$|A|$ = magnitude of the phasor at $t = 0$.

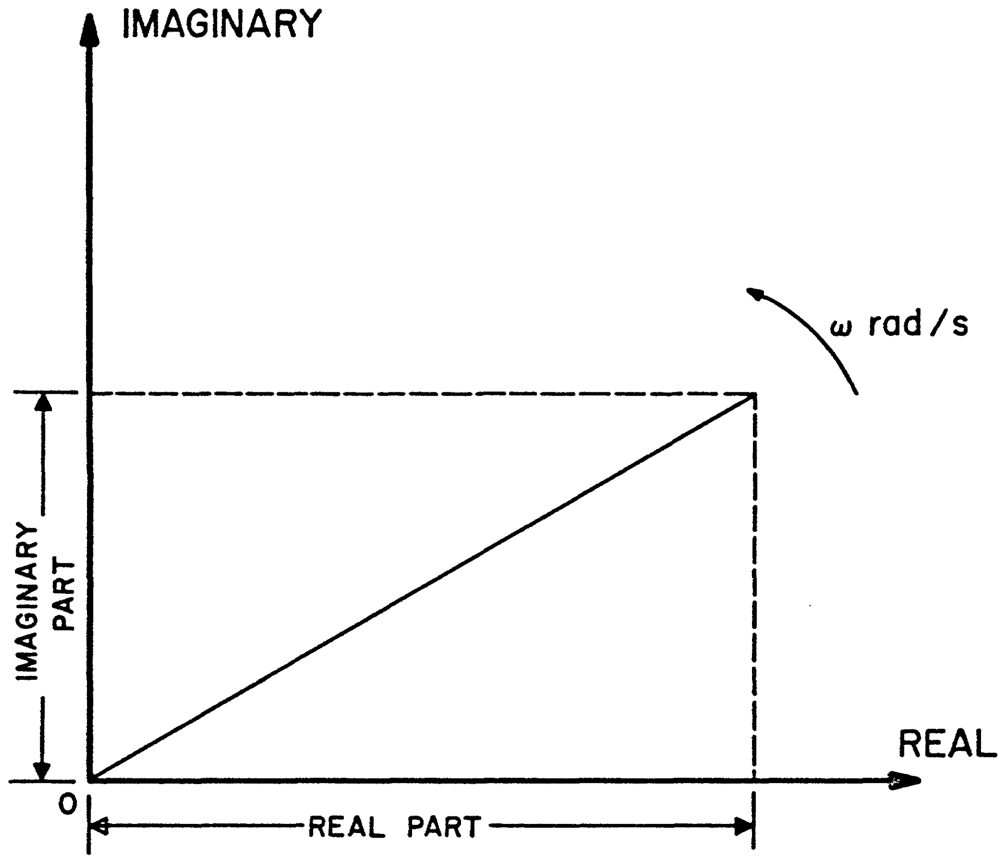

A.1 Graphical representation of a phasor.

Similar considerations hold when dealing with sinusoidally time-varying vectors.

To illustrate the application of phasor concept, let us derive the expression for time average electromagnetic body force component F_z [i.e. Eq. (3.15b)]. From Eq. (3.10), the instantaneous value of this quantity can be written, in phasor notation, as

$$F_z' = \mu_0 \, \mathrm{Re}(\hat{H}_\theta \, e^{j\omega t}) \times \mathrm{Re}(\hat{J}_r \, e^{j\omega t}) \tag{A.3}$$

$$= \mu_0 \, |\hat{H}_\theta| \cos(\omega t + \phi_1) \times |\hat{J}_r| \cos(\omega t + \phi_2)$$

$$= \mu_0 \, |\hat{H}_\theta||\hat{J}_r| \, [\cos(\omega t + \phi_1) \cos(\omega t + \phi_2)]$$

$$= \frac{1}{2}\mu_0 \, |\hat{H}_\theta| \, |\hat{J}_r| \, [\underbrace{\cos(2\omega t + \phi_1 + \phi_2)}_{\mathrm{I}} + \underbrace{\cos(\phi_1 - \phi_2)}_{\mathrm{II}}] \tag{A.4}$$

The time-average value can be found as follows:

$$F_z = \frac{1}{T} \int_0^T F_z' \, dt \tag{A.5}$$

where T is the period.

The time-average value of the first term in Eq. (A.4) is equal to zero, thus

$$F_z = \frac{1}{2}\mu_0 \, |\hat{H}_\theta| \, |\hat{J}_r| \cos(\phi_1 - \phi_2)$$

$$= \frac{1}{2}\mu_0 \, \mathrm{Re}[\, |\hat{H}_\theta| \, |\hat{J}_r| \, e^{j(\phi_1 - \phi_2)}]$$

$$F_z = \frac{1}{2}\mu_0 \, \mathrm{Re}[\, |\hat{H}_\theta| \, e^{j\,\phi_1} \cdot |\hat{J}_r| \, e^{-j\phi_2}]$$

$$= \frac{1}{2}\mu_0 \, \mathrm{Re}(\hat{H}_\theta \bar{J}_r) \qquad (3.15b)$$

where $\bar{J}_r$ is the complex conjugate of $\hat{J}_r$.

Following a similar approach, expressions can be derived for other time-averaged parameters such as F_r [Eq. (3.15a)], Q_j [Eq. (3.16)], etc.

APPENDIX B

BOUNDARY CONDITIONS ON VORTICITY

In this appendix, expressions will be derived for vorticity at the axis of symmetry and at the walls.

B.1 Vorticity at the Axis of Symmetry [39]

Form Eq. (3.23b) in the text,

$$\overline{V}_z = \frac{1}{\rho r} \frac{\partial \psi}{\partial r}$$

It follows that in order for $\overline{V}_z$ to be finite at $r = 0$, $\frac{\partial \psi}{\partial r}$ must tend to zero at the same rate as r near the axis. It follows that in the immediate vicinity of the axis, the $\psi \sim r$ distribution is parabolic. Furthermore, because of symmetry the second term in the $\psi \sim r$ expansion should be the fourth power one; thus:

$$\psi - \psi_0 \simeq ar^2 + br^4 \qquad \text{(B.1)}$$

where ψ_0 is the stream function at the axis and a and b are constants for a fixed z.

Using the definition of vorticity [Eq. (3.22)], the symmetry condition $\overline{V}_r = 0$ at the $r = 0$ and Eq. (B.1) we can write

$$\xi = -\frac{8br}{\rho} \qquad \text{(B.2)}$$

Thus $\xi = 0$ at $r = 0$, $\frac{\xi}{r}$ on the other hand is finite. If 1 and 2 denote the nodes which are once and twice removed from the node 0 on the symmetry axis, we can evaluate b from

$$\psi_1 - \psi_0 = ar_1^2 + br_1^4$$

$$\psi_2 - \psi_0 = ar_2^2 + br_2^4 \qquad \text{(B.3a,b)}$$

Then Eq. (B.2) gives;

$$\left(\frac{\xi}{r}\right)_0 = \frac{8}{\rho}\left[\frac{\psi_0 - \psi_2}{r_2^2} + \frac{\psi_1 - \psi_0}{r_1^2}\right]/(r_2^2 - r_1^2) \qquad \text{(3.89b)}$$

B.2. Vorticity at a Wall [53]

Let us illustrate the calculation of wall vorticity w·r·t slag-electrode interface. As seen in Fig. B.1, 0 is a node on the wall and 1 is the adjacent node in the z-direction. Using Taylor series expansion, the value of stream function at node 1, ψ_1 can be expressed as

$$\psi_1 = \psi_0 + \frac{\partial\psi}{\partial z}\Big|_0 \Delta + \frac{1}{2}\frac{\partial^2\psi}{\partial z^2}\Big|_0 \Delta^2 + \frac{1}{6}\frac{\partial^3\psi}{\partial z^3}\Big|_0 \Delta^3 + 0(\Delta^4) \qquad \text{(B.4)}$$

where $\Delta = z_1 - z_0$ (B.5)

From Eq. (3.23a)

$$\frac{\partial\psi}{\partial z}\Big|_0 = -\rho r\overline{V}_r\Big|_0 = 0 \qquad \text{(B.6)}$$

(no slip condition)

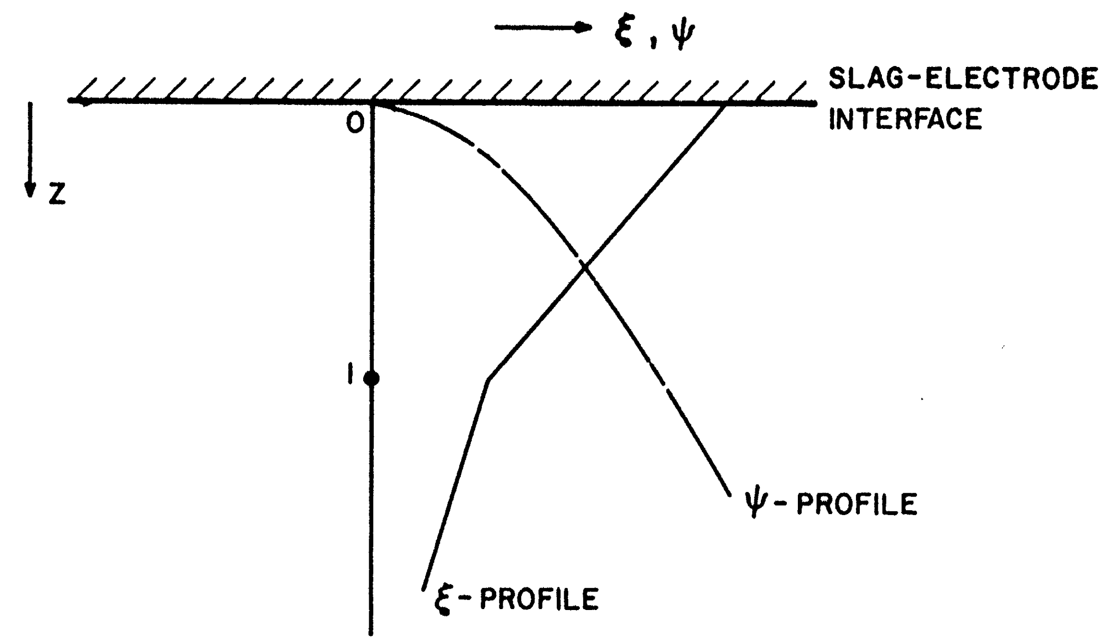

B.1 Evaluation of wall vorticity.

and $$\frac{\partial^2\psi}{\partial z^2}\Big|_0 = -\rho r \frac{\partial \overline{V}_r}{\partial z}\Big|_0 \tag{B.7}$$

From Eq. (3.22)

$$\xi\big|_0 = \frac{\partial \overline{V}_r}{\partial z}\Big|_0 - \cancelto{0}{\frac{\partial \overline{V}_z}{\partial r}\Big|_0}$$

$$= -\frac{1}{\rho r}\frac{\partial^2\psi}{\partial z^2}\Big|_0 \tag{B.8}$$

Thus from Eq. (B. 8) we can write

$$\frac{\partial^2\psi}{\partial z^2}\Big|_0 = -\rho r\, \xi\big|_0 \tag{B.9}$$

and $$\frac{\partial^3\psi}{\partial z^3}\Big|_0 = -\rho r \frac{\partial \xi}{\partial z}\Big|_0 \tag{B.10}$$

Using Eqs. (B.6), (B.9) and (B.10) in Eq. (B.4) gives

$$\psi_1 = \psi_0 - \rho r \left[\frac{1}{2}\xi_0 + \frac{1}{6}\frac{\partial \xi}{\partial z}\Big|_0 \Delta\right] \Delta^2 \tag{B.11}$$

If as shown in Fig. B.1, ξ is taken as varying linearly with z in the vicinity of the wall,

$$\frac{\partial \xi}{\partial z}\Big|_0 \Delta = (\xi_1 - \xi_0) \tag{B.12}$$

Solving for ξ_0 from Eq. (B.11) then gives,

$$\left(\frac{\xi}{r}\right)_0 = \frac{3(\psi_0 - \psi_1)}{\rho r^2 (z_1 - z_0)^2} - \frac{1}{2}\left(\frac{\xi}{r}\right)_1 \tag{3.91c}$$

Following an identical approach, expression for vorticity at the slag-metal interface can be derived. For the vertical surfaces, (i.e. $r = R_e$, $Z_1 \leq z \leq Z_2$ and $r = R_m$, $Z_1 \leq z \leq Z_3$), a similar approach is used but instead of assuming a linearly varying vorticity, the vorticity transport equation is used to give an expression for the normal gradient of vorticity at the wall.

APPENDIX C

CALCULATION OF RADIATION VIEW FACTORS

In this appendix, radiation view factors appearing in Eqs. (3.97) and (3.99) are calculated using the compilation made by Leunberger and Person [54] for finite coaxial cylinders. Fig. C.1 shows a schematic representation of the system for calculating view factors. Symbols s, e, m and t represent free surface of the slag, outer surface of the electrode, inner surface of the mold and top (open) surface respectively.

View factors are calculated with the aid of "view factor algebra" which relies on the reciprocity rule and on the fact that radiation is conserved. According to Leunberg and Person [54]

$$F_{es}(z) = \frac{1}{2\pi}\left[\cos^{-1}\frac{A_2}{A_1} - \frac{x}{R_e}\left\{\frac{A_3}{\sqrt{A_3^2 - 4R_e^2R_m^2}}\cos^{-1}\frac{A_2}{A_1}\frac{R_e}{R_m} - \cos^{-1}\frac{R_e}{R_m}\right\}\right] \qquad (C.1)$$

where

$$A_1 = x^2 + R_m^2 - R_e^2$$

$$A_2 = x^2 - R_m^2 + R_e^2$$

$$A_3 = x^2 + R_m^2 + R_e^2$$

$$x = L - z \qquad (C.2,3,4,5)$$

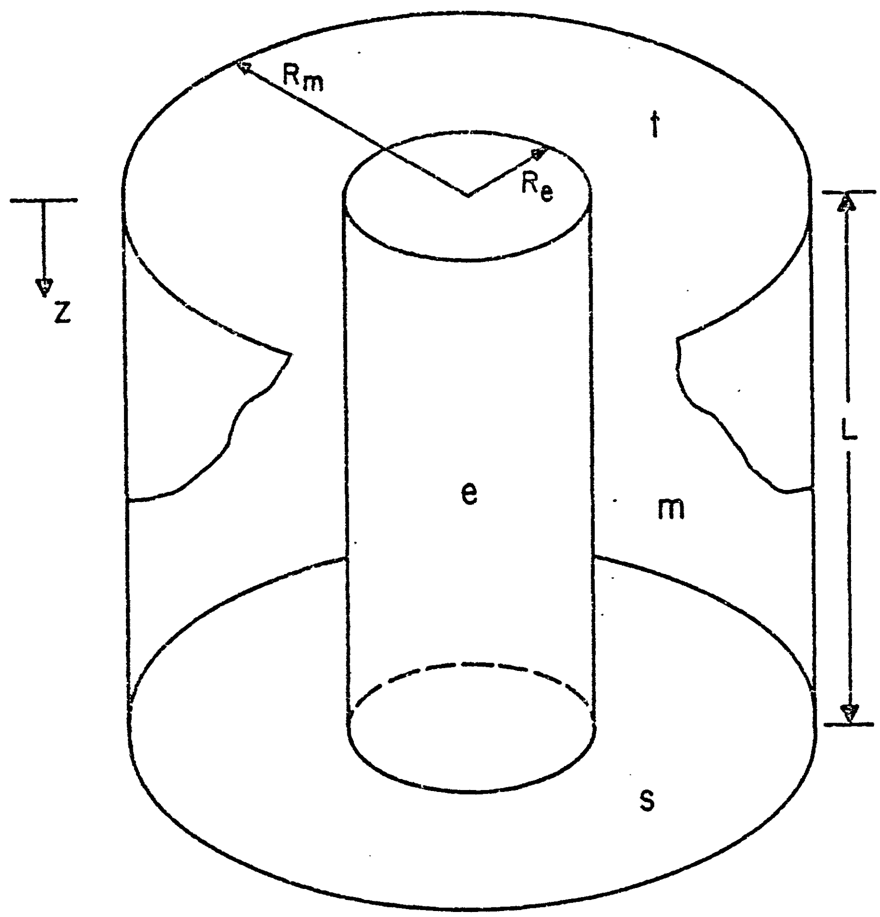

C.1 Schematic representation of the system for calculating view factors.

The view factor $F_{et}(z)$ can be evaluated by using Eq. (C.1) with $x = z$. Then $F_{em}(z)$ can be calculated using,

$$F_{em}(z) = 1 - F_{es}(z) - F_{et}(z) \tag{C.6}$$

Let us now consider the evaluation of F'_{sm} and F'_{se}. First we note that,

$$F'_{ms} + F'_{mm} + F'_{mt} + F'_{me} = 1 \tag{C.7}$$

where ' indicates that the view factors are w·r·t·the entire surface.

$$F'_{ms} = F'_{mt} \tag{C.8}$$

Thus, $$F'_{ms} = \frac{1}{2}\left(1 - F'_{mm} - F'_{me}\right) \tag{C.9}$$

Again, from reference 54,

$$F'_{me} = \frac{R_e}{R_m} \{1 - \frac{1}{\pi} \cos^{-1} \frac{A_5}{A_4} - \frac{1}{A_6} [A_7 \cos^{-1} \frac{R_e}{R_m} \frac{A_5}{A_4} + A_5 \sin^{-1} \frac{R_e}{R_m} - \frac{\pi}{2} A_4]\} \tag{C.10}$$

where

$$A_4 = L^2 + R_m^2 - R_e^2$$

$$A_5 = L^2 - R_m^2 + R_e^2$$

$$A_6 = 2R_mR_e \tag{C.11,12,13, 14}$$

$$A_7 = \sqrt{(L^2 + R_m^2 + R_e^2)^2 - 4R_e^2R_m^2}$$

and

$$F'_{mm} = 1 - \frac{R_e}{R_m} + \frac{1}{\pi}\left\{ 2 \frac{R_e}{R_m} \tan^{-1} A_{11} - \frac{L}{2R_m} \left[A_8 \sin^{-1} A_9 \right.\right.$$

$$\left.\left. - \sin^{-1} A_{10} + \frac{\pi}{2} (A_8 - 1) \right] \right\} \qquad (C.15)$$

where

$$A_{11} = \frac{2\sqrt{R_m^2 - R_e^2}}{L}$$

$$A_8 = \frac{\sqrt{4R^2 + L^2}}{L}$$

$$A_9 = \frac{A_{11}^2 + A_{10}}{A_{11}^2 + 1}$$

$$A_{10} = 1 - 2 \left(\frac{R_e}{R_m}\right)^2 \qquad (C.16,17,18,19)$$

Thus after calculating F'_{me} from Eq. (C.10) and F'_{mm} from Eq. (C.15), we can calculate F'_{ms} from Eq. (C.9).

Then, from reciprocity rule,

$$F'_{sm} = \frac{2R_m L}{R_m^2 - R_e^2} F'_{ms} \qquad (C.20)$$

similarly noting that [54]

$$F'_{st} = 1 - \frac{L}{R_m^2 - R_e^2} \left[R_e - R_m (F'_{mm} + 2F'_{me} - 1) \right]$$

$$(C.21)$$

and that $F'_{se} + F'_{sm} + F'_{st} = 1$

we can calculate

$$F'_{se} = 1 - F'_{sm} - F'_{st} \tag{C.22}$$

APPENDIX D

USE OF TEMPERATURE DEPENDENT ELECTRICAL CONDUCTIVITY IN THE SLAG

The magnetohydrodynamic form of Maxwell's equation (for low magnetic Reynolds no.) can be written as:

$$\mu_0 \frac{\partial H}{\partial t} = - \left[\nabla \times \left(\frac{\nabla \times H}{\sigma}\right) \right] \tag{D.1}$$

In cylindrical coordinate and for axial symmetry ($H_r = H_z = \frac{\partial}{\partial \theta} = 0$), Eq.(D.1) can be written as follows:

$$\mu_0 \frac{\partial H_\theta}{\partial t} = \frac{\partial}{\partial z} \left[\frac{1}{\sigma} \frac{\partial H_\theta}{\partial z}\right] + \frac{\partial}{\partial r}\left[\frac{1}{\sigma} \frac{1}{r} \frac{\partial}{\partial r}(rH_\theta)\right] \tag{D.2}$$

Expanding the terms in Eq.(D.2) gives:

$$\sigma\mu_0 \frac{\partial H_\theta}{\partial t} = \left[\frac{\partial^2 H_\theta}{\partial z^2} + \frac{\partial}{\partial r} \left(\frac{1}{r} \frac{\partial}{\partial r}(rH_\theta)\right)\right] - \left[\frac{\partial H_\theta}{\partial z} \frac{\partial \ell n\sigma}{\partial z} + \frac{1}{r} \frac{\partial}{\partial r}(rH_\theta) \frac{\partial \ell n\sigma}{\partial r}\right] \tag{D.3}$$

For the calculations reported in the text, the second term on the r.h.s. of Eq. (D.3) has been neglected. However, in some of the calculations the temperature dependence of σ , appearing on the $\ell \cdot h \cdot s$ of Eq.(D.3) has been accounted for. The basic approach in these latter calculations involved:

(1) Solution of field equations for a specified temperature distribution in slag

(2) Values for electromagnetic force and Joule heat rate generated in step 1 was then used to solve flow and temperature equations.

(3) Temperature field generated in step 2 was used to calculate the new distribution of σ in slag.

Steps 1 to 3 were repeated until the temperature fields in slag calculated in two consecutive iterations agreed within a specified limit. It is to be noted that each of steps 1 and 2 is iterative in addition to the overall process being iterative.

The temperature dependence of electrical conductivity was deduced from data published by Mitchell and Cameron [60] on 70% CaF_2, 30% Al_2O_3 slags. Their data in the range 1500 °C - 1700 °C, can be represented by the following equation:

$$\ell n\sigma = \frac{-9888}{T} + 10.467$$

where σ is in $ohm^{-1}m^{-1}$ and T is in °K.

APPENDIX E

THE COMPUTER PROGRAM

The computer program used for the solution of the governing differential equations is presented in this Appendix. A brief introduction to the program and the functions of various subroutines have already been given in Chapter IV. The computer program given here incorporates wall function approach for turbulence quantities and for temperature. However, the computed results reported in the thesis did not utilize this feature.

E.1 List of Fortran Symbols

Symbol	Meaning
A(I,J,K)	The dependent variables for flow and temperature equations and V_z, V_r, μ_t, μ_{eff}, K, ρ, C_p.
B(I,J,K)	Variables for electromagnetic field.
AE, AW, AN, AS	A_j' of Eq. (4.8)
ANAME (6, 12)	An alphameric array containing the names of variables for flow and temperature equations.

ASYMBL	An alphameric array containing the names of residuals as defined by Eq. (4.40).
AKEFF	Effective thermal conductivity in metal pool.
APP	$a_{\phi,p}$ of Eq (4.11 a,b,c,d)
BNAME (6,10)	An alphameric array containing the names of variables for electromagnetic field.
BE(I), BW(I), BN(J), BS(J)	B_j' of Eq. (4.8)
BPP	$b_{\phi,p}$ of Eq. (4.8)
BBE, BBW, BBN, BBS	The group of terms $c_{\phi,j}(b_{\phi,j} + b_{\phi,p})B_j'$ in Eq. (4.8).
BETA	Coefficient of volume expansion (β).
C1, C2, C3, CD	Constants in the turbulence model.
CC,CP	The convergence criteria for flow and temperature equations, magnetic field equations.
CU	Total current (maximum value), kA

CAPPA	Von Karman's constant (κ)
D	S in Eq. (3.75)
D1, D2, DN, DS	Parameters in Eqs. (4.15) and (4.16).
E	The wall roughness factor, E in Eq. (4.30)
ES, EE, EM	Emissivities of slag surface (ε_s) of electrode (ε_e) and of mold (ε_m)
FES, FEM, FSM, FSE	Radiation view factors F_{es}, F_{em}, F'_{sm}, F'_{se}
FR	Geometric factors to account for the fact that control volumes for integration in near wall regions are different from those in the interior of the domain.
GAMA	Interfacial tension between molten metal and slag (γ).
HC	Heat transfer coefficient between electrode and gas
HW	Overall heat transfer coefficients at interfaces defined by Eq. (3.104).

HCD	$\pi R_e^2 V_{me} \rho_e C_{P,d}$ in Eq. (3.76)
HL	Heat of fusion
I	Index for constant - z grid lines
IE	The number of differential equations (for flow and heat transfer) to be solved.
I1, I2, I3, I4, I5, IA, J1	Indices defined in Fig. 5.2
IN	The total number of constant z grid lines
IP	The number of successive iterations for which print-out is to be produced
IV	The number of variables whose values are to be printed out.
J	Index for constant-r lines.
JN	The total number of constant-r lines.
K	The index which denotes the dependent variable in question.

MIT		The maximum number of iterations for magnetic field equations
MPRINT		The number of iterations between print-out cycles for magnetic field variables.
NEP		Dissipation rate of turbulence energy
NF		Stream function
NK		Turbulence energy
NMT		Turbulent viscosity
NMU		Effective viscosity
NRO	Indices for flow and heat tr. variables	Density
NSP		Specific heat
NT		Temperature
NTC		Thermal conductivity
NVI		Velocity in z-direction
NV2		Velocity in r-direction
NW		Vorticity (ξ/r)

NHR		Real part of magnetic field intensity
NHI		Imaginary part of magnetic field intensity
NH		Magnetic field intensity
NJRR		Real part of current density in r-direction
NJRI	Indices for electromagnetic field variables	Imaginary part of current density in r-direction
NJR		Current density in r-direction
NJZR		Real part of current density in z-direction
NJZI		Imaginary part of current density in z-direction
NJZ		Current density in z-direction
NJJ		Joule heat ($kCal/m^3s$)
NMAX		The maximum number of iterations for flow and heat transfer equations.

NPRINT	The number of iterations between print out cycles for flow and heat tr. variables
P	Magnetic permeability, μ_0.
PR(K)	The Prandtl or Schmidt numbers.
QS	Q_S of Eq (3.76)
R(J)	r
RE, RM	Radius of electrode (R_e), radius of mold (R_m)
RES	The maximum residual $(1 - \phi_p^N/\phi_p^{N-1})_{max}$ for all of the ϕ equations.
ROREF(5)	Reference densities for various media.
RP(K)	Relaxation parameters for flow and temperature equations.
RS	The residual at a particular node.
RSDU(K)	The maximum value of RS for each ϕ equation.
SB	10^{12} x Stefan-Boltzmann constant $(kCal/m^2sK^4)$

S(4)	Electrical conductivities of electrode, slag, molten metal, ingot.
SN1, SN2, SN3, SN4	Local heat transfer coefficients in regions defined in Fig. 4.6.
SOURCE	$S_{\phi,p}$ of Eq. (4.8).
SPREF(5)	Reference specific heats
TLM, TSM, TLS, TA, TM, TW	$T_{\ell,m}$, $T_{s,m}$, $T_{\ell,s}$, T_a, T_m, T_w
TF, TB	T_f, T_B in Eq. (3.74).
TCREF(5)	Reference thermal conductivities.
TAUW1, TAUW2, TAUW3, TAUW4	Shear stress values in regions defined in Fig. 4.6.
TAU	Residence time of a droplet.
UP	Velocity parallel to a wall.
VOLT	Voltage.
VE	Melting rate of electrode.
VC	Casting rate.
W	Relaxation parameters for magnetic field equations.

X(7)	Defined in Fig. 5.2.
X1(I)	z-coordinate of the grid nodes.
X2(J)	r-coordinate of the grid nodes.
YL(J)	Position of liquidus isotherm.
YS(J)	Position of solidus isotherm.
ZMUREF	Reference value for viscosity.

```
      COMMON/CDVAR/A(71,15,12)                                          SAR00010
      COMMON/CNAME/ANAME(6,12),ASYMBL(10),BNAME(6,10)                   SAR00020
      COMMON/CNUMB/NW,NF,NK,NEP,NV1,NV2,NT,NMU,NRO,NTC,NSP,NMT          SAR00030
      COMMON/CGRID/IN,INM,JN,JNM,I1,I2,I3,I4,I5,IA,J1                   SAR00040
      COMMON/CCORD/IMIN(15),IMAX(15),X1(71),X2(15),R(15)                SAR00050
      COMMON/CCRIT/NWI,NWJ,NFI,NFJ,GOSA,TOTA                            SAR00060
      COMMON/CITER/NMAX,NPRINT,NITER,IP,IE,IV,CC                        SAR00070
      COMMON/CRLAX/RP(10),RSDU(10),SAN(10)                              SAR00080
      COMMON/CFLD/B(71,15,10),LF,CU                                     SAR00090
      COMMON/CPROP/ROREF(5),ZMUREF(2),PR(10),GAMA                       SAR00100
      COMMON/CDROP/TAU,HCD,D,QS,QM                                      SAR00110
      COMMON/CAVM/AVM(20)                                               SAR00120
      COMMON/CLS/YL(15),YS(15)                                          SAR00130
      INM=IN-1                                                          SAR00140
      JNM=JN-1                                                          SAR00150
C*** READ ALPHAMERIC INFORMATION FOR HEADINGS AND TITLES                 SAR00160
      READ(5,200)ANAME,ASYMBL,BNAME                                     SAR00170
C**    COMPUTE AND PRINT COORDINATES                                    SAR00180
      CALL  CORD                                                        SAR00190
      WRITE(6,12) I1,I2,I3,I4,J1                                        SAR00200
      WRITE(6,101)   (X1(I),I=1,IN)                                     SAR00210
      WRITE(6,102)   (X2(J),J=1,JN)                                     SAR00220
C**   INITIALIZE                                                        SAR00230
      CALL INIT                                                         SAR00240
C *** READ INFORMATION FROM PREVIOUS CALCULATIONS                        SAR00250
      DO 21 K=1,5                                                       SAR00260
      DO 21 J=1,JN                                                      SAR00270
   21 READ(4,14) (B(I,J,K),I=1,IN)                                      SAR00280
      DO 22 K=1,5                                                       SAR00290
      DO 22 J=1,JN                                                      SAR00300
   22 READ(4,14) (A(I,J,K),I=1,IN)                                      SAR00310
      DO 25 J=1,JN                                                      SAR00320
   25 READ(4,18) YL(J),YS(J)                                            SAR00330
   14 FORMAT(/,7(1PE10.3))                                              SAR00340
   18 FORMAT(2(F10.4))                                                  SAR00350
C *** PERFORM ELECTRO MAGNETIC FIELD CALCULATIONS                        SAR00360
                                                                  PAGE    1
```

```
      CALL FIELD
      IF(LF EQ 2) GO TO 30
C****    PERFORM FLUID FLOW CALCULATIONS
C *** INITIAL GUESS FOR PROPERTIES
      CALL PROP(1)
      CALL VFDROP
      NITER=0
    1 CONTINUE
      NITER=NITER+1
C*** CAUSE ONE CYCLE OF ITERATION TO BE PERFORMED
      CALL  EQN
C*** TEST IF PRINTOUT TO BE PRODUCED
      IF((NITER+NPRINT-IP)/NPRINT NE NITER/NPRINT)   GO TO 10
      CALL PRINT(1,IV,1)
      WRITE(6,103)  (ASYMBL(K),K=1,10)
      WRITE(6,104)NITER,(RSDU(K),K=1,IE),(SAN(K),K=1,IE),NWJ,NWI,NFJ,NFI
   10 CONTINUE
C**  TEST IF MAXIUM NUMBER OF ITERATONS PERFORMED
      IF(NITER.EQ NMAX)   GO TO 8
      RES=0
      DO 7 K=1,IE
      IF(ABS(RES) LT ABS(RSDU(K)))  RES=RSDU(K)
      RSDU(K)=0.
    7 CONTINUE
      SANWF=0.
      DO 3 K=1,IE
      IF(ABS(SANWF).LT.ABS(SAN(K)))  SANWF=SAN(K)
      SAN(K)=0
    3 CONTINUE
C*** TEST IF CONVERGENCE CRITERION SATISFIED
      IF(ABS(SANWF).GT..006) GO TO 1
      WRITE(6,105)  NITER
      CALL PRINT(1,8,1)
      WRITE(6,225)
      CALL PRINT(9,10,2)
      GO TO 9
```

```
  8 WRITE(6,106) NITER
    CALL PRINT(5,7,1)
  9 CONTINUE
30  CONTINUE
    STOP
12  FORMAT(/,4H I1=,I2,4H I2=,I2,4H I3=,I2,4H I4=,I2,4H J1=,I2)
101 FORMAT(25HODISTANCES IN DIRECTION-1/(1H 4E25.8))
102 FORMAT(25HODISTANCES IN DIRECTION-2/(1H 4E25.8))
103 FORMAT(36HOMAXIMUM RESIDUAL FOR EACH VARIABLE://
   16HONITER,10(3X,A6), 3X, 16H NWJ NWI NFJ NFI//)
104 FORMAT(1HO I3,3X,10(F9.4),  5X,I2,3(I4))
106 FORMAT(32HOTHE PROCESS DID NOT CONVERGE IN,I5,13H   ITERATIONS)
105 FORMAT(32HOTHE PROCESS        CONVERGED IN,I5,13H   ITERATIONS)
200 FORMAT( 6A6)
225 FORMAT(/,50H DRIVING FORCES ARE FIRST ELECTROMAG THEN BUOYANCY)
    END
```

```
      BLOCK DATA
      COMMON/CNUMB/NW,NF,NK,NEP,NV1,NV2,NT,NMU,NRO,NTC,NSP,NMT
      COMMON/CCORD/IMIN(15),IMAX(15),X1(71),X2(15),R(15)
      COMMON/CGRID/IN,INM,JN,JNM,I1,I2,I3,I4,I5,IA,J1
      COMMON/CDIM/X(7),RE,RM
      COMMON/CITER/NMAX,NPRINT,NITER,IP,IE,IV,CC
      COMMON/CCONT/C1,C2,C3,CD
      COMMON/CRLAX/RP(10),RSDU(10),SAN(10)
      COMMON/CEMP/WF,P,S(4)
      COMMON/CHJ/NHR,NHI,NH,NJRR,NJRI,NJR,NJZR,NJZI,NJZ,NJJ
      COMMON/FRLAX/W(2),SUM(2),SUM1(2)
      COMMON/FITER/MIT,MPRINT,CP
      COMMON/CTHERM/TCREF(5),SPREF(5),BETA(2),ES,EE,EM,SB,HL
      COMMON/CTEMP/TLM,TSM,TLS,TA,TM,TW
      COMMON/CTRVL/VE,VC
      COMMON/CHEAT/HC,HW(4)
      COMMON/CPROP/ROREF(5),ZMUREF(2),PR(10),GAMA
      COMMON/CVF/FES(21),FEM(21),FSM,FSE
      COMMON/CDROP/TAU,HCD,D,QS,QM
      COMMON/CTAUW/TAUW1(20),TAUW2(15),TAUW3(21),TAUW4(10),CAPPA,E
      COMMON/CFLD/B(71,15,10),LF,CU
C **  PROGRAM AND PRINT OUT CONTROL DATA
      DATA NW,NF,NK,NEP,NV1,NV2,NT,NMU,NRO,IE,IV/1,2,3,4,6,7,5,8,9,5,5/
     1,NMAX,NPRINT,IP,CC/600,200,1,0.005/
     2,RP/0.1,1.2,0.5,0.5,0.5,5*1.0/
     3,NTC,NSP,NMT/10,11,12/
      DATA RSDU,SAN/10*0.0,10*0.0/
      DATA NHR,NHI,NH,NJRR,NJRI,NJR,NJZR,NJZI,NJZ,NJJ/1,2,6,3,4,
     17,9,10,8,5/
     1,W,SUM,SUM1/1 50,1.20,2*0.0,2*0 0/
     2,MIT,MPRINT,CP/400,200,0.005/
C***  PHYSICAL DATA
      DATA ROREF/7 2E+03,2.8E+03,7.2E+03,7.2E+03,7.2E+03/
     1,ZMUREF/1.0E-02,6.0E-03/
     2,PR/1 0,1 0,1 0,1.3,6*1 0/
     3,TCREF/7.5E-03,2.500E-03,3.7E-03,7.5E-03,7.5E-03/
```

```
     4,SPEEF,HL/0.12,0.20,0.18,0.18,0.18,59.0/                              SAR01250
     5,TLM,TSM,TLS,TA,TM,TW/1723.0,1523.0,1650.0,323.0,323.0,330.0/         SAR01260
     6,ES,EE,EM,SB/0.60,0.40,1.00,13.70/                                    SAR01270
     7,BETA/1.0E-04,1.0E-03/                                                SAR01280
     8,VE,VC,HC/6.31E-04,2.05E-04,6.0E-03/                                  SAR01290
     9,GAMA/0.9/                                                            SAR01300
     1,HW/1.50E-01,6.50E-02,6.50E-02,4.5E-02/                               SAR01310
     2,CAPPA,E/0.40,9.0/                                                    SAR01320
      DATA C1,C2,C3,CD/1.44,1.92,1.0,0.09/                                  SAR01330
      DATA WF,P/3.77E+02,1.26E-06/                                          SAR01340
     1,S/7.14E+05,2.5E+02,7.14E+05,7.14E+05/                                SAR01350
     2,CU/2.404/                                                            SAR01360
C***  GRID DATA                                                             SAR01370
      DATA IN,JN/51,12/                                                     SAR01380
     1,X/0.3,0.32,0.361,0.370,0.380,0.450,0.730/                            SAR01390
     2,RE,RM/0.0285,0.05/                                                   SAR01400
     3,I1,I2,IA,I3,I4,I5,J1/16,19,24,27,31,41,7/                            SAR01410
     4,IMIN/7*2,5*17/                                                       SAR01420
     5,IMAX/12*50/                                                          SAR01430
      END                                                                   SAR01440
```

```
      SUBROUTINE CORD                                          SAR01450
      COMMON/CCORD/IMIN(15),IMAX(15),X1(71),X2(15),R(15)       SAR01460
      COMMON/CGRID/IN,INM,JN,JNM,I1,I2,I3,I4,I5,IA,J1          SAR01470
      COMMON/CDIM/X(7),RE,RM                                   SAR01480
      COMMON/CB/BE(71),BW(71),BN(15),BS(15)                    SAR01490
      COMMON/CEMP/WF,P,S(4)                                    SAR01500
      COMMON/CGEOM/FR(4)                                       SAR01510
      COMMON/CX/D1(71,15),D2(71,15),DN(15),DS(15)              SAR01520
      X1(1)=0.0                                                SAR01530
      X2(1)=0 0                                                SAR01540
      R(1)=X2(1)                                               SAR01550
      DZ1=X(1)/FLOAT(I1-1)                                     SAR01560
      DZ2=(X(2)-X(1))/FLOAT(I2-I1)                             SAR01570
      DZ3=(X(3)-X(2))/FLOAT(IA-I2)                             SAR01580
      DZ4=(X(4)-X(3))/FLOAT(I3-IA)                             SAR01590
      DZ5=(X(5)-X(4))/FLOAT(I4-I3)                             SAR01600
      DZ6=(X(6)-X(5))/FLOAT(I5-I4)                             SAR01610
      DZ7=(X(7)-X(6))/FLOAT(IN-I5)                             SAR01620
      DR1=RE/FLOAT(J1-1)                                       SAR01630
      DR2=(RM-RE)/FLOAT(JN-J1)                                 SAR01640
      DO 10 I=2,IN                                             SAR01650
      IF(I LE I1) DX1=DZ1                                      SAR01660
      IF(I.GT.I1.AND.I.LE.I2) DX1=DZ2                          SAR01670
      IF(I.GT.I2.AND.I.LE.IA) DX1=DZ3                          SAR01680
      IF(I.GT.IA.AND.I.LE.I3) DX1=DZ4                          SAR01690
      IF(I GT.I3.AND.I.LE.I4) DX1=DZ5                          SAR01700
      IF(I.GT.I4.AND.I.LE.I5) DX1=DZ6                          SAR01710
      IF(I.GT.I5.AND.I.LE.IN) DX1=DZ7                          SAR01720
   10 X1(I)=X1(I-1)+DX1                                        SAR01730
      DO 50 J=2,JN                                             SAR01740
      DX2=DR1                                                  SAR01750
      IF(J.GT.J1.AND.J.LE.JN) DX2=DR2                          SAR01760
      X2(J)=X2(J-1)+DX2                                        SAR01770
      R(J)=X2(J)                                               SAR01780
   50 CONTINUE                                                 SAR01790
C **  CALCULATE BE,BW,BN,BS,DN,DS,D1,D2                        SAR01800
                                                                  PAGE   6
```

```
      DO 20 J=2,JNM                                               SAR01810
      IL=IMIN(J)                                                  SAR01820
      IH=IMAX(J)                                                  SAR01830
      DO 20 I=IL,IH                                               SAR01840
      DX1=1./(X1(I+1)-X1(I-1))                                    SAR01850
      BW(I)=DX1/(X1(I)-X1(I-1))                                   SAR01860
      BE(I)=DX1/(X1(I+1)-X1(I))                                   SAR01870
      DX2=1.0/(X2(J+1)-X2(J-1))                                   SAR01880
      A1=DX2/(X2(J+1)-X2(J))                                      SAR01890
      DN(J)=2./(R(J+1)+R(J))*A1                                   SAR01900
      BN(J)=(1.+R(J+1)/R(J))*0.5*A1                               SAR01910
      A2=DX2/(X2(J)-X2(J-1))                                      SAR01920
      DS(J)=2./(R(J-1)+R(J))*A2                                   SAR01930
      BS(J)=(1 +R(J-1)/R(J))*0.5*A2                               SAR01940
      D1(I,J)=R(J)*(DN(J)+DS(J))+BE(I)+BW(I)                      SAR01950
      S1=S(2)                                                     SAR01960
      IF(I.LE.I2.AND.J.LE.J1) S1=S(1)                             SAR01970
      IF(I GT.I3) S1=S(1)                                         SAR01980
      D2(I,J)=0.5*WF*P*S1                                         SAR01990
      DD=D1(I,J)**2+D2(I,J)**2                                    SAR02000
      D1(I,J)=D1(I,J)/DD                                          SAR02010
      D2(1,J)=D2(I,J)/DD                                          SAR02020
      DN(J)=R(J+1)*DN(J)                                          SAR02030
      DS(J)=R(J-1)*DS(J)                                          SAR02040
   20 CONTINUE                                                    SAR02050
      FR(1)=2.-(X2(JNM)-X2(JNM-1))/(X2(JN)-X2(JNM-1))             SAR02060
      FR(2)=2.-(X1(I2+2)-X1(I2+1))/(X1(I2+2)-X1(I2))              SAR02070
      FR(3)=2.-(X1(I3-1)-X1(I3-2))/(X1(I3)-X1(I3-2))              SAR02080
      FR(4)=2.-(X2(J1+2)-X2(J1+1))/(X2(J1+2 )-X2(J1))             SAR02090
      RETURN                                                      SAR02100
      END                                                         SAR02110
```

```
      SUBROUTINE INIT                                                   SAR02120
      COMMON/CFLD/B(71,15,10),LF,CU                                     SAR02130
      COMMON/CHJ/NHR,NHI,NH,NJRR,NJRI,NJR,NJZR,NJZI,NJZ,NJJ             SAR02140
      COMMON/CCORD/IMIN(15),IMAX(15),X1(71),X2(15),R(15)                SAR02150
      COMMON/CGRID/IN,INM,JN,JNM,I1,I2,I3,I4,I5,IA,J1                   SAR02160
      COMMON/CDIM/X(7),RE,RM                                            SAR02170
      COMMON/CDVAR/A(71,15,12)                                          SAR02180
      COMMON/CNUMB/NW,NF,NK,NEP,NV1,NV2,NT,NMU,NRO,NTC,NSP,NMT          SAR02190
      COMMON/CTEMP/TLM,TSM,TLS,TA,TM,TW                                 SAR02200
      COMMON/CLS/YL(15),YS(15)                                          SAR02210
C*** SET VALUES IN STROE TO ZERO                                        SAR02220
      DO 30 K=1,12                                                      SAR02230
      DO 30 J=1,JN                                                      SAR02240
      DO 30 I=1,IN                                                      SAR02250
      A(I,J,K)=0.0                                                      SAR02260
      IF(K.GT.10) GO TO 30                                              SAR02270
      B(I,J,K)=0.0                                                      SAR02280
   30 CONTINUE                                                          SAR02290
      DO 31 J=1,J1                                                      SAR02300
      DO 31 I=1,I2                                                      SAR02310
   31 B(I,J,NHR)=CU*R(J)/(2.0*3.14*RE*RE)                               SAR02320
C *** INITIAL GUESS FOR LIQUIDUS SOLIDUS ISOTHERMS                      SAR02330
      DO 32 J=1,JN                                                      SAR02340
      YL2=0.016*(RM-R(J))                                               SAR02350
      YL(J)=0.00+SQRT(YL2)                                              SAR02360
      YS2=0.0360*(RM-R(J))                                              SAR02370
      YS(J)=0.015+SQRT(YS2)                                             SAR02380
   32 CONTINUE                                                          SAR02390
C *** INITIAL GUESS FOR TEMPERATURE                                     SAR02400
      DO 50 J=1,JN                                                      SAR02410
      DO 50 I=1,I3                                                      SAR02420
      IF(J.GT.J1.AND.I.LT.I1) GO TO 50                                  SAR02430
      A(I,J,NT)=1800.0                                                  SAR02440
      IF(J.LE.J1.AND.I.LE.I2) A(I,J,NT)=1500.0                          SAR02450
   50 CONTINUE                                                          SAR02460
      I31=I3+1                                                          SAR02470
```

```
      DO 54 J=1,JN
      DO 54 I=I31,IN
      XSM=X1(I)-X1(I3)
      IF(XSM.LE.YL(J)) A(I,J,NT)=1750.0
      IF(XSM.GT.YL(J).AND.XSM.LE.YS(J)) A(I,J,NT)=1650.0
      IF(XSM.GT.YS(J)) A(I,J,NT)=1500.0
   54 CONTINUE
C***  FIXED BOUNDARY CONDITIONS
      DO 11 I=I1,IN
   11 B(I,JN,NHR)=CU/(2.0*3.14*RM)
      J12=J1+1
      DO 12 J=J12,JN
      B(I1,J,NHR)=CU/(2.0*3.14*R(J))
   12 CONTINUE
      DO 20 J=2,JNM
      IL=I1+1
      IF(J.LE.J1) IL=I2+1
      IH=I3-1
      DO  20  I=IL,IH
      A(I,J,NK)=0.0001
      A(I,J,NEP)=0.00001
   20 CONTINUE
      DO 14 J=1,J1
   14 A(I2,J,NT)=TLM
      DO 17 I=I1,IH
   17 A(I,JN,NT)=TLS
      RETURN
      END
```

```
      SUBROUTINE FIELD                                                  SAR02760
      COMMON/CGRID/IN,INM,JN,JNM,I1,I2,I3,I4,I5,IA,J1                   SAR02770
      COMMON/CHJ/NHR,NHI,NH,NJRR,NJRI,NJR,NJZR,NJZI,NJZ,NJJ             SAR02780
      COMMON/CFLD/B(71,15,10),LF,CU                                     SAR02790
      COMMON/CEMP/WF,P,S(4)                                             SAR02800
      COMMON/CB/BE(71),BW(71),BN(15),BS(15)                             SAR0281C
      COMMON/CX/D1(71,15),D2(71,15),DN(15),DS(15)                       SAR02820
      COMMON/CCORD/IMIN(15),IMAX(15),X1(71),X2(15),R(15)                SAR02830
      COMMON/FRLAX/W(2),SUM(2),SUM1(2)                                  SAR0284C
      COMMON/FITER/MIT,MPRINT,CP                                        SAR02850
      COMMON/CAVM/AVM(20)                                               SAR02860
      NIT=0                                                             SAR02870
    1 CONTINUE                                                          SAR02880
C***   BOUNDARY I=1,J<J1                                                SAR02890
      J11=J1-1                                                          SAR02900
      XQ=X1(2)-X1(1)                                                    SAR02910
      XR=X1(3)-X1(1)                                                    SAR02920
      BB=XR*XR/(XR*XR-XQ*XQ)                                            SAR02930
      DO 10 K=NHR,NHI                                                   SAR0294C
      DO 10 J=2,J11                                                     SAR02950
      Z=B(1,J,K)                                                        SAR02960
      B(1,J,K)=BB*B(2,J,K)+(1.-BB)*B(3,J,K)                             SAR0297C
      SUM(K)=SUM(K)+ABS(Z-B(1,J,K))                                     SAR02980
      SUM1(K)=SUM1(K)+ABS(B(1,J,K))                                     SAR02990
   10 B(1,J,K)=Z+W(K)*(B(1,J,K)-Z)                                      SAR03000
C***  INTERIOR POINTS                                                   SAR03010
      DO 11 J=2,JNM                                                     SAR03020
      IL=IMIN(J)                                                        SAR03030
      IF(J.EQ.J1) IL=I1+1                                               SAR0304C
      IH=IMAX(J)                                                        SAR03050
      DO 19 I=IL,IH                                                     SAR03060
      IF(J.EQ.J1.AND.I.LE.I2) GO TO 30                                  SAR0307C
      IF(I.EQ.I2.AND.J.LT.J1) GO TO 14                                  SAR03080
      IF(I.EQ.I3) GO TO 14                                              SAR03090
      R1=DN(J)*B(I,J+1,NHR)+DS(J)*B(I,J-1,NHR)                          SAR03100
     1+BE(I)*B(I+1,J,NHR)+BW(I)*B(I-1,J,NHR)                            SAR03110
```

```
      R2=DN(J)*B(I,J+1,NHI)+DS(J)*B(I,J-1,NHI)
     1+BE(I)*B(I+1,J,NHI)+BW(I)*B(I-1,J,NHI)
      DO 17 K=NHR,NHI
      Z=B(I,J,K)
      IF(K.EQ.NHI) GO TO 15
      S1=R1
      S2=R2
      GO TO 16
   15 S1=R2
      S2=-R1
   16 B(I,J,K)=D1(I,J)*S1+D2(I,J)*S2
      SUM(K)=SUM(K)+ABS(Z-B(I,J,K))
      SUM1(K)=SUM1(K)+ABS(B(I,J,K))
   17 B(I,J,K) =Z+W(K)*(B(I,J,K)-Z)
      GO TO 111
C *** BOUNDARY J=J1,I1<I<I2
   30 BB=(X2(J1)-X2(J1-1))/(X2(J1+1)-X2(J1))*S(1)/S(2)
      DO 31 K=NHR,NHI
      Z=B(I,J,K)
      B(I,J,K)=R(J-1)*B(I,J-1,K)+R(J+1)*BB*B(I,J+1,K)
      B(I,J,K)=B(I,J,K)/R(J)/(1.+BB)
      SUM(K)=SUM(K)+ABS(Z-B(I,J,K))
      SUM1(K)=SUM1(K)+ABS(B(I,J,K))
   31 B(I,J,K)=Z+W(K)*(B(I,J,K)-Z)
      GO TO 111
C***  BOUNDARY I=I3,OR I=I2
   14 CON1=S(2)/S(3)
      CON2=S(1)/S(2)
      CON=CON1
      IF(I.EQ.I2) CON=CON2
      XQ=X1(I)-X1(I-1)
      XR=X1(I+1)-X1(I)
      DO 141 K=NHR,NHI
      BB=1./(1.+XQ/XR*CON)
      Z=B(I,J,K)
      B(I,J,K)=BB*B(I-1,J,K)+(1.-BB)*B(I+1,J,K)
```

```
      SUM(K)=SUM(K)+ABS(Z-B(I,J,K))                                     SAR03480
      SUM1(K)=SUM1(K)+ABS(B(I,J,K))                                     SAR03490
  141 B(I,J,K) =Z+W(K)*(B(I,J,K)-Z)                                     SAR03500
  111 CONTINUE                                                          SAR03510
  19  CONTINUE                                                          SAR03520
  11  CONTINUE                                                          SAR03530
C***  BOUNDARY I=IN                                                     SAR03540
      XQ=X1(IN)-X1(INM)                                                 SAR03550
      XR=X1(IN)-X1(INM-1)                                               SAR03560
      BB=XR*XR/(XR*XR-XQ*XQ)                                            SAR03570
      DO 151 K=NHR,NHI                                                  SAR03580
      DO 151 J=2,JNM                                                    SAR03590
      Z=B(IN,J,K)                                                       SAR03600
      B(IN,J,K)=BB*B(INM,J,K)+(1.-BB)*B(INM-1,J,K)                      SAR03610
      SUM(K) =SUM(K)+ABS(Z-B(IN,J,K))                                   SAR03620
  151 SUM1(K)=SUM1(K)+ABS(B(IN,J,K))                                    SAR03630
C***  CHECK FOR CONVERGENCE                                             SAR03640
      CF1=SUM(NHR)/SUM1(NHR)                                            SAR03650
      CF2=SUM(NHI)/SUM1(NHI)                                            SAR03660
      CFF=CF1                                                           SAR03670
      IF(CF1.LT.CF2) CFF=CF2                                            SAR03680
      IF(CFF.LE.CP) GO TO 9                                             SAR03690
      NIT=NIT+1                                                         SAR03700
C***  CHECK FOR PRINT OUT                                               SAR03710
      K1=NIT/MPRINT                                                     SAR03720
      K2=K1*MPRINT                                                      SAR03730
      IF(NIT.NE.K2) GO TO 5                                             SAR03740
      CALL PRINT(1,2,2)                                                 SAR03750
      WRITE(6,104) NIT,CF1,CF2                                          SAR03760
  104 FORMAT(/,6H  NIT=,I4/,6H  CF1=,E14.8,6H  CF2=,E14.8/)             SAR03770
   5  CONTINUE                                                          SAR03780
C***  CHECK FOR MAX. NO. OF ITERATIONS                                  SAR03790
      IF(NIT.LT.MIT) GO TO 1                                            SAR03800
      WRITE(6,106) NIT                                                  SAR03810
  106 FORMAT(32H0THE FLD.EQN DID NOT CONVERGE IN,I5,13H   ITERATIONS)   SAR03820
      LF=2                                                              SAR03830
```

```
      GO TO 20                                                          SAR03840
    9 CONTINUE                                                          SAR03850
      LF=1                                                              SAR03860
      DO 18 I=1,IN                                                      SAR03870
      DO 18 J=1,JN                                                      SAR03880
   18 B(I,J,NH)=SQRT(B(I,J,NHR)**2+B(I,J,NHI)**2)                       SAR03890
      DO 29 J=2,JNM                                                     SAR03900
      DO 191 I=1,IN                                                     SAR03910
      IF(I.LT.I1.AND.J.GT.J1) GO TO 191                                 SAR03920
      IF(I.EQ.1.AND.J.LT.J1) GO TO 193                                  SAR03930
      IF(I.EQ.IN) GO TO 193                                             SAR03940
      IF(J.EQ.J1.AND.I.LE.I1) GO TO 192                                 SAR03950
      IF(I.EQ.I1.AND.J.GT.J1) GO TO 196                                 SAR03960
      DFW=(X1(I+1)-X1(I))*BW(I)                                         SAR03970
      DBE=(X1(I)-X1(I-1))*BE(I)                                         SAR03980
      B(I,J,NJRR)=DBE*(B(I,J,NHR)-B(I+1,J,NHR))                         SAR03990
     1+DFW*(B(I-1,J,NHR)-B(I,J,NHR))                                    SAR04000
      B(I,J,NJRI)=DBE*(B(I,J,NHI)-B(I+1,J,NHI))                         SAR04010
     1+DFW*(B(I-1,J,NHI)-B(I,J,NHI))                                    SAR04020
  193 DF=X2(J+1)-X2(J)                                                  SAR04030
      DB=X2(J)-X2(J-1)                                                  SAR04040
      B(I,J,NJZR)=(DB*DB*B(I,J+1,NHR)-DF*DF*B(I,J-1,NHR)                SAR04050
     1+(DF*DF-DB*DB)*B(I,J,NHR))/(DB*DF*(DB+DF))+B(I,J,NHR)/R(J)        SAR04060
      B(I,J,NJZI)=(DB*DB*B(I,J+1,NHI)-DF*DF*B(I,J-1,NHI)                SAR04070
     1+(DF*DF-DB*DB)*B(I,J,NHI))/(DB*DF*(DB+DF))+B(I,J,NHI)/R(J)        SAR04080
      GO TO 191                                                         SAR04090
  192 B(I,J,NJZR)=(B(I,J,NHR)-B(I,J-1,NHR))/(X2(J)-X2(J-1))             SAR04100
     1+B(I,J,NHR)/R(J)                                                  SAR04110
      B(I,J,NJZI)=(B(I,J,NHI)-B(I,J-1,NHI))/(X2(J)-X2(J-1))             SAR04120
     1+B(I,J,NHI)/R(J)                                                  SAR04130
      GO TO 191                                                         SAR04140
C ***  JR AT I=I1                                                        SAR04150
  196 B(I,J,NJRR)=(B(I,J,NHR)-B(I+1,J,NHR))/(X1(I+1)-X1(I))             SAR04160
   26 B(I,J,NJRI)=(B(I,J,NHI)-B(I+1,J,NHI))/(X1(I+1)-X1(I))             SAR04170
  191 CONTINUE                                                          SAR04180
   29 CONTINUE                                                          SAR04190
```

```
C***  JZ AT THE CENTER                                                    SAR04200
      DO 21 I=1,IN                                                        SAR04210
      B(I,1,NJZR)=(B(I,2,NHR)-B(I,1,NHR))/(X2(2)-X2(1))*2.                SAR04220
   21 B(I,1,NJZI)=(B(I,2,NHI)-B(I,1,NHI))/(X2(2)-X2(1))*2.                SAR04230
C***   JZ AT J=JN                                                         SAR04240
      DO 25 I=I1,IN                                                       SAR04250
      B(I,JN,NJZR)=(B(I,JN,NHR)-B(I,JNM,NHR))/(X2(JN)-X2(JNM))            SAR04260
     1+B(I,JN,NHR)/R(JN)                                                  SAR04270
   25 B(I,JN,NJZI)=(B(I,JN,NHI)-B(I,JNM,NHI))/(X2(JN)-X2(JNM))            SAR04280
     1+B(I,JN,NHI)/R(JN)                                                  SAR04290
      DO 195 I=1,IN                                                       SAR04300
      DO 195 J=1,JN                                                       SAR04310
      B(I,J,NJZ)=SQRT(B(I,J,NJZR)**2+B(I,J,NJZI)**2)                      SAR04320
  195 B(I,J,NJR)=SQRT(B(I,J,NJRR)**2+B(I,J,NJRI)**2)                      SAR04330
      DO 115 I=1,IN                                                       SAR04340
      DO 115 J=1,JN                                                       SAR04350
      IF(J.GT.J1.AND.I.LT.I1) GO TO 115                                   SAR04360
      S1=S(2)                                                             SAR04370
      IF(I.LE.I2.AND.J.LE.J1) S1=S(1)                                     SAR04380
      IF(I.GT.I3) S1=S(3)                                                 SAR04390
      B(I,J,NJJ)=(B(I,J,NJRR)**2+B(I,J,NJRI)**2+B(I,J,NJZR)**2+B(I,J,     SAR04400
     1NJZI)**2)                                                           SAR04410
      B(I,J,NJJ)=119.531*B(I,J,NJJ)/S1                                    SAR04420
  115 CONTINUE                                                            SAR04430
C     CALCULATE VOLTAGE                                                   SAR04440
      SUMI=0.                                                             SAR04450
      DO 200 I=I1,I3                                                      SAR04460
      N=I-I1+1                                                            SAR04470
      JL=J1                                                               SAR04480
      IF(I.GE.I2) JL=1                                                    SAR04490
      SUMJ=0.                                                             SAR04500
      DO 201 J=JL,JNM                                                     SAR04510
      DX2=0.5*(X2(J+1)-X2(J))                                             SAR04520
  201 SUMJ=SUMJ+(R(J+1)*B(I,J+1,NJJ)+R(J)*B(I,J,NJJ))*DX2                 SAR04530
  200 AVM(N)=SUMJ                                                         SAR04540
      N3=I3-I1                                                            SAR04550
```

```
      DO 203 N=1,N3                                                     SAR04560
      I=N+I1-1                                                          SAR04570
      DZ=(X1(I+1)-X1(I))*0.5                                            SAR04580
  203 SUMI=SUMI+(AVM(N)+AVM(N+1))*DZ                                    SAR04590
      VOLT=6.286*4.185*SUMI/CU*1.414                                    SAR04600
      WRITE(6,110) NIT                                                  SAR04610
      CALL PRINT(5,8,2)                                                 SAR04620
      WRITE(6,204) VOLT                                                 SAR04630
  110 FORMAT(32HOTHE FIELD EQUATION CONVERGED IN,I5,13H   ITERATIONS)   SAR04640
  204 FORMAT(/,9H VOLTAGE=,F10.3)                                       SAR04650
   20 CONTINUE                                                          SAR04660
      RETURN                                                            SAR04670
      END                                                               SAR04680
```

```
      SUBROUTINE VFDROP
      COMMON/CVF/FES(21),FEM(21),FSM,FSE
      COMMON/CGRID/IN,INM,JN,JNM,I1,I2,I3,I4,I5,IA,J1
      COMMON/CPROP/ROREF(5),ZMUREF(2),PR(10),GAMA
      COMMON/CTRVL/VE,VC
      COMMON/CDIM/X(7),RE,RM
      COMMON/CCORD/IMIN(15),IMAX(15),X1(71),X2(15),R(15)
      COMMON/CTHERM/TCREF(5),SPREF(5),BETA(2),ES,EE,EM,SB,HL
      COMMON/CDROP/TAU,HCD,D,QS,QM
C  *** CALCULATION OF VIEW FACTORS
      RM2=RM*RM
      RE2=RE*RE
      XL=X1(I1)
      DO 10 I=1,I1
      Z=XL-X1(I)
      A1=Z*Z+RM2-RE2
      A2=Z*Z+RE2-RM2
      A3=Z*Z+RM2+RE2
      A4=A3/SQRT(A3*A3-4.0*RE2*RM2)
      A4=A4*ARCOS(RE/RM*A2/A1)-ARCOS(RE/RM)
      FES(I)=(ARCOS(A2/A1)-Z/RE*A4)*0.1591
      Z=X1(I)
      A1=Z*Z+RM2-RE2
      A2=Z*Z+RE2-RM2
      A3=Z*Z+RM2+RE2
      A4=A3/SQRT(A3*A3-4.0*RE2*RM2)
      A4=A4*ARCOS(RE/RM*A2/A1)-ARCOS(RE/RM)
      FET    =(ARCOS(A2/A1)-Z/RE*A4)*0.1591
      FEM(I)=1.0-FES(I)-FET
   10 CONTINUE
      Z=XL
      A1=Z*Z+RM2-RE2
      A2=Z*Z+RE2-RM2
      A3=Z*Z+RM2+RE2
      A4=    SQRT(A3*A3-4.0*RE2*RM2)
      A4=A4*ARCOS(RE/RM*A2/A1)+A2*ARSIN(RE/RM)-1.5708*A1
```

```
      A4=(ARCOS(A2/A1)-A4/(2.0*RE*Z))*0.31831
      FME=RE/RM*(1.0-A4)
      Z2=Z*Z
      A1=4.0*(RM2-RE2)/Z2
      A2=SQRT(A1)
      A3=SQRT(4.0*RM2/Z2+1.0)
      A4=ARSIN((A1+(1.0-2.0*RE2/RM2))/(1.0+A1))
      A4=A3*A4-ARSIN(1.-2.*RE2/RM2)+1.5708*(A3-1.)
      A4=2.*RE/RM*ATAN(A2)-0.5*Z/RM*A4
      FMM=1.-RE/RM+0.31831*A4
      FSM=RM*Z/(RM2-RE2)*(1.-FMM-FME)
      FST=1.-Z/(RM2-RE2)*(RE-RM*(FMM+2.*FME-1.))
      FSE=1.-FSM-FST
      WRITE(6,4) (FES(I),I=1,I1)
    4 FORMAT(25H0VIEW FACTORS FES(I)  ARE/(1H 7E14.4))
      WRITE(6,5) (FEM(I),I=1,I1)
    5 FORMAT(25H0VIEW FACTORS FEM(I)  ARE/(1H 7E14.4))
      WRITE(6,8) FSM,FSE
    8 FORMAT(/,10H    FSM  =,E14.4,10H    FSE  =,E14.4)
C *** CALCULATION OF DROP PARAMETERS
      RO=ROREF(2)
      RO2=RO*RO
      DRO=ROREF(3)-RO
      DP=2.8566*SQRT(GAMA/9.81/DRO)
      VU=ZMUREF(1)
      VU4=VU**4
      PP=(GAMA**3)*RO2/(9.81*DRO*VU4)
      P1=PP**0.85
      Y=1.3333*DP*DP*RO2*GAMA*GAMA/VU4/P1
      IF(Y.LT.70.0) GO TO 15
      Z=(22.222*Y)**0.422
      GO TO 16
   15 Z=(0.75*Y)**0.784
   16 RN=(Z-0.75)*(PP**0.15)
      VDT=RN*VU/DP/RO
C *** CALCULATION OF RESIDENCE TIME
```

```
      Z=X1(I3)-X1(I2)                                                   SAR05410
      A=DRO/(ROREF(3)+0.5*RO)*9.81                                      SAR05420
      C=2.*A/VDT                                                        SAR05430
      AM=4.*EXP(C*Z/VDT)                                                SAR05440
      TAU=AM-2.+SQRT(AM*AM-4.*AM)                                       SAR0545C
      TAU=ALOG(TAU*0.5)/C                                               SAR05460
      VDA=Z/TAU                                                         SAR05470
C *** CALCULATE D=6.HD/DP/RO/CPD AND HCD=F.MD.CPD                        SAR05480
      PRN=SPREF(2)*VU/TCREF(2)                                          SAR05490
      RN=VDA*DP*RO/VU                                                   SAR05500
      SN=0.8*SQRT(RN)*(PRN**0.333)                                      SAR05510
      HD=TCREF(2)*SN/DP                                                 SAR05520
      SPRF3=SPREF(3)                                                    SAR05530
      D  =6.*HD/(DP*SPRF3*ROREF(3))                                     SAR05540
      HCD=3.1416*SPRF3*RE2*VE*ROREF(3)                                  SAR05550
      WRITE(6,17) DP,VDT,RN,HD,TAU,D,HCD                                SAR05560
   17 FORMAT(/,5H  DP=,F12.5,/,5H VDT=,F12.4,/,5H  RN=,F12.3,/,         SAR05570
     15H  HD=,F12.3,/,5H TAU=,F12.3,/,5H   D=,F12.3,/,5H HCD=,F12.4)    SAR05580
      RETURN                                                            SAR05590
      END                                                               SAR05600
```

```
      SUBROUTINE EQN                                                    SAR05610
      COMMON/CDVAR/A(71,15,12)                                          SAR05620
      COMMON/CNUMB/NW,NF,NK,NEP,NV1,NV2,NT,NMU,NRO,NTC,NSP,NMT          SAR05630
      COMMON/CRLAX/RP(10),RSDU(10),SAN(10)                              SAR05640
      COMMON/CCRIT/NWI,NWJ,NFI,NFJ,GOSA,TOTA                            SAR05650
      COMMON/CITER/NMAX,NPRINT,NITER,IP,IE,IV,CC                        SAR05660
C*** OBTAIN EFFECTIVE VISCOSITY                                         SAR0567C
      CALL  VISCOS                                                      SAR05680
C*** VORTICITY SUB-CYCLE                                                SAR05690
      GOSA=0.0                                                          SAR05700
      TOTA=0.0                                                          SAR05710
      CALL  VORITY                                                      SAR05720
      IF(GOSA.EQ.0.0.AND.TOTA.EQ.0.0) GO TO 10                          SAR0573C
      SAN(NW)=GOSA/TOTA                                                 SAR05740
      GO TO 40                                                          SAR05750
   10 SAN(NW)=1.                                                        SAR05760
   40 CONTINUE                                                          SAR05770
C*** STREAM FUNCTION SUB-CYCLE                                          SAR05780
      GOSA=0.0                                                          SAR05790
      TOTA=0.0                                                          SAR0580C
      CALL  STRFUN                                                      SAR05810
      IF(GOSA.EQ.0.0.AND.TOTA.EQ.0.0) GO TO 20                          SAR05820
      SAN(NF)=GOSA/TOTA                                                 SAR0583C
      GO TO 50                                                          SAR05840
   20 SAN(NF)=1.                                                        SAR05850
   50 CONTINUE                                                          SAR0586C
      CALL  VELDIS                                                      SAR05870
      CALL WALL                                                         SAR05880
C*** SUB-CYCLE FOR TURBULENT  VARIABLES                                 SAR05890
      DO  41  K=NK,NEP                                                  SAR05900
      GOSA=0.0                                                          SAR05910
      TOTA=0.0                                                          SAR05920
      CALL TURVAR(K)                                                    SAR05930
      IF(GOSA.EQ.0.0.AND.TOTA.EQ.0.0) GO TO 30                          SAR05940
      SAN(K)=GOSA/TOTA                                                  SAR05950
      GO TO 41                                                          SAR05960
```

```
   30 SAN(K)=1.                                                SAR05970
   41 CONTINUE                                                 SAR05980
C *** TEMPERATURE SUB CYCLE                                    SAR05990
      GOSA=0.0                                                 SAR06000
      TOTA=0.0                                                 SAR06010
      CALL TEMPR                                               SAR06020
      IF(GOSA.EQ.0.0.AND.TOTA.EQ.0.0) GO TO 25                 SAR06030
      SAN(NT)=GOSA/TOTA                                        SAR06040
      GO TO 26                                                 SAR06050
   25 SAN(NT)=1.                                               SAR06060
  26  CONTINUE                                                 SAR06070
C*** INITIATE ITERATION ON BOUNDARY NODES                      SAR06080
      CALL  BOUND                                              SAR06090
C *** READJUST PROPERTIES AND ISOTHERMS                        SAR06100
      CALL PROP(2)                                             SAR06110
      RETURN                                                   SAR06120
      END                                                      SAR06130
```

```
      SUBROUTINE VORITY                                                 SAR06140
      COMMON/CB/BE(71),BW(71),BN(15),BS(15)                             SAR06150
      COMMON/CDVAR/A(71,15,12)                                          SAR06160
      COMMON/CNUMB/NW,NF,NK,NEP,NV1,NV2,NT,NMU,NRO,NTC,NSP,NMT          SAR0617C
      COMMON/CCORD/IMIN(15),IMAX(15),X1(71),X2(15),R(15)                SAR06180
      COMMON/CCRIT/NWI,NWJ,NFI,NFJ,GOSA,TOTA                            SAR06190
      COMMON/CRLAX/RP(10),RSDU(10),SAN(10)                              SAR06200
      COMMON/CGRID/IN,INM,JN,JNM,I1,I2,I3,I4,I5,IA,J1                   SAR0621C
      COMMON/CTHERM/TCREF(5),SPREF(5),BETA(2),ES,EE,EM,SB,HL            SAR06220
      DO 11 J=2,JNM                                                     SAR06230
      IL=I1+1                                                           SAR06240
      IF(J.LE.J1) IL=I2+1                                               SAR06250
      IH=I3-1                                                           SAR06260
      DO  11  I=IL,IH                                                   SAR0627C
      CALL  SORCE(SOURCE,I,J,NW)                                        SAR06280
      CALL  CONVEC(AE,AW,AN,AS,I,J,NW)                                  SAR06290
      RSQ=R(J)*R(J)                                                     SAR06300
      BBE=2.*RSQ*BE(I)                                                  SAR06310
      BBW=2.*RSQ*BW(I)                                                  SAR06320
      BBN=(R(J+1)*R(J+1)+RSQ)*BN(J)                                     SAR0633C
      BBS=(R(J-1)*R(J-1)+RSQ)*BS(J)                                     SAR06340
C     IMPLICIT VORTICITY CALCULATIONS                                   SAR06350
      TERM1=A(I+1,J,NW)                                                 SAR06360
      TERM2=A(I-1,J,NW)                                                 SAR06370
      TERM3=A(I,J-1,NW)                                                 SAR06380
      TERM4=A(I,J+1,NW)                                                 SAR06390
      TERM5=0.0                                                         SAR0640C
      IF(J.NE.JNM) GO TO 12                                             SAR06410
      DX2=X2(JN)-X2(JNM)                                                SAR06420
      DT=A(I,JNM,NT)-A(I,JN,NT)                                         SAR06430
      BT=BETA(1)                                                        SAR06440
      BOU= 2.452*A(I,JN,NRO)*BT*DX2*DT/A(I,JNM,NMU)/R(JN)               SAR06450
      TERM4     =3.*(A(I,JN,NF)-A(I,JNM,NF))/DX2/DX2/RSQ  /A(I,JN,NRO)  SAR0646C
      TERM4=TERM4+BOU                                                   SAR06470
      TERM5=0.5*(AN+A(I,J+1,NMU)*BBN)                                   SAR06480
      GO TO 14                                                          SAR06490
```

```
12   IF(I.NE.(I2+1)) GO TO 15                                                SAR06500
     IF(J.GT.J1) GO TO 15                                                    SAR06510
     DX12=(X1(I2+1)-X1(I2))**2                                               SAR06520
     TERM2      =3.*(A(I2,J,NF)-A(I2+1,J,NF))/DX12/RSQ/A(I2,J,NRO)           SAR06530
     TERM5=0.5*( AW+A(I-1,J,NMU)*BBW)                                        SAR06540
     GO TO 14                                                                SAR06550
15   IF(J.NE.(J1+1)) GO TO 16                                                SAR06560
     IF(I.GT.I2) GO TO 16                                                    SAR06570
     DX2=X2(J1+1)-X2(J1)                                                     SAR06580
     DX22=DX2*DX2                                                            SAR06590
     BT=BETA(1)                                                              SAR06600
     DT=A(I,J1,NT)-A(I,J1+1,NT)                                              SAR06610
     BOU= 2.452*A(I,J1,NRO)*BT*DX2*DT/A(I,J1+1,NMU)/R(J1)                    SAR06620
     TERM3      =3.*(A(I,J1,NF)-A(I,J1+1,NF))/DX22/RSQ/A(I,J1,NRO)           SAR06630
     TERM3=TERM3+BOU                                                         SAR06640
     TERM5=0.5*(AS+A(I,J-1,NMU)*BBS)                                         SAR06650
     GO TO 14                                                                SAR06660
16   IF(I.NE.(I3-1))  GO TO 14                                               SAR06670
     DX12=(X1(I3)-X1(I3-1))**2                                               SAR06680
     TERM1      =3.*(A(I3,J,NF)-A(I3-1,J,NF))/(DX12*RSQ*A(I3,J,NRO))         SAR06690
     TERM5=0.5*( AE+A(I+1,J,NMU)*BBE)                                        SAR06700
14   CONTINUE                                                                SAR06710
     ANUM=(AE+A(I+1,J,NMU)*BBE)*TERM1                                        SAR06720
    1+(AW+A(I-1,J,NMU)*BBW)*TERM2                                            SAR06730
    2+(AS+A(I,J-1,NMU)*BBS)*TERM3                                            SAR06740
    3+(AN+A(I,J+1,NMU)*BBN)*TERM4        +SOURCE                             SAR06750
     ADNM=AE+AW+AN+AS+A(I,J,NMU)*(BBE+BBW+BBN+BBS)+TERM5                     SAR06760
     IF(ADNM.EQ.0.)  GO TO 4                                                 SAR06770
     Z=A(I,J,NW)                                                             SAR06780
     A(I,J,NW)=ANUM/ADNM                                                     SAR06790
     IF(Z.EQ.0.0.AND.A(I,J,NW).EQ.0.0)  GO TO 1                              SAR06800
     RS=1.-Z/A(I,J,NW)                                                       SAR06810
     GO TO 3                                                                 SAR06820
   1 RS=0.                                                                   SAR06830
   3 CONTINUE                                                                SAR06840
     GOSA=GOSA+ABS(Z-A(I,J,NW))                                              SAR06850
```

```
      TOTA=TOTA+ABS(A(I,J,NW))                                          SAR0686C
C*** UNDER- OR OVER-RELAX                                               SAR06870
      A(I,J,NW)=Z+RP(NW)*(A(I,J,NW)-Z)                                  SAR06880
C*** STORE MAXIMUM RESIDUAL                                             SAR06890
      IF(ABS(RS).LE.ABS(RSDU(NW))) GO TO 4                              SAR06900
      RSDU(NW)=RS                                                       SAR06910
      NWJ=J                                                             SAR0692C
      NWI=I                                                             SAR06930
    4 CONTINUE                                                          SAR06940
   11 CONTINUE                                                          SAR06950
      RETURN                                                            SAR0696C
      END                                                               SAR06970
```

```
      SUBROUTINE STRFUN
      COMMON/CB/BE(71),BW(71),BN(15),BS(15)
      COMMON/CDVAR/A(71,15,12)
      COMMON/CNUMB/NW,NF,NK,NEP,NV1,NV2,NT,NMU,NRO,NTC,NSP,NMT
      COMMON/CCORD/IMIN(15),IMAX(15),X1(71),X2(15),R(15)
      COMMON/CCRIT/NWI,NWJ,NFI,NFJ,GOSA,TOTA
      COMMON/CRLAX/RP(10),RSDU(10),SAN(10)
      COMMON/CGRID/IN,INM,JN,JNM,I1,I2,I3,I4,I5,IA,J1
      DO 21 J=2,JNM
      IL=I1+1
      IF(J.LE.J1) IL=I2+1
      IH=I3-1
      DO 21 I=IL,IH
      CALL  SORCE(SOURCE,I,J,NF)
      RISQ=1./R(J)/R(J)
      ROP=A(I,J,NRO)
      BBE=4./(A(I+1,J,NRO)+ROP)*RISQ*BE(I)
      BBW=4./(A(I-1,J,NRO)+ROP)*RISQ*BW(I)
      BBN=16./(A(I,J+1,NRO)+ROP)/((R(J+1)+R(J))**2)*BN(J)
      BBS=16./(A(I,J-1,NRO)+ROP)/((R(J-1)+R(J))**2)*BS(J)
      ANUM=BBE*A(I+1,J,NF)+BBW*A(I-1,J,NF)+BBN*A(I,J+1,NF)
     1+BBS*A(I,J-1,NF)+SOURCE
      ADNM=BBE+BBW+BBN+BBS
      IF(ADNM.EQ.0.)  GO TO 5
      Z=A(I,J,NF)
      A(I,J,NF)=ANUM/ADNM
      IF(Z.EQ.0.0.AND.A(I,J,NF).EQ.0.0)  GO TO 8
      RS=1.-Z/A(I,J,NF)
      GO TO 6
    8 RS=0.0
    6 CONTINUE
      GOSA=GOSA+ABS(Z-A(I,J,NF))
      TOTA=TOTA+ABS(A(I,J,NF))
      A(I,J,NF)=Z+RP(NF)*(A(I,J,NF)-Z)
      IF(ABS(RS).LE.ABS(RSDU(NF))) GO TO 5
      RSDU(NF)=RS
```

```
      NFJ=J                                                             SAR07340
      NFI=I                                                             SAR07350
    5 CONTINUE                                                          SAR07360
   21 CONTINUE                                                          SAR07370
      RETURN                                                            SAR07380
      END                                                               SAR07390
```

```
      SUBROUTINE TURVAR(K)
      COMMON/CDVAR/A(71,15,12)
      COMMON/CNUMB/NW,NF,NK,NEP,NV1,NV2,NT,NMU,NRO,NTC,NSP,NMT
      COMMON/CBB/BBE,BBW,BBN,BBS,BPP
      COMMON/CSORSE/SOURCE,SPRIME
      COMMON/CCRIT/NWI,NWJ,NFI,NFJ,GOSA,TOTA
      COMMON/CCORD/IMIN(15),IMAX(15),X1(71),X2(15),R(15)
      COMMON/CRLAX/RP(10),RSDU(10),SAN(10)
      COMMON/CB/BE(71),BW(71),BN(15),BS(15)
      COMMON/CGRID/IN,INM,JN,JNM,I1,I2,I3,I4,I5,IA,J1
      COMMON/CPROP/ROREF(5),ZMUREF(2),PR(10),GAMA
      DO 31 J=2,JNM
      IL=I1+1
      IF(J.LE.J1) IL=I2+1
      IH=I3-1
      DO  31  I=IL,IH
      BPP=A(I,J,NMU)
      BBE=(A(I+1,J,NMU)+BPP)/PR(K)*BE(I)
      BBW=(A(I-1,J,NMU)+BPP)/PR(K)*BW(I)
      BBN=(A(I,J+1,NMU)+BPP)/PR(K)*BN(J)
      BBS=(A(I,J-1,NMU)+BPP)/PR(K)*BS(J)
      SPRIME=0.
      CALL  SORCE(SOURCE,I,J,K)
      CALL  CONVEC(AE,AW,AN,AS,I,J,K)
      ANUM=(AE+BBE)*A(I+1,J,K)+(AW+BBW)*A(I-1,J,K)+(AN+BBN)*A(I,J+1,K)
     1+(AS+BBS)*A(I,J-1,K)+SOURCE
      ADNM=AE+AW+AN+AS+BBE+BBW+BBN+BBS+SPRIME
      IF(ADNM.EQ.0.) GO TO 6
      Z=A(I,J,K)
      A(I,J,K)=ANUM/ADNM
      IF(Z.EQ.0.0.AND.A(I,J, K).EQ.0.0)  GO TO 3
      RS=1.-Z/A(I,J,K)
      GO TO 5
    3 RS=0.0
    5 CONTINUE
      GOSA=GOSA+ABS(Z-A(I,J,K))
```

```
      TOTA=TOTA+ABS(A(I,J,K))                                           SAR07760
      A(I,J,K)=Z+RP(K)*(A(I,J,K)-Z)                                     SAR07770
      IF(A(I,J, K).LE.0.0)  A(I,J, K)=0.0                               SAR07780
      IF(ABS(RS).LT.ABS(RSDU(K)))  GO TO 6                              SAR07790
      RSDU(K)=RS                                                        SAR07800
    6 CONTINUE                                                          SAR07810
   31 CONTINUE                                                          SAR07820
      RETURN                                                            SAR07830
      END                                                               SAR07840
```

```
      SUBROUTINE TEMPR                                                  SAR07850
      COMMON/CDVAR/A(71,15,12)                                          SAR07860
      COMMON/CNUMB/NW,NF,NK,NEP,NV1,NV2,NT,NMU,NRO,NTC,NSP,NMT          SAR07870
      COMMON/CCRIT/NWI,NWJ,NFI,NFJ,GOSA,TOTA                            SAR07880
      COMMON/CCORD/IMIN(15),IMAX(15),X1(71),X2(15),R(15)                SAR0789C
      COMMON/CRLAX/RP(10),RSDU(10),SAN(10)                              SAR07900
      COMMON/CB/BE(71),BW(71),BN(15),BS(15)                             SAR07910
      COMMON/CGRID/IN,INM,JN,JNM,I1,I2,I3,I4,I5,IA,J1                   SAR0792C
      COMMON/CAVT/TB                                                    SAR07930
      COMMON/CTRVL/VE,VC                                                SAR07940
      COMMON/CDROP/TAU,HCD,D,QS,QM                                      SAR07950
      COMMON/CLS/YL(15),YS(15)                                          SAR07960
      COMMON/CTHERM/TCREF(5),SPREF(5),BETA(2),ES,EE,EM,SB,HL            SAR07970
      COMMON/CPROP/ROREF(5),ZMUREF(2),PR(10),GAMA                       SAR07980
      COMMON/CBB/BBE,BBW,BBN,BBS,BPP                                    SAR0799C
      COMMON/CSNW/SN1(20),SN2(15),SN3(21),SN4(10)                       SAR08000
      COMMON/CSORSE/SOURCE,SPRIME                                       SAR0801C
      COMMON/CTEMP/TLM,TSM,TLS,TA,TM,TW                                 SAR08020
      COMMON/CFLD/B(71,15,10),LF,CU                                     SAR08030
      COMMON/CHJ/NHR,NHI,NH,NJRR,NJRI,NJR,NJZR,NJZI,NJZ,NJJ             SAR08040
      COMMON/CAVM/AVM(20)                                               SAR0805C
C *** CALCULATE AVERAGE BULK TEMPERATURE OF SLAG,TB                     SAR08060
      J11=J1-1                                                          SAR08070
      DO 33 I=I2,I3                                                     SAR08080
      N=I-I2+1                                                          SAR08090
      SUMT=0.                                                           SAR08100
      DO 34 J=1,J11                                                     SAR08110
      DR=R(J+1)-R(J)                                                    SAR0812C
   34 SUMT=SUMT+(R(J)*A(I,J,NT)+R(J+1)*A(I,J+1,NT))*DR                  SAR08130
   33 AVM(N)=SUMT/R(J1)/R(J1)                                           SAR08140
      N3=I3-I2                                                          SAR08150
      SUMT=0.                                                           SAR08160
      DO 35 N=1,N3                                                      SAR08170
      I=N+I2-1                                                          SAR08180
      DZ=(X1(I+1)-X1(I))*0.5                                            SAR0819C
   35 SUMT=SUMT+(AVM(N)+AVM(N+1))*DZ                                    SAR08200
```

```
      TB=SUMT/(X1(I3)-X1(I2))                                           SAR08210
      TF=TB-(TB-TLM)/EXP(D*TAU)                                         SAR08220
      QS=HCD*(TF-TLM)                                                   SAR08230
C *** CALCULATE VOLUME OF THE METAL POOL                                 SAR08240
      SUMV=0.                                                           SAR08250
      DO 14 J=1,JNM                                                     SAR08260
      DX=R(J+1)-R(J)                                                    SAR08270
      SUMV=SUMV+(R(J)*YL(J)+R(J+1)*YL(J+1))*DX                          SAR08280
   14 CONTINUE                                                          SAR08290
      VOL=SUMV*3.14                                                     SAR08300
      QM=QS/VOL                                                         SAR08310
      DO 10 J=2,JNM                                                     SAR08320
      IL=2                                                              SAR08330
      IF(J.EQ.J1) IL=I2+1                                               SAR0834C
      IF(J.GT.J1) IL=I1+1                                               SAR08350
      DO 11 I=IL,INM                                                    SAR08360
      IF(I.EQ.I2.AND.J.LE.J1) GO TO 11                                  SAR08370
      IF(I.EQ.I3) GO TO 11                                              SAR08380
      IF(J.GT.J1.AND.I.LE.I2) GO TO 20                                  SAR08390
      IF(I.GT.I2.AND.I.LT.I3) GO TO 20                                  SAR08400
      VV=VE                                                             SAR0841C
      IF(I.GT.I3) VV=VC                                                 SAR08420
      AEW=VV/(X1(I+1)-X1(I-1))*A(I,J,NRO)*A(I,J,NSP)                    SAR08430
      BPP=A(I,J,NTC)                                                    SAR0844C
      BBE=(A(I+1,J,NTC)+BPP)*BE(I)                                      SAR08450
      BBW=(A(I-1,J,NTC)+BPP)*BW(I)                                      SAR08460
      BBN=(A(I,J+1,NTC)+BPP)*BN(J)                                      SAR0847C
      BBS=(A(I,J-1,NTC)+BPP)*BS(J)                                      SAR08480
      IF(I.LT.I3) GO TO 36                                              SAR08490
      XSM=X1(I)-X1(I3)                                                  SAR08500
      IF(XSM.GT.YL(J).AND.XSM.LE.YS(J)) GO TO 31                        SAR0851C
      SOURCE=QM                                                         SAR08520
      GO TO 32                                                          SAR08530
   31 SOURCE=ADF(I,J,1,NT)/(TLM-TSM)                                    SAR08540
      SOURCE=-VC*HL*A(I,J,NRO)*SOURCE                                   SAR08550
      GO TO 32                                                          SAR08560
```

```
36   SOURCE=0.                                                           SAR08570
32   CONTINUE                                                            SAR08580
     ANUM=BBE*A(I+1,J,NT)+BBW*A(I-1,J,NT)+BBN*A(I,J+1,NT)                SAR08590
    1+BBS*A(I,J-1,NT)+SOURCE+AEW*(A(I-1,J,NT)-A(I+1,J,NT))               SAR08600
     ADNM=BBE+BBW+BBN+BBS                                                SAR08610
     GO TO 21                                                            SAR08620
20   CONTINUE                                                            SAR08630
     CALL  SORCE(SOURCE,I,J,NT)                                          SAR08640
     BPP=A(I,J,NMT)*A(I,J,NSP)/PR(NT)+A(I,J,NTC)                         SAR08650
     BBE=(A(I+1,J,NMT)*A(I+1,J,NSP)/PR(NT)+A(I+1,J,NTC)+BPP)*BE(I)       SAR08660
     BBW=(A(I-1,J,NMT)*A(I-1,J,NSP)/PR(NT)+A(I-1,J,NTC)+BPP)*BW(I)       SAR08670
     BBN=(A(I,J+1,NMT)*A(I,J+1,NSP)/PR(NT)+A(I,J+1,NTC)+BPP)*BN(J)       SAR08680
     BBS=(A(I,J-1,NMT)*A(I,J-1,NSP)/PR(NT)+A(I,J-1,NTC)+BPP)*BS(J)       SAR08690
     SPRIME=0.                                                           SAR08700
     CALL  CONVEC(AE,AW,AN,AS,I,J,NT)                                    SAR08710
     AEW=     VC/(X1(I+1)-X1(I-1))*A(I,J,NRO)*A(I,J,NSP)                 SAR08720
     AE=AE-AEW                                                           SAR08730
     AW=AW+AEW                                                           SAR08740
     K=NT                                                                SAR08750
     ANUM=(AE+BBE)*A(I+1,J,K)+(AW+BBW)*A(I-1,J,K)+(AN+BBN)*A(I,J+1,K)    SAR08760
    1+(AS+BBS)*A(I,J-1,K)+SOURCE                                         SAR08770
     ADNM=AE+AW+AN+AS+BBE+BBW+BBN+BBS+SPRIME                             SAR08780
21   CONTINUE                                                            SAR08790
     IF(ADNM.EQ.0.) GO TO 11                                             SAR08800
     Z=A(I,J,NT)                                                         SAR08810
     A(I,J,NT)=ANUM/ADNM                                                 SAR08820
     IF(Z.EQ.0.0.AND.A(I,J,NT).EQ.0.0)   GO TO 1                         SAR08830
     RS=1.-Z/A(I,J,NT)                                                   SAR08840
     GO TO 3                                                             SAR08850
   1 RS=0.                                                               SAR08860
   3 CONTINUE                                                            SAR08870
     GOSA=GOSA+ABS(Z-A(I,J,NT))                                          SAR08880
     TOTA=TOTA+ABS(A(I,J,NT))                                            SAR08890
     A(I,J,NT)=Z+RP(NT)*(A(I,J,NT)-Z)                                    SAR08900
     IF(ABS(RS).LE.ABS(RSDU(NT))) GO TO 4                                SAR08910
     RSDU(NT)=RS                                                         SAR08920
```

```
    4 CONTINUE                                                   SAR08930
   11 CONTINUE                                                   SAR08940
   10 CONTINUE                                                   SAR0895C
      RETURN                                                     SAR08960
      END                                                        SAR08970
```

```
      SUBROUTINE WALL                                                   SAR08980
      COMMON/CDVAR/A(71,15,12)                                          SAR08990
      COMMON/CNUMB/NW,NF,NK,NEP,NV1,NV2,NT,NMU,NRO,NTC,NSP,NMT          SAR09000
      COMMON/CGRID/IN,INM,JN,JNM,I1,I2,I3,I4,I5,IA,J1                   SAR09010
      COMMON/CCORD/IMIN(15),IMAX(15),X1(71),X2(15),R(15)                SAR09020
      COMMON/CPROP/ROREF(5),ZMUREF(2),PR(10),GAMA                       SAR09030
      COMMON/CTHERM/TCREF(5),SPREF(5),BETA(2),ES,EE,EM,SB,HL            SAR09040
      COMMON/CCONT/C1,C2,C3,CD                                          SAR09050
      COMMON/CTAUW/TAUW1(20),TAUW2(15),TAUW3(21),TAUW4(10),CAPPA,E      SAR09060
      COMMON/CSNW/SN1(20),SN2(15),SN3(21),SN4(10)                       SAR0907C
      A1=ROREF(2)*CD**0.25                                              SAR09080
      PRL=SPREF(2)*ZMUREF(1)/TCREF(2)                                   SAR09090
      RECPRT=1./PR(NT)                                                  SAR09100
      PRRAT=PRL*RECPRT                                                  SAR09110
      PJAY=9.*(PRRAT-1.)/(PRRAT**0.25)                                  SAR09120
C     ***********  AT J=JN,TAUW1     , SN1                              SAR09130
      YP=X2(JN)-X2(JNM)                                                 SAR0914C
      IL=I1+1                                                           SAR09150
      IH=I3-1                                                           SAR09160
      DO 1 I=IL,IH                                                      SAR09170
      N=I-IL+1                                                          SAR09180
      A2=A1*SQRT(A(I,JNM,NK))                                           SAR09190
      YPP=YP*A2/ZMUREF(1)                                               SAR0920C
      UP=ABS(A(I,JNM,NV1))                                              SAR09210
      IF(YPP.GT.11.5) GO TO 2                                           SAR09220
      TAUW1(N)=ZMUREF(1)*UP/YP                                          SAR09230
      GO TO 3                                                           SAR09240
    2 TAUW1(N)=CAPPA*UP*A2/ALOG(YPP*E)                                  SAR09250
    3 FRIC=TAUW1(N)/(UP*UP*ROREF(2))                                    SAR0926C
      SN1(N)=FRIC*RECPRT/(1.+PJAY*SQRT(FRIC))                           SAR09270
    1 SN1(N)=SN1(N)*ROREF(2)*SPREF(2)*UP                                SAR09280
C ***                AT I=I2+1,1<J<J1                                   SAR09290
      YP=X1(I2+1)-X1(I2)                                                SAR0930C
      DO 4 J=2,J1                                                       SAR09310
      A2=A1*SQRT(A(I2+1,J,NK))                                          SAR09320
      YPP=YP*A2/ZMUREF(1)                                               SAR0933C
```

```
      UP=ABS(A(I2+1,J,NV2))                                             SAR09340
      IF(YPP.GT.11.5) GO TO 5                                           SAR09350
      TAUW2(J)=ZMUREF(1)*UP/YP                                          SAR09360
      GO TO 6                                                           SAR09370
    5 TAUW2(J)=CAPPA*UP*A2/ALOG(YPP*E)                                  SAR09380
    6 FRIC=TAUW2(J)/(UP*UP*ROREF(2))                                    SAR09390
      SN2(J)=FRIC*RECPRT/(1.+PJAY*SQRT(FRIC))                           SAR09400
      SN2(J)=SN2(J)*ROREF(2)*SPREF(2)*UP                                SAR09410
   40 CONTINUE                                                          SAR09420
    4 CONTINUE                                                          SAR09430
C ***                AT I=I3-1,1<J<JN , TAUW3    ,SN3                   SAR09440
      YP=X1(I3)-X1(I3-1)                                                SAR09450
      DO 7 J=2,JNM                                                      SAR09460
      A2=A1*SQRT(A(I3-1,J,NK))                                          SAR09470
      YPP=YP*A2/ZMUREF(1)                                               SAR09480
      UP=ABS(A(I3-1,J,NV2))                                             SAR09490
      IF(YPP.GT.11.5) GO TO 8                                           SAR09500
      TAUW3(J)=ZMUREF(1)*UP/YP                                          SAR09510
      GO TO 9                                                           SAR09520
    8 TAUW3(J)=CAPPA*UP*A2/ALOG(YPP*E)                                  SAR09530
    9 FRIC=TAUW3(J)/(UP*UP*ROREF(2))                                    SAR09540
      SN3(J)=FRIC*RECPRT/(1.+PJAY*SQRT(FRIC))                           SAR09550
      SN3(J)=SN3(J)*ROREF(2)*SPREF(2)*UP                                SAR09560
      TCM=A(I3-1,J,NTC)                                                 SAR09570
      SN3(J)=TCM/(X1(I3)-X1(I3-1))                                      SAR09580
   70 CONTINUE                                                          SAR09590
    7 CONTINUE                                                          SAR09600
C ***                AT J=J1+1,I1<I<I2                                  SAR09610
      IF(I1.EQ.I2) GO TO 15                                             SAR09620
      YP=X2(J1+1)-X2(J1)                                                SAR09630
      IL=I1+1                                                           SAR09640
      I21=I2-1                                                          SAR09650
      DO 10 I=IL,I2                                                     SAR09660
      N=I-IL+1                                                          SAR09670
      A2=A1*SQRT(A(I,J1+1,NK))                                          SAR09680
      YPP=YP*A2/ZMUREF(1)                                               SAR09690
```

```
      UP=ABS(A(I,J1+1,NV1))                                             SAR09700
      IF(YPP.GT.11.5) GO TO 11                                          SAR09710
      TAUW4(N)=ZMUREF(1)*UP/YP                                          SAR09720
      GO TO 12                                                          SAR09730
11    TAUW4(N)=CAPPA*UP*A2/ALOG(YPP*E)                                  SAR09740
12    FRIC=TAUW4(N)/(UP*UP*ROREF(2))                                    SAR09750
      SN4(N)=FRIC*RECPRT/(1.+PJAY*SQRT(FRIC))                           SAR09760
      SN4(N)=SN4(N)*ROREF(2)*SPREF(2)*UP                                SAR09770
      TCM=A(I,J1+1,NTC)                                                 SAR09780
      SN4(N)=TCM/(X2(J1+1)-X2(J1))                                      SAR09790
100   CONTINUE                                                          SAR09800
10    CONTINUE                                                          SAR09810
15    CONTINUE                                                          SAR09820
      RETURN                                                            SAR09830
      END                                                               SAR0984C
```

```
      SUBROUTINE BOUND                                                  SAR09850
      COMMON/CDVAR/A(71,15,12)                                          SAR09860
      COMMON/CNUMB/NW,NF,NK,NEP,NV1,NV2,NT,NMU,NRO,NTC,NSP,NMT          SAR09870
      COMMON/CDROP/TAU,HCD,D,QS,QM                                      SAR09880
      COMMON/CCORD/IMIN(15),IMAX(15),X1(71),X2(15),R(15)                SAR09890
      COMMON/CGRID/IN,INM,JN,JNM,I1,I2,I3,I4,I5,IA,J1                   SAR09900
      COMMON/CRLAX/RP(10),RSDU(10),SAN(10)                              SAR09910
      COMMON/CPROP/ROREF(5),ZMUREF(2),PR(10),GAMA                       SAR09920
      COMMON/CLS/YL(15),YS(15)                                          SAR09930
      COMMON/CTHERM/TCREF(5),SPREF(5),BETA(2),ES,EE,EM,SB,HL            SAR09940
      COMMON/CSNW/SN1(20),SN2(15),SN3(21),SN4(10)                       SAR09950
      COMMON/CVF/FES(21),FEM(21),FSM,FSE                                SAR09960
      COMMON/CTEMP/TLM,TSM,TLS,TA,TM,TW                                 SAR09970
      COMMON/CHEAT/HC,HW(4)                                             SAR09980
      J11=J1-1                                                          SAR09990
C *** AT I=1,J<J1                                                       SAR10000
      DO 50 J=1,J1                                                      SAR10010
   50 A(1,J,NT)=(4.*A(2,J,NT)-A(3,J,NT))/3.                             SAR10020
C ***  AT THE CENTER                                                    SAR10030
      R3SQ =R(3)*R(3)                                                   SAR10040
      R2SQ =R(2)*R(2)                                                   SAR10050
      BB =R3SQ /(R3SQ -R2SQ )                                           SAR10060
      DO 41 I=2,INM                                                     SAR10070
      A(I,1,NT)=BB*A(I,2,NT)+(1.-BB)*A(I,3,NT)                          SAR10080
      IF(I.LT.I2.OR.I.GT.I3) GO TO 41                                   SAR10090
      A(I,1,NW)=(A(I,1,NF)-A(I,3,NF))/R3SQ+(A(I,2,NF)-A(I,1,NF))/R2SQ   SAR10100
      A(I,1,NW) =8.*A(I,1,NW) / A(I,1,NRO)/(R3SQ-R2SQ)                  SAR10110
      A(I,1,NK)=BB*A(I,2,NK)+(1.-BB)*A(I,3,NK)                          SAR10120
      A(I,1,NEP)=BB*A(I,2,NEP)+(1.-BB)*A(I,3,NEP)                       SAR10130
   41 CONTINUE                                                          SAR10140
C*** AT SIDE WALL                                                       SAR10150
C **@ VORTICITY                                                         SAR10160
      DX2=X2(JN)-X2(JNM)                                                SAR10170
      DO 42 I=I1,I3                                                     SAR10180
      Z=A(I,JN,NW)                                                      SAR10190
      DT=A(I,JNM,NT)-A(I,JN,NT)                                         SAR10200
```

```
      BT=BETA(1)
      BOU= 2.452*A(I,JN,NRO)*BT*DX2*DT/A(I,JNM,NMU)/R(JN)
      A(I,JN,NW)=3.*(A(I,JN,NF)-A(I,JNM,NF))/DX2/DX2/R(JN)/A(I,JN,NRO)
      A(I,JN,NW)=A(I,JN,NW)/R(JNM)-0.5*A(I,JNM,NW)+BOU
      A(I,JN,NW)=Z+RP(NW)*(A(I,JN,NW)-Z)
   42 CONTINUE
C *** TEMPERATURE
      J=JN
      DO 54 I=I3,INM
      XSM=X1(I)-X1(I3)
      IF(I.LT.I3) HTW=HW(1)
      IF(I.GE.I3.AND.XSM.LE.YL(J)) HTW=HW(2)
      IF(XSM.GT.YL(J).AND.XSM.LE.YS(J)) HTW=HW(3)
      IF(XSM.GT.YS(J)) HTW=HW(4)
      TT=TW
      BB=(X2(JN)-X2(JNM))*HTW*2./A(I,JN,NTC)
      A(I,JN,NT)=4.*A(I,JNM,NT)-A(I,JNM-1,NT)
   54 A(I,JN,NT)=(A(I,JN ,NT)+BB*TT)/(3.+BB)
      IF(A(I3,JN,NT).LT.TLM) A(I3,JN,NT)=TLM
C*** AT FREE SURFACE
C *** FIRST CALCULATE THE AVERAGE SLAG TEMPERATURE(AT SURFACE)
      SUMT=0.
      DO 51 J=J1,JNM
      DR=R(J+1)-R(J)
   51 SUMT=SUMT+(R(J)*A(I1,J,NT)+R(J+1)*A(I1,J+1,NT))*DR
      TSA=SUMT/(R(JN)*R(JN)-R(J1)*R(J1))
      TSA=TSA*0.0010
C *** NOW CALCULATE AV. ELECTRODE SURFACE TEMPERATURE,TEA
      SUMT=0.
      I11=I1-1
      DO 52 I=1,I11
      DZ=(X1(I+1)-X1(I))*0.5
   52 SUMT=SUMT+(A(I,J1,NT)+A(I+1,J1,NT))*DZ
      TEA=SUMT/(X1(I1)-X1(1))*0.001
      TM1=TM*0.001
      XQ=X1(I1+1)-X1(I1)
```

```
      XR=X1(I1+2)-X1(I1)                                                SAR10570
      BB=XR*XR/(XR*XR-XC*XQ)                                            SAR10580
      A2=TSA**4-FSM*EM*TM1**4-EE*FSE*TEA**4                             SAR10590
      J12=J1+1                                                          SAR10600
      DO 44 J=J12,JNM                                                   SAR10610
      AK=A(I1,J,NTC)+A(I1,J,NMT)*A(I1,J,NSP)/PR(NT)                     SAR10620
      A1=SB*ES*XQ/AK*2.                                                 SAR10630
C *** NEGLECT CONVECTIVE TR. AT THE SLAG SURFACE                          SAR10640
      A3=0.                                                             SAR10650
      A(I1,J,NT)=4.*A(I1+1,J,NT)-A(I1+2,J,NT)-A1*A2+A3*TA               SAR10660
      A(I1,J,NT)=A(I1,J,NT)/(3.+A3)                                     SAR10670
      A(I1,J,NK)=BB*A(I1+1,J,NK)+(1.-BB)*A(I1+2,J,NK)                   SAR10680
      A(I1,J,NEP)=BB*A(I1+1,J,NEP)+(1.-BB)*A(I1+2,J,NEP)                SAR10690
   44 CONTINUE                                                          SAR10700
C *** AT SLAG-METAL INTERFACE Z=Z3 ,ASSUMED TO BE A SOLID WALL            SAR10710
      DX12=(X1(I3)-X1(I3-1))**2                                         SAR10720
      DO 43 J=2,JNM                                                     SAR10730
      RSQ=R(J)*R(J)                                                     SAR10740
      A(I3,J,NW)=3.*(A(I3,J,NF)-A(I3-1,J,NF))/(DX12*RSQ*ROREF(2))       SAR10750
     1-0.5*A(I3-1,J,NW)                                                 SAR10760
      XF=X1(I3+1)-X1(I3)                                                SAR10770
      TCM=A(I3,J,NTC)                                                   SAR10780
      BB=SN3(J)*XF/TCM                                                  SAR10790
      ANUM=A(I3+1,J,NT)+BB*A(I3-1,J,NT)                                 SAR10800
      ADNM=1.+BB                                                        SAR10810
      Z=A(I3,J,NT)                                                      SAR10820
      A(I3,J,NT)=ANUM/ADNM                                              SAR10830
      A(I3,J,NT)=Z+RP(NT)*(A(I3,J,NT)-Z)                                SAR10840
   43 CONTINUE                                                          SAR10850
C ***  AT I=I2,J<J1                                                     SAR10860
      DX12=(X1(I2+1)-X1(I2))**2                                         SAR10870
      DO 40 J=2,J1                                                      SAR10880
      RSQ=R(J)*R(J)                                                     SAR10890
      A(I2,J,NW)=3.*(A(I2,J,NF)-A(I2+1,J,NF))/DX12/RSQ/A(I2,J,NRO)      SAR10900
      A(I2,J,NW)=A(I2,J,NW)-0.5*A(I2+1,J,NW)                            SAR10910
   40 CONTINUE                                                          SAR10920
```

```
C ***  AT THE CORNER I=I2,J=J1                                          SAR10930
      RSQ=R(J1)*R(J1)                                                   SAR1094C
      DXSS=(X2(J1+1)-X2(J1))**2+(X1(I2+1)-X1(I2))**2                    SAR10950
      A(I2,J1,NW)=3.*(A(I2,J1,NF)-A(I2+1,J1+1,NF))/DXSS/RSQ/A(I2,J1,NRO)SAR10960
      A(I2,J1,NW)=A(I2,J1,NW)-0.5*A(I2+1,J1+1,NW)                       SAR1097C
C *** TEMP. AT J=J1,2<I<I1                                              SAR10980
      DX2=R(J1)-R(J11)                                                  SAR10990
      DO 53 I=2,I11                                                     SAR1100C
      A1=HC*DX2*2./A(I,J1,NTC)                                          SAR11010
      A2=EE*SB*DX2*2./A(I,J1,NTC)                                       SAR11020
      Z=A(I,J1,NT)                                                      SAR11030
      A4=ES*FES(I)*TSA**4                                               SAR11040
      A5=EM*FEM(I)*TM1**4                                               SAR11050
      A3=0.0001*A(I,J1,NT)                                              SAR11060
      DNM=3.+A1+A2*(A3**3)                                              SAR11070
      ANM=4.*A(I,J11,NT)-A(I,J11-1,NT)+A1*TA+A2*(A4+A5)                 SAR11080
      A(I,J1,NT)=ANM/DNM                                                SAR11090
  53  A(I,J1,NT)=Z+RP(NT)*(A(I,J1,NT)-Z)                                SAR11100
C ***  AT J=J1, I1<I<I2                                                 SAR11110
      IF(I1.EQ.I2) GO TO 47                                             SAR11120
      DX2=X2(J1+1)-X2(J1)                                               SAR11130
      DX22=DX2*DX2                                                      SAR11140
      I21=I2-1                                                          SAR11150
      RSQ=R(J1)*R(J1+1)                                                 SAR11160
      XB=X2(J1)-X2(J11)                                                 SAR11170
      BT=BETA(1)                                                        SAR11180
      DO 45 I=I1,I21                                                    SAR11190
      TCM=A(I,J11,NTC)                                                  SAR11200
      IF(I.EQ.I1) GO TO 48                                              SAR11210
      BB=SN4(I-I1)                                                      SAR11220
      GC TO 49                                                          SAR11230
  48  BB=A(I,J1+1,NTC)/DX2                                              SAR11240
  49  BB=BB*2.*XB/TCM                                                    SAR11250
      A(I,J1,NT)=4.*A(I,J11,NT)-A(I,J11-1,NT)+BB*A(I,J1+1,NT)           SAR11260
      A(I,J1,NT)=A(I,J1,NT)/(3.+BB)                                     SAR11270
      Z=A(I,J1,NW)                                                      SAR11280
```

```
      DT=A(I,J1,NT)-A(I,J1+1,NT)                                        SAR11290
      BOU= 2.452*A(I,J1,NRO)*BT*DX2*DT/A(I,J1+1,NMU)/R(J1)              SAR11300
      A(I,J1,NW)=3.*(A(I,J1,NF)-A(I,J1+1,NF))/DX22/RSQ/A(I,J1,NRO)      SAR11310
      A(I,J1,NW)=A(I,J1,NW)-0.5*A(I,J1+1,NW)+BOU                        SAR11320
      A(I,J1,NW)=Z+RP(NW)*(A(I,J1,NW)-Z)                                SAR11330
   45 CONTINUE                                                          SAR11340
   47 CONTINUE                                                          SAR11350
C *** AT I=IN                                                           SAR11360
      XQ=X1(IN)-X1(INM)                                                 SAR11370
      XR=X1(IN)-X1(INM-1)                                               SAR11380
      BB=XR*XR/(XR*XR-XQ*XQ)                                            SAR11390
      DO 55 J=1,JN                                                      SAR11400
   55 A(IN,J,NT)=BB*A(INM,J,NT)+(1.-BB)*A(INM-1,J,NT)                   SAR11410
      RETURN                                                            SAR11420
      END                                                               SAR11430
```

```
      SUBROUTINE CONVEC(AE,AW,AN,AS,I,J,K)
      COMMON/CDVAR/A(71,15,12)
      COMMON/CNUMB/NW,NF,NK,NEP,NV1,NV2,NT,NMU,NRO,NTC,NSP,NMT
      COMMON/CCORD/IMIN(15),IMAX(15),X1(71),X2(15),R(15)
      COMMON/CGRID/IN,INM,JN,JNM,I1,I2,I3,I4,I5,IA,J1
      COMMON/CBB/BBE,BBW,BBN,BBS,BPP
      COMMON/CSORSE/SOURCE,SPRIME
      COMMON/CTAUW/TAUW1(20),TAUW2(15),TAUW3(21),TAUW4(10),CAPPA,E
      COMMON/CCONT/C1,C2,C3,CD
      COMMON/CSNW/SN1(20),SN2(15),SN3(21),SN4(10)
      COMMON/CGEOM/FR(4)
C*********************************************
C   SUBROUTINE FOR CALCULATION OF AE,AW,AN,AS
C*********************************************
C
C*** CALCULATION MEAN MASS FLOW RATE AT FOUR TUBES OF THE TANK
      DV=R(J)*(X1(I+1)-X1(I-1))*(X2(J+1)-X2(J-1))
      G1PW=(A(I,J+1,NF)-A(I,J-1,NF)+A(I-1,J+1,NF)-A(I-1,J-1,NF))/DV
      G1PE=(A(I,J+1,NF)-A(I,J-1,NF)+A(I+1,J+1,NF)-A(I+1,J-1,NF))/DV
      G2PS=(A(I-1,J,NF)-A(I+1,J,NF)+A(I-1,J-1,NF)-A(I+1,J-1,NF))/DV
      G2PN=(A(I-1,J,NF)-A(I+1,J,NF)+A(I-1,J+1,NF)-A(I+1,J+1,NF))/DV
C *** ACCOUNT FOR THE WALL FUNCTION
      IF(K.EQ.NW.OR.K.EQ.NF) GO TO 10
      IF(I.EQ.(I3-1).AND.K.EQ.NT) GO TO 10
      IF(J.EQ.(J1+1).AND.K.EQ.NT) GO TO 10
      IF(J.NE.JNM) GO TO 7
      G1PE=-(A(I,J-1,NF)+A(I,J,NF)+A(I+1,J,NF)+A(I+1,J-1,NF))/DV
      G1PW=-(A(I,J-1,NF)+A(I,J,NF)+A(I-1,J,NF)+A(I-1,J-1,NF))/DV
      BBE=BBE*FR(1)
      BBW=BBW*FR(1)
      BBN=0.0
      G2PN=0.
      IF(K.NE.NK) GO TO 15
      DX=X2(JN)-X2(JNM-1)
      UA=ABS(A(I,JNM,NV1)+A(I,JNM-1,NV1))/DX
      TAUW=TAUW1(I-I1)
```

```
      GO TO 20                                                          SAR11800
15    IF(K.NE.NEP) GO TO 16                                             SAR11810
      YP=X2(JN)-X2(JNM)                                                 SAR11820
      GO TO 21                                                          SAR11830
16    B1=FR(1)                                                          SAR11840
      B2=2.*R(J+1)/R(J)/(X2(J+1)-X2(J-1))                               SAR11850
      SNW=SN1(I-I1)                                                     SAR11860
      TWALL=A(I,J+1,NT)                                                 SAR11870
      GO TO 22                                                          SAR11880
7     IF(I.NE.(I2+1)) GO TO 8                                           SAR11890
      IF(J.GT.J1) GO TO 8                                               SAR11900
      G2PN=-(A(I,J+1,NF)+A( I,J,NF)+A(I+1,J,NF)+A(I+1,J+1,NF))/DV       SAR11910
      G2PS=-(A(I,J-1,NF)+A( I,J,NF)+A(I+1,J,NF)+A(I+1,J-1,NF))/DV       SAR11920
      G1PW=0.                                                           SAR11930
      BBN=BBN*FR(2)                                                     SAR11940
      BBS=BBS*FR(2)                                                     SAR11950
      BBW=0.0                                                           SAR11960
      IF(K.NE.NK) GO TO 17                                              SAR11970
      DX=X1(I2+2)-X1(I2)                                                SAR11980
      UA=ABS(A(I2+1,J,NV2)+A(I2+2,J,NV2))/DX                            SAR11990
      TAUW=TAUW2(J)                                                     SAR12000
      GO TO 20                                                          SAR12010
17    IF(K.NE.NEP) GO TO 18                                             SAR12020
      YP=X1(I)-X1(I-1)                                                  SAR12030
      GO TO 21                                                          SAR12040
18    B1=FR(2)                                                          SAR12050
      B2=2./(X1(I+1)-X1(I-1))                                           SAR12060
      SNW=SN2(J)                                                        SAR12070
      TWALL=A(I-1,J,NT)                                                 SAR12080
      GO TO 22                                                          SAR12090
8     IF(I.NE.(I3-1)) GO TO 9                                           SAR12100
      G2PN= (A(I,J+1,NF)+A( I,J,NF)+A(I-1,J,NF)+A(I-1,J+1,NF))/DV       SAR12110
      G2PS= (A(I,J-1,NF)+A( I,J,NF)+A(I-1,J,NF)+A(I-1,J-1,NF))/DV       SAR12120
      G1PE=0.                                                           SAR12130
      BBE=0.0                                                           SAR12140
      BBN=BBN*FR(3)                                                     SAR12150
```

```
      BBS=BBS*FR(3)                                                     SAR12160
      IF(K.NE.NK) GO TO 25                                              SAR1217C
      DX=X1(I+1)-X1(I-1)                                                SAR12180
      UA=ABS(A(I3-1,J,NV2)+A(I3-2,J,NV2))/DX                            SAR12190
      TAUW=TAUW3(J)                                                     SAR1220C
      GO TO 20                                                          SAR12210
 25   IF(K.NE.NEP) GO TO 26                                             SAR12220
      YP=X1(I+1)-X1(I)                                                  SAR1223C
      GO TO 21                                                          SAR12240
 26   B1=FR(3)                                                          SAR12250
      B2=2./(X1(I+1)-X1(I-1))                                           SAR1226C
      SNW=SN3(J)                                                        SAR12270
      TWALL=A(I+1,J,NT)                                                 SAR12280
      GO TO 22                                                          SAR12290
 9    IF(J.NE.(J1+1)) GO TO 10                                          SAR1230C
      IF(I.GT.I2) GO TO 10                                              SAR12310
      G1PE= (A(I,J+1,NF)+A(I,J,NF)+A(I+1,J,NF)+A(I+1,J+1,NF))/DV        SAR12320
      G1PW= (A(I,J+1,NF)+A(I,J,NF)+A(I-1,J,NF)+A(I-1,J+1,NF))/DV        SAR12330
      G2PS=0.                                                           SAR1234C
      BBS=0.                                                            SAR12350
      BBE=BBE*FR(4)                                                     SAR1236C
      BBW=BBW*FR(4)                                                     SAR1237C
      IF(K.NE.NK) GO TO 27                                              SAR12380
      DX=X2(J1+2)-X2(J1)                                                SAR12390
      UA=ABS(A(I,J1+1,NV1)+A(I,J1+2,NV1))/DX                            SAR12400
      TAUW=TAUW4(I-I1)                                                  SAR12410
      GO TO 20                                                          SAR12420
 27   IF(K.NE.NEP) GO TO 28                                             SAR12430
      YP=X2(J1+1)-X2(J1)                                                SAR12440
      GO TO 21                                                          SAR12450
 28   B1=FR(4)                                                          SAR1246C
      B2=2.*R(J-1)/R(J)/(X2(J+1)-X2(J-1))                               SAR12470
      SNW=SN4(I-I1)                                                     SAR12480
      TWALL=A(I,J-1,NT)                                                 SAR12490
      GO TO 22                                                          SAR12500
 20   SOURCE=UA*TAUW                                                    SAR12510
```

```
      SPRIME=UA*CD*A(I,J,NRC)**2*A(I,J,NK)/TAUW                          SAR12520
      GO TO 10                                                           SAR12530
   21 SOURCE     =(CD**0.75)*(A(I,J,NK )**1.50)/CAPPA/YP                 SAR12540
      SPRIME=1.                                                          SAR12550
      AE=0.                                                              SAR12560
      AW=0.                                                              SAR12570
      AN=0.                                                              SAR12580
      AS=0.                                                              SAR12590
      BBE=0.                                                             SAR12600
      BBW=0.                                                             SAR12610
      BBN=0.                                                             SAR12620
      BBS=0.                                                             SAR12630
      GO TO 100                                                          SAR12640
   22 SOURCE=SOURCE*B1+B2*SNW*TWALL                                      SAR12650
      SPRIME=SNW*B2                                                      SAR12660
   10 CONTINUE                                                           SAR12670
C*** COMPUTE AE,AW,AN,AS                                                 SAR12680
      APP=1.                                                             SAR12690
      IF(K.EQ.NW) APP=R(J)*R(J)                                          SAR12700
      IF(K.EQ.NT) APP=A(I,J,NSP)                                         SAR12710
      AW=0.5*APP*(ABS(G1PW)+G1PW)                                        SAR12720
      AE=0.5*APP*(ABS(G1PE)-G1PE)                                        SAR12730
      AN=0.5*APP*(ABS(G2PN)-G2PN)                                        SAR12740
      AS=0.5*APP*(ABS(G2PS)+G2PS)                                        SAR12750
  100 CONTINUE                                                           SAR12760
      RETURN                                                             SAR12770
      END                                                                SAR12780
```

```
      SUBROUTINE PRINT(NBEGIN,NTOTAL,LP)                              SAR12790
      COMMON/CNAME/ANAME(6,12),ASYMBL(10),BNAME(6,10)                 SAR12800
      COMMON/CDVAR/A(71,15,12)                                        SAR12810
      COMMON/CFLD/B(71,15,10),LF,CU                                   SAR12820
      COMMON/CGRID/IN,INM,JN,JNM,I1,I2,I3,I4,I5,IA,J1                 SAR12830
      COMMON/CAVT/TB                                                  SAR12840
      COMMON/CNUMB/NW,NF,NK,NEP,NV1,NV2,NT,NMU,NRO,NTC,NSP,NMT        SAR12850
      COMMON/CAK/AKEFF                                                SAR12860
      COMMON/CLS/YL(15),YS(15)                                        SAR12870
      COMMON/CTRVL/VE,VC                                              SAR12880
      JX=JN/10                                                        SAR12890
      IF(JX.LT.1) JX=1                                                SAR12900
      IX=IN/10                                                        SAR12910
      IF(IX.LT.1) IX=1                                                SAR12920
      DO 10 K=NBEGIN,NTOTAL                                           SAR12930
      IF(LP.EQ.2) GO TO 11                                            SAR12940
      WRITE(6,100) (ANAME(L,K),L=1,6)                                 SAR12950
      GO TO 12                                                        SAR12960
   11 WRITE(6,100) (BNAME(L,K),L=1,6)                                 SAR12970
   12 CONTINUE                                                        SAR12980
      DO 2 L=1,JN,JX                                                  SAR12990
      J=JN+1-L                                                        SAR13000
      IS=26                                                           SAR13010
      IF(LP.EQ.2) GO TO 15                                            SAR13020
      WRITE(6,103) (A(I,J,K),I=I1,IS,1),J                             SAR13030
      GO TO 16                                                        SAR13040
   15 WRITE(6,103) (B(I,J,K),I=I1,IS,1),J                             SAR13050
   16 CONTINUE                                                        SAR13060
    2 CONTINUE                                                        SAR13070
      IF(LP.EQ.1) GO TO 18                                            SAR13080
      WRITE(6,104) (I,I=I1,IS,1)                                      SAR13090
      GO TO 10                                                        SAR13100
   18 WRITE(6,104) (I,I=I1,IS,1)                                      SAR13110
   10 CONTINUE                                                        SAR13120
      IF(LP.EQ.2) GO TO 20                                            SAR13130
      WRITE(6,201)                                                    SAR13140
```

```
      DO 202 J=1,J1                                                    SAR13150
  202 WRITE(6,203) J,(A(I,J,NT),I=1,I1)                                SAR13160
      WRITE(6,204)                                                     SAR1317C
      I31=IS+1                                                         SAR13180
      DO 205 J=1,JN                                                    SAR13190
      WRITE(6,203) J,(A(I,J,NT),I=I31,IN,1)                            SAR13200
  205 WRITE(6,207) YL(J),YS(J)                                         SAR13210
      WRITE(6,212) VE,TB,AKEFF                                         SAR13220
   20 CONTINUE                                                         SAR13230
      RETURN                                                           SAR1324C
  100 FORMAT(1H130X,21HTHE DISTRIBUTION OF   ,6A6/                     SAR13250
     126X,51H---------------------------------------------------/      SAR13260
     21H0110X,1HJ//)                                                   SAR1327C
  103 FORMAT(1H0,3X,11(1PE10.3),3X,I2,/)                               SAR13280
  104 FORMAT(1H0//3H  I,4X,10(I2,8X),I2/4H ---)                        SAR13290
  201 FORMAT(/,32H TEMP. DISTRIBUTION IN ELECTRODE)                    SAR13300
  204 FORMAT(/,32H TEMP. DISTRIBUTION IN      METAL)                   SAR13310
  203 FORMAT(/,10H J        =,I2,/,10(3X,F8.1))                        SAR13320
  207 FORMAT(/,4H YL=,F10.4,4H YS=,F10.4)                              SAR13330
  212 FORMAT(/,4H VE=,E12.4,4H TB=,F12.2,7H AKEFF=,E12.3)              SAR13340
      END                                                              SAR13350
```

```
      SUBROUTINE SORCE(SOURCE,I,J,K)
      COMMON/CFLD/B(71,15,10),LF,CU
      COMMON/CDVAR/A(71,15,12)
      COMMON/CNUMB/NW,NF,NK,NEP,NV1,NV2,NT,NMU,NRO,NTC,NSP,NMT
      COMMON/CCONT/C1,C2,C3,CD
      COMMON/CTURB/GK(71,15)
      COMMON/CTRVL/VE,VC
      COMMON/CHJ/NHR,NHI,NH,NJRR,NJRI,NJR,NJZR,NJZI,NJZ,NJJ
      COMMON/CCORD/IMIN(15),IMAX(15),X1(71),X2(15),R(15)
      COMMON/CEMP/WF,P,S(4)
      COMMON/CDROP/TAU,HCD,D,QS,QM
      COMMON/CTHERM/TCREF(5),SPREF(5),BETA(2),ES,EE,EM,SB,HL
      COMMON/CGRID/IN,INM,JN,JNM,I1,I2,I3,I4,I5,IA,J1
      COMMON/CLS/YL(15),YS(15)
      COMMON/CTEMP/TLM,TSM,TLS,TA,TM,TW
      GO TO (1,2,3,4,5,6,6,6,6),K
  6   SOURCE=0.0
      RETURN
C ***  FOR VORTICITY/R
  1   SOURCE=B(I,J,NHR)*B(I,J,NJRR)+B(I,J,NHI)*B(I,J,NJRI)
      SOURCE=(1.0E+06)*P*SOURCE
      B(I,J,NJZR)=SOURCE
      BT=BETA(1)
      IF(I.GE.I3) BT=BETA(2)
      B1=ADF(I,J,2,NT)
      B2=R(J)*A(I,J,NRO)*BT*9.81*B1
      B(I,J,NJZI)=B2
      SOURCE=SOURCE+B2
      RETURN
C*** FOR STREAM FUNCTION
    2 SOURCE=A(I,J,NW)
      RETURN
C*** FOR TURBULENCE ENERGY
    3 CONTINUE
      B1=ADF(I,J,1,NV1)
      B2=ADF(I,J,2,NV2)
```

```
      B3=ADF(I,J,2,NV1)
      B4=ADF(I,J,1,NV2)
      B5=A(I,J,NV2)/R(J)
      GK(I,J)=A(I,J,NMT) *(2.0*(B1**2+B2**2+B5**2)+(B3+B4)**2)
      DK=A(I,J,NRO)*A(I,J,NEP)
      SOURCE=GK(I,J)-DK
      RETURN
C***  TURB.ENERGY DISSIPATION
    4 CONTINUE
      IF(A(I,J,NK).EQ.0.0) GO TO 100
      TERM1=0.0
      TERM2=C1*GK(I,J)*A(I,J,NEP)/A(I,J,NK)
      TERM3=C2*A(I,J,NRO)*(A(I,J,NEP)**2)/A(I,J,NK)
      SOURCE=TERM1+TERM2-TERM3
      RETURN
  100 SOURCE=0.0
      RETURN
C *** SOURCE FOR TEMPERATURE
    5 CONTINUE
      IF(J.GT.J1) GO TO 8
      Z=X1(I3)-X1(I2)
      SOURCE=B(I,J,NJJ)-QS/(3.14*R(J1)*R(J1)*Z)
      GO TO 9
    8 SOURCE=B(I,J,NJJ)
    9 CONTINUE
      RETURN
      END
```

```
      SUBROUTINE VELDIS                                                 SAR1399C
      COMMON/CDVAR/A(71,15,12)                                          SAR14000
      COMMON/CNUMB/NW,NF,NK,NEP,NV1,NV2,NT,NMU,NRO,NTC,NSP,NMT          SAR14010
      COMMON/CCORD/IMIN(15),IMAX(15),X1(71),X2(15),R(15)                SAR1402C
      COMMON/CGRID/IN,INM,JN,JNM,I1,I2,I3,I4,I5,IA,J1                   SAR14030
      COMMON/CPROP/ROREF(5),ZMUREF(2),PR(10),GAMA                       SAR14040
      DO 50  J=2,JNM                                                    SAR1405C
      IL=I1+1                                                           SAR14060
      IF(J.LE.J1) IL=I2+1                                               SAR14070
      IH=I3-1                                                           SAR14080
      DO 51  I=IL,IH                                                    SAR1409C
      A(I,J,NV1)=ADF(I,J,2,NF)/R(J)/A(I,J,NRO)                          SAR14100
      A(I,J,NV2)=-ADF(I,J,1,NF)/R(J)/A(I,J,NRO)                         SAR14110
 51   CONTINUE                                                          SAR1412C
  50  CONTINUE                                                          SAR14130
      IL=I1+1                                                           SAR14140
      IH=I3-1                                                           SAR14150
      DO 54  I=IL,IH                                                    SAR14160
      A(I,1,NV1)=2.0*A(I,2,NF)/(R(2)*R(2))/A(I,1,NRO)                   SAR14170
 54   CONTINUE                                                          SAR14180
      J12=J1+1                                                          SAR14190
      DO 40  J=J12,JNM                                                  SAR14200
      A(I1,J,NV2)=-ADF(I1,J,1,NF)/R(J)/A(I1,J,NRO)                      SAR14210
  40  CONTINUE                                                          SAR14220
      RETURN                                                            SAR14230
      END                                                               SAR14240
```

```
      SUBROUTINE VISCOS                                                 SAR14250
      COMMON/CDVAR/A(71,15,12)                                          SAR14260
      COMMON/CNUMB/NW,NF,NK,NEP,NV1,NV2,NT,NMU,NRO,NTC,NSP,NMT          SAR14270
      COMMON/CGRID/IN,INM,JN,JNM,I1,I2,I3,I4,I5,IA,J1                   SAR14280
      COMMON/CRLAX/RP(10),RSDU(10),SAN(10)                              SAR14290
      COMMON/CCONT/C1,C2,C3,CD                                          SAR14300
      COMMON/CPROP/ROREF(5),ZMUREF(2),PR(10),GAMA                       SAR14310
      COMMON/CCORD/IMIN(15),IMAX(15),X1(71),X2(15),R(15)                SAR14320
C*** CALCULATE TURBULENT VISCOSITY                                      SAR14330
      I31=I3-1                                                          SAR14340
      DO 10 J=1,JNM                                                     SAR14350
      DO  11 I=I1,I31                                                   SAR14360
      IF(J.LE.J1.AND.I.LE.I2) GO TO 12                                  SAR14370
      IF(A(I,J,NEP).LE.0.0.OR.A(I,J,NK).LE.0.0) GO TO 20                SAR14380
      A(I,J,NMT) =A(I,J,NRO)*CD*(A(I,J,NK)**2)/A(I,J,NEP)               SAR14390
      GO TO 21                                                          SAR14400
   20 CONTINUE                                                          SAR14410
      A(I,J,NMT)=0.                                                     SAR14420
   21 CONTINUE                                                          SAR14430
      Z=A(I,J,NMU)                                                      SAR14440
      EMU=ZMUREF(1)                                                     SAR14450
      A(I,J,NMU)=EMU    +A(I,J,NMT)                                     SAR14460
      A(I,J,NMU)=Z+RP(NMU)*(A(I,J,NMU)-Z)                               SAR14470
  12  CONTINUE                                                          SAR14480
  11  CONTINUE                                                          SAR14490
   10 CONTINUE                                                          SAR14500
      RETURN                                                            SAR14510
      END                                                               SAR14520
```

```
      SUBROUTINE PROP(L)                                                SAR14530
      COMMON/CDVAR/A(71,15,12)                                          SAR1454C
      COMMON/CNUMB/NW,NF,NK,NEP,NV1,NV2,NT,NMU,NRO,NTC,NSP,NMT          SAR14550
      COMMON/CPROP/ROREF(5),ZMUREF(2),PR(10),GAMA                       SAR14560
      COMMON/CLS/YL(15),YS(15)                                          SAR1457C
      COMMON/CCORD/IMIN(15),IMAX(15),X1(71),X2(15),R(15)                SAR14580
      COMMON/CTHERM/TCREF(5),SPREF(5),BETA(2),ES,EE,EM,SB,HL            SAR14590
      COMMON/CAK/AKEFF                                                  SAR1460C
      COMMON/CTEMP/TLM,TSM,TLS,TA,TM,TW                                 SAR14610
      COMMON/CTRVL/VE,VC                                                SAR14620
      COMMON/CDROP/TAU,HCD,D,QS,QM                                      SAR14630
      COMMON/CSNW/SN1(20),SN2(15),SN3(21),SN4(10)                       SAR14640
      COMMON/CAVM/AVM(20)                                               SAR14650
      COMMON/CFLD/B(71,15,10),LF,CU                                     SAR14660
      COMMON/CHJ/NHR,NHI,NH,NJRR,NJRI,NJR,NJZR,NJZI,NJZ,NJJ             SAR14670
      COMMON/CGRID/IN,INM,JN,JNM,I1,I2,I3,I4,I5,IA,J1                   SAR14680
      IF(L.EQ.2) GO TO 1                                                SAR1469C
      DO 2 I=1,I3                                                       SAR14700
      DO 2 J=1,JN                                                       SAR14710
      IF(I.LE.I2.AND.J.LE.J1) GO TO 3                                   SAR14720
      A(I,J,NRO)=ROREF(2)                                               SAR14730
      A(I,J,NMU)=ZMUREF(1)                                              SAR14740
      A(I,J,NTC)=TCREF(2)                                               SAR14750
      A(I,J,NSP)=SPREF(2)                                               SAR1476C
      GO TO 2                                                           SAR14770
    3 A(I,J,NRO)=ROREF(1)                                               SAR14780
      A(I,J,NTC)=TCREF(1)                                               SAR14790
      A(I,J,NSP)=SPREF(1)                                               SAR14800
      A(I,J,NMU)=ZMUREF(1)                                              SAR14810
    2 CONTINUE                                                          SAR1482C
      AKEFF=TCREF(3)                                                    SAR1483C
    1 CONTINUE                                                          SAR14840
      IF(L.EQ.1) GO TO 5                                                SAR14850
C *** REPOSITION THE ISOTHERMS                                          SAR1486C
      LIQ=0                                                             SAR14870
      DO 10 J=1,JN                                                      SAR14880
```

```
      DO 11 I=I3,IN                                               SAR14890
      IF(LIQ.EQ.1) GO TO 14                                       SAR14900
      TL=A(I,J,NT)-TLM                                            SAR14910
      TLA=ABS(TL)/TLM                                             SAR14920
      IF(TLA.GT.0.0002) GO TO 12                                  SAR14930
      YL(J)=X1(I)-X1(I3)                                          SAR14940
      LIQ=1                                                       SAR1495C
      GO TO 11                                                    SAR14960
   12 IF(TL.GT.0.) GO TO 11                                       SAR14970
      DXT=(X1(I)-X1(I-1))/(A(I,J,NT)-A(I-1,J,NT))                 SAR14980
      YL(J)=X1(I-1)+DXT*(TLM-A(I-1,J,NT))-X1(I3)                  SAR14990
      LIQ=1                                                       SAR15000
   14 TS=A(I,J,NT)-TSM                                            SAR1501C
      TSA=ABS(TS)/TSM                                             SAR15020
      IF(TSA.GT.0.0002) GO TO 15                                  SAR15030
      YS(J)=X1(I)-X1(I3)                                          SAR15040
      LIQ=0                                                       SAR15050
      GO TO 10                                                    SAR15060
   15 IF(TS.GT.0.) GO TO 16                                       SAR15070
      DXT=(X1(I)-X1(I-1))/(A(I,J,NT)-A(I-1,J,NT))                 SAR1508C
      YS(J)=X1(I-1)+DXT*(TSM-A(I-1,J,NT))-X1(I3)                  SAR15090
      LIQ=0                                                       SAR15100
      GO TO 10                                                    SAR1511C
   16 LIQ=1                                                       SAR1512C
   11 CONTINUE                                                    SAR15130
   10 CONTINUE                                                    SAR1514C
C     RECALCULATE VE,VC                                           SAR15150
      DR=R(2)-R(1)                                                SAR15160
      DXF=X1(I2+1)-X1(I2)                                         SAR15170
      DXB=X1(I2)-X1(I2-1)                                         SAR15180
      A1=TCREF(1)/DXB*0.5                                         SAR15190
      A3=   1./(R(J1)*R(J1)*ROREF(1)*HL)                          SAR15200
      XF=X1(I2+1)-X1(I2)                                          SAR1521C
      AVM(1)=0.                                                   SAR15220
      DO 60 J=2,J1                                                SAR15230
      A4=A1*(4.*A(I2-1,J,NT)-3.*A(I2,J,NT)-A(I2-2,J,NT))          SAR15240
```

```
     1+SN2(J)*(A(I2+1,J,NT)-A(I2,J,NT))                                 SAR15250
 60   AVM(J)=R(J)*A4                                                     SAR15260
      SUMV=0.                                                            SAR15270
      J11=J1-1                                                           SAR15280
      DO 61 J=1,J11                                                      SAR15290
      DX2=X2(J+1)-X2(J)                                                  SAR15300
 61   SUMV=SUMV+(AVM(J)+AVM(J+1))*DX2                                    SAR15310
      Z=VE                                                               SAR15320
      VE=A3*SUMV                                                         SAR15330
      VC=VE*R(J1)*R(J1)/(R(JN)*R(JN))                                    SAR15340
      VC=VC*ROREF(1)/ROREF(5)                                            SAR15350
      HCD=HCD*VE/Z                                                       SAR15360
C *** FIRST CALCULATE THE AVERAGE KEFF IN THE SLAG                        SAR15370
      SUMI=0.                                                            SAR15380
      DO 62 I=I1,I3                                                      SAR15390
      N=I-I1+1                                                           SAR15400
      JL=J1                                                              SAR15410
      IF(I.GE.I2) JL=1                                                   SAR15420
      SUMJ=0.                                                            SAR15430
      DO 64 J=JL,JNM                                                     SAR15440
      DX2=0.5*(X2(J+1)-X2(J))                                            SAR15450
 64   SUMJ=SUMJ+(A(I,J,NMT)*R(J)+A(I,J+1,NMT)*R(J+1))*DX2                SAR15460
      RAV=(R(JN)+R(JL))*0.5                                              SAR15470
 62   AVM(N)=SUMJ/(X2(JN )-X2(JL))/RAV                                   SAR15480
      N3=I3-I1                                                           SAR15490
      DO 66 N=1,N3                                                       SAR15500
      I=N+I1-1                                                           SAR15510
      DZ=(X1(I+1)-X1(I))*0.5                                             SAR15520
 66   SUMI=SUMI+(AVM(N)+AVM(N+1))*DZ                                     SAR15530
      AVMU=SUMI/(X1(I3)-X1(I1))                                          SAR15540
      AKEFF=AVMU*SPREF(2)/TCREF(2)+1.                                    SAR15550
      AKEFF=AKEFF*TCREF(3)*0.3333                                        SAR15560
      IF(AKEFF.LT.TCREF(3)) AKEFF=TCREF(3)                               SAR15570
 5    CONTINUE                                                           SAR15580
      DO 4 J=1,JN                                                        SAR15590
 4    A(I3,J,NTC)=AKEFF                                                  SAR15600
```

```
C  *** ASSIGN THE PROPERTIES TO PROPER DOM AINS                         SAR15610
      I31=I3+1                                                          SAR15620
      DO 54 J=1,JN                                                      SAR15630
      DO 54 I=I31,IN                                                    SAR15640
      XSM=X1(I)-X1(I3)                                                  SAR15650
      IF(XSM.GT.YL(J)) GO TO 55                                         SAR15660
      A(I,J,NRO)=ROREF(3)                                               SAR15670
      A(I,J,NTC)=AKEFF                                                  SAR15680
      A(I,J,NSP)=SPREF(3)                                               SAR15690
      GO TO 54                                                          SAR15700
   55 IF(XSM.GT.YS(J)) GO TO 56                                         SAR15710
      A(I,J,NRO)=ROREF(4)                                               SAR15720
      A(I,J,NTC)=TCREF(4)                                               SAR15730
      A(I,J,NSP)=SPREF(4)                                               SAR15740
      GO TO 54                                                          SAR15750
   56 A(I,J,NRO)=ROREF(5)                                               SAR15760
      A(I,J,NTC)=TCREF(5)                                               SAR15770
      A(I,J,NSP)=SPREF(5)                                               SAR15780
   54 CONTINUE                                                          SAR15790
      RETURN                                                            SAR15800
      END                                                               SAR15810
```

```
      FUNCTION ADF(I,J,LX,K)                                            SAR15820
      COMMON/CDVAR/A(71,15,12)                                          SAR15830
      COMMON/CCORD/IMIN(15),IMAX(15),X1(71),X2(15),R(15)                SAR15840
      COMMON/CGRID/IN,INM,JN,JNM,I1,I2,I3,I4,I5,IA,J1                   SAR15850
C     FUNCTION FOR EVALUATION OF FIRST DERIVATIVES                      SAR15860
      M=1                                                               SAR15870
      PP=1.                                                             SAR15880
      IF(J.EQ.1) M=2                                                    SAR15890
      IF(J.EQ.JN)  M=4                                                  SAR15900
      IF(I.EQ.I1) M=3                                                   SAR15910
      IF(I.EQ.IN)  M=5                                                  SAR15920
      GO TO (1,2,3,4,5),M                                               SAR15930
C*** M=1, FOR POINTS NOT ON ANY OF THE BOUNDARIES                        SAR15940
    1 IF(LX.EQ.2)  GO TO 11                                             SAR15950
      PN=1.                                                             SAR15960
      BENQ=A(I+1,J,K)                                                   SAR15970
      BWSR=A(I-1,J,K)                                                   SAR15980
      BP=A(I,J,K)                                                       SAR15990
      XENQ=X1(I+1)-X1(I)                                                SAR16000
      XWSR=X1(I)-X1(I-1)                                                SAR16010
      GO TO 100                                                         SAR16020
   11 PN=1.                                                             SAR16030
      BENQ=A(I,J+1,K)                                                   SAR16040
      BWSR=A(I,J-1,K)                                                   SAR16050
      BP=A(I,J,K)                                                       SAR16060
      XENQ=X2(J+1)-X2(J)                                                SAR16070
      XWSR=X2(J)-X2(J-1)                                                SAR16080
      GO TO 100                                                         SAR16090
C *** FOR POINTS ON THE SYMMETRY AXIS                                   SAR16100
    2 IF(LX.EQ.1)  GO TO 1                                              SAR16110
      PN=-1.                                                            SAR16120
      BENQ=A(I,J+1,K)                                                   SAR16130
      BWSR=A(I,J+2,K)                                                   SAR16140
      BP=A(I,J,K)                                                       SAR16150
      XENQ=X2(J+1)-X2(J)                                                SAR16160
      XWSR=X2(J+2)-X2(J)                                                SAR16170
```

```
      GO TO 100
C*** M=3, FOR POINTS ON THE BOUNDARY I=I1
    3 IF(LX.EQ.2)  GO TO 11
      PN=-1.
      BENQ=A(I+1,J,K)
      BWSR=A(I+2,J,K)
      BP=A(I,J,K)
      XENQ=X1(I+1)-X1(I)
      XWSR=X1(I+2)-X1(I)
      GO TO 100
C*** M=4, FOR POINTS ON THE BOUNDARY J=JN
    4 IF(LX.EQ.1)  GO TO 1
      PN=-1.
      PP=-1.
      BENQ=A(I,J-1,K)
      BWSR=A(I,J-2,K)
      BP=A(I,J,K)
      XENQ=X2(J)-X2(J-1)
      XWSR=X2(J)-X2(J-2)
      GO TO 100
C*** M=5, FOR POINTS ON THE BOUNDARY I=IN
    5 IF(LX.EQ.2)  GO TO 11
      PN=-1.
      PP=-1.
      BENQ=A(I-1,J,K)
      BWSR=A(I-2,J,K)
      BP=A(I,J,K)
      XENQ=X1(I)-X1(I-1)
      XWSR=X1(I)-X1(I-2)
  100 CONTINUE
      ADF=((XENQ*XENQ-XWSR*XWSR)*BP+
     1XWSR*XWSR*BENQ-XENQ*XENQ*BWSR)/(XENQ*XWSR*(PN*XENQ+XWSR))*PP
      RETURN
      END
```

```
VORTICITY
STREAM FUNCT:ON
TURBULENCE ENERGY
TURBULENCE DISSIPATION
TEMPERATURE
DIR.-1 VELOCITY
DIR.-2 VELOCITY
EFFECTIVE VISCOSITY
DENSITY
THERMAL CONDUCTIVITY
SPECIFIC HEAT
TURBULENT VISCOSITY
RSVORTRSSTRMRSTENGRSDISPRSTEMPSANVOR
SANSTMSANTKESANDSPSANTMP
RE MAGNETIC FLUX INTENSITY
IM MAGNETIC FLUX INTENSITY
RE CURRENT IN DIR.-R
IM CURRENT IN DIR.-R
JOULE HEAT
MAGNETIC FLUX INTENSITY
CURRENT IN DIR.-R
CURRENT IN DIR.-Z
RE CURRENT IN DIR.-Z
IM CURRENT IN DIR.-Z
```

REFERENCES

1. A. Mitchell, S. Joshi and J. Cameron; Met. Trans., 2, 561 (1971).

2. J.F. Elliott and M.A. Maulvault; Proc. Elec. Conf. AIME, 28, 13 (1970).

3. J. Mendrykowski, J.J. Poveromo, J. Szekely and A. Mitchell; Met. Trans., 3, 1761 (1972).

4. R.C. Sun and J.W. Pridgeon; Second Int. Symp. on ESR, Mellon Inst., Pittsburgh (1969).

5. B.E. Paton, B.I. Medovar, V.F. Demchenko, J.G. Khorungy, V.L. Shevtzov, J.P. Shtanko and A.G. Bogachenko; Fifth Int. Symp. on ESR, Mellon Inst; Pittsburgh (1974).

6. S. Joshi; Ph.D. Thesis, Dept. of Met., Univ. of British Columbia (1971).

7. M.A. Maulvault; Ph.D. Thesis, Dept. of Met. and Mat. Sc., Mass. Inst. of Tech. (1971).

8. L.F. Carvajal and G.E. Geiger, Met. Trans., 2, 2087 (1971).

9. A. Mitchell, J. Szekely, and J.F. Elliott, Proc. Conf. on ESR, Sheffield, England, 3 (1973).

10. B.E. Paton, B.I. Medovar, D.A. Kozlitin, Yu. G. Emel'-yanenko, Yu. A. Sterebogen and V.M. Baglai; Proc. Conf. on ESR, Sheffield, England, 16 (1973).

11. J.F. Elliott and M. Maulvault; Proc. Fourth Int. Symp. on ESR, Tokyo, 69 (1973).

12. A.S. Ballantyne and A. Mitchell; Ironmaking and Steel-making, No. 4, 222 (1977).

13. A.H. Dilawari and J. Szekely; Met. Trans., 8B, 227 (1977).

14. A.H. Dilawari and J. Szekely; Proc. Fifth Int. Conf. on Vac. Met. and ESR Processes, Munich, 157 (1976).

15. A.H. Dilawari and J. Szekely; Met. Trans., 9B, 77 (1978).

16. J. Kreyenberg and K. Schwerdtfeger; Arch. Eisenhutten-wes, No. 1, 1 (1979).

17. M. Kawakami and K.S. Gogo; Proc. Sixth Int. Conf. on Vac. Met. and ESR, San Diego (1979).

18. C.L. Jeanfils, J.H. Chen and H.J. Klein, ibid.

19. M. Choudhary and J. Szekely; ibid.

20. J. Szekely and M. Choudhary; Proc. Int. Conf. on Heat and Mass Transfer in Met. Systems, Dubrovnik, Yugoslavia (1979).

21. M. Inoue and T. Iwasaki, quoted in the paper by Kawakami and Goto (reference 17).

22. M. Choudhary and J. Szekely, Met. Trans. (submitted for publication).

23. M. Etienne and A. Mitchell; Proc. Elec. Furn. Conf. AIME, 28, 28 (1970).

24. C.K. Copper et al., Proc. Elec. Furn. Conf. AIME, 28, 8 (1970).

25. C.F. Knights and R. Perkins; Proc. Conf. on ESR, Sheffield, England, 35 (1973).

26. K. Schwerdtfeger, W. Wepner and G. Pateisky; Ironmaking and Steelmaking, No. 3, 135 (1978).

27. S. Kou, D.R. Poirier and M.C. Flemings; Met. Trans., 9B, 711 (1978).

28. S.D. Ridder, F.C. Reyes, S. Chakravorty, R. Mehrabian, J.D. Nauman, J.H. Chen and H.J. Klein; Met. Trans; 9B, 415 (1978).

29. R. Mehrabian and S. Ridder; paper presented at the fall meeting of TMS - AIME, Milwaukee, Wisconsin (1979).

30. J. Szekely and R.T. Yadoya; Math. Process Models in Iron and Steelmaking, Amsterdam, 165 (1973).

31. J. Szekely and K. Nakanishi; Met. Trans., 6B, 245 (1975).

32. J. Szekely and C.W. Chang; Ironmaking and Steelmaking, 4, No. 3, 190, 196 (1977).

33. E.D. Tarapore and J.W. Evans; Met. Trans., 7B, 343 (1976).

34. J. Szekely, H.J. Wang and K.M. Kiser; Met. Trans., 7B, 287 (1976).

35. J. Szekely, A.H. Dilawari and R. Metz; Met. Trans., 10B, 33 (1979).

36. B.E. Launder and D.B. Spalding; Lectures in Math. Models of Turbulence, Academic Press, London and New York (1972).

37. International Conference on Injection Metallurgy, Lulea, Sweden (1977).

38. J. Szekely; Proc. Int. Conf. on Heat and Mass Transfer in Met. Systems, Dubrovnik, Yugoslavia (1979).

39. A.D. Gosman, W.M. Pun, A.K. Runchal, D.B. Spalding and M. Wolfshtein; Heat and Mass Transfer in Recirculating Flows, Academic Press, London and New York (1969).

40. W.E. Duckworth and G. Hoyle; Electro-slag Refining, Chapman and Hall, London (1969).

41. Report of the Committee on Electroslag Remelting and Plasma Arc Melting, National Materials Advisory Board, National Academy of Science, Washington (1976).

42. J. Campbell, J. of Metals, 24, 23 (1970).

43. W.F. Hughes and F.J. Young, The Electromagnetodynamics of Fluids, John Wiley and Sons, N.Y. (1966).

44. N. Narayana Rao, Basic Electromagnetics with Applications; Prentice-Hall, Inc. (1972).

45. R.B. Bird, W.E. Stewart and E.N. Lightfoot, Transport Phenomena, John Wiley and Sons, N.Y. (1960).

46. B.E. Launder and D.B. Spalding; Computer Methods in Applied Mechanics and Engr., 3, 269 (1974).

47. H. Tennekes and J.L. Lumley; A First Course in Turbulence, MIT Press (1972).

48. J.O. Hinze, Turbulence, McGraw Hill (1959).

49. H. Lamb, Hydrodynamics, Dover Publications, New York (1945).

50. S. Hu and R.C. Kintner; A.I.Ch.E.J., 1, 42 (1955).

51. S. Sideman and H. Shabtal, Can. J. Chem. Eng., 42, 107 (1964).

52. K.E. Spelles; Proc. Phys. Soc., 65B, 541 (1952).

53. P.J. Roache, Computational Fluid Dynamics, Hermosa Publishers, New Mexico (1972).

54. H. Leunberger and R.A. Person, Compilation of Radiation Shape Factors for Cylindrical Assemblies, ASME Report 56-A-144 (1956).

55. W.M. Pun and D.B. Spalding; A General Computer Program for Two-Dimensional Elliptic Flows, Report no. HTS/76/2, Heat Transfer Section, Imperial College of Science and Technology (1976).

56. H. Schlichting, Boundary-Layer Theory, McGraw Hill (1968).

57. P.O. Mellberg, Proc. Fourth Int. Symp. on ESR, Tokyo, 13 (1973).

58. M. Hajduk and T. El Gammal, Stahl u Eisen, No. 3, 113 (Feb. 1979).

59. A.H. Dilawari and J. Szekely, Ironmaking and Steelmaking, No. 5, 308 (1977).

60. A. Mitchell and J. Cameron; Met. Trans; 2, 3361 (1971).

61. K. Yamaguchi, M. Funazu and T. Ichihara, Proc. Fourth Int. Symp. on ESR, Tokyo, 91 (1973).

62. D.M. Longbottom, A.A. Greenfield, G. Hoyle and M.J. Rhydderch; ibid, 126 (1973).

BIOGRAPHICAL NOTE

The author was born in Bihar, India on June 26, 1952. After finishing high school in Calcutta he attended Indian Institute of Technology, Kharagpur, from 1969 to 1974 and obtained the degree of Bachelor of Technology (Honours) in Chemical Engineering. During both high school and undergraduate years he received numerous awards for achievements in academics and extra-curricular activities. On completion of his undergraduate studies in 1974, Department of Chemical Engineering awarded him Professor S.K. Nandi Gold Medal for being the "best all rounder" Chemical Engineering student in the class of 1974, the Institute Silver Medal for securing first rank in B. Tech. examinations and an award for the Best Undergraduate Thesis.

In June 1974, the author married Saraswati Jha. In September 1974, he joined State University of New York at Buffalo and obtained the degree of Master of Science in Chemical Engineering in June 1976. His thesis work was on the effect of flow maldistribution on the performance of catalytic packed bed reactors. He joined the Department of Materials Science and Engineering at MIT in September 1976. In 1978, the department awarded him Falih N. Darmara Materials Achievement Award "in recognition of outstanding academic performance, excellent research work and extra curricular activities". The same year he received the

Annual Student Paper Award of the Eastern Iron and Steel Section of AIME for a paper "Optimization of Burden Size for a Blast Furnace".

As a research associate (Summers of 1976, 1977, 1978) at both SUNY at Buffalo and at MIT, the author has worked on a number of projects, both experimental and theoretical. He has worked on a broad range of problems as parts of various consulting assignments. Some of the assignments have involved heat transfer and fluid flow calculations in an electric furnace smelter, heat transfer calculations for recuperators using impinging jets, material and energy balance analysis for coal gasification and direct reduction processes, etc. He has also published papers in the areas of chemical reaction engineering, gas-solid reaction, and modelling of electroslag refining process.

The author is a student member of AIME and ASM. He is also a member of Sigma Xi.